Thermodynamics and Indefinite Causal Order

A thesis by

Otavio Augusto Dantas Molitor

for the title of Doctor of Philosophy (PhD)

Supervisor

dr hab. Łukasz Rudnicki

Faculty of Physics, Mathematics and Informatics
University of Gdańsk

Gdańsk, Poland

2024

To my beloved Dorota,
thank you for your love, care,
understanding and support,
without you I wouldn't have gotten here…

Acknowledgements

First and foremost, I thank My Lord and God for allowing me to reach this point in my life. It was never easy, but I always had all the necessary blessings to go forward and move until the end. Glory to Him!

I thank my (already!) wife Dorota for all the love, care, understanding and help during these years. This relationship started in the first months of the doctorate and quickly developed into the seed of a beautiful family, where we already have two sweet frenchies, Mania and Sorca. I could not be happier! In this relationship, I also was adopted by my Polish family. Being embraced as a son, a grandson, a nephew and a cousin for me was a huge blessing. From the bottom of my heart, thank you Magda (mama), Sławek (tata), babcia Dorota, babcia Ula, ciocia Tania, ciocia Iza and all other family members. I love you guys!

Of course, the basis comes from my Brazilian family, which always supported me and gave me the conditions, material and immaterial, to conduct my studies. I miss them every day and some times it feels harder to not have my parents, my sister, grandparents, aunts, uncles and cousins around, but it is part of life and here in Poland I found my place. I always carry them in my heart and prayers. Needless to say, I love you too!

From the professional side, I thank my supervisor Łukasz Rudnicki for having me as his student and Ewa Kaszewska from the International Centre for Theory of Quantum Technologies (ICTQT) for greatly helping me with administrative issues, specially when I was moving to Poland. Moreover, I am grateful to Pedro Ruas Dieguez from ICTQT, for his great help with the challenging Chapter 6 of the thesis and for valuable feedback about its quality. Equally important was the collaboration with Lucas Chibebe Céleri from the Federal University of Goiás, Brazil and Matheus Capela from the Basque Country University, Spain, which helped understanding important concepts of indefinite causal order in terms of process matrices and how to make the connection with thermodynamics. The International Network on Acausal Quantum Technologies (INAQT) also gave me the opportunity to meet numerous prestigious researchers through the organization of its online seminars. These meetings helped me maturing as a researcher and a co-organizer of scientific gatherings. Correspondence with Esther Hänggi from the Lucerne University of Applied Sciences and Arts, Switzerland, greatly helped me to understand one of her papers, which was central in one one the results of the thesis. I extend my thanks to the other academic and administrative people that helped me at some extent, from the University of Gdańsk and elsewhere.

“In the beginning God made heaven and earth.
The earth was invisible and unfinished;
and darkness was over the deep.
The Spirit of God was hovering over the water.
Then God said: ’Let there be light’; and there was light.
God saw the light; it was good; and God divided the light from the darkness.
God called the light Day; the darkness He called Night; and there was evening and morning, one day.”

— Genesis 1:1-5

“Na początku Bóg stworzył niebo i ziemię.
Ziemia zaś była bezładem i pustkowiem;
ciemność była nad powierzchnią bezmiaru wód.
Duch Boży unosił się nad wodami.
Wtedy Bóg rzekł: ’Niechaj się stanie światłość!’ I stała się światłość.
Bóg widząc, że światłość jest dobra, oddzielił ją od ciemności.
I nazwał Bóg światłość dniem, a ciemność nazwał nocą. I tak upłynął wieczór i poranek - dzień pierwszy.”

— Księga Rodzaju 1:1-5

Abstract

Apart from an initial spark in the early 1990's, the idea of superposing the time evolution of quantum systems was put aside. Many years later, in the quest of formulating a successful theory of quantum gravity, the concept of indefinite causal order (ICO) was developed, which itself contains superposition of time evolutions. Physically, ICO would be the result of having uncertainty in the spacetime metric itself, inserting quantum uncertainty into the core of general relativity. The ICO concept can be operationally incorporated in the so-called process matrix formalism, which is a generalization of the density matrix acting on two or more quantum channels, returning some probability distribution over different measurement results. It happens that process matrices that cannot be decomposed as convex combinations of causally-ordered terms, whose technical denomination is causal non-separability, are said to contain ICO. Moreover, there are process matrices containing ICO that violate what are called causal inequalities (CIs), analogous to Bell inequalities, and those that do not violate them. The former has to this day only an abstract description and no exact physical mechanism originating it has been completely thought through. Largely due to it, it is not known if they are in fact physical. The latter can be collectively called controlled-superposition of causal orders (cSCO), whose main implementation is known as the quantum switch (QS). This process has been already implemented in the laboratory by different research groups and has been suggested to offer advantages in areas such as quantum computation, quantum communications, quantum metrology and quantum thermodynamics. Within the two categories of ICO processes, this thesis puts forward studying them in the context of thermodynamics. For those process matrices violating CIs, we focus on finding out whether thermodynamics through its second law constrains their existence. By combining different models from the literature, we develop a framework in which the second law of thermodynamics (SLT) is never violated by any bipartite process matrix with two-dimensional systems. Considering the universality of the SLT, this is an indicative that these ICO processes are indeed physical. Our results agree with previous research output where ICO processes were shown to not allow extra work extraction when compared to causally-ordered strategies. Nevertheless, the result is not conclusive and further studies must be done. On the other hand, for the processes that do not violate CIs, specially the QS, we present technical results of applying it to activate passive states and the instabilities of the QS for a control degree-of-freedom that interacts with a thermal environment. Both have considerable impact for including thermal effects in the description of technological implementations of the QS. We consider that this thesis adds valuable knowledge to the growing efforts of understanding ICO and harnessing it for real life applications.

Keywords: Indefinite Causal Order; Thermodynamics; Causal Inequalities; Quantum Switch; Quantum Information Theory.

Podsumowanie

Po początkowym zrywie na początku lat 90-tych, pomysł superpozycji ewolucji czasowych układów kwantowych został odłożony na bok. Wiele lat później, w poszukiwaniu sformułowania udanej teorii grawitacji kwantowej, opracowano pojęcie nieokreślonego porządku przyczynowego (ICO), które samo w sobie zawiera superpozycję ewolucji czasowych. Fizycznie, ICO byłoby wynikiem niepewności w samej metryce czasoprzestrzeni, wprowadzając niepewność kwantową do rdzenia ogólnej teorii względności. Pojęcie ICO może być operacyjnie włączone do tzw. formalizmu macierzy procesów, który jest uogólnieniem macierzy gęstości działających na dwa lub więcej kanałów kwantowych, zwracających rozkład prawdopodobieństwa różnych wyników pomiarów. Okazuje się, że macierze procesów, które nie mogą zostać rozłożone jako kombinacje wypukłe wyrazów uporządkowanych przyczynowo, których techniczna nazwa to nieoddzielność przyczynowa, są określane jako zawierające ICO. Ponadto istnieją macierze procesów zawierające ICO, które łamią tzw. nierówności przyczynowe (CI), analogiczne do nierówności Bella, oraz takie, które ich nie łamią. Pierwsze mają do dziś jedynie abstrakcyjny opis, a żaden dokładny mechanizm fizyczny, który je wywołuje, nie został całkowicie opracowany. Głównie z tego powodu nie wiadomo, czy są one w rzeczywistości fizyczne. Drugie można zbiorczo nazwać kontrolowaną superpozycją porządków przyczynowych (cSCO), której główna implementacja jest znana jako kwantowy przełącznik (QS). Ten proces został już zaimplementowany w laboratoriach przez różne grupy badawcze i zasugerowano, że może on oferować zalety w obszarach takich jak obliczenia kwantowe, komunikacja kwantowa, metrologia kwantowa i termodynamika kwantowa. W ramach dwóch kategorii procesów ICO, niniejsza praca proponuje badanie ich w kontekście termodynamiki. Dla tych macierzy procesów, które łamią CI, koncentrujemy się na ustaleniu, czy termodynamika przez swoje drugie prawo ogranicza ich istnienie. Łącząc różne modele z literatury, opracowujemy ramy, w których drugie prawo termodynamiki (SLT) nigdy nie jest łamane przez żadną macierz procesów dwu-dzielnych z układami dwu-wymiarowymi. Biorąc pod uwagę uniwersalność SLT, wskazuje to, że te procesy ICO są faktycznie fizyczne. Nasze wyniki zgadzają się z wcześniejszymi badaniami, w których pokazano, że procesy ICO nie pozwalają na ekstrahowanie pracy w porównaniu do strategii uporządkowanych przyczynowo. Niemniej jednak, wynik nie jest ostateczny i wymagają dalszych badań. Z drugiej strony, dla procesów, które nie łamią CI, szczególnie dla QS, przedstawiamy wyniki techniczne dotyczące jego zastosowania do aktywacji stanów pasywnych oraz niestabilności QS dla stopnia swobody kontrolującego, który wchodzi w interakcję z termalnym środowiskiem. Oba te aspekty mają istotny wpływ na uwzględnianie efektów termicznych w opisie technologicznych implementacji QS. Uważamy, że niniejsza praca wnosi cenną wiedzę do rosnących wysiłków w zrozumieniu ICO i wykorzystaniu go w zastosowaniach w rzeczywistości.

Słowa kluczowe: Nieokreślony Porządek Przyczynowy; Termodynamika; Nierówności Przyczynowe; Kwantum Switch; Teoria Informacji Kwantowej.

List of Publications during Doctoral Studies

Peer-reviewed

- O. A. D. Molitor, A. H. A. Malavazi, R. D. Baldijão, A. C. Orthey, I. L. Paiva, and P. R. Dieguez, Communications Physics **7**, 373 (2024).
- O. A. D. Molitor and Ł. Rudnicki, Entropy **26**, 153 (2024).

Pre-prints

- Ł. Rudnicki, W. Kłobus, O. A. D. Molitor, and W. Laskowski, *Salient signatures of entanglement in the surrounding environment*, 2022. arXiv:2209.05197 [quant-ph].

List of Symbols & Abbreviations

(a, b)	Excludes *a and b*
$(a, b]$	Excludes a, includes b
$:=$	Defined as
$[a, b)$	Includes a, excludes b
$[a, b]$	Includes *a and b*
$[X, Y]_+$	Anti-commutator between X and Y
$[X, Y]_-$	Commutator between X and Y
$\circ$	Map composition
$\times$	Cartesian product
$\dagger$	Hermitian conjugate
δ_{ij}	Kronecker delta
$\equiv$	Equivalent to
$\forall$	For all
$\hbar$	Reduced Planck constant: $1.054\,571\,817\ldots \times 10^{34}$ J·s
$\in$	Belongs to
ln	Natural logarithm
$\mapsto$	Maps to
$\mathbb{C}$	The set of Complex Numbers
$\mathbb{N}$	The set of Natural Numbers
$\mathbb{R}$	The set of Real Numbers
$\mathbb{Z}$	The set of Integer Numbers
$\mathcal{E}$	Internal energy
$\mathcal{H}$	Hilbert space
$\mathcal{I}$	Available information
$\mathcal{L}(\mathcal{H})$	Linear space of operators upon the Hilbert space $\mathcal{H}$
$\mathcal{O}$	Order of the function
$\mathcal{Q}, q$	Heat

$\mathcal{S}$	von Neumann entropy
$\mathcal{W}$	Work
$\mathbb{1}$	Identity operator
$\mathfrak{C}$	Relative entropy of coherence
$\mathfrak{I}$	Identity map
$\mathfrak{M}$	Manifold
$\mathfrak{p}$	Probability density function
$\mathfrak{S}$	Decomposition entropy
μ	Causal witness
$\nleftrightarrow$	No causal relation (space-like separated)
$\oplus$	Sum modulo 2
$\otimes$	Tensor product
ρ	Density operator/matrix
σ_α	The $\alpha \in \{x \leftrightarrow 1, y \leftrightarrow 2, z \leftrightarrow 3\}$ Pauli operator/matrix
$\succeq 0$	Positive semi-definite
$\mathrm{D}(\mathcal{H})$	Density operator space upon the Hilbert space $\mathcal{H}$
Θ	Gibbs thermal state
tr	The trace operation
tr_X	The partial trace operation over some subsystem X
*	Complex conjugation
$^\intercal$	Matrix transposition
a	Annihilation operator of the quantum harmonic oscillator
$a^\dagger$	Creation operator of the quantum harmonic oscillator
C	Control
c	Speed of light in vacuum: 299 792 458 $\mathrm{m{\cdot}s^{-1}}$
D	Relative entropy
E	Environment
e	Euler number: 2.718 . . .
G	Gravitational constant: $6.674\,30 \times 10^{-11}\ \mathrm{m^3{\cdot}kg^{-1}{\cdot}s^{-2}}$
H	Hamiltonian
I	Mutual information
k_B	Boltzmann constant: $1.380\,649 \times 10^{23}\ \mathrm{J{\cdot}K^{-1}}$
l_P	Planck length
m_P	Planck mass

P	Probability
S	System
V	Interaction Hamiltonian
W	Process matrix
per se	(Latin) By itself
AdS	Anti-de Sitter
BW	Bäumeler-Wolf
CFT	Conformal field theory
CI	Causal inequality
COP	Coefficient of performance
CPTP	Completely positive trace-preserving
cSCO	Controlled superposition of causal orders
DOF	Degree-of-freedom
e.g.	Example given
EC	Excitation conserving
EUR	Entropic uncertainty relation
eV	Electron-volt: 1.602×10^{-19} J
FGUR	Fine-grained uncertainty relation
FLT	First law of thermodynamics
FT	Fluctuation theorem
GPS	Global positioning system
GR	General relativity
h.c.	Hermitian conjugate
i.d.	(Latin) Id est: that is
ICO	Indefinite causal order
iff	if and only if
LGYNI	Lazy guess your neighbour's input
LHC	Large Hadron Collider
LHS	Left-hand side
MUBs	Mutually-unbiased bases
OCB	Oreshkov-Costa-Brukner
QFT	Quantum field theory
QG	Quantum gravity
QM	Quantum mechanics

QS Quantum switch

RHS Right-hand side

SCO Superposition of causal orders

SEC Strict energy conservation

SLT Second law of thermodynamics

SMI Shannon measure of information

TLGYNI Thermal lazy guess your neighbour's input

UR Uncertainty relation

List of Figures

2.1 **Scheme of what an indefinite causal order would look like from a superposition perspective** . . . 8
2.2 **Scheme of a process matrix W acting on two Choi-Jamiołkowski (CJ) matrices M_x^{Alice} and M_y^{Alice}** . . . 10
2.3 **Diagram presenting the main groups of process matrices according to causal non-separability and violation of causal inequalities** . . . 13

3.1 **Generic representation of superposition of causal orders (SCO) for two quantum channels** . . . 15
3.2 **Generic representation of controlled superposition of causal orders (cSCO) for two quantum channels** . . . 16
3.3 **Experimental setup employed in Ref. [7]** . . . 21
3.4 **Experimental setup used in Ref. [8]** . . . 22
3.5 **Experimental setup of Ref. [9]** . . . 23

4.1 **The internal energy difference Δ_{QS} as a function of the inverse temperature of the system β and for different values of $|t|$, when the unitaries are rotations around the x and y axes of the Bloch sphere** . . . 32
4.2 **Angle φ_M (radians) for which $\Delta_{S,M}$ is minimum as a function of $\alpha_x = \alpha_y = \alpha$ (left) and $\Delta_{S,M}$ as a function of the angle φ_M and for $\alpha = \pi/4, \pi/2, 3\pi/4$ (right)** . . . 33
4.3 **Minimum min Δ_{QS} for $U(2)$ unitaries as a function of $|t|$** . . . 34
4.4 **Plot of min $\Delta_{S,M}$ for general $U(2)$ unitaries as a function of φ_M (radians)** 35
4.5 **Density plots of Δ_{QS} as a function of $|\alpha_1|$ and $|\alpha_2|$, when unitaries are displacemenets operators** . . . 38
4.6 **Plot of Δ_{QS} when the unitaries are displacement operators as a function of $|\alpha| = |\alpha_1| = |\alpha_2|$ and for different $|t|$** . . . 39
4.7 **Plots of Δ_{QS} when the unitaries are the displacement and squeeze operators as a function of $|\alpha|$ and $|z|$** . . . 41
4.8 **Plots of $\Delta^0_{S,M}$ as a function of $|\alpha|$ and $|z|$, when the unitaries are the displacement operator and the squeeze operator, and $\xi - 2\phi = 0$** . . . 44
4.9 **Plots of $\Delta^\pi_{S,M}$ as a function of $|\alpha|$ and $|z|$, when the unitaries are the displacement operator and the squeeze operator, and $\xi - 2\phi = \pi$** . . . 45
4.10 **Plots of $\Delta_{S,M}$ when the unitaries are the displacement operator and the squeeze operator, as a function of $|\alpha| = |z|$ and for $\beta \to \infty$** . . . 46

5.1 **Depiction of the collisional model framework** . . . 49

5.2 **Quantum circuit representation of the quantum switch with an open control** . . . 53
5.3 **Monotonic decay of $|b^{\pm}_{\text{indef}}(n, g\tau)|$ as a function of n.** . . . 56
5.4 **Effect of temperature on $|b^{+}_{\text{def}}(n, f_E, g\tau)|$ (a) and $|b^{-}_{\text{def}}(n, f_E, g\tau)|$ (b) as a function of n** . . . 57
5.5 **Available information in the system S (a qubit) after applying the QS, collisions and measuring the control in the $|+\rangle_C$ state as a function of the measuring strength ϵ, in the case of monitoring MUBs quantum maps** . . . 62
5.6 **Available information in the system S (a qubit) after applying the QS, collisions and measuring the control in the $|-\rangle_C$ state as a function of the measuring strength ϵ, in the case of monitoring MUBs quantum maps** . . . 63
5.7 **Flow chart depiction of the open control QS-fueled refrigeration cycle** 65
5.8 **Representation of the open control QS-fueled quantum refrigeration cycle up to the measurement of the control and storage of the result** . 66
5.9 **Refrigeration condition for closed control (zero collisions, $n = 0$) as a function of β_{cold} and β_{hot}** . . . 68
5.10 **Ratio between the coefficient of performance after n collisions (COP_n) and the coefficient of performance for closed control (COP_0) as a function of n and $\beta_E/\beta_{\text{hot}}$** . . . 69
5.11 **Heat flowing between control C and cold bath, as a function of $\beta_{\text{cold}}/\beta_{\text{hot}}$ and ω/ω_S, for $n = 100$** . . . 70
5.12 **Ratio between the coefficient of performance after n collisions (COP_n) and the coefficient of performance for closed control (COP_0) as a function of n and ω/ω_S, when taking into account the heat from the control q_n** . . . 71

6.1 **Representation of local laboratories operated by Alice and Bob** . . . 74
6.2 **Representation of local labs operated by Alice, Bob and Charlie** . . . 76
6.3 **The engine connecting uncertainty relations and the second law of thermodynamics** . . . 78
6.4 **Thermal lazy-guess your neighbour's input (TLGYNI) game played between Alice and Bob from the perspective of communicated and received states** . . . 84

A.1 **Circuit connection between quantum channels** . . . 100

List of Tables

5.1 **Post-measurement state and measurement probability for the states $|\pm\rangle_C$ in the limits of low/high temperature and $n \to \infty$** 58

6.1 **Summary of causal upper bounds and ICO violations for bipartite and tripartite systems** 76

Contents

List of Symbols & Abbreviations vii

List of Figures viii

List of Tables x

1 Introduction 1

2 Indefinite causal order 5
2.1 Key hypotheses of indefinite causal order . . . 6
2.2 An imagined scenario . . . 7
2.3 Operational description: process matrices . . . 9
2.3.1 Definition . . . 9
2.3.2 Characterization . . . 10
2.3.3 Causal non-separability . . . 12

3 Superposition of causal orders 14
3.1 Concept . . . 14
3.2 Controlled-superposition of causal orders: the quantum switch . . . 17
3.3 Non-violation of causal inequalities . . . 19
3.4 Experimental implementations . . . 21

4 Passive states activation using the quantum switch 25
4.1 Passive states in (quantum) thermodynamics . . . 26
4.2 The quantum switch alone is not a thermodynamic resource . . . 27
4.3 Conditions for activation using the quantum switch . . . 28
4.3.1 Without post-selection . . . 28
4.3.2 With post-selection . . . 29
4.4 Examples . . . 30
4.4.1 Two-level system (qubit) . . . 30
4.4.1.1 Rotation operators . . . 31
4.4.1.2 General $U(2)$ unitaries . . . 33
4.4.2 Quantum harmonic oscillator . . . 36
4.4.2.1 Displacement operators . . . 36
4.4.2.2 Displacement and squeeze operators . . . 39

5 Quantum switch with open control dynamics 47

5.1 Collisional model for open system dynamics . . . 48
5.1.1 First law of thermodynamics . . . 50
5.1.2 Second law of thermodynamics . . . 51
5.1.3 Energy-conserving interactions . . . 51
5.2 Quantum switch with an open control . . . 52
5.2.1 General evolution of the composite state . . . 54
5.2.2 Control post-selection . . . 55
5.3 Examples . . . 59
5.3.1 Monitoring of mutually-unbiased bases (MUBs) . . . 59
5.3.2 Quantum switch-based refrigerator . . . 64

6 Thermodynamics and causal inequalities 72
6.1 Causal inequalities . . . 73
6.2 Connecting the second law of thermodynamics and causal inequalities . . . 77
6.2.1 The idealized engine of Hänggi and Wehner . . . 77
6.2.2 The thermal lazy-guess your neighbour's input game . . . 81
6.2.3 Example . . . 90
6.2.3.1 Initial states well-defined . . . 90
6.2.3.2 Measurements well-defined . . . 92
6.3 Relation to already existing results and future directions . . . 93

7 Conclusion 96

A Choi-Jamiołkowski matrices 99

B Process matrix characterization 101

C Uncertainties 104
C.1 Alternative formulations of URs . . . 107
C.1.1 Entropic uncertainty relations (EURs) . . . 107
C.1.2 Fine-grained uncertainty relations (FGURs) . . . 108

Bibliography 110

Chapter 1

Introduction

"But how could you live and have no story to tell?"

— Fyodor Dostoevsky, White Nights.

The work of theoretical physics is to synthesize more and more natural phenomena into a single theoretical framework and hand to the experimentalist to test it, confirming it or not according to the outcomes of some experiment(s) in the laboratory or observations of some naturally occurring phenomenon. In the process, new phenomena can be discovered and the underlying theory expanded, or even completely reviewed, as it was the case when *quantum mechanics* (QM) came to light in the first half of the 20^{th} century. Indeed, even Albert Einstein (1879 – 1955) tried to formulate a *unified field theory* which would entail all the fundamental forces of physical nature then known (gravity and electromagnetism), however, he never came up with a consistent theory. Later on, many advances towards the goal of a "theory of everything" have been established: *quantum electrodynamics* (interaction between light and matter), *electroweak theory* (unification of electromagnetic and weak forces), *quantum chromodynamics* (quantum field theory of the strong force between gluons and quarks) and finally the *standard model of particle physics*, putting together in a single description the electroweak and strong interactions, plus the Higgs mechanism – responsible for giving mass to gauge bosons – and the Yukawa interaction – which then couples the Higgs field to fermions and render them mass. Gravity, the weakest of all forces, has not yet been included in the description. A quantum gravity (QG) theory, merging QM and *general relativity* (GR) is the Holy Grail of fundamental physics, and even though it has been developed for a long time, we still do not have a definite theory (the battle between *loop quantum gravity* and *string theory* is still ongoing) and even further away from an experimental confirmation, since the energy scales are huge compared to what our current technological capabilities can offer.

Thinking from a more conceptual and probabilistic perspective, Lucien Hardy almost twenty years ago (2005) proposed in Ref. [1] that a successful QG theory should have a *metric tensor* – the mathematical representation of spacetime – that is both dynamic and uncertain, or *indeterminate*, as requested by GR and QM, respectively. Some

years afterwards (2012), Ognyan Oreshkov, Fabio Costa and Časlav Brukner, used the work of Hardy as an inspiration for developing an operational framework for dealing with situations where the causal relations between laboratories are uncertain: the *process matrix formalism*. It consists of a generalization of the density matrix, capable of encoding in its structure the information that two or more parties do not have their causal relation on spacetime well defined. That is, these process matrices in general cannot be decomposed as convex combinations of causally-ordered processes (i.e. time-like and space-like separated events). By means of these process matrices which are *causally non-separable*, one can calculate probability distributions, which in turn might violate some special inequalities, known as *causal inequalities* (CIs). Important is the fact that not all process matrices having ICO in their structure can violate a CI. As a matter of fact, controlled-superposition of causal orders (cSCO), for which the *quantum switch* (QS) [2] is the most famous implementation, which are causally non-separable, were shown to not violate *any* CIs [3, 4]. In this endeavour, there is some analogy with separable and Bell-local states vs. entangled states in the context of quantum non-locality. Bell-local states do not violate any Bell inequality [5], but they are not separable [6]. The relationship between these quantities, ICO and quantum non-locality or quantum entanglement, is not yet fully understood and it is indeed a very interesting research topic.

In the last decade, a few experiments have claimed to implement ICO in its weaker form: the QS with two more gates in superposition [7–11]. Putting this together with the known task advantages of using the QS in the areas of quantum computation [7, 12, 13], quantum communications [14–16], quantum metrology [17] and quantum thermodynamics [10, 18–23], makes this specific implementation of ICO the most favored in current research. However, as previously said, this form of ICO does not violate any CI, thus, even though resourceful, they are limited. On the physicality of CI-violating ICO processes, Araújo *et al.* [24] *postulated* that not all process matrices are physical by means of a mathematical argument: if a process matrix is not purifiable, then isometries are not conserved by this particular process matrix. In their work they studied two cases, both violating a CI: the Oreshkov-Costa-Brukner (OCB) process matrix [25]), a two-party process matrix, which then would be non-physical and the the Bäumeler-Wolf (BW) process matrix [26]), a three-party process matrix, which according to their postulate is physical. An urgent question then arises: are there *physical* constraints for the existence of processes containing ICO that violate CIs? An interesting prospect is to put process matrices to the test of the *second law of thermodynamics* (SLT), one of the pillars of physics, classical and quantum. Recently, Gianluca Francica in Ref. [27] formulated a "game" of work extraction between two parties, which admits the implementation of process matrices connecting them. It was found that *no* ICO strategy can lead to more thermodynamic work being extracted than any definite order scenario. It is argued in this work that it would be a sign of compliance of (two-party) process matrices containing ICO with the SLT. Nonetheless, it is still an open question whether thermodynamics is indeed a physical limitation to the implementation of ICO processes that violate CIs. It is important to remark, though, that even in the case that thermodynamics does not impose constraints on ICO processes violating CIs, some other physicality condition might limit their existence (see for example Ref. [28]).

Given this open problem, the present thesis has as main goal investigating whether

two-party process matrices violating CIs are contrained by the SLT. We do so by combining the thermodynamic cycle of Esther Hänggi and Stephanie Wehner [29] with the *lazy guess your neighbour input* (LGYNI) game of Ref. [25], from which we get an *entropic uncertainty relation* (EUR) for the binary entropy functions of the probabilities of the game. We move forward to show that the SLT does not constrain any parameter of the bipartite process matrix in the LGYNI scenario. It does not matter if a given process matrix does not violate a CI or maximally violates it, like the OCB process matrix, the inequality is never surpassed, attesting that for two-party process matrices, thermodynamics *is not* a limiting feature. Nonetheless, our argument goes in line with what was presented in Ref. [27] and points out in the direction that, at least two-party process matrices, the SLT is not a physical constraint for process matrices violating CIs or any process matrix allowed by QM. As already said, this does not rule out other physical limitations [28] (also remember the postulate of Ref. [24]), which can possibly constrain what process matrices are indeed physical. In any case, this is out of the scope of this thesis, remaining as objective of further investigation. Moreover, from a more technical perspective, this thesis also presents other results concerning the QS in situations where thermodynamics is relevant. In the first, we show how the QS alone cannot activate *passive states* (i.e. states from which no work can be extracted with cyclic unitaries), it needs extra resources coming from the control degree-of-freedom (DOF), namely non-diagonal control Hamiltonian in the computational basis and state of the control containing coherences. In the case that we do not post-select (i.e. measure) the control in a coherent state, both requirements on the control DOF are needed, while for post-selection only the coherence in the initial state of the control really matters. We derive necessary, but not sufficient conditions for state activation for both cases. Moreover, we apply the framework to qubits and quantum harmonic oscillators, showing that state activation is very sensitive to both the initial state of the control and the measurement state. These results were already peer-reviewed and published [23]. Our work is a direct expansion of Ref. [20], in which the topic of state activation via the QS was first discussed. Lastly, we also present results concerning the situation in which, after applying the QS and before post-selection, the control DOF interacts with an environment in the *collisional model* formalism. We find an elegant analytical expression for the state system-control for an arbitrary number of collisions with a thermal environment (i.e. bath). Moreover, we arrive at the conclusion that the state used for the post-selection of the control has considerable importance, depending on the temperature regime. This result shows how unstable the QS is due to thermal fluctuations and by applying our model to the QS-based refrigerator of Felce *et al.* [18] and maps which implement monitoring of mutually-unbiased bases (MUBs), we present how useful it is to include open-system features into account. This work was published in *Communication Physics* [30]. Throughout the whole thesis, many definitions are repeated, in order to facilitate the life of the reader, which will not need to be coming back and forth through the chapters.

In Chapter 2, we start by discussing a bit of the philosophy behind ICO, its motivations and the problem that it aims to solve. In the same chapter, we present in detail what is a process matrix and characterize it, that is, show what is the structure that it must contain. In the sequence, in Chapter 3 we explain what is superposition of causal orders, both in its "pure" form and controlled one, focusing on the case of the QS. We argue briefly why the QS (and any other cSCO process) does not violate any CI. To conclude the chap-

ter, we describe selected experiments from the literature where the QS was implemented. Passing to Chapters 4 and 5, we discuss in detail the works of Refs. [23, 30] respectively. Both articles were peer-reviewed (the first published in Entropy and the second in Communication Physics) and I was their first author. In the first one, we study how the QS can be used to activate *passive states*, a particular problem within quantum thermodynamics. This was first carried out in Ref. [20], but our work goes beyond and presents a more complete survey of how the QS *alone* cannot activate passive states and what are the additional features that are needed for this goal. Moreover, we set very general initial and measurement states of the control, allowing for the search of the combinations that maximize work extraction if the state can be activated. Finally, we apply our model to different kinds of systems: (i) a two-level system (qubit), where the unitary operations are rotations around the Bloch sphere; and (ii) a quantum harmonic oscillator, with unitary operations being displacement and squeeze operators. In the second paper, we treat the situation in which the control degree-of-freedom (DOF) of the QS is subject to interaction with an environment, which is assumed to have a *collisional model* [31–40]. A general expression for the open system dynamics of the post-QS of the composite state system-control is derived, as well as general expressions for the state of the system post-measurement in the $\{|+\rangle_C, |-\rangle_C\}$ basis of the control. We study the behaviour of the "definite order" and "indefinite order" terms with number of collisions for the limits of high and low temperature of the environment, finding that the post-selection state has a considerable impact on how resilient the "indefinite order" terms are to decoherence. The framework is applied to two different cases: the QS-based quantum refrigerator of Ref. [18] and monitoring maps of *mutually-unbiased bases* (MUB). Finally, we pass to the results presented in Chapter 6, where we begin by discussing CIs, with examples for two (Alice and Bob) and three-party (Alice, Bob and Charlie) scenarios. With these in hands, we pass to the indication that the SLT does not constraint bipartite, two-dimensional process matrices. We say that it is an indication, because using a specific setup, based on the thermodynamic engine of Ref. [29], we are not able to violate the SLT of thermodynamics for any combination of parameters of the process matrix. This is a "negative" result, in the sense that we could not show that thermodynamics is a constraint for certain process matrices, but only in a specific case. This, of course, does not rule out violation of the SLT by some process matrix in another setup. Nevertheless, our result has the inherent value of showing a setup in which there is no contradiction between the SLT and bipartite, two-dimensional process matrices, and whoever looks for violations of the SLT from now on should search somewhere else. Except for where some order of magnitude analysis is done, units are such that $\hbar = k_B = 1$.

In the end, we pass to the Conclusion. There we sum up all the discussions developed in this thesis. We give special focus to the findings of Chapter 6, as they present a partial answer to the question of physical constraints to ICO. The other results are commented in a resumed way, where the importance of each one is pointed out. As a last discussion, we talk about future directions that the studies presented in this thesis can lead to, for instance expanding the analysis to higher number of parties and higher dimensions.

Chapter 2

Indefinite causal order

> *"Science cannot solve the ultimate mystery of nature. And that is because, in the last analysis, we ourselves are a part of the mystery that we are trying to solve."*
>
> — Max Planck.

Understanding physical nature and predicting its behaviour has been the main goal of modern physics, both for philosophical and technological reasons. While *quantum mechanics* (QM) has been a successful theory, in the sense that it explains with good precision physical phenomena in the scale of an atom (and below) and has been used for cutting edge technologies[1], it still has unresolved questions: (i) it lacks a physical explanation for entanglement; (ii) the measurement problem; (iii) the interpretation problem, that is, if the Copenhagen interpretation of quantum mechanics or another (of many) is more suited [41]; and (iv) the ontological issue, i.e. if the quantum state has a real physical meaning. A few of these issues are discussed in Ref. [42]. Nonetheless, it is still the best available physical description of very small systems, either moving "slowly" – non-relativistic QM – or "fast" – relativistic QM or *quantum field theory* (QFT). On the other side of the spectrum of physical theories, one has *general relativity* (GR), a classical theory that is the one that most-accurately describes gravity and very massive objects, such as black holes, stars and galaxies. Apart from its success through the decades, especially in the fields of cosmology and astrophysics, but also to some degree in technology (e.g. global positioning system, GPS), it fails to account for *dark matter* and *dark energy*, postulated entities to fit observation data from cosmological bodies (e.g. supernovae). For dealing with discrepancies, new theories have been proposed (see Ref. [43] for a review), which to this day have not yet been successful in superseding GR. In any case, even though these theories have their limitations, we take them as the best so far and set them as the basis for a successful future theory that describes phenomena from the very small to the very large and from the very slow to the very fast.

For a long time, scientists have tried to merge QM and GR into one theory, generi-

[1] The "first quantum revolution" brought the development of lasers, transistor electronics and atomic clocks. The "second quantum revolution" promises even more striking technologies: quantum computation, quantum metrology, quantum communications and quantum cryptography.

cally called *quantum gravity* (QG). To this day, only static approximations were achieved, such as *QFT in curved spacetime*. Except for *string theory*, which poses a complete new physical paradigm, QG theories normally try to *quantize* gravity, that is, apply a quantization procedure (e.g. canonical quantization, path integrals) to the gravitational field, represented in GR by the *metric tensor* $g_{\mu\nu}(x^\mu)$ (μ and ν are the indices of the tensor, and x^μ are the spacetime coordinates). Considerable problems arise in this endeavour. First, naive quantization of the metric tensor leads to non-renormalizable quantum fields [44]. Second, the scale in which genuine quantum gravity effects are expected to happen is prohibitive for any conceivable experiments. To have a grasp of the quantities, consider the *Planck length*, where quantum gravity effects are considerable:

$$l_P := \sqrt{\frac{\hbar G}{c^3}} \sim 1.616 \times 10^{-35}\,\mathrm{m}, \tag{2.1}$$

where $\hbar = h/2\pi$ is the reduced Planck constant, G is the gravitational constant and c is the speed of light in vacuum. Moreover, the *Planck mass* is:

$$m_P := \frac{\hbar}{l_p\, c} \sim 1.22 \times 10^{19}\ \mathrm{GeV} \cdot \mathrm{c}^{-2}. \tag{2.2}$$

This mass scale is 10^{19} times higher than the proton mass and more than 10^{15} times higher than the maximum collision energy of the Large Hadron Collider (LHC), the state-of-the-art when it comes to particle colliders. This means that one would need to build a collider with dimensions of a *galaxy* to observe particles at this scale (i.e. *gravitons*, the theorized QG particles). Evidently, this is completely out of question [45]. As physics needs to be experimentally tested, this is very frustrating for anyone that is willing to see this problem solved. Nonetheless, recent developments on *table-top quantum gravity experiments* [46], in which non-gravitational systems containing some sufficient amount of entanglement may express quantum gravity effects, as shown by the *holographic principle* and the anti-de Sitter/conformal field theory (AdS/CFT) correspondence, give hope to those that are eager to see in the near future experimental tests of QG.

2.1 Key hypotheses of indefinite causal order

Not diving inside the "hardcore" physics of QG, one is still able to wonder what characteristics a successful QG theory would have. As proposed by Lucien Hardy [1], a QG theory consistent with both QM and GR should:

- Have a *dynamical* metric tensor, that is, it evolves following a dynamical equation, in this case the Einstein's equations (consistency with GR);
- Contain some sort of uncertainty in the metric tensor, which, before any measurement is performed, has no deterministic value, therefore the metric has a *probabilistic behaviour* (consistency with QM).

Thus, as the *causal structure* between events on spacetime is determined by the metric, which tells us what is time-like and space-like separated, if it contains some degree of uncertainty in the sense of pre-measurement indeterminacy, then the causal structure itself is undetermined, what is called in the literature *indefinite causal order* (ICO). Following these assumptions, Ognyan Oreshkov, Fabio Costa and Časlav Brukner showed in

Ref. [25] that for definite causal structure, i.e. events are time-like or space-like separated, or a probabilistic combination of them, there exists an upper bound for the "success probability" of a game played between two parties, where locally QM holds for each one. Here one has what is called a *causal inequality* (CI), which will be key for the main result of this thesis in Chapter 6. By introducing a mathematical object known as the *process matrix* (more details in Section 2.3), a generalization of the density matrix, they showed that the upper bound can be violated for a specific process matrix that does not admit a decomposition into a convex combination of causally-ordered terms. This "non-decomposability" is known in the literature as *causal non-separability*. This opened a path of investigation focused on an operational description of physical phenomena that supposedly a true QG theory could explain the mechanism. The main object of study of this operational description is the calculation of probabilities which form a specific CI, whose bound sets the emergence of a new resource to be used for some task. It has many analogies with *quantum non-locality*, in the sense that it deals with probabilities that cannot be generated by some other theory, i.e. local hidden-variable theories. This relationship is briefly discussed in Chapter 6.

In this chapter, we start with an imagined scenario in which causal non-separability could be found in nature (Section 2.2). Also, we define what are process matrices (Section 2.3.1), we characterize them (Section 2.3.2) and explain what is causal non-separability (Section 2.3.3). The main goal of this chapter is to didactically introduce the concept of ICO and how operational (probabilistic) calculations can be done through process matrices. In the next chapters, we shall look at specific characteristics of ICO and how it relates to thermodynamics from different perspectives.

2.2 An imagined scenario

We make now a hypothesis exercise[2]. Check Fig. 2.1 for a schematic representation of the scenario described below. Imagine that some region of spacetime (more formally, a *Lorentzian manifold* $\mathfrak{M}$) has a metric tensor $g^{(1)}_{\mu\nu}(x^\mu)$, which is subject to Einstein's equations of GR, i.e. it is dynamic. Now, assume that there exists some Hilbert space $\mathcal{H}$ in which a ket state $|g^{(1)}_{\mu\nu}(x^\mu)\rangle$ has a one-to-one correspondence to the metric tensor $g^{(1)}_{\mu\nu}(x^\mu)$ (isomorphism) (for a recent and more rigorous treatment, check Ref. [47]). This metric tensor defines at each point the *light-cone*, which is determinant to say if two events on this manifold are space-like or time-like separated. On the other hand, the same cut of spacetime could have another metric tensor $g^{(2)}_{\mu\nu}(x^\mu)$. In fact, since dynamic metric is assumed, there can be a continuous transformation from one metric tensor to the second. The $g^{(2)}_{\mu\nu}(x^\mu)$ metric, in its turn, also has an isomorphic ket state in $\mathcal{H}$: $|g^{(2)}_{\mu\nu}(x^\mu)\rangle$. Since $\mathcal{H}$ is a complex vector space, the ket state

$$|g^{(3)}_{\mu\nu}(x^\mu)\rangle = \alpha|g^{(1)}_{\mu\nu}(x^\mu)\rangle + \beta\,|g^{(2)}_{\mu\nu}(x^\mu)\rangle, \tag{2.3}$$

with $\alpha, \beta \in \mathbb{C}$, is also a valid ket state. This is indeed the *superposition principle* applied to the metric tensors in this isomorphism framework. The state from Eq. (2.3) contains un-

[2]Based on Časlav Brukner's presentation during the 1st in-person meeting of the INAQT (International Network for Acausal Quantum Technologies) Network, Glasgow (Scotland, United Kingdom). January 23–25, 2023.

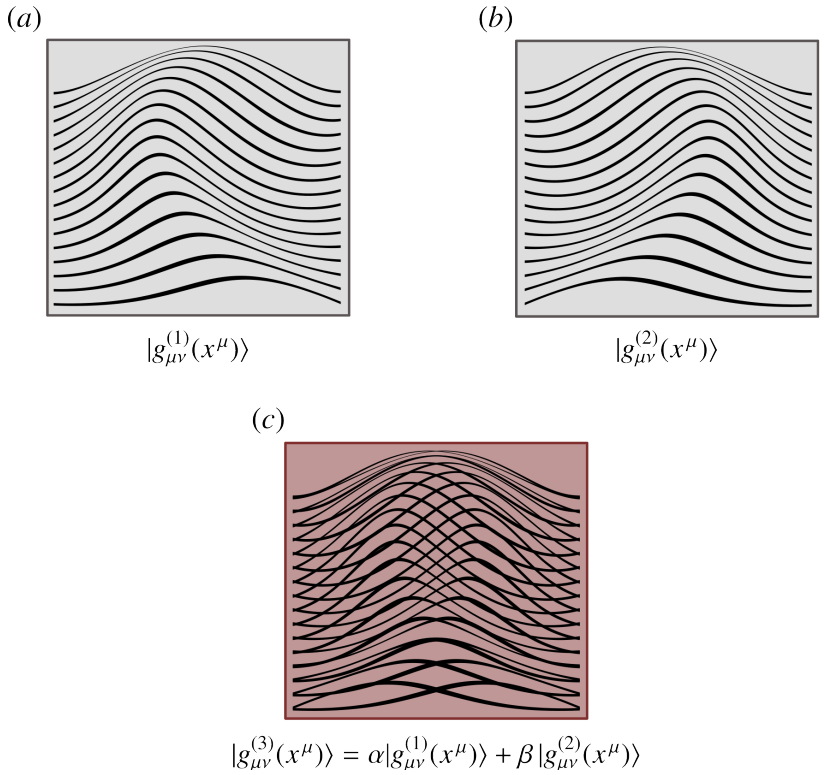

Figure 2.1: **Scheme of what an indefinite causal order would look like from a superposition perspective.** (a) Some region of spacetime is well described by a metric tensor $g^{(1)}_{\mu\nu}(x^\mu)$. Assuming that there is some quantum state that incorporates this information, we call it $|g^{(1)}_{\mu\nu}(x^\mu)\rangle$. (b) The same region might assume another metric configuration, whose ket state is $|g^{(2)}_{\mu\nu}(x^\mu)\rangle$. (c) Quantum states admit superposition, therefore the metric states could coherently form a "superposed" metric state $|g^{(3)}_{\mu\nu}(x^\mu)\rangle = \alpha|g^{(1)}_{\mu\nu}(x^\mu)\rangle + \beta\,|g^{(2)}_{\mu\nu}(x^\mu)\rangle$.

certainty, in the sense that it has a probability $|\alpha|^2$ to be in $|g^{(1)}_{\mu\nu}(x^\mu)\rangle$ and a probability $|\beta|^2$ to be in $|g^{(2)}_{\mu\nu}(x^\mu)\rangle$. Moreover, there are "interference" terms $\alpha\beta^*$ and $\alpha^*\beta$ that appear relative to other bases, such as $\{|g^{(+)}_{\mu\nu}(x^\mu)\rangle, |g^{(-)}_{\mu\nu}(x^\mu)\rangle\}$, with $|g^{(\pm)}_{\mu\nu}(x^\mu)\rangle := (|g^{(1)}_{\mu\nu}(x^\mu)\rangle + |g^{(2)}_{\mu\nu}(x^\mu)\rangle)/\sqrt{2}$. The indeterminacy of which metric tensor connects the points on spacetime may lead to ICO, in the sense that there is some coherent superposition of causally-ordered events, such as event A being in the past of event B, and vice-versa (other combinations are also possible, such as time-like and space-like separated events). Clearly, such a situation cannot be decomposed as a convex combination of terms with well-defined causal structure.

The above imagined scenario does not explain itself: first, we are far from actually knowing if there is such a thing as isomorphism between the manifold where metric tensors live and some Hilbert space $\mathcal{H}$; second, the physics behind superposition of metric tensors is not defined, even though there can be some speculation about singularities of spacetime, such as black holes, where the QM *and* GR are expected to "merge". To solve the first point, one would probably need to go the hard path of stating axioms and building from first principle a whole new theory of QG, which brings us to the problems aforementioned. While a solution to the second one demands a great deal of imagination and speculation, which might of course be done through exhaustive collection of outer space observations (e.g. black holes and gravitational waves) and table-top experiments,

as proposed in Ref. [46]. Nonetheless, it is important to some degree to use imagination when trying to understand physical phenomena, as it can lead us on a path not previously imagined[3]. In the following section, we present the operational framework that will be used for dealing with ICO, the *process matrix formalism*.

2.3 Operational description: process matrices

In this section, the main operational tool for ICO is treated: the process matrix formalism. We define it mathematically (Section 2.3.1), characterize it (Section 2.3.2) and discuss formally what we mean by causal non-separability (Section 2.3.3).

2.3.1 Definition

Imagine that two parties, Alice and Bob, dispose of *quantum instruments* $\mathcal{M}_x^{\text{Alice}}$ and $\mathcal{M}_y^{\text{Bob}}$, respectively, where x, y are encoding variables. Their input (output) Hilbert spaces are $\mathcal{H}_{A_{I(O)}}$ and $\mathcal{H}_{B_{I(O)}}$. Quantum instruments are completely positive (CP), but *not* trace-preserving maps, meaning that,

$$\text{tr}\left\{\mathcal{M}_{x(y)}^{\text{Alice(Bob)}}(\rho)\right\} < 1, \qquad \forall \rho \in \text{D}\left(\mathcal{H}_{A_I(B_I)}\right), \tag{2.4}$$

where $\text{tr}\{O\}$ denotes the trace over the operator O. Of course, if we sum over the variables x and y, the trace is preserved and we have completely positive trace-preserving (CPTP) maps:

$$\sum_x \text{tr}\left\{\mathcal{M}_x^{\text{Alice}}(\rho)\right\} = \sum_y \text{tr}\left\{\mathcal{M}_y^{\text{Bob}}(\rho)\right\} = 1, \qquad \forall \rho \in \text{D}(\mathcal{H}_{A_I(B_I)}). \tag{2.5}$$

Now, assume that there is a bi-linear function ω, which takes as inputs two quantum instruments and outputs a probability $P(x, y)$:

$$\omega\left(\mathcal{M}_x^{\text{Alice}}, \mathcal{M}_y^{\text{Bob}}\right) = P(x, y). \tag{2.6}$$

Taking into account the Choi-Jamiołkowski (CJ) isomorphism (see Appendix A), quantum instruments can be written as matrices, such that:

$$\mathcal{M}_x^{\text{Alice}} \leftrightarrow M_x^{\text{Alice}} \in \mathcal{L}(\mathcal{H}_{A_I} \otimes \mathcal{H}_{A_O}), \tag{2.7}$$

and

$$\mathcal{M}_y^{\text{Bob}} \leftrightarrow M_y^{\text{Bob}} \in \mathcal{L}(\mathcal{H}_{B_I} \otimes \mathcal{H}_{B_O}), \tag{2.8}$$

known as *CJ matrices*. Therefore, the bi-linear function ω on quantum instruments can be rewritten as a bi-linear function $\tilde{\omega}$ on CJ matrices:

$$P(x, y) = \omega\left(\mathcal{M}_x^{\text{Alice}}, \mathcal{M}_y^{\text{Bob}}\right) = \tilde{\omega}\left(M_x^{\text{Alice}}, M_y^{\text{Bob}}\right), \tag{2.9}$$

where

$$\tilde{\omega} : \mathcal{L}(\mathcal{H}_{A_I} \otimes \mathcal{H}_{A_O}) \times \mathcal{L}(\mathcal{H}_{B_I} \otimes \mathcal{H}_{B_O}) \to \mathbb{R}, \tag{2.10}$$

[3] As a matter of fact, imagination was crucial for Albert Einstein when developing both his special and general theories of relativity. Of course, a great deal of complex calculations were needed, but the initial spark came from mental exercises.

with $\times$ denoting the Cartesian product. Moreover, a bi-linear function acting on the Cartesian product of vector spaces $V_A \times V_B$ is isomorphic to a linear function on the tensor product of the same vector spaces $V_A \otimes V_B$ [25]. Putting this together with the *Hilbert-Schmidt scalar product*, there is an isomorphism that allows us to write:

$$P(x,y) = \mathrm{tr}\left\{W\left(M_x^{\mathrm{Alice}} \otimes M_y^{\mathrm{Bob}}\right)\right\}, \tag{2.11}$$

where

$$W \in \mathcal{L}(\mathcal{H}_{A_I} \otimes \mathcal{H}_{A_O} \otimes \mathcal{H}_{B_I} \otimes \mathcal{H}_{B_O}), \tag{2.12}$$

is the so-called *process matrix*. A process matrix is represented schematically as shown in Fig. 2.2. It is a monolithic block that contains some inner structure, depending on the specific case. The general form of W will be determined in Section 2.3.2.

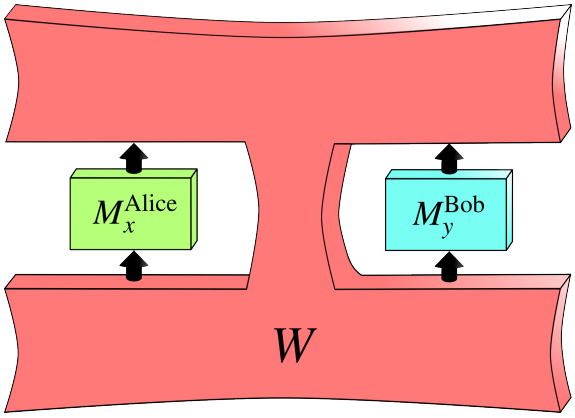

Figure 2.2: **Scheme of a process matrix W acting on two Choi-Jamiołkowski (CJ) matrices M_x^{Alice} and M_y^{Alice}.** The process matrix W connects the CJ matrices in some general fashion, which might express indefinite causal order (ICO) in the final probability distribution $P(x,y)$.

Remarkably, the concept of process matrix can be expanded to the case where there is a "global" past P_G and a "global" future F_G. In this case [48]:

$$M_{x,y}^{W} = \mathrm{tr}_{A_I A_O B_I B_O}\left\{W_{\mathrm{ext}}\left(\mathbb{1}_{P_G} \otimes M_x^{\mathrm{Alice}} \otimes M_y^{\mathrm{Bob}} \otimes \mathbb{1}_{F_G}\right)\right\}, \tag{2.13}$$

is the CJ matrix of the *quantum supermap* $\mathcal{M}_{x,y}^{W}(\rho_{P_G}) = \rho_{F_G}(x,y)$ taking a state ρ_{P_G} in the global past and mapping it to a non-normalized state $\rho_{F_G}(x,y)$ in the global future. The process matrix W_{ext} is an extended process matrix living in $\mathcal{L}(\mathcal{H}_{P_G} \otimes \mathcal{H}_{A_I} \otimes \mathcal{H}_{A_O} \otimes \mathcal{H}_{B_I} \otimes \mathcal{H}_{B_O} \otimes \mathcal{H}_{F_G})$. In the above equation, $\mathbb{1}_X$ is the identity operator in $\mathcal{L}(\mathcal{H}_X)$ and $\mathrm{tr}_X\{O\}$ denotes the partial trace of operator O over the subsystem X.

2.3.2 Characterization

We need to guarantee that the probabilities $P(x,y)$ are non-negative for any positive semi-definite input CJ matrices:

$$\mathrm{tr}\left\{W\left(M_x^{\mathrm{Alice}} \otimes M_y^{\mathrm{Bob}}\right)\right\} \geqslant 0, \qquad \forall M_x^{\mathrm{Alice}}, M_y^{\mathrm{Bob}} \succeq 0, \tag{2.14}$$

with ≥ 0 denoting that the matrix is positive semi-definite. Also, in the case that the parties share some quantum state ρ_{shared} in $\mathrm{D}(\mathcal{H}_{A_I'B_I'})$, which can even be entangled, the extended process matrix $W' = \rho_{\text{shared}} \otimes W$ should fulfill[4]:

$$\mathrm{tr}\left\{W'\left(M_x^{\text{Alice'}} \otimes M_y^{\text{Bob'}}\right)\right\} \geqslant 0, \qquad \forall M_x^{\text{Alice'}}, M_y^{\text{Bob'}} \geq 0, \tag{2.15}$$

where $M_x^{\text{Alice'}}$ and $M_y^{\text{Bob'}}$ are the CJ matrices of the extended quantum instruments. The two previous conditions together imply that W itself is positive semi-definite [49]:

$$W \geq 0. \tag{2.16}$$

By noticing that summing over the indices of quantum instruments gives us CPTP maps,

$$\mathcal{M}^{\text{Alice}} := \sum_x \mathcal{M}_x^{\text{Alice}}, \qquad \mathcal{M}^{\text{Bob}} := \sum_y \mathcal{M}_y^{\text{Bob}}, \tag{2.17}$$

whose CJ matrices M^{Alice} and M^{Bob} must fulfill

$$\mathrm{tr}_{A_O}\left\{M^{\text{Alice}}\right\} = \mathbb{1}_{A_I}, \qquad \mathrm{tr}_{B_O}\left\{M^{\text{Bob}}\right\} = \mathbb{1}_{B_I}, \tag{2.18}$$

one has that:

$$\begin{aligned} \mathrm{tr}\left\{W\left(M^{\text{Alice}} \otimes M^{\text{Bob}}\right)\right\} &= \sum_{x,y} \mathrm{tr}\left\{W\left(M_x^{\text{Alice}} \otimes M_y^{\text{Bob}}\right)\right\} \\ &= \sum_{x,y} P(x,y) \\ &\equiv 1, \end{aligned} \tag{2.19}$$

for any pairs of CPTP maps $\mathcal{M}^{\text{Alice}}$ and $\mathcal{M}^{\text{Bob}}$.

We move further and derive the necessary and sufficient conditions for W to fulfill the above conditions [25] (details are presented in Appendix B). The most general form of a two-party process matrix is:

$$W = \frac{1}{d_{A_I} d_{B_I}} \left(\mathbb{1}_{A_I A_O B_I B_O} + \xi_{B\to A} + \xi_{A\to B} + \xi_{A\leftrightarrow B}\right), \tag{2.20}$$

where $\mathbb{1}_{A_I A_O B_I B_O} := \mathbb{1}_{A_I} \otimes \mathbb{1}_{A_O} \otimes \mathbb{1}_{B_I} \otimes \mathbb{1}_{B_O}$ and

$$\xi_{B\to A} := \sum_{i,j>0} a_{ij} \left(\xi_i^{A_I} \otimes \mathbb{1}_{A_O} \otimes \mathbb{1}_{B_I} \otimes \xi_j^{B_O}\right) + \sum_{i,j,k>0} b_{ijk} \left(\xi_i^{A_I} \otimes \mathbb{1}_{A_O} \otimes \xi_j^{B_I} \otimes \xi_k^{B_O}\right), \tag{2.21}$$

$$\xi_{A\to B} := \sum_{i,j>0} c_{ij} \left(\mathbb{1}_{A_I} \otimes \xi_i^{A_O} \otimes \xi_j^{B_I} \otimes \mathbb{1}_{B_O}\right) + \sum_{i,j,k>0} d_{ijk} \left(\xi_i^{A_I} \otimes \xi_j^{A_O} \otimes \xi_k^{B_I} \otimes \mathbb{1}_{B_I}\right), \tag{2.22}$$

$$\begin{aligned} \xi_{A\leftrightarrow B} := &\sum_{i>0} e_i \left(\xi_i^{A_I} \otimes \mathbb{1}_{A_O} \otimes \mathbb{1}_{B_I} \otimes \mathbb{1}_{B_O}\right) + \sum_{i>0} f_i \left(\mathbb{1}_{A_I} \otimes \mathbb{1}_{A_O} \otimes \xi_i^{B_I} \otimes \mathbb{1}_{B_O}\right) \\ &+ \sum_{i,j>0} g_{ij} \left(\xi_i^{A_I} \otimes \mathbb{1}_{A_O} \otimes \xi_j^{B_I} \otimes \mathbb{1}_{B_O}\right), \end{aligned} \tag{2.23}$$

[4]For simplicity, we assume that the shared quantum state is measured and thrown away. It could be post-processed afterwards, but as noted in Ref. [25], it does not influence the characterization of W.

with $a_{ij}, b_{ijk}, c_{ij}, d_{ijk}, e_i, f_i, g_{ij} \in \mathbb{R}$ and d_X is the dimension of Hilbert space $\mathcal{H}_X$. All terms in Eq. (2.20) have a straightforward interpretation. First, the identity operator $\mathbb{1}_{A_I A_O B_I B_O}$ is such that:

$$\begin{aligned} \mathrm{tr}\{W\} &= \frac{\mathrm{tr}\{\mathbb{1}_{A_I A_O B_I B_O}\}}{d_{A_I} d_{B_I}} \\ &= d_{A_O} d_{B_O}, \end{aligned} \tag{2.24}$$

which guarantees probability normalization. Second, Eq. (2.21) contains terms connecting causally the output of Bob to the input of Alice: the first is simply a channel connection from B to A, while the second is a channel *with memory*. Third, in Eq. (2.22) we have the other way around, the same type of terms, but with the opposite order: from Alice to Bob. Fourth, in Eq. (2.23) there are terms that do not connect causally Alice and Bob (local and bi-partite state preparation), thus are related to when they are spatially separated. At all times, only *uni-directional signalling* was assumed, that is, at one time just one of the parties is sending information to their partner.

2.3.3 Causal non-separability

From Eq. (2.20), it is clear that in general one cannot write any process matrix as a convex combination of causally-ordered terms, that is:

$$W \neq \lambda\, W_{A\to B} + (1-\lambda)\, W_{B\to A}, \qquad \text{in general} \tag{2.25}$$

where $\lambda \in [0,1]$ and $W_{A\to B}$ ($W_{B\to A}$) is the causally-ordered process matrix from A (B) to B (A). A process matrix W that follows the relation of Eq. (2.25) is said to be *causally non-separable* [3, 25, 50, 51]. This is considered to be the main indicator if a process matrix contains ICO. It is important to note that, not all causally non-separable processes can be put together in the same category. As it will be shown in Chapter 6, an important element for studying ICO is what is called *causal inequality* (CI). These are constructed from probability distributions and can only be violated when causality is a priori undefined. The problem is that not all processes that are causally non-separable can violate a CI. As a matter of fact, a special kind of ICO, called *controlled-superposition of causal order* (cSCO) has causally non-separable process matrix, but does not violate *any* CI [3, 4]. The Oreshkov-Costa-Brukner (OCB) process matrix [25], on the other hand, is causally non-separable *and* violates a CI. The main groups of process matrices are organized in a diagram in Fig. 2.3.

Here an interesting analogy is found with the case of separable and Bell-local states vs. entangled states. For instance, a bi-partite density matrix ρ_{AB} is said to be separable if:

$$\rho_{AB} = \sum_{\lambda} P(\lambda)\, \rho_A(\lambda) \otimes \rho_B(\lambda), \tag{2.26}$$

where $P(\lambda)$ is some probability distribution over the variable λ and $\rho_{A(B)}(\lambda)$ is a local density matrix living in $\mathrm{D}(\mathcal{H}_{A(B)})$. States like the one in Eq. (2.26) are always Bell-local, but the opposite is not true [6]. So, even though both do not violate a Bell inequality, they have an important difference in that regard. Entangled states, of course, cannot be decomposed as Eq. (2.26) and they violate a Bell inequality. We are going to discuss more on this analogy in Chapter 6.

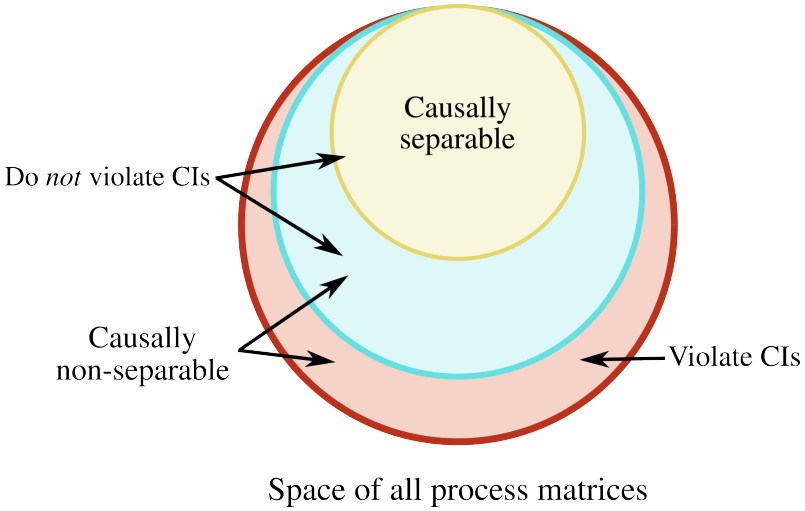

Figure 2.3: **Diagram presenting the main groups of process matrices according to causal non-separability and violation of causal inequalities.** According to Eq. (2.20), the most general process matrices are not causally separable. There are two different groups inside this category: those that violate causal inequalities (CIs) and those that do not violate them. Finally, the most restrict group is of those process matrices which are causally separable and of course do not violate CIs as well.

In this chapter, we presented the main assumptions behind the concept of ICO: dynamic and uncertain metric tensor. We also discussed what is the main motivation for studying this topic, that is, establishing a operational framework which would correspond to probabilities calculated within a successful QG theory. Moreover, an intellectual exercise was given, which provides some reasoning behind the possibility of ICO in a physical scenario. Finally, the main instrument for studying ICO, the process matrix formalism, was defined, characterized and used for defining causal non-separability. In Chapter 6, we shall introduce and discuss what are causal inequalities, which are crucial for showing that in a specific setup, based on the thermodynamic engine of Ref. [29], thermodynamics is not a physical constraint for bipartite, two-dimensional process matrices. This is not, however, a general proof, but it serves as an indication that maybe the second law of thermodynamics is not violated by any bipartite, two-dimensional process matrix.

Chapter 3

Superposition of causal orders

"Thoroughly conscious ignorance is the prelude to every real advance in science."

—James Clerk Maxwell.

In Chapter 2, the fundamentals of indefinite causal order (ICO) were presented: its main motivation and characterisation based on causal non-separability. As noted in the same chapter, one way of looking at ICO is through some sort of "higher-level superposition", for example, superposition of metric tensors. On the quantum channel level, one can assume the existence of superposition of the order of application of two or more quantum channels, something called *superposition of causal orders* (SCO). Historically speaking, the first paper that we know that considered superposing time-evolutions was Ref. [52]. Moreover, when it comes to *causal inequalities* (CIs) [25, 26, 50, 53–55] there are processes that even though are represented by a causally non-separable process matrix, *do not* violate *any* CI (more details about CIs in Chapter 6). These processes can be represented as quantum circuits, in contrast to other "stronger" processes, like the Oreshkov-Costa-Brukner (OCB) process [25], which has no circuit representation. The non-separable processes that do not violate CIs that are known fall in the category of SCO with an extra degree-of-freedom, called the *control*. These processes shall be called *controlled-SCO* or cSCO. In this Chapter, the concept of SCO is discussed (Section 3.1), together with the controlled case known in the literature as the *quantum switch* (QS) [12] (Section 3.2). Moreover, we show how these processes cannot violate CIs (Section 3.3). Finally, in recent years cSCO processes have been implemented in the laboratory, hence we present in Section 3.4 a few examples from the literature.

3.1 Concept

Quantum coherence [56–61] is a very useful resource in quantum information technologies and is a characteristic feature of quantum mechanics itself. It stems from *quantum superposition*, which states that the sum of quantum states with complex phases mul-

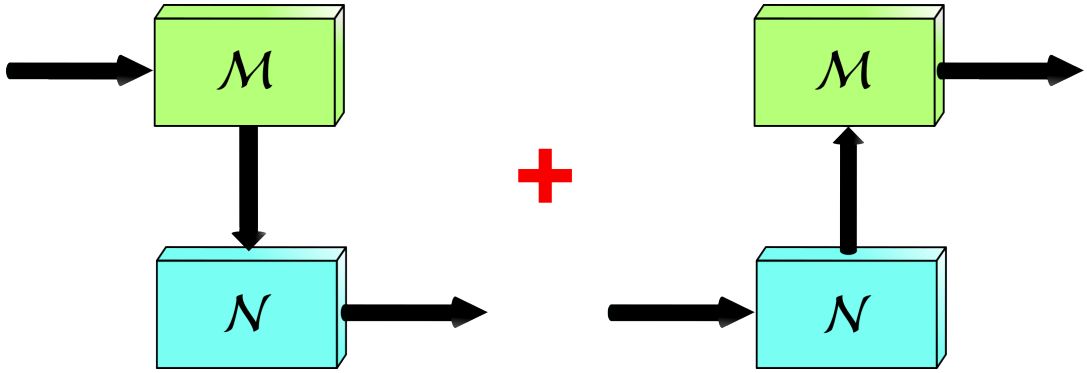

Figure 3.1: **Generic representation of superposition of causal orders (SCO) for two quantum channels.** The simplest case of SCO is when the order of application of two quantum channels $\mathcal{M}$ and $\mathcal{N}$ is put in superposition, in analogy with superposition of quantum states.

tiplied by them is still a valid quantum state. That is, given two states $|\psi_1\rangle$ and $|\psi_2\rangle$ in the Hilbert space $\mathcal{H}$, the state

$$|\Psi\rangle = \alpha|\psi_1\rangle + \beta\,|\psi_2\rangle, \tag{3.1}$$

where $\alpha, \beta \in \mathbb{C}$ are complex numbers satisfying $|\alpha|^2 + |\beta|^2 = 1$, is also a quantum state in $\mathcal{H}$. The density operator representing this new state,

$$\begin{aligned} \rho &= |\Psi\rangle\langle\Psi| \\ &= |\alpha|^2|\psi_1\rangle\langle\psi_1| + |\beta|^2|\psi_2\rangle\langle\psi_2| + \alpha\beta^*|\psi_1\rangle\langle\psi_2| + \alpha^*\beta|\psi_2\rangle\langle\psi_1|, \end{aligned} \tag{3.2}$$

where * denotes complex conjugation, contains *populations*, the first two terms in the right-hand-side (RHS), and quantum coherences, the last two terms in the RHS. Thus, the linearity of quantum theory, represented by quantum superposition, is in the very heart of quantum coherence.

Given that superposition of quantum states exists and is well known, would it also be true for the order in which quantum channels are applied to some system? After all, we know from the Choi-Jamiołkowski isomorphism [62, 63] that states and channels are intimately connected. We then expect that somehow we can "sum" two[1] different orderings of quantum channels $\mathcal{M}$ and $\mathcal{N}$ to get a new quantum channel (see Fig. 3.1). Such a superposition, dubbed SCO, would produce off-diagonal terms that have analogy with quantum coherence present in quantum states. Interestingly, SCO contains *causal non-separability* (defined in Chapter 2), i.e. their process matrix W *cannot* be decomposed as a convex sum of causally ordered applications of the channels. In our two channel case:

$$W \neq \lambda\, W_{\mathcal{M}\to\mathcal{N}} + (1-\lambda)\, W_{\mathcal{N}\to\mathcal{M}}, \tag{3.3}$$

where $\lambda \in [0,1]$ is a probability, $W_{\mathcal{M}\to\mathcal{N}}$ is the process matrix for applying first quantum channel $\mathcal{M}$ then $\mathcal{N}$, and $W_{\mathcal{N}\to\mathcal{M}}$ is the process matrix for the opposite order.

Remarkably, in Ref. [64] the author showed that the existence of "pure" SCO is very constrained. By "pure", we mean superposition of quantum channels without the

[1] This can be extended to an arbitrarily large number N of quantum channels and their $N!$ orderings.

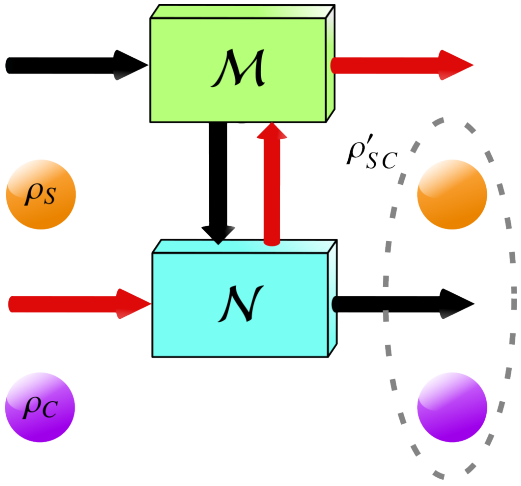

Figure 3.2: **Generic representation of controlled superposition of causal orders (cSCO) for two quantum channels.** A control C degree-of-freedom (DOF) sets the order in which two quantum channels $\mathcal{M}$ and $\mathcal{N}$ are applied to a target quantum system in state ρ_S (black and red paths). If the initial state of the control ρ_C is a coherent state, we expect that the order in which $\mathcal{M}$ and $\mathcal{N}$ happen will be in superposition (initially system and control are uncorrelated $\rho_S \otimes \rho_C$). The final composite state system-control ρ'_{SC} is then a correlated state.

help of an auxiliary system, known in the literature as the *control* C. The state of the latter is what determines the ordering of quantum channels, therefore, if it is prepared in a coherent state, this will ensure SCO. In Fig. 3.2 we show schematically how this works. An extra degree-of-freedom (DOF), called the control C, sets the order in which two quantum channels are applied to a target quantum system ρ_S. For some basis, one state of C gives first $\mathcal{M}$ then $\mathcal{N}$, while for the other state of the basis we have first $\mathcal{N}$ and then $\mathcal{M}$. Initially, system and control are uncorrelated $\rho_S \otimes \rho_C$, so that, if the control is in some coherent state, which comes from superposition of the basis states, this will result in a correlated final state ρ'_{SC}, that in its turn has coherence on the side of the system. To have a better idea of how it works from a mathematical perspective, consider that the quantum channels $\mathcal{M}$ and $\mathcal{N}$ have Kraus operators $\{M_i\}_{i=0,\dots,d_S-1}$ and $\{N_i\}_{i=0,\dots,d_S-1}$, respectively ($d_S = \dim(\mathcal{H}_S)$ is the dimension of the Hilbert space $\mathcal{H}_S$ of the system)[2]. Then, we can define the controlled Kraus operators K_{ij}:

$$K_{ij} = M_i N_j \otimes |\psi_1\rangle\langle\psi_1|_C + N_j M_i \otimes |\psi_2\rangle\langle\psi_2|_C, \tag{3.4}$$

where $\{|\psi_1\rangle_C, |\psi_2\rangle_C\}$ forms a basis in the Hilbert space $\mathcal{H}_C$ of the control. Thus, the final composite state system-control after applying the controlled Kraus operators is:

$$\rho'_{SC} = \sum_{i,j=0}^{d_S-1} K_{ij}(\rho_S \otimes \rho_C)K_{ij}^\dagger, \tag{3.5}$$

[2]Being Kraus operators of a completely positive trace-preserving (CPTP) map, these satisfy $\sum_i M_i^\dagger M_i = \mathbb{1}$ and $\sum_i N_i^\dagger N_i = \mathbb{1}$.

which, for some initial pure state $|\Psi\rangle_C = \alpha|\psi_1\rangle_C + \beta|\psi_2\rangle_C$ of the control, becomes:

$$\begin{aligned}\rho'_{SC} = \sum_{i,j=0}^{d_S-1} \Big(&|\alpha|^2 M_i N_j \rho_S N_j^\dagger M_i^\dagger \otimes |\psi_1\rangle\langle\psi_1|_C + |\beta|^2 N_j M_i \rho_S M_i^\dagger N_j^\dagger \otimes |\psi_2\rangle\langle\psi_2|_C \\ &+ \alpha\beta^* M_i N_j \rho_S M_i^\dagger N_j^\dagger \otimes |\psi_1\rangle\langle\psi_2|_C + \alpha^*\beta N_j M_i \rho_S N_j^\dagger M_i^\dagger \otimes |\psi_2\rangle\langle\psi_1|_C \Big).\end{aligned} \tag{3.6}$$

This state clearly has two "population" terms with well-ordered Kraus operators, i.e. the first two inside the sum, while the last two terms have scrambled Kraus operators and resembles a coherence. Also, ρ'_{SC} has an evident non-separable format, which confirms the previous reasoning. Interestingly, if one traces out the control,

$$\begin{aligned}\mathrm{tr}_C\{\rho'_{SC}\} &= \sum_{i,j=0}^{d_S-1} \left(|\alpha|^2 M_i N_j \rho_S N_j^\dagger M_i^\dagger + |\beta|^2 N_j M_i \rho_S M_i^\dagger N_j^\dagger \right) &(3.7)\\ &= |\alpha|^2 \mathcal{M}\circ\mathcal{N}(\rho_S) + |\beta|^2 \mathcal{N}\circ\mathcal{M}(\rho_S), &(3.8)\end{aligned}$$

the coherences disappear. Here a parallel with entanglement is visible: for entangled states, if one traces out one of the subsystems, the resultant state is a mixed state, while in the case of cSCO, tracing out the control makes the correlated state to become a convex combination of causally ordered quantum channels applied to the target quantum system S. To use the "coherence" generated by cSCO, one them must first post-process the final state before tracing out the control DOF. What is vastly done in the literature is to measure the control in some basis, renormalize the final state and then trace out C. This is known as *post-selection*. How to do it will be presented in the next section, where we discuss the standard implementation of cSCO, known as the *quantum switch* (QS).

3.2 Controlled-superposition of causal orders: the quantum switch

The quantum switch (QS) traditionally has two steps: (i) superposed application of two (or more) quantum channels to some target system S and (ii) post-selection of the control to keep coherences in the final local state of S. Here we present them together as a package, but in Chapters 4 and 5 they will be separated with specific technical purposes.

We come back to the two quantum channels scenario of Fig. 3.2 and assume that the control can be effectively described by a two-level system (qubit): even if it has more energy levels, just two are necessary for our purposes. We go on to model its Hamiltonian as:

$$H_C = \epsilon_0 |0\rangle\langle 0|_C + \epsilon_1 |1\rangle\langle 1|_C, \tag{3.9}$$

with $\epsilon_1 > \epsilon_0$, thus $|0\rangle_C$ is identified with the *ground state* and $|1\rangle_C$ with the *excited state*. This basis is then the one that controls the application of the two quantum channels $\mathcal{M}$ and $\mathcal{N}$ onto ρ_S. The controlled Kraus operators are:

$$K_{ij} = M_i N_j \otimes |0\rangle\langle 0|_C + N_j M_i \otimes |1\rangle\langle 1|_C, \tag{3.10}$$

thus, the state of the composite state system-control after applying the QS *supermap*[3] $\mathcal{S}_{\mathcal{M},\mathcal{N}}$ is:

$$\rho'_{SC} = \rho_{SC}^{\mathcal{M}\leftrightarrow\mathcal{N}} := \mathcal{S}_{\mathcal{M},\mathcal{N}}(\rho_S \otimes \rho_C) = \sum_{i,j=0}^{d_S-1} K_{ij}\,(\rho_S \otimes \rho_C)K_{ij}^\dagger. \tag{3.11}$$

As we already know from the previous section, the interesting behavior happens when the control is in a general state whose density operator is ρ_C, which might contain *coherences*. By combining Eqs. (3.10)-(3.11), the composite state system-control is explicitly:

$$\begin{aligned}\rho_{SC}^{\mathcal{M}\leftrightarrow\mathcal{N}} = {}& \langle 0|\rho_C|0\rangle_C\, M_i N_j \rho_S N_j^\dagger M_i^\dagger \otimes |0\rangle\langle 0|_C + \langle 0|\rho_C|1\rangle_C\, M_i N_j \rho_S M_i^\dagger N_j^\dagger \otimes |0\rangle\langle 1|_C \\ & + \langle 1|\rho_C|0\rangle_C\, N_j M_i \rho_S N_j^\dagger M_i^\dagger \otimes |1\rangle\langle 0|_C + \langle 1|\rho_C|1\rangle_C\, N_j M_i \rho_S M_i^\dagger N_j^\dagger \otimes |1\rangle\langle 1|_C,\end{aligned} \tag{3.12}$$

which can be conveniently cast in the form [22, 30]:

$$\rho_{SC}^{\mathcal{M}\leftrightarrow\mathcal{N}} = A_{++}\otimes\rho_C + A_{+-}\otimes\rho_C\,\sigma_z + A_{-+}\otimes\sigma_z\rho_C + A_{--}\otimes\sigma_z\rho_C\,\sigma_z \tag{3.13}$$

with

$$A_{xy} := \frac{1}{4}\sum_{i,j=0}^{d_S-1}\left[M_i, N_j\right]_x \rho_S \left[M_i, N_j\right]_y^\dagger, \tag{3.14}$$

where $x, y \in \{+,-\}$, $[X,Y]_+ = XY + YX$ is the anti-commutator, $[X,Y]_- = XY - YX$ is the commutator and σ_z is the z-Pauli matrix. Since the quantum state $|+\rangle = (|0\rangle + |1\rangle)/\sqrt{2}$ has maximum coherence in the computational basis, we shall consider it as the initial state of the control: $\rho_C = |+\rangle\langle +|_C$. Indeed, in the literature this is widely used as the state of the control that generates quantum superposition in the order of the quantum channels applied to the system S. Therefore, Eq. (3.13) becomes

$$\rho_{SC}^{\mathcal{M}\leftrightarrow\mathcal{N}} = A_{++}\otimes|+\rangle\langle+|_C + A_{+-}\otimes|+\rangle\langle-|_C + A_{-+}\otimes|-\rangle\langle+|_C + A_{--}\otimes|-\rangle\langle-|_C. \tag{3.15}$$

The next step is to post-select this bipartite state, i.e. measure the control DOF, renormalize the final state, and then trace out C. To do so, we consider measurements in the $\{|+\rangle_C, |-\rangle_C\}$ basis, thus:

$$\rho_{S,\pm} = \frac{\mathrm{tr}_C\{(\mathbb{1}_S\otimes|\pm\rangle\langle\pm|_C)\,\rho_{SC}^{\mathcal{M}\leftrightarrow\mathcal{N}}(\mathbb{1}_S\otimes|\pm\rangle\langle\pm|_C)\}}{\mathrm{tr}\{(\mathbb{1}_S\otimes|\pm\rangle\langle\pm|_C)\,\rho_{SC}^{\mathcal{M}\leftrightarrow\mathcal{N}}\}}, \tag{3.16}$$

which explicitly reads:

$$\rho_{S,\pm} = \frac{A_{\pm\pm}}{\mathrm{tr}\{A_{\pm\pm}\}}. \tag{3.17}$$

This state has been shown to enable different kinds of advantages when compared to the "definite order" scenario. Examples of tasks are found in different areas: quantum computation [12, 13], quantum communications [14–16], quantum metrology [17] and quantum thermodynamics [10, 18–22].

[3] The name *supermap* is due to the fact that the QS takes two quantum channels as inputs and has another quantum channel as an output.

For the sake of completeness, the process matrix of the QS is given by [48]:

$$
\begin{aligned}
W_{\mathrm{QS}} = |0\rangle\langle 0|_{P_C} \otimes \Bigg(\sum_{i,i',j,j',k,k'=0}^{d_S-1} & |i\rangle\langle i'|_{P_S} \otimes |i\rangle\langle i'|_{M_I} \otimes |j\rangle\langle j'|_{M_O} \otimes |j\rangle\langle j'|_{N_I} \otimes |k\rangle\langle k'|_{N_O} \\
& \otimes |k\rangle\langle k'|_{F_S} \Bigg) \otimes |0\rangle\langle 0|_{F_C} + |0\rangle\langle 1|_{P_C} \otimes \Bigg(\sum_{i,i',j,j',k,k'=0}^{d_S-1} |i\rangle\langle i'|_{P_S} \otimes |i\rangle\langle j'|_{M_I} \otimes |j\rangle\langle k'|_{M_O} \\
& \otimes |j\rangle\langle i'|_{N_I} \otimes |k\rangle\langle j'|_{N_O} \otimes |k\rangle\langle k'|_{F_S} \Bigg) \otimes |0\rangle\langle 1|_{F_C} + |1\rangle\langle 0|_{P_C} \otimes \Bigg(\sum_{i,i',j,j',k,k'=0}^{d_S-1} |i\rangle\langle i'|_{P_S} \\
& \otimes |j\rangle\langle i'|_{M_I} \otimes |k\rangle\langle j'|_{M_O} \otimes |i\rangle\langle j'|_{N_I} \otimes |j\rangle\langle k'|_{N_O} \otimes |k\rangle\langle k'|_{F_S} \Bigg) \otimes |1\rangle\langle 0|_{F_C} + |1\rangle\langle 1|_{P_C} \\
& \otimes \Bigg(\sum_{i,i',j,j',k,k'=0}^{d_S-1} |i\rangle\langle i'|_{P_S} \otimes |j\rangle\langle j'|_{M_I} \otimes |k\rangle\langle k'|_{M_O} \otimes |i\rangle\langle i'|_{N_I} \otimes |j\rangle\langle j'|_{N_O} \otimes |k\rangle\langle k'|_{F_S} \Bigg) \\
& \otimes |1\rangle\langle 1|_{F_C},
\end{aligned}
\tag{3.18}
$$

where $M_{I(O)}$ is the label for the Hilbert space of the input (output) of the quantum channel $\mathcal{M}$, $N_{I(O)}$ is the label for the Hilbert space of the input (output) of the quantum channel $\mathcal{N}$, P_C (F_C) represents the Hilbert space of the initial (final) state of the control and P_S (F_S) represents the Hilbert space of the initial (final) state of the system. One can use the QS process matrix with specific goals, such as certification of causal non-separability by means of *causal witnesses* in simulations and experiments. We shall see one clear example where it is useful in Section 3.4.

3.3 Non-violation of causal inequalities

Even though the quantum switch (QS), and more generally controlled superposition of causal orders (cSCO), presents causal non-separability and can be used for advantages in multiple tasks, ranging from computation and communications to thermodynamics and metrology, they *cannot* violate causal inequalities (CIs). These are inequalities that can only be violated by processes that have causal non-separability. However, it is not a sufficient condition, as shown by the case of cSCO. More than that, in Ref. [51] it was shown that there are causally non-separable processes, which are not necessarily cSCO processes, that admit a *causal model* and therefore *do not* violate a CI.

The fact that the QS cannot violate CIs was originally pointed out in Ref. [3]. Its causal non-separability comes from an extra degree-of-freedom (DOF) that controls the order of application of quantum channels. This control is what "lends" the superposition and ultimately the coherences to the target system. As noted before, when one traces out this DOF, a convex combination of causally ordered application of quantum channels is obtained. Take for instance the process matrix of the QS from Eq. (3.18). By tracing out

the future of the control, we get:

$$\begin{aligned}\mathrm{tr}_{F_C}\{W_{\mathrm{QS}}\} = |0\rangle\langle 0|_{P_C} \otimes \sum_{i,i',j,j',k,k'=0}^{d_S-1} \Big(& |i\rangle\langle i'|_{P_S} \otimes |i\rangle\langle i'|_{M_I} \otimes |j\rangle\langle j'|_{M_O} \otimes |j\rangle\langle j'|_{N_I} \otimes |k\rangle\langle k'|_{N_O} \\ & \otimes |k\rangle\langle k'|_{F_S} \Big) + |1\rangle\langle 1|_{P_C} \otimes \sum_{i,i',j,j',k,k'=0}^{d_S-1} \Big(|i\rangle\langle i'|_{P_S} \otimes |j\rangle\langle j'|_{M_I} \otimes |k\rangle\langle k'|_{M_O} \otimes |i\rangle\langle i'|_{N_I} \\ & \otimes |j\rangle\langle j'|_{N_O} \otimes |k\rangle\langle k'|_{F_S} \Big).\end{aligned} \tag{3.19}$$

Noting that the Choi-Jamiołkowski (CJ) matrix [62, 63] for a quantum channel Φ is (check Appendix A):

$$J(\Phi) := \left[\sum_{j,j'=0}^{d_S-1} |j\rangle\langle j'| \otimes \Phi(|j\rangle\langle j'|) \right]^{\intercal}, \tag{3.20}$$

where $^{\intercal}$ denotes matrix transposition, the CJ matrix of the identity map $\Im$ from the past of the system S to the quantum channel $\mathcal{M}$, from it to quantum channel $\mathcal{N}$ and then from the latter to the future of the system S is:

$$\begin{aligned}J(\Im_{P_S\to M_I,M_O\to N_I,N_O\to F_S}) = & \sum_{i,i'=0}^{d_S-1} (|i\rangle\langle i'|_{P_S} \otimes |i\rangle\langle i'|_{M_I}) \otimes \sum_{j,j'=0}^{d_S-1} (|j\rangle\langle j'|_{M_O} \\ & \otimes |j\rangle\langle j'|_{N_I}) \otimes \sum_{k,k'=0}^{d_S-1} (|k\rangle\langle k'|_{N_O} \otimes |k\rangle\langle k'|_{F_S}).\end{aligned} \tag{3.21}$$

Thus, we immediately see that,

$$\mathrm{tr}_{F_C}\{W_{\mathrm{QS}}\} = |0\rangle\langle 0|_{P_C} \otimes J(\Im_{P_S\to M_I,M_O\to N_I,N_O\to F_S}) + |1\rangle\langle 1|_{P_C} \otimes J(\Im_{P_S\to N_I,N_O\to M_I,M_O\to F_S}), \tag{3.22}$$

which is simply a mixture of definite order terms. Indeed, if we want to calculate probabilities in a scenario where Alice and Bob have quantum instruments (CP maps) $\mathcal{M}^{\mathrm{Alice}}_{x,a} = \mathcal{M}$ and $\mathcal{M}^{\mathrm{Bob}}_{y,b} = \mathcal{N}$, respectively ($x, a, y, b$ are labels), we get:

$$\begin{aligned}P(x,y|a,b) &= \mathrm{tr}\{(\rho_C \otimes \rho_S \otimes M^{\mathrm{Alice}}_{x,a} \otimes M^{\mathrm{Bob}}_{y,b})\, \mathrm{tr}_{F_C F_S}\{W_{\mathrm{QS}}\}\} \\ &= \langle 0|\rho_C|0\rangle\, P_{\mathrm{A}\to\mathrm{B}}(x,y|a,b) + \langle 1|\rho_C|1\rangle\, P_{\mathrm{B}\to\mathrm{A}}(x,y|a,b),\end{aligned} \tag{3.23}$$

where ρ_C and ρ_S are the initial states of control and system, $M^{\mathrm{Alice}}_{x,a} := J(\mathcal{M}^{\mathrm{Alice}}_{a,x})$ and $M^{\mathrm{Bob}}_{b,y} := J(\mathcal{M}^{\mathrm{Bob}}_{b,y})$ are the CJ matrices of the corresponding quantum instruments, and we defined:

$$P_{\mathrm{A}\to\mathrm{B}}(x,y|a,b) := \mathrm{tr}\left\{\mathcal{M}^{\mathrm{Bob}}_{y,b} \circ \mathcal{M}^{\mathrm{Alice}}_{x,a}(\rho_S)\right\}, \tag{3.24}$$

$$P_{\mathrm{B}\to\mathrm{A}}(x,y|a,b) := \mathrm{tr}\left\{\mathcal{M}^{\mathrm{Alice}}_{x,a} \circ \mathcal{M}^{\mathrm{Bob}}_{y,b}(\rho_S)\right\}. \tag{3.25}$$

As a consequence, it is clear that, if none of the definite order probabilities cannot violate a certain CI, a convex combination of them ($\langle 0|\rho_C|0\rangle + \langle 1|\rho_C|1\rangle = 1$), like the one in Eq. (3.23), cannot either. This is the most straightforward way to show that cSCO cannot violate CIs. For the sake of completeness, we point out that in Ref. [4] the authors arrived at the same conclusion, but by showing that any quantum circuit containing cSCO can be simulated by a classical causal model. Nonetheless, it is still an open question whether "pure" SCO can violate causal inequalities; the work of Ref. [64] showed that these processes are very constrained, but they are not completely crossed-out of existence.

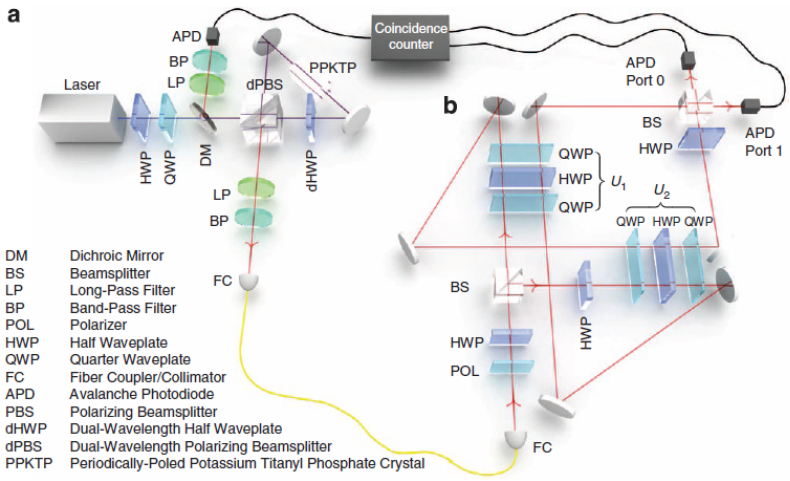

Figure 3.3: **Experimental setup employed in Ref. [7].** This optical setup is composed of (a) a Sagnac source and (b) a Mach-Zender inteferometer with unitaries U_1 in one arm and U_2 in the second arm. Each unitary is composed of three waveplates acting on the polarization of the incoming photon. Using the path as a control degree-of-freedom for superposing the order of application of the unitary gates, this setup, after the photon counting, is able to determine if U_1 and U_2 commute or anti-commute. This schematic was directly obtained from Ref. [7].

3.4 Experimental implementations

Just a few years after the ideas of indefinite causal order (ICO), and more specifically the quantum switch (QS), were conceived, the first experiment showing that it was attainable to put quantum channels in superposition was done [7]. The authors implemented on a quantum optics platform a QS in which the target system is the *polarization* of a photon and the control is the path in a Mach-Zender interferometer. The quantum channels are simply unitary gates (Pauli gates plus identity) and controlled-superposition of causal orders (cSCO) is attested by checking unbalance between commutation and anti-commutation contributions to photon counting. A schematic of the optical setup used by the authors of Ref. [7] is found in Fig. 3.3. Given that in one arm of the interferometer the unitary is U_1 and in the other arm U_2, one has that the output state system-control, for initial control state $|+\rangle_C = (|0\rangle_C + |1\rangle_C)/\sqrt{2}$, is:

$$|\Psi\rangle_{SC} = \frac{[U_1, U_2]_+}{2}|\psi\rangle_S \otimes |0\rangle_C + \frac{[U_1, U_2]_-}{2}|\psi\rangle_S \otimes |1\rangle_C, \tag{3.26}$$

where $|\psi\rangle_S$ is the input state of the system. Thus, by measuring the control qubit, one can infer if the unitaries commute or anti-commute. Here, the very nature of cSCO is present, since the unitaries are used only once, that is, on average the photon passes through the gates just once. This is in stark contrast with causally separable quantum circuits, which do not allow determining if two unitaries commute or anti-commute with a single use of the gates [2].

Another remarkable experiment was performed a few years later by the authors of Ref. [8]. Again a quantum optics setup was used, where the target quantum system is

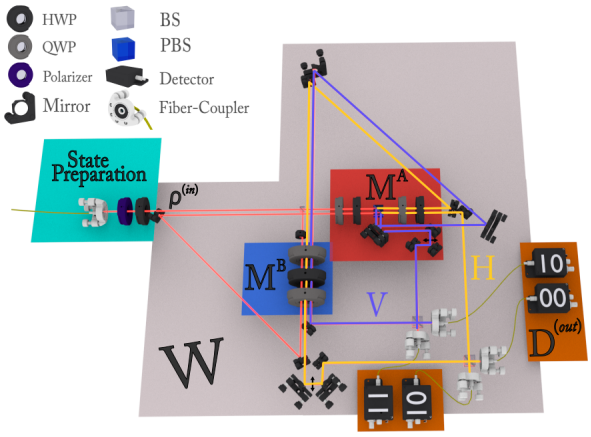

Figure 3.4: **Experimental setup used in Ref. [8].** Photons are prepared by a Type-II spontaneous-parametric-down-conversion source, which is not shown in the drawing. Two Mach-Zender interferometers are implemented, each containing a quantum channel: measurement plus re-preparation (M^A) and unitary gate (M^B). The order in which these are applied depends on the path that the photon takes, that is, if it goes first to one Mach-Zender interferometer or the other. Thus, the path is used as the control degree-of-freedom (DOF). The outputs are encoded as two bits: the first is 0 (1) if the photon is detected coming from the yellow (violet) interferometer, while the second bit is simply the result of polarization measurement and is indicated by which exit of a beam splitter the photon goes through. The W represents the process matrix connecting the interferometers and acronyms are: half-wave plate (HWP), quarter-wave plave (QWP), beam splitter (BS) and polarizer beam splitter (PBS). The schematic was directly obtained from Ref. [8].

the polarization of a photon and the control degree-of-freedom (DOF) is encoded in the path that it takes: first one Mach-Zender interferometer and then the second, or the other way around (for better visualization, the schematic of the experimental setup is shown in Fig. 3.4). The quantum channels consist of one measurement and re-preparation and the other a unitary operation. Assuming that a process matrix W connects one interferometer to the other and that it might have some sort of causal non-separability, a quantity dubbed CNS(W) (from "causal non-separability") [3] is extracted from the experiment. It is defined as:

$$\mathrm{CNS}(W) := -\mathrm{tr}\{\mu W\}, \tag{3.27}$$

where μ is called the *causal witness* and CNS(W) thus has a strong analogy with "generalized robustness of entanglement" [65]. As a quantifier of causal non-separability, whenever CNS(W) is positive we certify that W is causally non-separable. In Ref. [3] the authors go on to state that CNS(W) is the maximum amount of noise that can be inserted in the process so that it remains causally non-separable (if it flips sign, than it becomes causally separable). To certify the protocol of Ref. [8], they prepared the QS in their experimental platform, thus we know that the process matrix is the one in Eq. (3.18). The causal witness μ can be decomposed as:

$$\mu = \sum_{a,d,x,y,z} \alpha_{a,d,x,y,z}\, \rho^{(\mathrm{in})}_z \otimes M^A_{x,a} \otimes U^B_y \otimes D^{\mathrm{out}}_d, \tag{3.28}$$

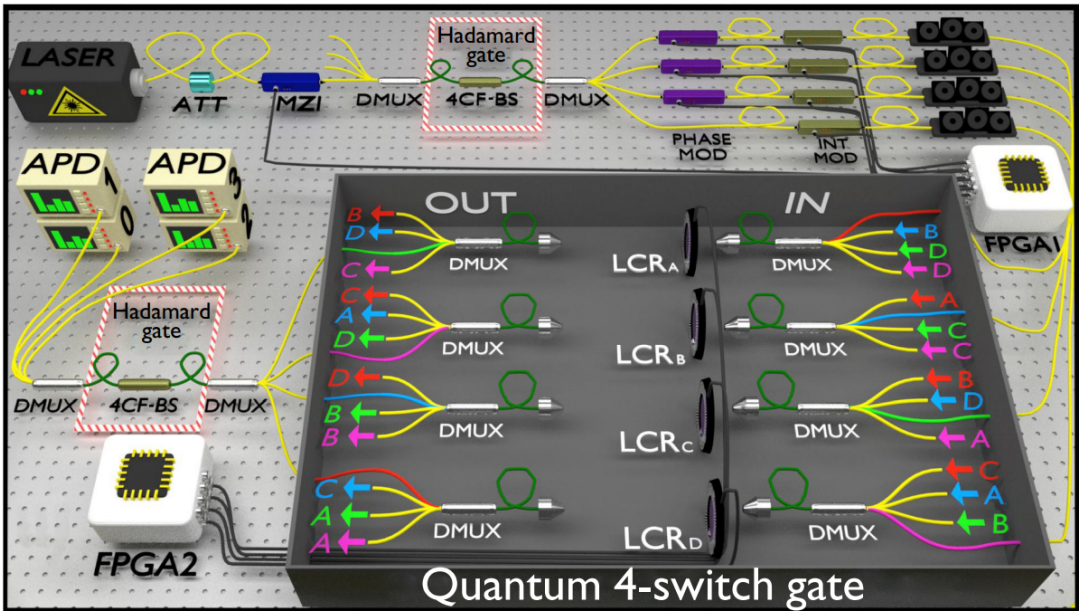

Figure 3.5: **Experimental setup of Ref. [9].** On the upper part, we have the single-photon preparation stage. The acronyms are ATT (attenuator), MZI (Mach-Zehnder interferometer), DMUX (demultiplexer), 4CF-BS (four-core fiber beam splitter), PHASE MOD (phase modulator), INT MOD (intensity modulator) and FPGA (field-programmable gate array). The photon might then be in four different spatial modes, which is a characteristic of the optical fibers being used. This is employed as the control degree-of-freedom (DOF), while the polarization is the target system. Each optical fiber entering the black-box is a different spatial mode. Inside the black-box we have the FPGA-controlled liquid crystal reflectors (LCRs) implementing the four unitaries: U_1, U_2, U_3 and U_4 from $\mathrm{LCR_A}$, $\mathrm{LCR_B}$, $\mathrm{LCR_C}$ and $\mathrm{LCR_D}$, respectively. Take for instance the green fiber on the "IN" side. If the photons enters the black-box through it, it will go first to $\mathrm{LCR_C}$, then to $\mathrm{LCR_B}$ (green C), $\mathrm{LCR_D}$ (green B) and finally $\mathrm{LCR_A}$ (green D). After that, on the "OUT" side, the photon will exit through the green optical fiber. This sequence corresponds to the gate ordering $U_A U_D U_B U_C$. After being properly post-processed, the photon is measured with the help of single-photon detectors (APDs). The schematic was directly obtained from Ref. [9].

where $\alpha_{a,d,x,y,z} \in \mathbb{R}$ are normalization coefficients, $\rho_z^{(\mathrm{in})}$ are the possible input states (with label z), $M^A_{x,a}$ is the Choi-Jamiołkowski matrix of the quantum channel of one of the interferometers (a, x are input/output encoding variables), U^B_y are the unitaries of the second interferometer (labeled by the variable y) and D^{out}_d are the measurement performed on the photon after the interferometers (labeled by the bit d). Therefore, the $\mathrm{CNS}(W_{\mathrm{QS}})$ becomes:

$$\mathrm{CNS}(W_{\mathrm{QS}}) = -\sum_{a,d,x,y,z} \alpha_{a,d,x,y,z}\, P(x,y,z|a,d), \tag{3.29}$$

with probabilities

$$P(x,y,z|a,d) = \mathrm{tr}\left\{\left(\rho_z^{(\mathrm{in})} \otimes M^A_{x,a} \otimes U^B_y \otimes D^{\mathrm{out}}_d\right) W_{\mathrm{QS}}\right\}, \tag{3.30}$$

which are the outputs of the experimental setup. After measuring in the laboratory all the probabilities, weighting them with the values of $\alpha_{a,d,x,y,z}$ and summing up, the authors

obtained:

$$\mathrm{CNS}(W_{\mathrm{QS}}) = 0.202 \pm 0.029, \tag{3.31}$$

attesting that there is causal non-separability in this optical setup.

A more elaborate experimental setup is the *4-switch* (QS with four gates) presented in Ref. [9]. Still an optical setup, here the difference lies on the fact that optical fibers are employed, instead of photons travelling in free-space. In Fig. 3.5 the schematic of the experiment is presented. The target system is the polarization of a photon that is produced from a laser source and the control DOF is the *spatial mode* of the fiber. Four modes of the optical fiber are used, which then corresponds to a four level control. Moreover, four unitary gates are implemented (U_A, U_B, U_C and U_D), each one generated by a controllable liquid crystal retarder (LCR). Even though $4! = 24$ permutations of these unitaries are possible, only four are effectively used: $U_D U_C U_B U_A$, $U_C U_D U_A U_B$, $U_A U_D U_B U_C$ and $U_B U_C U_A U_D$. The implemented 4-switch is used for a specific computational task: solve the "Hadamard promise problem", i.e. estimating the phase between the permutations of the four implemented gates. The authors show that their 4-switch setup is capable of estimating the phase with a number $O(N)$ of applications of the gates, while fixed order of the gates without cSCO does it with a number $O(N^2)$ of gates. The flexibility of this experimental setup — application of higher number of gates, simple re-routing of their order, precise control over their parameters through the LCRs — and the advantages that come with the use of optical fibers — no cumbersome alignment of lenses, high fidelity and rapidly increasing industrial technological improvements — make this 4-switch probably the most-promising experimental platform for testing cSCO in the present and for the near future.

Chapter 4

Passive states activation using the quantum switch

> *"Evil is evil, Stregobor. Lesser, greater, middling... it's all the same. I'm not judging you. I haven't only done good in my life either. But now, if I have to choose between one evil and another, then I prefer not to choose at all."*
>
> — Geralt of Rivia, the Witcher.

One specific matter to be addressed when investigating how indefinite causal order (ICO) in its weaker form (controlled-superposition of causal orders, cSCO) relates to thermodynamics, is to understand how *passive states* might be activated via the quantum switch (QS) plus post-selection. This was first studied in Ref. [20], where the authors studied the final state after applying the QS and post-selecting the control degree-of-freedom (DOF), identifying from its populations and coherences when state activation occurs. Meanwhile, this was widely reformulated and expanded in Ref. [23], in which the authors showed that: (i) the QS alone cannot activate passive states (Section 4.2), i.e. it is not a thermodynamical resource per se; (ii) what are the conditions for state activation on the energetic level (Section 4.3) and (iii) peculiarities of state activation in the different examples of qubits and quantum harmonic oscillators (Section 4.4). By diving into the case of QS applied to continuous-variables (CV) systems, the quantum harmonic oscillator (QHO) being its most prominent example, the authors contributed to an area still being poorly explored [66, 67].

In this chapter we first start with a quick introduction to what are passive states in (quantum) thermodynamics (Section 4.1). Then we pass to a general result in Section 4.2, showing that if one has a passive system and a control DOF implementing the QS, without any extra resources, such as coherence in the state of the control and post-selecting in an adequate basis, *no* state activation is possible. This is equivalent to say that the QS by itself is not a thermodynamical resource. Furthermore, in Section 4.3 we relax previous constraints and allow extra resources in the setup. With these inputs, we investigate general conditions for enabling state activation without and with post-selecting the con-

trol DOF (Sections 4.3.1 and 4.3.2, respectively). Finally, in Section 4.4 we explore how the state activation looks like for qubits (Section 4.4.1) and for QHOs (Section 4.4.2). In the former, the considered unitaries composing the QS are: (a) rotation operators around the x and y axes of the Bloch sphere (Section 4.4.1.1) and (b) general $U(2)$ unitaries (Section 4.4.1.2); while in the latter the unitaries are: (a) displacement operators (Section 4.4.2.1) and (b) displacement and squeeze[1] operators (Section 4.4.2.2).

4.1 Passive states in (quantum) thermodynamics

Consider a system S in some state ρ_S and with Hamiltonian H_S. If, by means of applying *any cyclic* unitary U – cyclic in the sense that some internal parameter of H_S is changed and comes back to the initial value – the inequality

$$\mathrm{tr}\{\rho_S H_S\} \leqslant \mathrm{tr}\{U\rho_S U^\dagger H_S\} \tag{4.1}$$

is respected, we say that ρ_S is *passive* with respect to H_S [68–70]. In other words: it is impossible to decrease the internal energy of S and thus extract energy from it.

A useful way to look at passive states is through the lens of *ergotropy* [71, 72]. Ergotropy is a measure of extractable work ($\mathcal{W}_{\max}$) in the following sense:

$$\mathcal{W}_{\max} := \mathrm{tr}\{\rho_S H_S\} - \min_U \mathrm{tr}\{U\rho_S U^\dagger H_S\}, \tag{4.2}$$

that is, for *all* possible unitaries U existing in the linear space formed from the Hilbert space of the system $\mathcal{L}(\mathcal{H}_S)$, we minimize the internal energy of the system and calculate the difference to the internal energy for the current state of the system ρ_S. From the above definition of passive state, we see that its extractable work is negative, i.e. it has no available work to be extracted. The upper bound for the ergotropy of a system S in state ρ_S is [73]:

$$\mathcal{W}_{\max} \leqslant \mathrm{tr}\{\rho_S H_S\} - \mathrm{tr}\{\Theta_\beta H_S\}, \tag{4.3}$$

where

$$\Theta_\beta := \frac{e^{-\beta H_S}}{Z_S} \tag{4.4}$$

is the Gibbs thermal state at inverse temperature β whose von Neumann entropy $\mathcal{S}(\rho) := -\mathrm{tr}\{\rho \ln \rho\}$ is the same as for the state ρ_S: $\mathcal{S}(\Theta_\beta) = \mathcal{S}(\rho_S)$. The partition function $Z_S = \mathrm{tr}\{\exp(\beta H_S)\}$ is a normalization constant. Hence, it shows that the Gibbs thermal state is the "most passive state of all passive states", and sets a reference point for maximum energy extraction. Here we have a striking connection with the second law of thermodynamics (SLT) in the *Kelvin-Planck formulation*: no work can be obtained from a device operating cyclically when connected to only one thermal bath.

[1] In the literature both "squeeze" and "squeezing" are used to refer to the same second order operators (second order with respect to the creation/annihilation operators of oscillation modes). Throughout this Chapter, we opt for "squeeze operator".

4.2 The quantum switch alone is not a thermodynamic resource

Since passive states cannot be activated by means of cyclic unitaries, we shall expect that this extends to the case of the QS when the control has no extra resources (i.e. coherence). This is so, because the QS is a *linear* combination of quantum channels acting only on the side of the system S, and then no *superadditivity*[2] or exotic feature is possible. It hints to the fact that the QS *alone* is not a thermodynamic resource, something already investigated in Ref. [74], where the authors show that the free energy of coherence is what moves the chains of gains of information capacity. Here, nonetheless, we go one step further and show in a simple and elegant way that indeed the QS is not capable of activating the passive state ρ_S of a system S *per se*.

The proof goes as follows. We have one system S in some passive state ρ_S with respect to its Hamiltonian H_S and a control C DOF in some other passive state ρ_C in reference to the local Hamiltonian H_C. The composite state system-control starts uncorrelated in the separable state $\rho_{SC} = \rho_S \otimes \rho_C$. Then, a controlled-unitary called onwards the QS-unitary (U_{QS}),

$$U_{\text{QS}} = U_2 U_1 \otimes |0\rangle\langle 0|_C + U_1 U_2 \otimes |1\rangle\langle 1|_C, \tag{4.5}$$

is applied to the system S. Here $\{|0\rangle_C, |1\rangle_C\}$ is the computational basis of the control (eigenstates of the z-Pauli operator). Notice that the unitary operators are applied just on the side of S, while on the side of C we have projectors; hence superadditivity is discarded in our setup. Define the internal energy of the composite state before the QS:

$$\begin{aligned} \mathcal{E}_{SC} &= \text{tr}\{\rho_{SC} H_{SC}\} \\ &= \text{tr}\{\rho_S H_S\} + \text{tr}\{\rho_C H_C\} =: \mathcal{E}_S + \mathcal{E}_C \end{aligned} \tag{4.6}$$

where $H_{SC} = H_S \otimes \mathbb{1}_C + \mathbb{1}_S \otimes H_C$ is the total Hamiltonian (no interactions between S and C), and the internal energy after applying the QS:

$$\mathcal{E}'_{SC} = \text{tr}\{U_{\text{QS}} \rho_{SC} U_{\text{QS}}^\dagger H_{SC}\}. \tag{4.7}$$

Then their difference,

$$\Delta_{\text{QS}} = \mathcal{E}'_{SC} - \mathcal{E}_{SC}, \tag{4.8}$$

shall be our quantifier of whether the composite state system-control was activated after applying the QS, i.e. $\Delta_{\text{QS}} < 0$. By explicitly expanding Eq. (4.7), we have:

$$\begin{aligned} \mathcal{E}'_{SC} = {} & \langle 0|\rho_C|0\rangle\, \mathcal{E}_{12} + \langle 1|\rho_C|1\rangle\, \mathcal{E}_{21} + \langle 0|\rho_C|0\rangle\langle 0|H_C|0\rangle \\ & + \langle 1|\rho_C|1\rangle\langle 1|H_C|1\rangle + \chi\, \langle 0|\rho_C|1\rangle\langle 1|H_C|0\rangle + \chi^*\, \langle 1|\rho_C|0\rangle\langle 0|H_C|1\rangle, \end{aligned} \tag{4.9}$$

where we defined

$$\mathcal{E}_{12} := \text{tr}\left\{U_2 U_1 \rho_S U_1^\dagger U_2^\dagger H_S\right\}, \qquad \mathcal{E}_{21} := \text{tr}\left\{U_1 U_2 \rho_S U_2^\dagger U_1^\dagger H_S\right\}, \tag{4.10}$$

[2] Superadditivity is when, given two objects x and y (scalars, fields, operators, etc.) and a function f operating on them, the inequality $f(x+y) \geqslant f(x) + f(y)$ holds.

and

$$\chi := \mathrm{tr}\left\{U_2 U_1 \rho_S U_2^\dagger U_1^\dagger\right\} \equiv |\chi| e^{i\phi}, \tag{4.11}$$

which is related to the unitary cross-map [20]. Of course, when the unitaries commute we have $\chi = 1$. Moreover, we define the unitary

$$U_{\phi,\pm} := \begin{pmatrix} 1 & 0 \\ 0 & \pm e^{-i\phi} \end{pmatrix}, \tag{4.12}$$

and the states

$$\tilde{\rho}_C := \left(\frac{1+|\chi|}{2}\right) U_{\phi,+}\rho_C U_{\phi,+}^\dagger + \left(\frac{1-|\chi|}{2}\right) U_{\phi,-}\rho_C U_{\phi,-}^\dagger, \tag{4.13}$$

$$\tilde{\rho}_S := \langle 0|\rho_C|0\rangle\, U_2 U_1 \rho_S U_1^\dagger U_2^\dagger + \langle 1|\rho_C|1\rangle\, U_1 U_2 \rho_S U_2^\dagger U_1^\dagger, \tag{4.14}$$

leading to

$$\mathcal{E}'_{SC} = \mathrm{tr}\{\tilde{\rho}_S H_S\} + \mathrm{tr}\{\tilde{\rho}_C H_C\} =: \tilde{\mathcal{E}}_S + \tilde{\mathcal{E}}_C. \tag{4.15}$$

From passivity of ρ_S and ρ_C, we clearly see that $\Delta_S := \tilde{\mathcal{E}}_S - \mathcal{E}_S \geqslant 0$ and $\Delta_C := \tilde{\mathcal{E}}_C - \mathcal{E}_C \geqslant 0$, thus combining this with Eqs. (4.6) and (4.15):

$$\tilde{\mathcal{E}}_{SC} \geqslant \mathcal{E}_{SC}, \tag{4.16}$$

therefore,

$$\Delta_{\mathrm{QS}} \geqslant 0 \tag{4.17}$$

always. The same is valid for the reduced state of the system $\rho'_S = \mathrm{tr}_C\{U_{\mathrm{QS}}\rho_{SC}U_{\mathrm{QS}}^\dagger\}$:

$$\begin{aligned} \mathrm{tr}\{\rho'_S H_S\} - \mathrm{tr}\{\rho_S H_S\} &= \mathrm{tr}\{\tilde{\rho}_S H_S\} - \mathrm{tr}\{\rho_S H_S\} \\ &= \tilde{\mathcal{E}}_S - \mathcal{E}_S \\ &\equiv \Delta_S \geqslant 0. \end{aligned} \tag{4.18}$$

Thus, we prove that having only the QS in hands is not enough to activate either the local state of the system or the composite state system-control in the case that both ρ_S and ρ_C are passive. As we show below, any ergotropy gains is the result of extra resources being added to the setup, such as coherence in the state of the control and non-diagonal Hamiltonian of the control in the computational basis.

4.3 Conditions for activation using the quantum switch

4.3.1 Without post-selection

What if then the state of the control has no more the constraint of being passive? In such a case ($\langle 0|\rho_C|1\rangle \neq 0$) we have that:

$$\Delta_C = 2\,\mathrm{Re}\{\langle 0|\rho_C|1\rangle\langle 1|H_C|0\rangle(\chi - 1)\}, \tag{4.19}$$

with $\mathrm{Re}\{z\}$ being the real component of the complex number z. The minimization of Eq. (4.19) is straightforward: $\langle 0|\rho_C|1\rangle = -e^{i\delta}/\sqrt{2}$, where δ cancels out the phase of $\langle 1|H_C|0\rangle(\chi - 1)$, then:

$$\min_{\rho_C} \Delta_C = -\sqrt{2}\,|\langle 1|H_C|0\rangle(\chi - 1)|\,. \tag{4.20}$$

The last expression shows that: (i) non-commuting unitaries are necessary for the possibility of state activation ($\chi \neq 1$); (ii) without any kind of post-selection, one must have the Hamiltonian of the control containing non-diagonal elements in the computational basis and it must be relatively large to compensate for the positive Δ_S and then have $\Delta_{\mathrm{QS}} < 0$; and (iii) the activation occurs for the composite state system-control as a whole.

4.3.2 With post-selection

When the condition of non-diagonal Hamiltonian of the control is not met (in the computational basis $\{|0\rangle_C, |1\rangle_C\}$, of course), the state of the system alone can still be activated by means of post-selecting the control C (i.e. measuring, tracing out C and renormalizing the final state). For the sake of generality, consider that the state of the control is prepared in the generic pure state $\rho_C = |\psi\rangle\langle\psi|_C$, with

$$|\psi\rangle_C = \cos\left(\frac{\theta_C}{2}\right)|0\rangle_C + e^{i\varphi_C}\sin\left(\frac{\theta_C}{2}\right)|1\rangle_C, \tag{4.21}$$

being a state parametrized in the Bloch sphere ($\theta_C \in [0,\pi]$, $\varphi_C \in [0,2\pi]$). It has three-dimensional Cartesian coordinates $(\sin\theta_C\cos\varphi_C, \sin\theta_C\sin\varphi_C, \cos\theta_C)$. Explicitly, the state post-QS ($\rho'_{SC} = U_{\mathrm{QS}}\,\rho_{SC}\,U_{\mathrm{QS}}^\dagger$) is:

$$\begin{aligned}\rho'_{SC} = {} & \cos^2\left(\frac{\theta_C}{2}\right) U_2U_1\,\rho_S\,U_1^\dagger U_2^\dagger \otimes |0\rangle\langle 0|_C + \frac{e^{i\varphi_C}}{2}\sin\theta_C\, U_2U_1\,\rho_S\,U_2^\dagger U_1^\dagger \otimes |0\rangle\langle 1|_C \\ & + \frac{e^{-i\varphi_C}}{2}\sin\theta_C\, U_1U_2\,\rho_S\,U_1^\dagger U_2^\dagger \otimes |1\rangle\langle 0|_C + \sin^2\left(\frac{\theta_C}{2}\right) U_1U_2\,\rho_S\,U_2^\dagger U_1^\dagger \otimes |1\rangle\langle 1|_C.\end{aligned} \tag{4.22}$$

We move forward and parameterize the measurement state also on the Bloch sphere:

$$|\psi_M\rangle_C = \cos\left(\frac{\theta_M}{2}\right)|0\rangle_C + e^{i\varphi_M}\sin\left(\frac{\theta_M}{2}\right)|1\rangle_C, \tag{4.23}$$

thus, using *Born's rule* and renormalizing the measured state, the post-selected state of the system is:

$$\rho_{S,M} = \frac{(\mathbb{1}_S \otimes \langle\psi_M|_C)\;\rho'_{SC}\;(\mathbb{1}_S \otimes |\psi_M\rangle_C)}{\mathrm{tr}\{(\mathbb{1}_S \otimes \langle\psi_M|_C)\;\rho'_{SC}\;(\mathbb{1}_S \otimes |\psi_M\rangle_C)\}}, \tag{4.24}$$

which, by using Eqs. (4.22) and (4.23), is equal to

$$\begin{aligned}\rho_{S,M} = \frac{1}{N_M}\Bigg(& \cos^2\left(\frac{\theta_C}{2}\right)\cos^2\left(\frac{\theta_M}{2}\right) U_2U_1\,\rho_S\,U_1^\dagger U_2^\dagger + \sin^2\left(\frac{\theta_C}{2}\right)\sin^2\left(\frac{\theta_M}{2}\right) U_1U_2\,\rho_S\,U_2^\dagger U_1^\dagger \\ & + \frac{e^{-i(\varphi_C+\varphi_M)}}{4}\sin\theta_M\sin\theta_C\, U_1U_2\,\rho_S\,U_1^\dagger U_2^\dagger + \frac{e^{i(\varphi_C+\varphi_M)}}{4}\sin\theta_M\sin\theta_C\, U_2U_1\,\rho_S\,U_2^\dagger U_1^\dagger\Bigg),\end{aligned} \tag{4.25}$$

where the normalization constant N_M is:

$$N_M = \frac{1}{2}\left(1 + \cos\theta_C\cos\theta_M + \sin\theta_C\sin\theta_M\,\mathrm{Re}\{\chi e^{i(\varphi_C+\varphi_M)}\}\right). \tag{4.26}$$

The state in Eq. (4.25) contains diagonal elements connected to the definite causal order (first U_1 then U_2 and vice-versa) and off-diagonal elements, where the order is "mixed" (not in the usual "onion" operator evolution shape). These "coherences" come exactly

from the coherences in the state of the control in the computational basis and constitute the previously introduced superposition of causal orders (SCO, Chapter 3).

The internal energy of the system after measuring the control is:

$$\mathcal{E}_{S,M} = \mathrm{tr}\{\rho_{S,M} H_S\}, \tag{4.27}$$

and the internal energy difference in the system before the QS and after the QS plus post-selection of the control is:

$$\Delta_{S,M} = \mathcal{E}_{S,M} - \mathcal{E}_S. \tag{4.28}$$

This energy difference, by using Eq. (4.25) is:

$$\begin{aligned}\Delta_{S,M} = \frac{1}{N_M}\Bigg(&\cos^2\left(\frac{\theta_C}{2}\right)\cos^2\left(\frac{\theta_M}{2}\right)\Delta_{12} + \sin^2\left(\frac{\theta_C}{2}\right)\sin^2\left(\frac{\theta_M}{2}\right)\Delta_{21} \\ &+ \frac{1}{2}\sin\theta_C \sin\theta_M \,\mathrm{Re}\{\Delta_F e^{i(\varphi_C+\varphi_M)}\}\Bigg),\end{aligned} \tag{4.29}$$

where we defined

$$\Delta_{12} := \mathrm{tr}\{U_2 U_1 \rho_S U_1^\dagger U_2^\dagger\} - \mathcal{E}_S, \qquad \Delta_{21} := \mathrm{tr}\{U_1 U_2 \rho_S U_2^\dagger U_1^\dagger\} - \mathcal{E}_S \tag{4.30}$$

and

$$\Delta_{\mathcal{F}} := \mathcal{F}_S - \chi\,\mathcal{E}_S, \qquad \mathcal{F}_S := \mathrm{tr}\{U_2 U_1 \rho_S U_2^\dagger U_1^\dagger H_S\}. \tag{4.31}$$

Given the passivity of ρ_S, we get that $\Delta_{12} \geqslant 0$ and $\Delta_{21} \geqslant 0$. Hence, by imposing $\Delta_{S,M} < 0$, we obtain the conditions for state of the system activation:

- $\theta_C \neq 0, \pi$ and $\theta_M \neq 0, \pi$ (i.e. the states cannot be either $|0\rangle$ or $|1\rangle$);
- $\tan(\varphi_C + \varphi_M) \neq \mathrm{Re}\{\Delta_F\}/\,\mathrm{Im}\{\Delta_F\}$;
- $\sin\theta_C \sin\theta_M \,\mathrm{Re}\{\Delta_F e^{i(\varphi_C+\varphi_M)}\} < 0$.

It is very important to state that these are *necessary* but not *sufficient* conditions.

4.4 Examples

To see how the previous conditions for state activation apply to specific cases, we shall test them when the system has two levels (qubit, Section 4.4.1) and when it is a QHO (Section 4.4.2). In the former, we have the unitaries as (a) rotations around the x and y axes of the Bloch sphere (Section 4.4.1.1), and (b) general $U(2)$ unitaries (Section 4.4.1.2); while in the latter the unitaries are (a) displacement operators (Section 4.4.2.1) and (b) displacement and squeeze operators (Section 4.4.2.2).

4.4.1 Two-level system (qubit)

Here we have the system being described as a two-level system (qubit), whose Hamiltonian H_S is:

$$H_S = \frac{\omega}{2}\left(\mathbb{1}_2 - \sigma_z^S\right), \tag{4.32}$$

where ω is the energy gap between the ground and excited states, $\mathbb{1}_2$ is the 2×2 identity matrix and σ_z^S is z-Pauli operator in $\mathcal{L}(\mathcal{H}_S)$. In this manner, $|0\rangle_S$ is the ground state with

energy 0 and $|1\rangle_S$ is the excited state with energy ω. The Hamiltonian of the control H_C, on the other hand, contains non-diagonal terms in the computational basis,

$$H_C = \frac{\omega}{2}\left(\mathbb{1}_2 - \sigma_z^C\right) + t\,|0\rangle\langle 1|_C + t^*|1\rangle\langle 0|_C, \tag{4.33}$$

where $t = |t|e^{i\theta} \in \mathbb{C}$ is related to the probability that the qubit will change spontaneously its state between $|0\rangle_C$ and $|1\rangle_C$[3]. Analogous to the system's Hamiltonian, the z-Pauli operator is employed in $\mathcal{L}(\mathcal{H}_C)$. Notice that the system and control are taken to be *resonant*, i.e. they have the same energy gap ω. This assumption does not affect the generality of the results presented in the continuation, at the same time that confers more compact expressions. Moreover, S and C do not interact, thus $H_{SC} = H_S \otimes \mathbb{1}_C + \mathbb{1}_S \otimes H_C$. The system is initialized in the Gibbs thermal state $\Theta_\beta = \exp(-\beta H_S)/Z_S$ with inverse temperature $\beta = 1/T$, which for the given H_S is:

$$\Theta_\beta = \left(\frac{1}{1+e^{-\beta\omega}}\right)|0\rangle\langle 0|_S + \left(1 - \frac{1}{1+e^{-\beta\omega}}\right)|1\rangle\langle 1|_S. \tag{4.34}$$

The control is initialized according to Eq. (4.21) and the composite state system-control is a separable one $\rho_{SC} = \Theta_\beta \otimes |\psi\rangle\langle\psi|_C$ before applying the QS.

4.4.1.1 Rotation operators

One possibility is to have the unitaries that are applied to the system to be *rotation operators*

$$\begin{aligned} U_1 &= R_x(\alpha_x) \\ &= \exp\left(-i\sigma_x^S \frac{\alpha_x}{2}\right), \end{aligned} \tag{4.35}$$

$$\begin{aligned} U_2 &= R_y(\alpha_y) \\ &= \exp\left(-i\sigma_y^S \frac{\alpha_y}{2}\right), \end{aligned} \tag{4.36}$$

which implement rotations of $\alpha_x \in [0, 2\pi]$ around the x-axis and $\alpha_y \in [0, 2\pi]$ around the y-axis of the Bloch sphere, respectively. Direct calculation leads to

$$\begin{aligned} \Delta_{\text{QS}} = \frac{\omega}{2}\Bigg[1 - \cos\alpha_x\cos\alpha_y + \frac{|t|}{\omega}\sin\alpha_x\sin\alpha_y\sin\theta_C\sin(\theta+\varphi_C)\Bigg]\tanh\left(\frac{\beta\omega}{2}\right) \\ - 2|t|\cos(\theta+\varphi_C)\sin\theta_C\sin^2\left(\frac{\alpha_x}{2}\right)\sin^2\left(\frac{\alpha_y}{2}\right). \end{aligned} \tag{4.37}$$

A common case in the literature is to consider $|\psi\rangle_C = |+\rangle_C = (|0\rangle_C + |1\rangle_C)/\sqrt{2}$ (it corresponds to $\theta_C = \pi/2, \varphi_C = 0$), thus:

$$\begin{aligned} \Delta_{\text{QS}} = \frac{\omega}{2}\Bigg[1 - \cos\alpha_x\cos\alpha_y + \frac{|t|}{\omega}\sin\alpha_x\sin\alpha_y\sin\theta\Bigg]\tanh\left(\frac{\beta\omega}{2}\right) \\ - 2|t|\cos\theta\sin^2\left(\frac{\alpha_x}{2}\right)\sin^2\left(\frac{\alpha_y}{2}\right). \end{aligned} \tag{4.38}$$

[3] In semiconductor-based qubits, for instance, electric potentials create "islands" (valleys of the electric potential formed upon the *two-dimensional electron gas, 2DEG*) where electrons can be stored. An electron inside one island can be encoded as the state $|0\rangle$ and if it is inside a second island, state $|1\rangle$. Then, by means of *quantum tunneling* the electron can jump from one island to the other, changing spontaneously the state of the system.

This quantity is plotted in Fig. 4.1. As expected from Eq. (4.20), whenever non-diagonal terms are null ($|t| = 0$), no activation is possible ($\Delta_{QS} \geqslant 0$). Also, for larger amplitude of these non-diagonal terms we have a better achievement of composite state system-control activation, so to say, more negative Δ_{QS} and for wider range of values of the inverse temperature β. Interestingly, in this specific case activation is better achieved for low β, that is, for *high* temperature T, which goes against the intuition that thermal noise would spoil state activation.

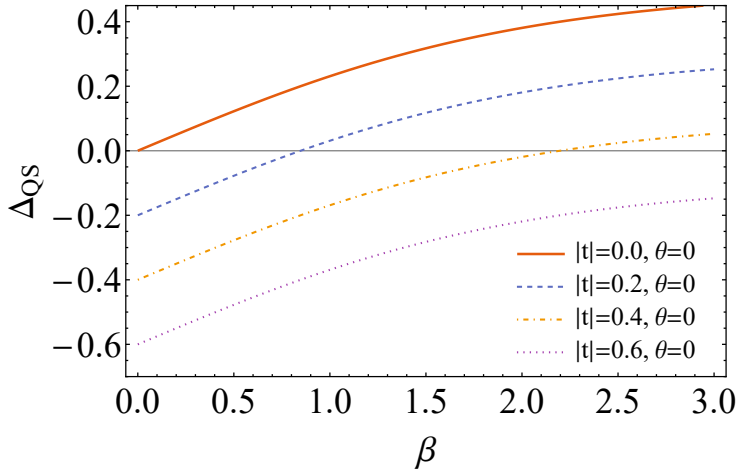

Figure 4.1: **The internal energy difference Δ_{QS} as a function of the inverse temperature of the system β and for different values of $|t|$, when the unitaries are rotations around the x and y axes of the Bloch sphere.** For $|t| = 0$ no activation occurs ($\Delta_{QS} \geqslant 0$), as expected. Nonetheless, for increasing $|t|$ the extractable energy grows and it is available for larger range of values of β. Here $\omega = 1.0$, $\alpha_x = \pi/2$, $\alpha_y = \pi$ and $\theta = 0$. Figure obtained from Ref. [23].

Moreover, if one measures the control with a parameterized state as in Eq. (4.23), the following necessary but not sufficient conditions for state activation of the system are found:

$$\sin\theta_C \neq 0, \quad \sin\theta_M \neq 0, \tag{4.39}$$

$$\tan(\varphi_C + \varphi_M) \neq (\cot\alpha_x \cot\alpha_y - \csc\alpha_x \csc\alpha_y)\sinh(\beta\omega), \tag{4.40}$$

and

$$\frac{\omega \sin\theta_C \sin\theta_M}{2(1+e^{\beta\omega})^2}\Big[(e^{2\beta\omega}-1)(1-\cos\alpha_x\cos\alpha_y)\cos(\varphi_C+\varphi_M) + 2e^{\beta\omega}\sin\alpha_x\sin\alpha_y\sin(\varphi_C+\varphi_M)\Big] < 0. \tag{4.41}$$

While the first two conditions are easy to analyze (neither the initial control state or the measurement state can be on the poles of the Bloch sphere, i.e. the states $\{|0\rangle_C, |1\rangle_C\}$), the other conditions are not straightforward. Thus, we pass to the simplifying case where $\beta \to 0$ (infinite temperature) and $\alpha_x = \alpha_y = \alpha$. Then the last two conditions reduce to:

$$\tan(\varphi_C + \varphi_M) \neq 0, \tag{4.42}$$

and

$$\sin\theta_C \sin\theta_M \sin(\varphi_C + \varphi_M) < 0. \tag{4.43}$$

For instance, if the control is prepared in the $|+\rangle_C$ state ($\theta_C = \pi/2$ and $\varphi_C = 0$), we finally arrive at the constraints for the measurement state:

$$\varphi_M \neq 0, \pi, \tag{4.44}$$

$$\sin\theta_M \sin\varphi_M < 0. \tag{4.45}$$

Since $\sin\theta_M > 0$, the angle φ_M must be in the $(\pi, 2\pi)$ range. One comment about this result is important. In the case that one prepares the control in the $|+\rangle_C$ state, measuring it in either $|+\rangle_C$ or $|-\rangle_C$ will *not* activate it in any circumstance. It goes against many of the QS setups in the literature, in which preparation and measurement are in the same basis of eigenstates of σ_x. Therefore, here we recognize a specific feature of state activation by means of the QS plus post-selection of the control.

In the end, considering the aforementioned simplifications ($\theta_C = \pi/2, \varphi = 0, \beta \to 0$, $\alpha_x = \alpha_y = \alpha$), we have the internal energy difference of the system to be equal to:

$$\Delta_{S,M} = \frac{\omega \sin\varphi_M}{2\cos\varphi_M + 4\cos\varphi_M \cot\alpha \csc\alpha + 4\csc^2\alpha \csc\theta_M}. \tag{4.46}$$

Given that $\theta_M \in (0, \pi)$, the previous expression has a minimum for $\varphi_M = \pi/2$. In Fig. 4.2 one has the plot of Eq. (4.46) for $\alpha = \pi/4, \pi/2, 3\pi/4$ and of the angle φ_M that leads to minimum $\Delta_{S,M}$ given a certain α. We clearly see from the plots that more activation is achieved, so to say, we have more negative $\Delta_{S,M}$, when we have rotation angle $\alpha = \pi/4$, while $\varphi_M \approx 11\pi/10$ rad leads to this minimum. Finally, since $\Delta_{12} = \Delta_{21} = 0$ in the considered limit of infinite temperature $\beta \to 0$, the previously presented conditions for state activation are not only necessary, but also sufficient. Hence, we see that for the whole range of $\varphi_M \in (\pi, 2\pi)$ activation is accomplished in the plots.

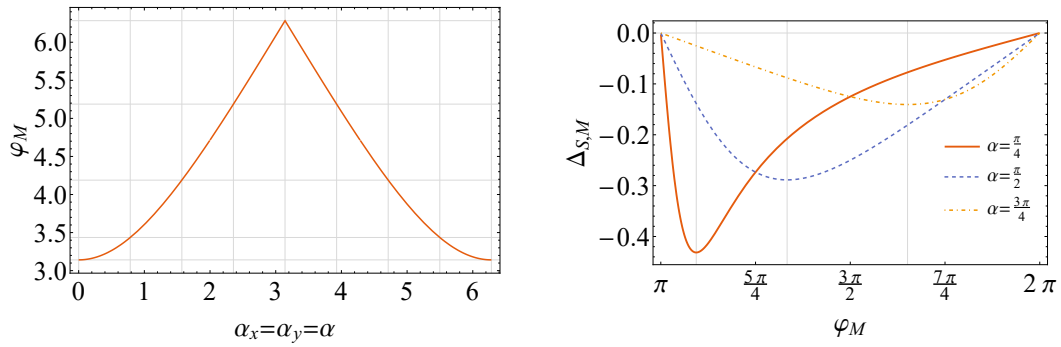

Figure 4.2: **Angle φ_M (radians) for which $\Delta_{S,M}$ is minimum as a function of $\alpha_x = \alpha_y = \alpha$ (left) and $\Delta_{S,M}$ as a function of the angle φ_M and for $\alpha = \pi/4, \pi/2, 3\pi/4$ (right).** In the plots the parameters are: $\theta_C = \pi/2$, $\varphi_C = 0$, $\omega = 1.0$, $\theta_M = \pi/2$ and $\beta \to 0$. Figure obtained from Ref. [23].

4.4.1.2 General $U(2)$ unitaries

The most general unitary operations in $\mathcal{L}(\mathcal{H}_S)$, where $\dim(\mathcal{H}_S) = 2$, are in the $U(2)$ group. These can be written in terms of rotations in the Bloch sphere in the following way [75]:

$$U_k = e^{i\alpha_k} R_z(\lambda_k) R_y(\gamma_k) R_z(\delta_k), \quad k = 1, 2 \tag{4.47}$$

The parameters $\alpha_{1,2}, \lambda_{1,2}, \gamma_{1,2}, \delta_{1,2}$ are in the range $[0, 2\pi]$, i.e. they are angles and R_y, R_z are rotation operators around the y and z axes of the Bloch sphere, respectively. Therefore, the previous scenario of rotations around the x and y axes of the Bloch sphere is a special case of these more general transformations.

Given the generality of the unitaries described by Eq. (4.47), obtaining a close, elegant and relatively short analytic expression for the internal energy difference is not achievable. Thus, we follow a more straightforward approach and analyze a numerical minimization of Δ_{QS} with fixed ω, β, $|t|$ and θ. For each combination of these physical parameters, we find combinations of λ_k, γ_k and δ_k (the α_k's cancel out when calculating the internal energy) that give a minimum $\min \Delta_{QS}$. Without loss of generality, we constrain the state of the control to be $|+\rangle_C$ ($\theta_C = \pi/2$, $\varphi_C = 0$).

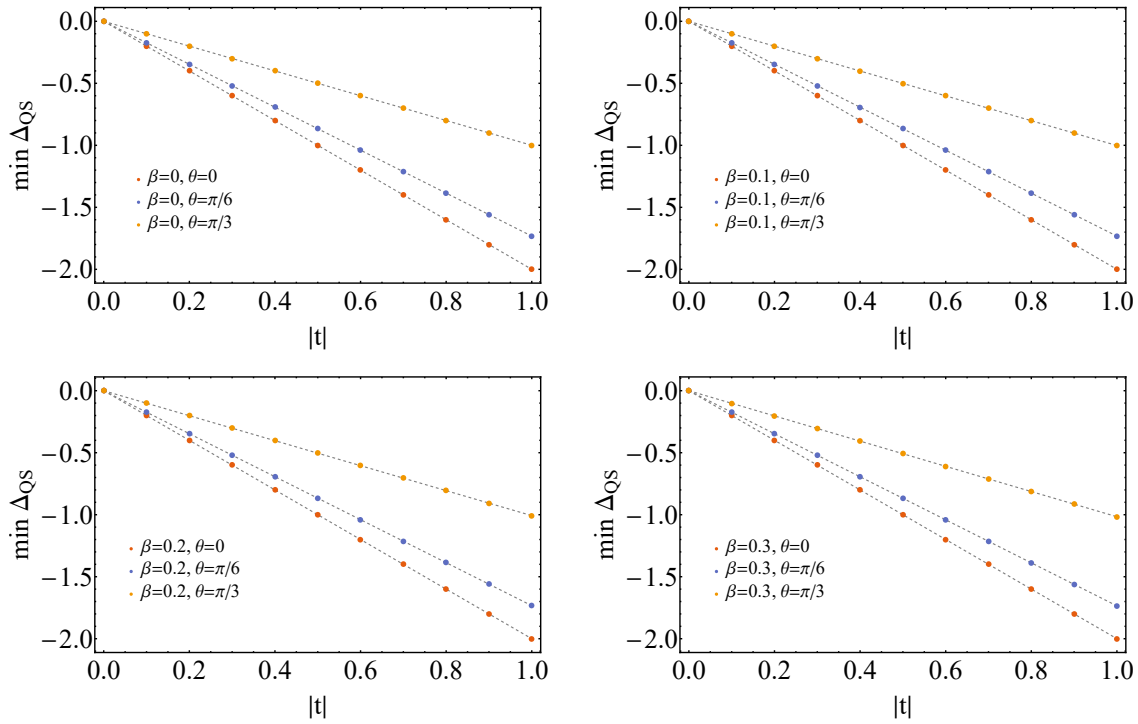

Figure 4.3: **Minimum $\min \Delta_{QS}$ for $U(2)$ unitaries as a function of $|t|$.** For the angles $\theta = 0, \pi/6$ and $\pi/3$, the minimization is done for the inverse temperatures: $\beta = 0.0$ (top left), $\beta = 0.1$ (top right), $\beta = 0.2$ (bottom left) and $\beta = 0.3$ (bottom right). Each point has a specific combination of $\lambda_{1,2}$, $\gamma_{1,2}$ and $\delta_{1,2}$ that leads to minimization of the internal energy variation. The dashed gray lines on the plots make evident the interesting fact that their slopes are *independent* of β. For all plots $\omega = 1.0$, $\theta_C = \pi/2$ and $\varphi_C = 0$. Figure partly obtained from Ref. [23].

In Fig. 4.3 one has the minimization results for four different inverse temperatures: $\beta = 0.0$ (top left), $\beta = 0.1$ (top right), $\beta = 0.2$ (bottom left) and $\beta = 0.3$ (bottom right). The exact values of the $\alpha_{1,2}, \lambda_{1,2}, \gamma_{1,2}, \delta_{1,2}$ that give the plotted minimum values are not important and therefore not shown. A very interesting feature that is readily noticed is that the slope of the dashed gray lines is *independent* of the inverse temperature β, they depend solely on the value of the phase θ of the non-diagonal elements of the Hamiltonian of the control. This can be understood by looking at the specific case in Eq. (4.38). We

have two terms, one dependent on β and one independent of it. In the case of general $U(2)$ rotations, we expect a similar decomposition and thus it is always possible to find a combination of rotation angles that cancels the term dependent on β and at the same time minimizes Δ_{QS}. Thus, we are allowed to set $\beta \to 0$ and get:

$$\Delta_{\text{QS}}^{\beta\to 0} = \left(\frac{12 - \epsilon(\lambda_1, \gamma_1, \delta_1, \lambda_2, \gamma_2, \delta_2)}{16}\right)|t|\cos\theta \tag{4.48}$$

with

$$\min \epsilon(\lambda_1, \gamma_1, \delta_1, \lambda_2, \gamma_2, \delta_2) = -20, \tag{4.49}$$

which, by being a constant, shows that $\min \Delta_{\text{QS}}$ is totally determined by $|t|$ and θ. Furthermore, we see that for all values of $|t|$ (except for $|t| = 0$, of course), it is always possible to activate the composite state system-control for some combinations of unitary angles.

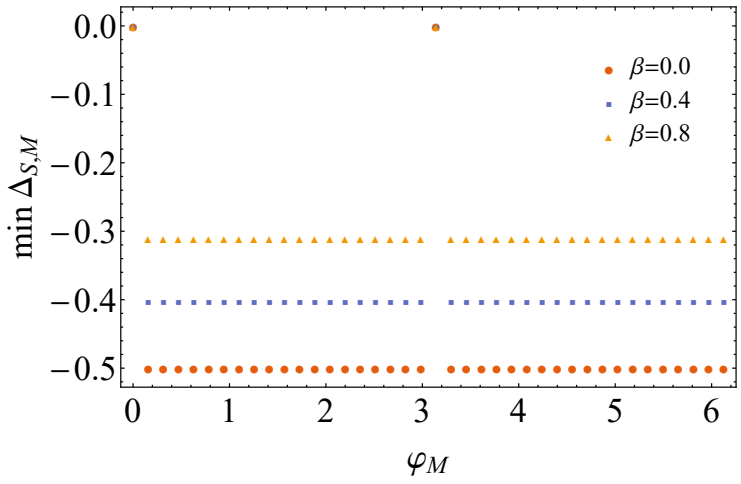

Figure 4.4: **Plot of min $\Delta_{S,M}$ for general $U(2)$ unitaries as a function of φ_M (radians).** Here we plot for three different inverse temperatures: $\beta = 0.0, 0.4$ and 0.8. We notice that for $\varphi_M = 0, \pi$, no state activation is possible ($\min \Delta_{S,M} = 0$), while for other values of φ_M the minimization gives always the same value of $\min \Delta_{S,M}$. We consider $\omega = 1.0$. Figure obtained from Ref. [23].

A similar numerical minimization can be done to the situation where one measures the control and post-selects the state of the system. Here we fix the initial state of the control to be again the $|+\rangle_C$ state ($\theta_C = \pi/2, \varphi_C = 0$) and the measurement state to be in the xy-plane of the Bloch sphere ($\theta_M = \pi/2$). In Fig. 4.4 is the plot of $\min \Delta_{S,M}$ as a function of the angle φ_M in radians. We see that for each chosen inverse temperature ($\beta = 0.0, 0.4$ and 0.8), the minimization procedure outside of the extreme points $\varphi_M = 0, \pi$, where no activation is possible, gives always the same value independent of φ_M. As we see that $\beta \to 0$ results in a more negative value than for finite temperatures $\beta > 0$, we set $\beta \to 0$ and obtain:

$$\Delta_{S,M}^{\beta\to 0} = \omega \frac{f(\lambda_1, \gamma_1, \delta_1, \lambda_2, \gamma_2, \delta_2)\sin\varphi_M}{32 + g(\lambda_1, \gamma_1, \delta_1, \lambda_2, \gamma_2, \delta_2)\cos\varphi_M}, \tag{4.50}$$

where $f(\lambda_1, \gamma_1, \delta_1, \lambda_2, \gamma_2, \delta_2)$ and $g(\lambda_1, \gamma_1, \delta_1, \lambda_2, \gamma_2, \delta_2)$ are complicated functions of the angles of the unitaries. Their numerical values, on the other hand, are:

$$\min f(\lambda_1, \gamma_1, \delta_1, \lambda_2, \gamma_2, \delta_2) = -16 \tag{4.51}$$

and

$$\min g(\lambda_1, \gamma_1, \delta_1, \lambda_2, \gamma_2, \delta_2) \approx -8.57. \tag{4.52}$$

4.4.2 Quantum harmonic oscillator

Another case that can be explored in the matter of state activation using the QS is to consider a quantum harmonic oscillator (QHO) as the system. This is the textbook case to treat continuous-variables (CVs) and can offer a considerable insight in physical platforms such as quantum optics setups, where the electromagnetic modes themselves can be seen as QHOs.

A convenient way to represent the Hamiltonian of a QHO is by using *creation* and *annihilation operators*, $a^\dagger$ and a, respectively. Thus,

$$H_S = \omega\left(a^\dagger a + \frac{\mathbb{1}_S}{2}\right), \tag{4.53}$$

where ω is the energy of each excitation/particle, $\mathbb{1}_S$ is the identity operator in $\mathcal{L}(\mathcal{H}_S)$ and the combination $a^\dagger a$ is known as the *number operator*, because it "counts" the number of excitations/particles in the system. Once again we take system and control to be resonant, something that does not constrain the generality of the results presented herein. Also, no interaction is considered to exist between S and C, then $H_{SC} = H_S \otimes \mathbb{1}_C + \mathbb{1}_S \otimes H_C$.

When it comes to the initial composite state, it is assumed to be a separable density operator $\Theta_\beta \otimes \rho_C$. It means that the system is in the Gibbs thermal state:

$$\Theta_\beta = \frac{e^{-\beta H_S}}{Z_S} = (1 - e^{-\beta\omega}) \sum_{n=0}^{\infty} e^{-\beta\omega n} |n\rangle\langle n|_S, \tag{4.54}$$

where $Z_S = \mathrm{tr}\{\exp(-\beta H_S)\}$ is the partition function, n is the number of excitations/particles and $|n\rangle_S$ is an eigenstate of $a^\dagger a$ with eigenvalue n; while the control is in the pure state $|\psi\rangle_C$ parameterized in the Bloch sphere.

4.4.2.1 Displacement operators

We first consider scenario where the unitaries U_1 and U_2 correspond to *displacement operators*. Hence [76]:

$$\begin{aligned} U_k &= D(\alpha_k) \\ &= \exp\left(\alpha_k a^\dagger - \alpha_k^* a\right), \qquad k = 1, 2 \end{aligned} \tag{4.55}$$

with $\alpha_k = |\alpha_k| e^{i\phi_k} \in \mathbb{C}$ being the complex displacement amplitudes. By direct calculation, we get:

$$\begin{aligned} \Delta_{\mathrm{QS}} &= \Delta_S + 2\,\mathrm{Re}\{\langle 0|\rho_C|1\rangle\langle 1|H_C|0\rangle(\chi - 1)\} \\ &= \Delta_S + \sin\theta_C\,\mathrm{Re}\left\{e^{i\varphi_C} t^*(\chi - 1)\right\}, \end{aligned} \tag{4.56}$$

where

$$\Delta_S = \cos^2\left(\frac{\theta_C}{2}\right)\mathcal{E}_{12} + \sin^2\left(\frac{\theta_C}{2}\right)\mathcal{E}_{21} - \mathcal{E}_S, \tag{4.57}$$

$$\mathcal{E}_{12} = \mathrm{tr}\{D(\alpha_2)D(\alpha_1)\,\Theta_\beta\,D^\dagger(\alpha_1)D^\dagger(\alpha_2)H_S\}, \tag{4.58}$$

$$\mathcal{E}_{21} = \mathrm{tr}\{D(\alpha_1)D(\alpha_2)\,\Theta_\beta\,D^\dagger(\alpha_2)D^\dagger(\alpha_1)H_S\}, \tag{4.59}$$

and

$$\begin{aligned}\mathcal{E}_S &= \mathrm{tr}\{\Theta_\beta H_S\}\\ &= \omega(1-e^{-\beta\omega})\sum_{n=0}^{\infty} e^{-\beta\omega n}\,\langle n|\left(a^\dagger a+\frac{\mathbb{1}}{2}\right)|n\rangle\\ &= \omega\left(\langle n\rangle_{\mathrm{th}}+\frac{1}{2}\right).\end{aligned} \tag{4.60}$$

The quantity

$$\langle n\rangle_{\mathrm{th}} = \frac{1}{e^{\beta\omega}-1}$$

is the *Bose-Einstein distribution* with zero chemical potential. Using the relation [76]:

$$D^\dagger(\alpha)\,a^\dagger D(\alpha) \equiv a^\dagger + \alpha^*,$$

and defining

$$\alpha' := \alpha_1 + \alpha_2, \tag{4.61}$$

we get the simplifications of Eqs. (4.58) and (4.59):

$$\mathcal{E}_{21} = \mathcal{E}_{12} = \mathcal{E}_S + \omega|\alpha'|^2. \tag{4.62}$$

Also, by means of the *braiding relation* between displacement operators [76]:

$$D(\alpha_2)D(\alpha_1) = \exp(\alpha_1^*\alpha_2 - \alpha_1\alpha_2^*)D(\alpha_1)D(\alpha_2), \tag{4.63}$$

we get

$$\begin{aligned}\chi &= \mathrm{tr}\{D(\alpha_2)D(\alpha_1)\,\Theta_\beta\,D^\dagger(\alpha_2)D^\dagger(\alpha_1)\}\\ &= \exp\left(\alpha_1^*\alpha_2-\alpha_1\alpha_2^*\right)\mathrm{tr}\{D(\alpha_1)D(\alpha_2)\,\Theta_\beta\,D^\dagger(\alpha_2)D^\dagger(\alpha_1)\}\\ &= \exp\left(\alpha_1^*\alpha_2-\alpha_1\alpha_2^*\right).\end{aligned} \tag{4.64}$$

Putting everything back together into Eq. (4.56), one gets:

$$\Delta_{\mathrm{QS}} = \omega|\alpha'|^2 + |t|\left(\cos\left(\theta-\varphi_C+2|\alpha_1||\alpha_2|\sin(\phi_1-\phi_2)\right)-\cos(\theta-\varphi_C)\right)\sin\theta_C. \tag{4.65}$$

This result reveals something: the inverse temperature β has *no* impact on the composite state system-control activation whatsoever. It happens, because putting back the result in Eq. (4.62) into Eq. (4.57) shows that $\mathcal{E}_S$, which is the only term left containing β, cancels out. Also, the *difference* between the displacement phases ϕ_1 and ϕ_2 is what matters, and not their absolute value. For instance, when the displacements are such that $\phi_1-\phi_2 = \pi\, m, m\in\mathbb{Z}$, ("parallel/anti-parallel" displacements):

$$\Delta_{\mathrm{QS}} > 0, \qquad \forall\omega, |\alpha'|, |t|, \theta, \theta_C, \varphi_C, \tag{4.66}$$

i.e., it is impossible to activate the composite state. On the other hand, for $\phi_1-\phi_2 = \pi/2$ activating the composite state system-control is achievable and it can be seen in Fig. 4.5,

where for larger $|t|$, the lower $|\alpha_1|$ and $|\alpha_2|$ are needed for activation. Moreover, consider then the case in which $\phi_1 - \phi_2 = \pi(2k-1)/2, k \in \mathbb{Z}$, $\theta = 0$, $|\alpha_1| = |\alpha_2| = |\alpha|$, $\theta_C = \pi/2$ and $\varphi_C = 0$. Then, the internal energy variation simplifies to:

$$\Delta_{\text{QS}} = 2\left(\omega|\alpha|^2 - |t|\sin^2\left(|\alpha|^2\right)\right), \tag{4.67}$$

whose plot is seen in Fig. 4.6 for a selection of $|t|$. Clearly, for non-zero $|t|$, as one increases $|\alpha|$, the internal energy difference eventually becomes negative and activation is possible. The curves are not monotonic: for a certain $|\alpha|_{\text{min}}$ we get minimum Δ_{QS} and if we further increase $|\alpha|$ the internal energy variation starts to increase, to the point that it gets positive again. The analytic expression for $|\alpha|_{\text{min}}$ is:

$$|\alpha|_{\text{min}} = \sqrt{\frac{\pi - \arcsin(\omega/|t|)}{2}}, \tag{4.68}$$

showing that solutions exist only for $\omega \leqslant |t|$ and when $|t| \gg \omega$ we have that $|\alpha|_{\text{min}} \approx \sqrt{\pi/2}$.

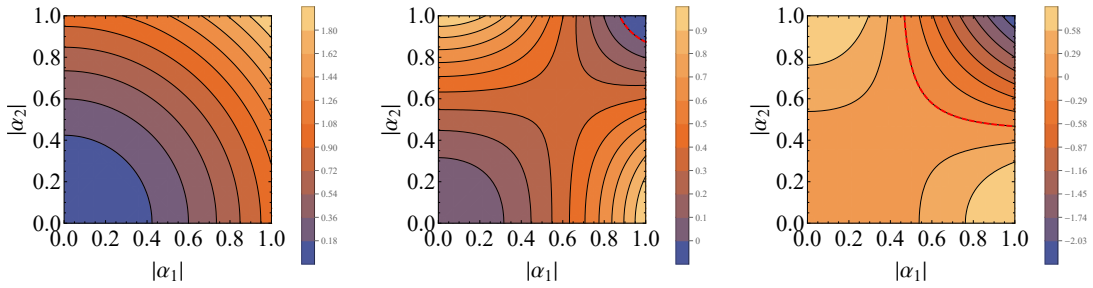

Figure 4.5: **Density plots of Δ_{QS} as a function of $|\alpha_1|$ and $|\alpha_2|$, when unitaries are displacemenets operators.** (Left) $|t| = 0$, (center) $|t| = 1.5$ and (right) $|t| = 3.0$. The parameters are: $\omega = 1.0$, $\theta_C = \pi/2$, $\varphi_C = 0$, $\theta = 0$ and $\phi_1 - \phi_2 = \pi/2$. The dashed red lines delimit where the internal energy difference is null and thus is a separation between activation and no activation of passive states. Figure obtained from Ref. [23].

Now, to consider activation only of the system S, we treat post-selection of its state by measuring the control C. The measurement parameterized on the Bloch sphere (Eq. (4.23)) gives us the general expression for the internal energy difference shown in Eq. (4.29). Using the displacement operators in place of the unitaries U_1 and U_2, we have that:

$$\begin{aligned}
\mathcal{F}_S &= \text{tr}\{D(\alpha_2)D(\alpha_1)\,\Theta_\beta\, D^\dagger(\alpha_2)D^\dagger(\alpha_1)H_S\} \\
&= \chi\,\text{tr}\{D(\alpha_1)D(\alpha_2)\,\Theta_\beta\, D^\dagger(\alpha_2)D^\dagger(\alpha_1)H_S\} \\
&= \chi\mathcal{E}_{21} \\
&= \chi(\mathcal{E}_S + \omega|\alpha'|^2),
\end{aligned} \tag{4.69}$$

thus:

$$\Delta_F = \chi\omega|\alpha'|^2. \tag{4.70}$$

The "causally ordered" terms $\mathcal{E}_{12}$ and $\mathcal{E}_{21}$ are the same as in the no-measurement scenario, hence:

$$\Delta_{12} = \Delta_{21} = \omega|\alpha'|^2. \tag{4.71}$$

The post-selected internal energy difference of the system is then:

$$\Delta_{S,M} = \omega|\alpha'|^2 \geqslant 0, \qquad \forall\theta_C, \varphi_C, \theta_M, \varphi_M. \tag{4.72}$$

This striking result tells us that, when using displacement operators in a QS setup, measuring the control never can lead to activation of the state of the system, for whatever measurement state. It is a direct result of the peculiar commutation relation between two displacement operators,

$$[D(\alpha_1), D(\alpha_2)]_- = (1 - \chi)D(\alpha_1)D(\alpha_2), \tag{4.73}$$

which means that applying in different causal orders displacements to a passive state (in our case the Gibbs thermal state) leads to final states differing only by a global phase χ. It does not matter which measurement basis is chosen for the control, the final state will be some convex combination of passive states. It is important to note, however, that previously we could activate the composite state system-control, because the Hamiltonian of the control had non-diagonal terms in the computational basis. In the post-selection case, this resource is not present and the state cannot be activated.

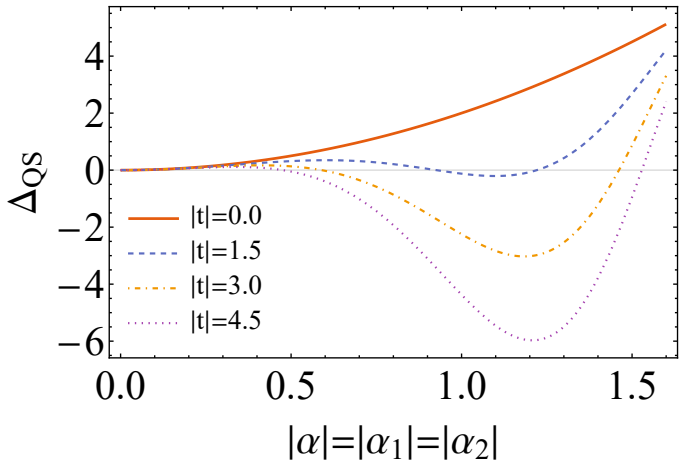

Figure 4.6: **Plot of Δ_{QS} when the unitaries are displacement operators as a function of $|\alpha| = |\alpha_1| = |\alpha_2|$ and for different $|t|$.** Activation of the composite state is achievable for a limited range of values of $|\alpha|$, where a $|\alpha|_{\min}$ leads to minimum Δ_{QS}. Here $\omega = 1.0$, $\theta = \varphi_C = 0$ and $\phi_1 - \phi_2 = \theta_C = \pi/2$. Figure obtained from Ref. [23].

4.4.2.2 Displacement and squeeze operators

In quantum optics setups, another important unitary operation is extensively used: the *squeeze operator*. It has an interesting feature of being non-linear in the creation/annihilation operators, more specifically, it is of second-order. We then keep U_1 as a displacement operator:

$$U_1 = D(\alpha) = \exp\left(\alpha a^\dagger - \alpha^* a\right), \tag{4.74}$$

where $\alpha = |\alpha|e^{i\phi} \in \mathbb{C}$ is the displacement complex amplitude, while we change U_2 to be a squeeze operator [76]:

$$U_2 = S(z) = \exp\left(\frac{1}{2} z a^\dagger a^\dagger - \frac{1}{2} z^* a\, a\right), \tag{4.75}$$

with $z = |z|e^{i\xi} \in \mathbb{C}$ being the squeeze complex amplitude.

The internal energy difference of system-control is then:

$$\Delta_{\mathrm{QS}} = \Delta_S + \sin\theta_C \,\mathrm{Re}\{e^{i\varphi_C} t^*(\chi - 1)\}, \tag{4.76}$$

with

$$\Delta_S = \cos^2\left(\frac{\theta_C}{2}\right)\mathcal{E}_{12} + \sin^2\left(\frac{\theta_C}{2}\right)\mathcal{E}_{21} - \mathcal{E}_S, \tag{4.77}$$

and

$$\mathcal{E}_{12} = \mathrm{tr}\{S(z)D(\alpha)\,\Theta_\beta\, D^\dagger(\alpha)S^\dagger(z)H_S\}, \tag{4.78}$$

$$\mathcal{E}_{21} = \mathrm{tr}\{D(\alpha)S(z)\,\Theta_\beta\, S^\dagger(z)D^\dagger(\alpha)H_S\}, \tag{4.79}$$

$$\chi = \mathrm{tr}\{S(z)D(\alpha)\,\Theta_\beta\, S^\dagger(z)D^\dagger(\alpha)\}. \tag{4.80}$$

The Baker-Campbell-Hausdorff (BCH) expansion of sandwiched displacement and squeeze operators with the creation/annihilation operators [76],

$$D^\dagger(\alpha)a^\dagger D(\alpha) = a^\dagger + \alpha^*, \qquad D^\dagger(\alpha)aD(\alpha) = a + \alpha$$

$$S^\dagger(z)a^\dagger S(z) = a^\dagger\cosh|z| + ae^{-i\xi}\sinh|z|, \qquad S^\dagger(z)aS(z) = a\cosh|z| + a^\dagger e^{i\xi}\sinh|z|$$

lead to

$$\mathcal{E}_{21} = \omega|\alpha|^2 + \frac{\omega}{2}\left(2\langle n\rangle_{\mathrm{th}} + 1\right)\cosh(2|z|) \tag{4.81}$$

$$\mathcal{E}_{12} = \mathcal{E}_{21} + \omega|\alpha|^2\cos(\xi - 2\phi)\sinh(2|z|). \tag{4.82}$$

Thus,

$$\begin{aligned}\Delta_S = &-\frac{\omega}{2} + \omega|\alpha|^2 + \frac{\omega\cosh(2|z|)}{2} + 2\omega\,\langle n\rangle_{\mathrm{th}}\sinh^2|z| \\ &+ \omega|\alpha|^2\cos^2\left(\frac{\theta_C}{2}\right)\cos(\xi - 2\phi)\sinh(2|z|).\end{aligned} \tag{4.83}$$

The calculation of χ is more demanding and requires the use of the braiding relation between displacement and squeeze operator [77]:

$$D(\alpha)S(z) = S(z)D(\gamma),$$

where

$$\gamma = |\alpha|e^{i\phi}\cosh|z| - |\alpha|e^{i(\xi-\phi)}\sinh|z|.$$

With the help of the *P-representation* of the Gibbs thermal state [76],

$$\Theta_\beta = \int P_T(\eta)\,|\eta\rangle\langle\eta|_S\,\mathrm{d}^2\eta,$$

with $|\eta\rangle_S$ being a *coherent state* and

$$P_T(\eta) = \frac{1}{\pi\langle n\rangle_{\mathrm{th}}}\exp\left(-\frac{|\eta|^2}{\langle n\rangle_{\mathrm{th}}}\right), \tag{4.84}$$

we get:

$$\begin{aligned}\chi &= \int P_T(\eta)\,\langle\eta|\,D^\dagger(\gamma)D(\alpha)\,|\eta\rangle\,\mathrm{d}^2\eta \\ &= \int P_T(\eta)\exp\left(\frac{\eta}{2}(\gamma^* - \alpha^*)\right)\exp\left(\frac{\eta^*}{2}(\alpha - \gamma)\right)\langle\eta + \gamma|\eta + \alpha\rangle\,\mathrm{d}^2\eta.\end{aligned} \tag{4.85}$$

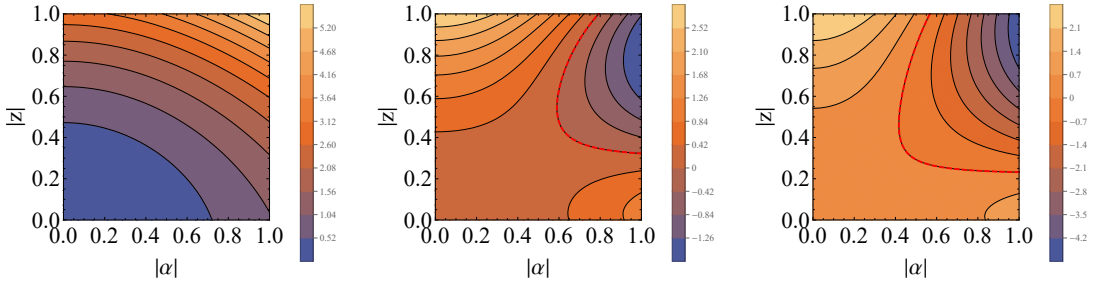

Figure 4.7: **Plots of Δ_{QS} when the unitaries are the displacement and squeeze operators as a function of $|\alpha|$ and $|z|$.** (Left) $|t| = 0$, (center) $|t| = 20$ and (right) $|t| = 30$. Dashed red lines show when $\Delta_{\mathrm{QS}} = 0$. Parameters are: $\omega = \beta = 1.0$, $\theta_C = \pi/2$, $\varphi_C = 0$ ($\rho_C = |+\rangle\langle+|_C$) and $\theta = \phi = \xi = 0$. Figure obtained from Ref. [23].

Knowing that any two coherent states $|\alpha\rangle$ and $|\beta\rangle$ have the inner product [76]:

$$\langle\alpha|\beta\rangle = \exp\left(\alpha^*\beta - \frac{|\alpha|^2}{2} - \frac{|\beta|^2}{2}\right),$$

the evaluation of the integral in Eq. (4.85) gives:

$$\chi = \langle\gamma|\alpha\rangle \exp\left(-\langle n\rangle_{\mathrm{th}} |\alpha - \gamma|^2\right). \tag{4.86}$$

Putting together Eqs. (4.81), (4.82), (4.83) and (4.86) into Eq. (4.76), we get:

$$\begin{aligned}\Delta_{\mathrm{QS}} = {} & \frac{\omega}{2} + \omega|\alpha|^2 + \frac{\omega\cosh(2|z|)}{2} + 2\omega\langle n\rangle_{\mathrm{th}}\sinh^2|z| \\ & + \omega|\alpha|^2\cos^2\left(\frac{\theta_C}{2}\right)\cos(\xi - 2\phi)\sinh(2|z|) + |t|\sin\theta_C\,\mathrm{Re}\{e^{i(\varphi_C-\theta)}(\chi - 1)\}.\end{aligned} \tag{4.87}$$

In Fig. 4.7 the latter expression is plotted for different values of $|t|$, and as a function of $|\alpha|$ and $|z|$. It is clearly seen that, in contrast to the case where both unitaries are the displacement operators, here one needs a considerably larger value of $|t|$ to activate the composite state system-control (the same energy scale $\omega = \beta = 1.0$ in both situations).

Now we check what happens when we measure the control in a state parameterized as in Eq. (4.23). The internal energy difference of the system is again:

$$\begin{aligned}\Delta_{S,M} = \frac{1}{N_M}\Bigg(&\cos^2\left(\frac{\theta_C}{2}\right)\cos^2\left(\frac{\theta_M}{2}\right)\Delta_{12} + \sin^2\left(\frac{\theta_C}{2}\right)\sin^2\left(\frac{\theta_M}{2}\right)\Delta_{21} \\ &+ \frac{1}{2}\sin\theta_C\sin\theta_M\,\mathrm{Re}\{\Delta_F e^{i(\varphi_C+\varphi_M)}\}\Bigg),\end{aligned} \tag{4.88}$$

with

$$N_M = \frac{1}{2}(1 + \cos\theta_C\cos\theta_M + \sin\theta_C\sin\theta_M\,\mathrm{Re}\{\chi e^{i(\varphi_C+\varphi_M)}\}), \tag{4.89}$$

but now:

$$\Delta_{12} := \mathrm{tr}\{S(z)D(\alpha)\,\Theta_\beta\,D^\dagger(\alpha)S^\dagger(z)\} - \mathcal{E}_S, \tag{4.90}$$

$$\Delta_{21} := \mathrm{tr}\{D(\alpha)S(z)\,\Theta_\beta\,S^\dagger(z)D^\dagger(\alpha)\} - \mathcal{E}_S, \tag{4.91}$$

and

$$\Delta_F := \mathcal{F}_S - \chi \mathcal{E}_S \tag{4.92}$$

with $\mathcal{F}_S$ being

$$\begin{aligned} \mathcal{F}_S &:= \mathrm{tr}\{S(z)D(\alpha)\,\Theta_\beta\, S^\dagger(z)D^\dagger(\alpha)H_S\} \\ &= \omega\frac{\chi}{2} + \mathrm{tr}\{S(z)D(\alpha)\,\Theta_\beta\, S^\dagger(z)D^\dagger(\alpha)a^\dagger a\}. \end{aligned} \tag{4.93}$$

By using the same braiding relation as before, we get:

$$\mathcal{F}_S = \omega\frac{\chi}{2} + \int P_T(\eta)\,\langle\eta|D^\dagger(\gamma)\,a^\dagger a\,D(\alpha)|\eta\rangle_S\,\mathrm{d}^2\eta, \tag{4.94}$$

with

$$\begin{aligned} \langle\eta|D^\dagger(\gamma)a^\dagger aD(\alpha)|\eta\rangle_S = \exp\left(\frac{\eta}{2}(\gamma^* - \alpha^*)\right)\exp\left(\frac{\eta^*}{2}(\alpha-\gamma)\right)(\eta^*+\gamma^*)(\eta+\alpha) \\ \times\,\langle\eta+\gamma|\eta+\alpha\rangle, \end{aligned} \tag{4.95}$$

which is obtained from the fact that coherent states are eigenvectors of the annihilation operator: $a|\alpha\rangle = \alpha|\alpha\rangle$. Integration on the complex plane (η has real and imaginary parts) of the previous integral gives:

$$\mathcal{F}_S = \omega\chi\left[\frac{1}{2} + \gamma^*\alpha + (1 + 2\gamma^*\alpha - |\alpha|^2 - |\gamma|^2)\langle n\rangle_{\mathrm{th}} - |\alpha-\gamma|^2\langle n\rangle_{\mathrm{th}}^2\right], \tag{4.96}$$

thus

$$\Delta_F = \omega\chi\left[\gamma^*\alpha + (2\gamma^*\alpha - |\gamma|^2 - |\alpha|^2)\langle n\rangle_{\mathrm{th}} - |\alpha-\gamma|^2\langle n\rangle_{\mathrm{th}}^2\right]. \tag{4.97}$$

Moreover,

$$\Delta_{21} = \omega|\alpha|^2 + \omega\,\langle n\rangle_{\mathrm{th}}(\cosh(2|z|) - 1) + \omega\sinh^2|z|, \tag{4.98}$$

$$\Delta_{12} = \Delta_{21} + \omega|\alpha|^2\cos(\xi - 2\phi)\sinh(2|z|), \tag{4.99}$$

and Eq. (4.88) becomes:

$$\begin{aligned} \Delta_{S,M} = \frac{1}{N_M}\Bigg[&\frac{\omega}{4}(1 + \cos\theta_C\cos\theta_M)(2|\alpha|^2 + (2\langle n\rangle_{\mathrm{th}} + 1)(\cosh(2|z|) - 1)) \\ &+ \omega|\alpha|^2\cos^2\left(\frac{\theta_C}{2}\right)\cos^2\left(\frac{\theta_M}{2}\right)\cos(\xi - 2\phi)\sinh(2|z|) \\ &+ \frac{1}{2}\sin\theta_C\sin\theta_M\,\mathrm{Re}\{\Delta_F e^{i(\varphi_C+\varphi_M)}\}\Bigg]. \end{aligned} \tag{4.100}$$

For a better interpretation of this result, we shall consider two specific combinations of ϕ

and ξ. First, for $\xi - 2\phi = 0$:

$$\begin{aligned}\Delta^0_{S,M} = \frac{1}{N^0_M}\Bigg\{&\frac{\omega}{4}(1+\cos\theta_C\cos\theta_M)[2|\alpha|^2 + (2\langle n\rangle_{\text{th}}+1)(\cosh(2|z|)-1)] \\ &+ \omega|\alpha|^2\cos^2\left(\frac{\theta_C}{2}\right)\cos^2\left(\frac{\theta_M}{2}\right)\sinh(2|z|) \\ &- \frac{\omega|\alpha|^2}{2}\sin\theta_C\sin\theta_M\exp\left(-2|z| - |\alpha|^2 e^{-|z|}(2\langle n\rangle_{\text{th}}+1)(\cosh|z|-1)\right) \\ &\times\left[\langle n\rangle^2_{\text{th}}(e^{2|z|}-2e^{|z|}+1) + \langle n\rangle_{\text{th}}(e^{2|z|}-2e^{|z|}+|\alpha|^2e^{-2|z|}) - e^{|z|}\right] \\ &\times\cos(\varphi_C+\varphi_M)\Bigg\},\end{aligned} \tag{4.101}$$

where

$$\begin{aligned}N^0_M =&\frac{1}{2}\Bigg(1+\cos\theta_C\cos\theta_M+\sin\theta_C\sin\theta_M \\ &\times\exp\left(-2|\alpha|^2\sinh^2\left(\frac{|z|}{2}\right)(\cosh|z|-\sinh|z|)\right)\cos(\varphi_C+\varphi_M)\Bigg),\end{aligned} \tag{4.102}$$

while for $\xi - 2\phi = \pi$:

$$\begin{aligned}\Delta^\pi_{S,M} = \frac{1}{N^\pi_M}\Bigg\{&\frac{\omega}{4}(1+\cos\theta_C\cos\theta_M)[2|\alpha|^2 + (2\langle n\rangle_{\text{th}}+1)(\cosh(2|z|)-1)] \\ &- \omega|\alpha|^2\cos^2\left(\frac{\theta_C}{2}\right)\cos^2\left(\frac{\theta_M}{2}\right)\sinh(2|z|) \\ &- \frac{\omega|\alpha|^2}{2}\sin\theta_C\sin\theta_M\exp\left(-\frac{|\alpha|^2}{2}(e^{|z|}-1)^2(2\langle n\rangle_{\text{th}}+1)\right) \\ &\times\left[\langle n\rangle^2_{\text{th}}(e^{2|z|}-2e^{|z|}+1) + \langle n\rangle_{\text{th}}(|\alpha|^2e^{4|z|}-2e^{|z|}+1) - e^{|z|}\right] \\ &\times\cos(\varphi_C+\varphi_M)\Bigg\},\end{aligned} \tag{4.103}$$

in which

$$\begin{aligned}N^\pi_M =&\frac{1}{2}\Bigg(1+\cos\theta_C\cos\theta_M+\sin\theta_C\sin\theta_M \\ &\times\exp\left(-\frac{|\alpha|^2}{2}(e^{|z|}-1)^2(2\langle n\rangle_{\text{th}}+1)\right)\cos(\varphi_C+\varphi_M)\Bigg).\end{aligned} \tag{4.104}$$

Plots of Eqs. (4.101) and (4.103) are found in Figs. 4.8 and 4.9, as functions of $|\alpha|$ and $|z|$, respectively. In the former, we get that only when the measurement state is $|-\rangle_C$ ($\theta_M = \pi/2$, $\varphi_M = \pi$) one is capable of activating the state of the system. This situation, nonetheless, must be taken with much care, as N^0_M converges to zero faster than the numerator of $\Delta^0_{S,M}$ for small $|\alpha|$ and $|z|$, leading to divergences. In the latter case, on the other hand, for all chosen measurement angles (fixed $\theta_M = \pi/2$ and $\varphi_M = 0, \pi/2, \pi, 3\pi/2$) one finds some set of parameter values where activation of the state of the system is achievable. Once again, when one measures the control in $|-\rangle_C$, divergences occur, due to the fast convergence of the denominator N^π_M to zero.

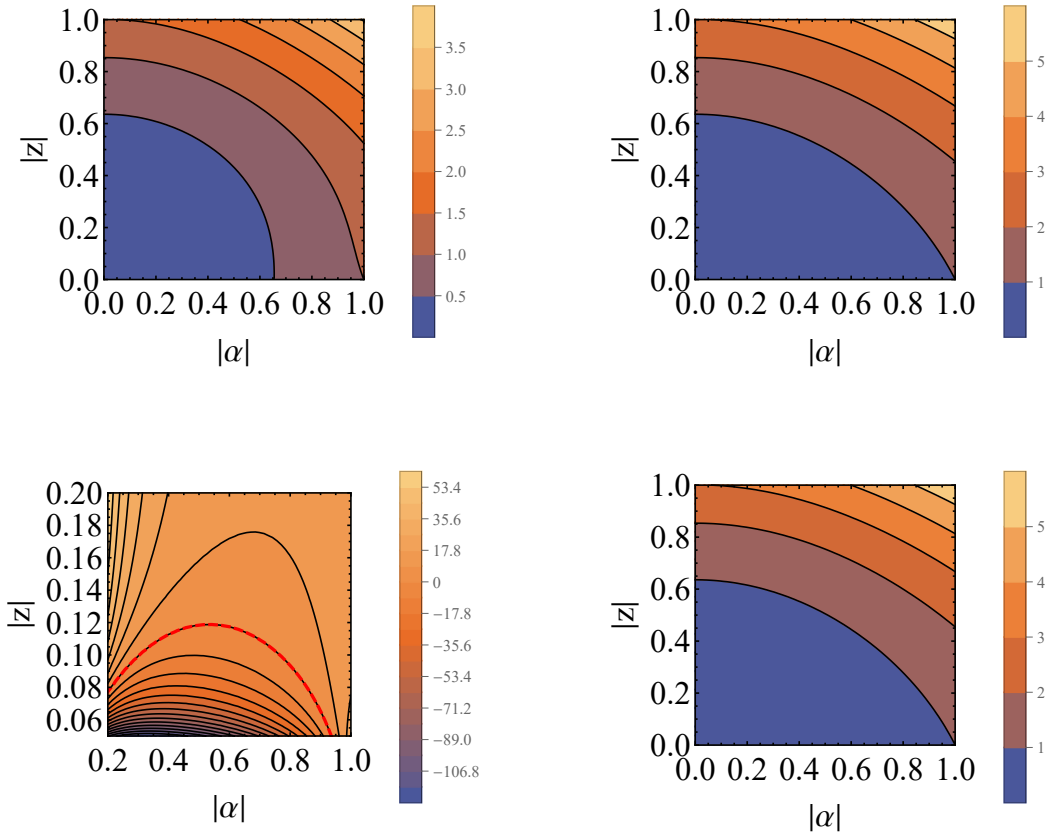

Figure 4.8: **Plots of $\Delta^0_{S,M}$ as a function of $|\alpha|$ and $|z|$, when the unitaries are the displacement operator and the squeeze operator, and $\xi - 2\phi = 0$.** (Top left) $\varphi_M = 0$, (top right) $\varphi_M = \pi/2$, (bottom left) $\varphi_M = \pi$, (bottom right) $\varphi_M = 3\pi/2$. Here the only scenario where activation happens is for $\varphi_M = \pi$, however one must take care of the fact that there is a steep divergence for small $|\alpha|$ and $|z|$. Parameters are: $\omega = \beta = 1.0$, $\theta_C = \pi/2$, $\varphi_C = 0$ and $\theta_M = \pi/2$. Figure obtained from Ref. [23].

Lastly, consider that the temperature tends to zero, what corresponds to $\beta \to \infty$, thus:

$$\langle n \rangle_{\text{th}} \to 0. \tag{4.105}$$

This means that the mean occupation number is zero and the Gibbs thermal state tends to:

$$\lim_{\beta \to \infty} \Theta_\beta \to |0\rangle\langle 0|_S . \tag{4.106}$$

Taken into account these simplifications, we turn back to Eqs. (4.101) and (4.103), simplify them and plot the final expressions as functions of $|\alpha| = |z|$ in Fig. 4.10. Interestingly, now that $\beta \to \infty$, no activation of the state of the system is possible when $\xi - 2\phi = 0$ (the divergence for $\theta_M = \pi/2$ and $\varphi_M = \pi$ persists). Nevertheless, when we pass to the case where $\xi - 2\phi = \pi$, whatever is the chosen measurement angle φ_M (for fixed $\theta_M = \pi/2$), the internal energy difference of the system can be negative, that is, activation is achieved. Also, in both plots one notices that the curves for $\varphi_M = \pi/2$ and $\varphi_M = 3\pi/2$ match each

other. These results reinforce that the combination of values of ξ and ϕ changes drastically the activation capabilities of our setup.

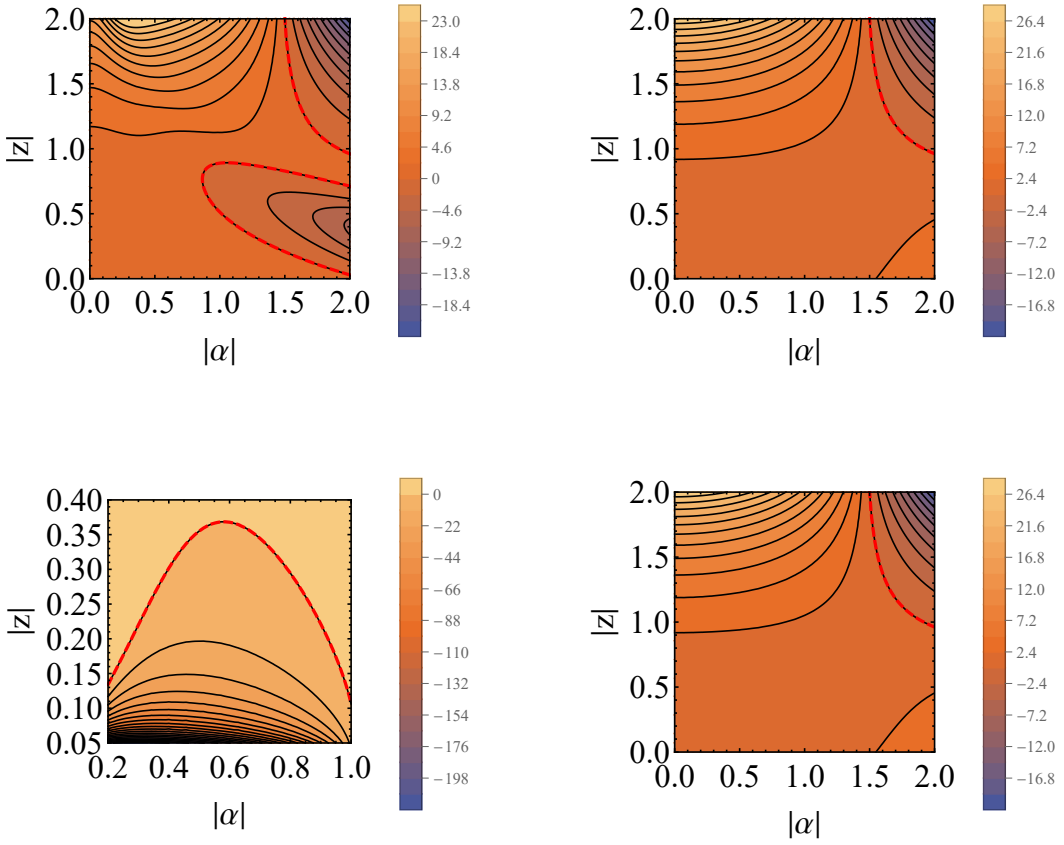

Figure 4.9: **Plots of $\Delta^{\pi}_{S,M}$ as a function of $|\alpha|$ and $|z|$, when the unitaries are the displacement operator and the squeeze operator, and $\xi - 2\phi = \pi$.** (Top left) $\varphi_M = 0$, (top right) $\varphi_M = \pi/2$, (bottom left) $\varphi_M = \pi$, (bottom right) $\varphi_M = 3\pi/2$. For all chosen measurement states, activation of the system is possible after post-selecting the control. As before, when $\varphi_M = \pi$ one finds a delicate scenario, since for small $|\alpha|$ and $|z|$ a divergence is found. Parameters are: $\omega = \beta = 1.0$, $\theta_C = \pi/2$, $\varphi_C = 0$ and $\theta_M = \pi/2$. Figure obtained from Ref. [23].

In chapter, we presented the work of Ref. [23], where the activation of passive states using the quantum switch (QS) was scrutinized. In "standard" quantum thermodynamics, unitaries are not capable of activating a passive state [68–71]. Starting from the work in Ref. [20], the question of whether the quantum switch (QS) [3, 7–10, 13–17, 78–93], an application of superposition of causal orders (SCO), which itself is a constrained version of indefinite causal order (ICO), started to be explored. Here we expanded this endeavour, by:

- Showing clearly that the QS *cannot* activate passive states by itself. The essential point here is that the QS enables extra resources to be used for state activation. Notably, non-diagonal elements in the Hamiltonian of the control in the computational basis and coherence in the initial state of the control are of fundamental impor-

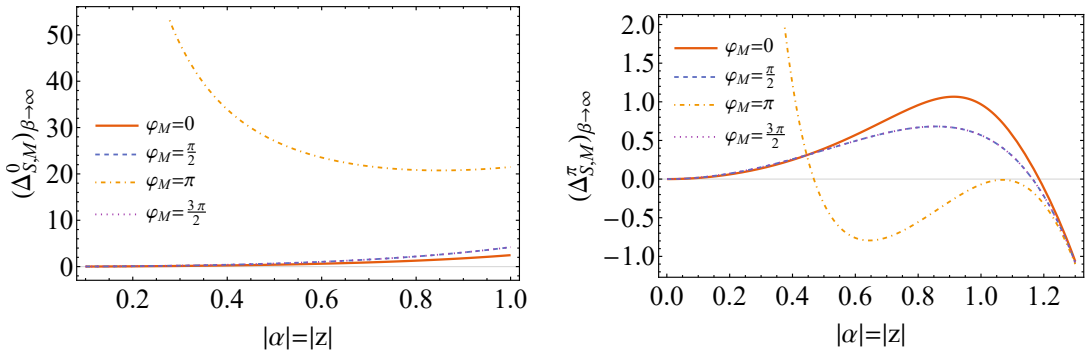

Figure 4.10: **Plots of $\Delta_{S,M}$ when the unitaries are the displacement operator and the squeeze operator, as a function of $|\alpha| = |z|$ and for $\beta \to \infty$.** (Left) $\xi - 2\phi = 0$ and (right) $\xi - 2\phi = \pi$. In each we have plots for different values of φ_M: $0, \pi/2, \pi$ and $3\pi/2$. Here we see that for $\xi - 2\phi = 0$ no state activation is achieved irrespective of φ_M. However, for $\xi - 2\phi = \pi$ for all possible φ_M activation can be done for some $|\alpha| = |z|$. In both left and right plots, the curves of $\varphi_M = \pi/2$ and $\varphi_M = 3\pi/2$ coincide and for $|\alpha| = |z| \to 0$ there is divergence of $\Delta^{0,\pi}_{S,M}$. Parameters are: $\omega = 1.0$, $\theta_C = \pi/2$, $\varphi_C = 0$ and $\theta_M = \pi/2$. Figure obtained from Ref. [23].

tance here. The latter has more prominence, since it is always needed, whether we measure the control or not;

- Finding *necessary* but not *sufficient* conditions for state activation. These conditions are obtained from direct inspection of the internal energy difference before and after applying the QS, and checking what is needed for it to be negative;
- Applying the basic framework to significant examples:
  - A system consisting of a qubit (two-level system), to which rotations around the Bloch sphere are the unitaries that are superposed through the QS. In a more specific scenario, only rotations around the x and y axes are considered, while in the most generic case unitaries of the $U(2)$ group (which themselves are combinations of rotations);
  - A system made of a quantum harmonic oscillator (QHO), a suitable mathematical model for continuous-variable (CV) systems. Two different scenarios were tested. First, both unitaries of the QS were displacement operators. In the second, one unitary is a displacement operator and the other is a squeeze operator.

Beyond the general proof of the "non-resourcefulness" of the QS for thermodynamic tasks by itself, needing extra input from the side of the control, through the analysis of the specific cases it becomes obvious that using the QS for the activation of passive states is *very* case-sensitive. Changing the dimensionality of the system strongly affects the behaviour for asymptotic temperature ($\beta = 1/T \to 0$ or $\beta = 1/T \to \infty$), at the same time that the other combination of physical parameters changes considerably what are the measurement states that allow state activation. Lastly, to our best knowledge, studying CV systems in the context of ICO was only done before in Refs. [66, 67].

Chapter 5

Quantum switch with open control dynamics

"A man who is certain he is right is almost sure he is wrong."
— Michael Faraday.

Even though closed quantum systems are extremely useful for understanding fundamental physics and have deemed us with plethora of new phenomena to be found in the laboratory, they are not always realistic. Quantum systems are ultimately coupled with their surroundings, which generally are very complicated arrangements of degrees-of-freedom (DOFs) known as *environment*. Even when a natural coupling is negligible, an external observer (classical, macroscopic object) that wants to learn something from a quantum system must eventually interact with it to extract some information. This indeed has a great overlap with the so-called "measurement problem of quantum mechanics" [41], a conceptual complication in the foundations of quantum theory for a century[1]. We keep ourselves to less philosophical enterprises and focus on the practical problem of physical systems described by quantum mechanics that couple with external DOFs (environment) and undergo processes generically known as *decoherence*.

From the possible ways of exploring the time evolution of a quantum system when interacting with an environment (e.g. quantum master equations in the Born-Markov and secular approximations [95]), here we choose to follow a more direct approach which does not rely on approximations *ab initio*. The *collisional model* framework[2] [31–40] relies on breaking the environment into small and identical pieces – *ancillae* – which interact for a definite time one-by-one with the quantum system being studied. These ancillae are thrown away after each interaction. Thus we have a great amount of freedom, because we can chose: the state of the environment ancillae, the interaction Hamiltonian and the

[1]The standard interpretation of quantum mechanics, known as the "Copenhagen interpretation" [41, 94], puts by hand the *Born rule* for measurement outcome probabilities and assumes the notion of "wave function collapse", object of heated debates until nowadays.

[2]The first papers that proposed the collisional model framework called it "repeated interactions."

time interval of each interaction. This can be explored for modelling a vast number of situations, from weak to strong interactions, as well as from "classical" environments (thermal) to "quantum" environments (containing some resource, e.g. quantum coherence). As shown in the literature [37], the collisional model framework is compatible with the more traditional way of treating open quantum dynamics, i.e. *Markovian master equations* [95].

Thus, in such a manner of modelling open system dynamics, we look at the previously presented quantum switch (QS) in Chapter 3 and ask ourselves how it is affected by the surrounding environment. More specifically, we scrutinize effects of a *thermal* environment on the control DOF. First, we choose this kind of environment, which corresponds to ancillae in the *Gibbs thermal state*, because it provides the best approximation for a thermal bath with fixed internal energy (state of maximum entropy). Second, we consider solely open dynamics of the control, since it is the DOF which determines the superposition of causal orders (SCO) in the QS and we want to attest how the post-selection of a control which interacted with the environment affects the final state of the quantum system. Here lies a very important point to be emphasized: the post-selection of the control is at the same time crucial and a delicate issue when one uses the QS[3]. This will become evident as we go through this chapter.

As a warm-up for the rest of the chapter, we start in Section 5.1 with a summarized presentation of the collisional model framework, its main assumptions and equations, as well as a short comment on its connection to quantum master equations. Then, in Section 5.2 we consider a generic QS putting in superposition two arbitrary quantum channels, in which a collisional model describes the interaction of the control with a surrounding thermal environment. Furthermore, the general expressions herein presented are applied to different cases in Sec. 5.3: (i) when the quantum channels have as *Kraus operators* projectors which are sets of mutually unbiased bases (MUB) and (ii) the QS-based refrigerator of Ref. [18].

5.1 Collisional model for open system dynamics

The collisional model relies on the simplifying assumption of two-body interactions between a quantum system and an environment that is then broken down to small pieces – ancillae – in a fixed state. In our case we want to study temperature-related effects, thus the ancillae are taken to be in the Gibbs thermal state:

$$\Theta_E := \frac{e^{-\beta_E H_E}}{Z_E}, \tag{5.1}$$

where $\beta_E = 1/T_E$, H_E and $Z_E = \mathrm{tr}\{\exp(-\beta_E H_E)\}$ are the inverse temperature, the Hamiltonian and the partition function of the thermal environment, respectively. We assume that such an environment, also called a *bath*, is much larger than the quantum system S under study and for all practical purposes it is an *infinite* source of thermal ancillae at the same inverse temperature β_E. Each of these thermal units comes in sequence to interact with a quantum system S, as shown in Fig. 5.1 (a). After $n-1$ interactions ("collisions"),

[3] As it was discussed in Chapter 4, based in Ref. [23], one can also harvest resources from the QS without post-selecting the control DOF.

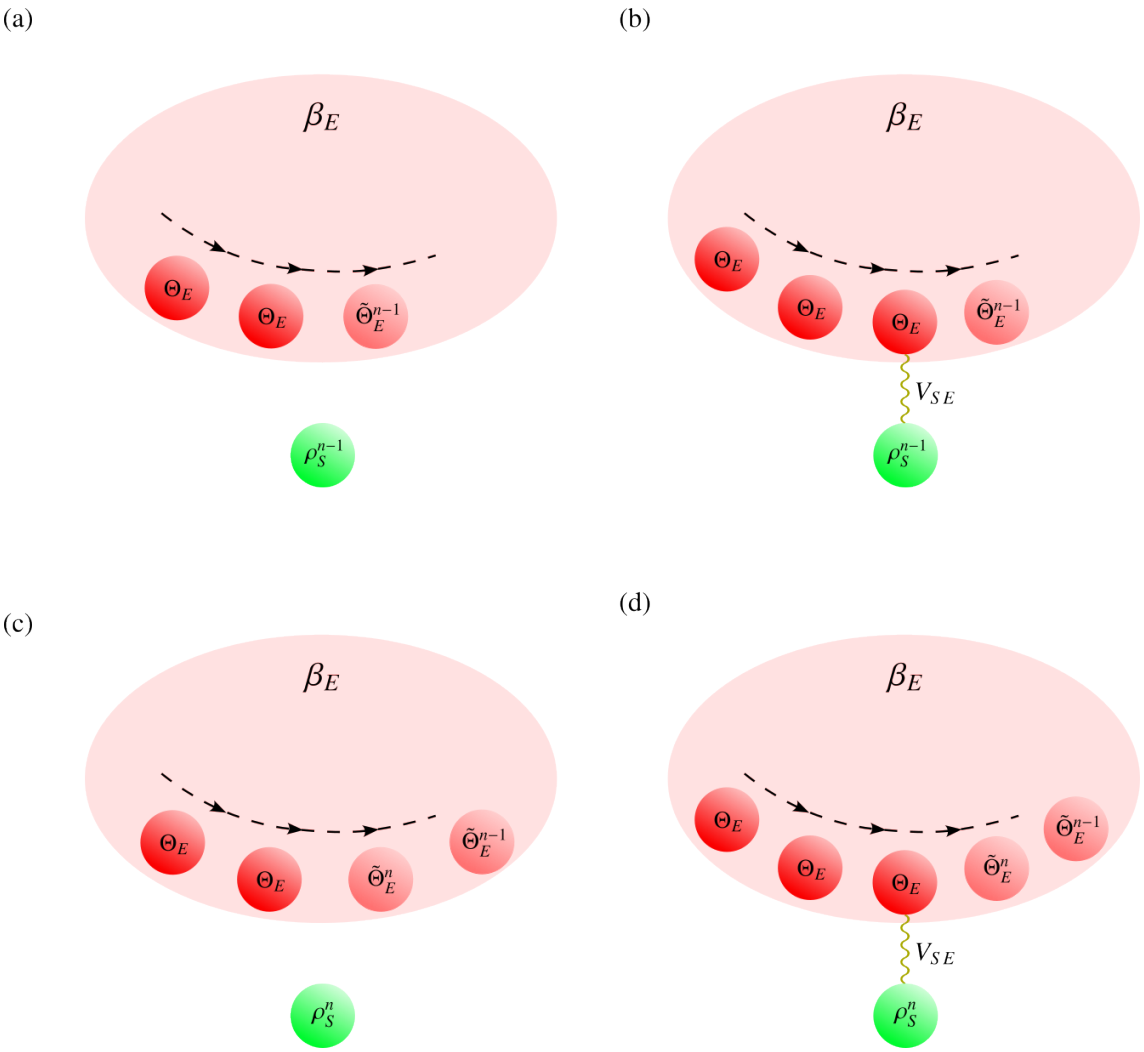

Figure 5.1: **Depiction of the collisional model framework.** The thermal environment (bath) at inverse temperature β_E consists of ancillae in the same Gibbs thermal state $\Theta_E = \exp(-\beta_E H_E)/Z_E$. (a) Between the $n-1$-th and n-th collision, the ancilla that previously interacted with the quantum system S and whose density operator $\tilde{\Theta}_E^{n-1}$ is thrown away and a new thermal unit approaches. The density operator of S is denoted ρ_S^{n-1}. (b) A new interaction ("collision") starts between system and environment ancilla, lasting for a time τ and mediated by the interaction Hamiltonian V_{SE}. The final state of S is ρ_S^n. (c) Similar to (a), the thermal ancilla that just interacted is discarded and makes room for a new one to come. (d) The interaction between system and environment is turned on again and the process keeps repeating itself.

the state of the system is ρ_S^{n-1} and the state of the ancilla that just interacted with it is $\tilde{\Theta}_E^{n-1}$. After throwing away this ancilla, the next one and the quantum system – which are considered to be initially *uncorrelated* – will interact for a time τ through the interaction Hamiltonian V_{SE} (Fig. 5.1 (b)). Then, as the previous ancilla that interacted with the system, this ancilla, now in state $\tilde{\Theta}_E^n$ is discarded and the quantum system is found to be in the state ρ_S^n (Fig. 5.1 (c)). Finally, the process repeats itself again and a fresh ancilla comes and interacts through V_{SE} for a time τ with the quantum system (Fig. 5.1 (d)). The

equation relating the system's density operator after ρ_S^n and before ρ_S^{n-1} the n-th collision is:

$$\rho_S^n = \mathrm{tr}_E\{\rho_{SE}^n\} := \mathrm{tr}_E\{U(\rho_S^{n-1} \otimes \Theta_E)U^\dagger\}, \tag{5.2}$$

where $\mathrm{tr}_E\{\cdot\}$ denotes trace over the *Hilbert space* $\mathcal{H}_E$ of the environment and U is the unitary dictating the time evolution of the composite state system-ancilla. The unitary $U = \exp(-iH_{\mathrm{tot}}\tau)$ is determined by the total Hamiltonian H_{tot}:

$$H_{\mathrm{tot}} = H_S \otimes \mathbb{1}_E + \mathbb{1}_S \otimes H_E + V_{SE}, \tag{5.3}$$

which is the sum of the local Hamiltonians with the interaction between system and thermal ancilla. Similarly, the density operator of each thermal unit after the n-th collision is given by:

$$\tilde{\Theta}_E^n = \mathrm{tr}_S\{U(\rho_S^{n-1} \otimes \Theta_E)U^\dagger\}. \tag{5.4}$$

5.1.1 First law of thermodynamics

As done in Ref. [39], we shall *define* the energy change of the thermal ancilla to be equal to *minus* the heat exchanged between the quantum system S and the environment:

$$Q_{SE}^n := -\mathrm{tr}_S\{(\tilde{\Theta}_E^n - \Theta_E)H_E\}. \tag{5.5}$$

The minus sign is simply a convention and the identification with heat comes from the fact that the Gibbs thermal state is diagonal in the computational basis, thus its energy changes come solely from population variations. As the composite system-ancilla is closed and the total Hamiltonian is time-independent during the interaction, energy must be conserved. Hence,

$$\mathrm{tr}\{U(\rho_S^{n-1} \otimes \Theta_E)U^\dagger H_{\mathrm{tot}}\} = \mathrm{tr}\{(\rho_S^{n-1} \otimes \Theta_E)H_{\mathrm{tot}}\}, \tag{5.6}$$

which by expanding the terms becomes:

$$\Delta\mathcal{E}_S^n = Q_{SE}^n + \mathcal{W}_{\mathrm{on/off}}^n, \tag{5.7}$$

where

$$\Delta\mathcal{E}_S^n = \mathrm{tr}\{(\rho_S^n - \rho_S^{n-1})H_S\}, \tag{5.8}$$

is the *total* internal energy variation of the quantum system S and

$$\begin{aligned} \mathcal{W}_{\mathrm{on/off}}^n &= \Delta\mathcal{E}_S^n - Q_{SE}^n \\ &= \mathrm{tr}\{\rho_{SE}^n V_{SE}\} - \mathrm{tr}\{(\rho_S^{n-1} \otimes \Theta_E)V_{SE}\} \\ &=: \Delta\langle V_{SE}\rangle_n, \end{aligned} \tag{5.9}$$

corresponds to the *on/off work* or variation of mean energy of the interaction. It is exactly how much of the energy trapped in the interaction changes from one collision to the next one and thus it identifies with an energetic cost for putting the system and ancilla to interact. As we can see, Eq. (5.7) is the *first law of thermodynamics* (FLT) in the collisional model setup.

5.1.2 Second law of thermodynamics

On the other hand, to get the *second law of thermodynamics* (SLT) for this framework is more delicate. Akin to a quantum information formalism, the entropy production (a quantifier of the SLT) is [96, 97]:

$$\begin{aligned}\Sigma_n &= \mathcal{I}(\rho^n_{SE} : \rho^{n-1}_S \otimes \Theta_E) + \mathcal{S}(\Theta^n_E \,\|\, \Theta_E) \\ &= \mathcal{S}(\rho^n_{SE} \,\|\, \rho^{n-1}_S \otimes \Theta_E) \geqslant 0 \end{aligned} \tag{5.10}$$

where

$$\begin{aligned}\mathcal{I}(\rho^n_{SE} : \rho^{n-1}_S \otimes \Theta_E) &= \mathcal{S}(\rho^n_{SE} \,\|\, \rho^{n-1}_S \otimes \Theta_E) \\ &= \mathcal{S}(\rho^{n-1}_S) + \mathcal{S}(\Theta_E) - \mathcal{S}(\rho^{n-1}_S \otimes \Theta_E) \end{aligned} \tag{5.11}$$

is the *mutual information* developed between system and environment ancilla after the n-th interaction, $\mathcal{S}(\rho) = -\mathrm{tr}\{\rho \ln \rho\}$ is the von Neumann entropy of ρ and $\mathcal{S}(\rho\|\sigma) = \mathrm{tr}\{\rho \ln \rho - \rho \ln \sigma\}$ is the quantum relative entropy between ρ and σ[4]. Interestingly, in the case that the environment is thermal, it is possible to show that [97]

$$\Sigma_n = \Delta\mathcal{S}^n_S - \beta_E \mathcal{Q}^n_{SE} \geqslant 0, \tag{5.12}$$

with $\Delta\mathcal{S}^n_S = \mathcal{S}(\rho^n_S) - \mathcal{S}(\rho^{n-1}_S)$ being the von Neumann entropy variation in the quantum system S between the n-th and $n-1$-th collisions. Here we see that the first term on the RHS corresponds to an internal entropy change and the second term is akin to a flux of entropy between system and thermal environment at inverse temperature β_E. In the light of classical thermodynamics, it is very similar to Clausius's statement of the SLT [98–100].

5.1.3 Energy-conserving interactions

To ensure *strict energy conservation* (SEC) in each collision, we enforce that the unitary U is such that [101]:

$$[U, H_S \otimes \mathbb{1}_E + \mathbb{1}_S \otimes H_E]_- = 0, \tag{5.13}$$

which implies that the interaction V_{SE} also commutes with the sum of the local Hamiltonians. An important consequence of this is that:

$$\mathcal{W}^n_{\text{on/off}} \equiv 0, \qquad \forall n \tag{5.14}$$

meaning that there is no energetic cost to put system and thermal environment to interact and thus, the mean energy trapped in the interaction is constant and can be ignored. Therefore,

$$\mathcal{Q}^n_{SE} = \mathrm{tr}\{(\rho^n_S - \rho^{n-1}_S) H_S\}, \tag{5.15}$$

and all the energy leaving (entering) the system enters (leaves) the environment ancilla. In thermodynamic scenarios, the SEC assumption is reasonable, since in the limit of macroscopic baths, the bulk energies are orders of magnitude higher than the energy at the

[4] As noted in Ref. [97], even though $\mathcal{S}(\rho\|\sigma) \geqslant 0$ and $\mathcal{S}(\rho\|\sigma) = 0$ iff $\rho = \sigma$, this is not stricly speaking a distance between the states, since the *triangle inequality* is not satisfied.

interface between environment and system, such that, even if they vary, their influence is negligible [101].

A further condition that can be enforced to the interaction, is that it is *excitation conserving* (EC), which can be guaranteed by the following form [37, 39]:

$$V_{SE} = \sum_k g_k \left(L_k^\dagger A_k + L_k A_k^\dagger \right), \tag{5.16}$$

where $\{L_k\}_k$ and $\{A_k\}_k$ are sets of *eigenoperators* of system and environment, respectively, i.e. they obey:

$$[H_S, L_k] = -\omega_k L_k, \quad [H_E, A_k] = -\omega_k A_k, \quad \forall k \tag{5.17}$$

in which we assume that the transition frequencies between levels of system and environment are the same (resonance). This latter assumption is reasonable, since resonant modes are the ones that interact the strongest when one physical system is put to interact with a second physical system. The general expression in Eq. (5.16) is EC, because as one can see, whenever an excitation is created (destroyed) in the system, another excitation is destroyed (created) in the environment. Such an assumption compels to real scenarios where either no non-linear effects happen (e.g. second-harmonic generation) and/or the order of magnitude of the energies into play are "low" (we are not in the limit of high energy physics, where particles pop out from the vacuum, for instance).

5.2 Quantum switch with an open control

We are now ready to combine the QS (Chapter 3) with open system dynamics applied to the control DOF. The quantum circuit scheme that represents our model is shown in Fig. 5.2. We start with a system S in some quantum state ρ_S living in $\mathcal{L}(\mathcal{H}_S)$, where $\dim(\mathcal{H}_S) =: d_S$. To this density operator two possible quantum channels might be applied, $\mathcal{M}$ and $\mathcal{N}$, with *Kraus operators* $\{M_i\}_{i=0}^{d_S^2-1}$ and $\{N_i\}_{i=0}^{d_S^2-1}$, respectively[5]. An ancillary system, or additional DOF, called the *control*[6] C, determines the order in which $\mathcal{M}$ and $\mathcal{N}$ are employed, depending on its state. Therefore, by setting the initial state of C to be the density operator $\rho_C = |+\rangle\langle+|_C$, which contains *maximum coherence* in the computational basis, we implement cSCO in our setting. The state post-QS will be denoted ρ_{SC}^0, where the "0" indicates that no collisions have occurred yet. Based on what we know from Chapter 3, the explicit expression for this state is:

$$\rho_{SC}^0 = A_{++} \otimes |+\rangle\langle+|_C + A_{+-} \otimes |+\rangle\langle-|_C + A_{-+} \otimes |-\rangle\langle+|_C + A_{--} \otimes |-\rangle\langle-|_C, \tag{5.18}$$

where

$$A_{xy} := \frac{1}{4} \sum_{i,j} \left[M_i, N_j \right]_x \rho_S \left[M_i, N_j \right]_y^\dagger, \tag{5.19}$$

with $x, y \in \{+, -\}$, and $[X, Y]_+$ being the anti-commutator and $[X, Y]_-$ the commutator.

[5] The quantum channels are completely positive trace-preserving (CPTP) maps, therefore their Kraus operators satisfy $\sum_i M_i^\dagger M_i = \sum_i N_i^\dagger N_i = \mathbb{1}_S$.

[6] As usual in the literature, we take the control to be a two-level system (qubit). Even when it is not, in practice only two states are necessary for the QS, so C is effectively treated as a qubit.

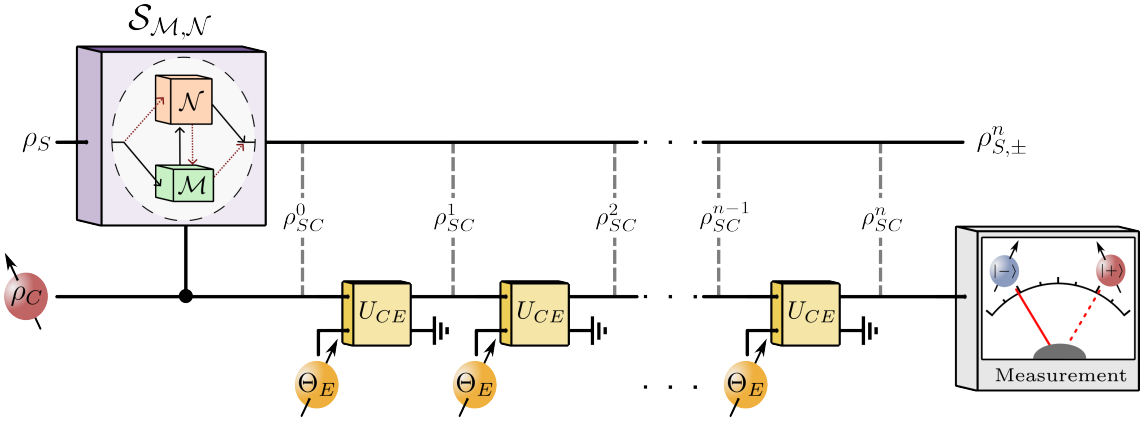

Figure 5.2: **Quantum circuit representation of the quantum switch with an open control.** The system is initially in ρ_S and the control in ρ_C. The system goes through the quantum switch (QS) supermap $\mathcal{S}_{\mathcal{M},\mathcal{N}}$, which implements a controlled superposition of the quantum channels $\mathcal{M}$ and $\mathcal{N}$. Right after the QS, the composite state system-control is denoted ρ^0_{SC}. This state suffers a sequence of collisions on the control degree-of-freedom (DOF) with environment ancillas set in the thermal state Θ_E. The collisions are modeled by the unitary U_{CE} and after each interaction the ancilla is thrown away. After n collisions, the state ρ^n_{SC} has its control DOF measured in the eigenbasis of σ_x (i.e. $\{|+\rangle, |-\rangle\}$) and, depending on the result of the measurement, the final local state of the system is either $\rho^n_{S,+}$ or $\rho^n_{S,-}$. Figure obtained from Ref. [30].

The joint state ρ^0_{SC} carries terms related to cSCO. Define the operators:

$$A_{\text{def}} := A_{++} + A_{--} = \frac{1}{2}\sum_{i,j}\left(M_i N_j \rho_S N_j^\dagger M_i^\dagger + N_j M_i \rho_S M_i^\dagger N_j^\dagger\right), \tag{5.20}$$

and

$$A_{\text{indef}} := A_{++} - A_{--} = \frac{1}{2}\sum_{i,j}\left(M_i N_j \rho_S M_i^\dagger N_j^\dagger + N_j M_i \rho_S N_j^\dagger M_i^\dagger\right). \tag{5.21}$$

Observe that A_{def} is a convex combination of two terms: one with $\mathcal{M}$ applied to the system, followed by $\mathcal{N}$, and the other term representing the opposite order. Therefore, A_{def} corresponds to a mixture of definite causal orders. However, A_{indef} corresponds to interference terms between the causal orders, i.e., terms without definite causal order in the quantum description. Since

$$A_{\pm\pm} = \frac{1}{2}A_{\text{def}} \pm \frac{1}{2}A_{\text{indef}}, \tag{5.22}$$

we indeed see that indefinite causal order leaves an imprint in linearly independent components of the joint system-control state.

For the open system dynamics of C, we need to define what are the local Hamiltonians – except for the system, which shall have a generic Hamiltonian H_S – and what is the interaction between C and the environment ancilla E. The local Hamiltonians are

$$H_\alpha = -\omega\frac{\sigma_x^\alpha}{2}, \qquad \alpha \in \{C, E\}, \tag{5.23}$$

where we assume that control and environment are resonant and the $\{|+\rangle, |-\rangle\}$ eigenbasis is selected for both. In the case of C it is convenient, since unnecessary phases will not appear in the state expression after each collision and it is the same basis in which post-selection will be done; while for the environment it is a matter of convention, the reference frame of E can be arbitrarily set. As for the interaction, we choose:

$$V_{CE} = \frac{g}{2}\left(\sigma_z^C \sigma_z^E + \sigma_y^C \sigma_y^E\right), \tag{5.24}$$

g being the interaction strength[7]. This interaction can be also written as

$$V_{CE} = g\left(|+\rangle\langle -|_C \otimes |-\rangle\langle +|_E + |-\rangle\langle +|_C \otimes |+\rangle\langle -|_E\right), \tag{5.25}$$

which is a Jaynes-Cummings-like coupling with a qubit reservoir [102]. Another interesting feature of the chosen interaction is that it is EC, as seen in Sec. 5.1.3. Taking all these Hamiltonians together, we will have SEC, as presented in the previously mentioned section, and all energy leaving (entering) the control enters (leaves) the environment. Thus, in the end we have the total Hamiltonian:

$$H_{\text{tot}} = H_S \otimes \mathbb{1}_C \otimes \mathbb{1}_E + \mathbb{1}_S \otimes H_C \otimes \mathbb{1}_E + \mathbb{1}_S \otimes \mathbb{1}_C \otimes H_E + \mathbb{1}_S \otimes V_{CE}, \tag{5.26}$$

which generates the unitary operator $U = \exp(-i\tau H_{\text{tot}})$ for the collision map:

$$\rho_{SC}^n = \text{tr}_E\{U(\rho_{SC}^{n-1} \otimes \Theta_E)U^\dagger\}. \tag{5.27}$$

5.2.1 General evolution of the composite state

We obtain a closed and elegant expression for the composite state system-control for *any* n:

$$\rho_{SC}^n = \mathcal{B}_{++}(n)\otimes|+\rangle\langle +|_C + \mathcal{B}_{+-}(n)\otimes|+\rangle\langle -|_C + \mathcal{B}_{-+}(n)\otimes|-\rangle\langle +|_C + \mathcal{B}_{--}(n)\otimes|-\rangle\langle -|_C, \tag{5.28}$$

where

$$\mathcal{B}_{+-}(n) = \mathcal{B}_{-+}^\dagger(n) := e^{in\tau\omega}\cos^n(g\tau)U_S^n A_{+-}U_S^{\dagger n} \tag{5.29}$$

and

$$\mathcal{B}_{\pm\pm}(n) := \frac{1}{2}\left\{1 \pm f_E\left[1 - \cos^{2n}(g\tau)\right]\right\}A_{\text{def}}^n \pm \frac{1}{2}\cos^{2n}(g\tau)A_{\text{indef}}^n, \tag{5.30}$$

in which we defined $U_S := \exp(-i\tau H_S)$, $f_E := \tanh(\beta_E\omega/2)$, $A_{\text{def/indef}}^n := U_S^n A_{\text{def/indef}} U_S^{\dagger n}$. For this collisional model setting we assume that $0 < g\tau \ll 1$, thus the cosines work effectively as *perturbative damping* factors: $\cos(g\tau) \sim 1 - g^2\tau^2/2$. As one can see, Eqs. (5.18)-(5.28) have the exact same format, differing only by the coefficients $A_{xy} \leftrightarrow \mathcal{B}_{xy}(n)$. These are continuously connected, since

$$\mathcal{B}_{xy}(n=0) \equiv A_{xy}, \qquad \forall x, y \tag{5.31}$$

[7] In many-body physics, this is an *isotropic yz*-interaction.

and then, from Eq. (5.28) we can obtain Eq. (5.18) by setting $n = 0$. Moreover, the local state of the system for any n,

$$\begin{aligned}\rho_S^n &= \mathrm{tr}_C\{\rho_{SC}^n\} \\ &= \mathcal{B}_{++}(n) + \mathcal{B}_{--}(n) \\ &= A_{\mathrm{def}}^n \\ &= \frac{1}{2}U_S^n[\mathcal{N}\circ\mathcal{M}(\rho_S) + \mathcal{M}\circ\mathcal{N}(\rho_S)]U_S^{\dagger n}, \quad \forall n \in \mathbb{N}\end{aligned} \tag{5.32}$$

which is a mixture of definite causal orders (first $\mathcal{M}$ then $\mathcal{N}$, and vice-versa) evolves unitarily on time through U_S^n. Therefore, from the point of view of the system S, if no post-selection is done on the side of the control C, the QS has *no* extraordinary impact, since SCO is just thrown away by eliminating the control DOF. Finally, for the asymptotic limit of $n \to \infty$ one has:

$$\begin{aligned}\lim_{n\to\infty}\rho_{SC}^n &\sim \left[\lim_{n\to\infty}\mathcal{B}_{++}(n)\right]\otimes|+\rangle\langle+|_C + \left[\lim_{n\to\infty}\mathcal{B}_{--}(n)\right]\otimes|-\rangle\langle-|_C \\ &= \left(\lim_{n\to\infty}A_{\mathrm{def}}^n\right)\otimes\left[\left(\frac{1+f_E}{2}\right)|+\rangle\langle+|_C + \left(\frac{1-f_E}{2}\right)|-\rangle\langle-|_C\right] \\ &= \rho_S^\infty\otimes\Theta_{\beta_E},\end{aligned} \tag{5.33}$$

that is, for an infinitely large amount of collisions, the local state of the system becomes a mixture of causal orders, the local state of the control is the thermal state referent to inverse temperature β_E – meaning that it thermalized with the environment – and *all* correlations, quantum or classical, between S and C disappear, since they are in a separable state.

5.2.2 Control post-selection

The standard procedure carried out in the literature of the QS to extract the correlations caused by SCO in the composite state system-control is to post-select C. We choose the post-selection basis to be the eigenbasis of the σ_x operator, i.e. $|\pm\rangle$, thus

$$\begin{aligned}\rho_{S,\pm}^n &= \frac{\mathrm{tr}_C\{(\mathbb{1}_S\otimes|\pm\rangle\langle\pm|_C)\rho_{SC}^n(\mathbb{1}_S\otimes|\pm\rangle\langle\pm|_C)\}}{\mathrm{tr}\{(\mathbb{1}_S\otimes|\pm\rangle\langle\pm|_C)\rho_{SC}^n\}} \\ &= \frac{\mathcal{B}_{\pm\pm}(n)}{p_{\mathrm{post}}^n(\pm)}\end{aligned} \tag{5.34}$$

is the post-selected state after n collisions on the control. In the above expression, the denominator

$$p_{\mathrm{post}}^n(\pm) := \mathrm{tr}\{(\mathbb{1}_S\otimes|\pm\rangle\langle\pm|_C)\rho_{SC}^n\}, \tag{5.35}$$

is the probability of detecting C in the state $|+\rangle_C$ or $|-\rangle_C$ after n interactions with E.

From Eq. (5.34), we see that the SCO features of the QS setup are inside $\mathcal{B}_{\pm\pm}(n)$. Studying the behavior of this function is then imperative to understand how the interaction with the environment affects the QS operation. First, we rewrite $\mathcal{B}_{\pm\pm}(n)$ as:

$$\mathcal{B}_{\pm\pm}(n) = \frac{b_{\mathrm{def}}^{\pm}(n, f_E, g\tau)}{2}A_{\mathrm{def}}^n + \frac{b_{\mathrm{indef}}^{\pm}(n, g\tau)}{2}A_{\mathrm{indef}}^n, \tag{5.36}$$

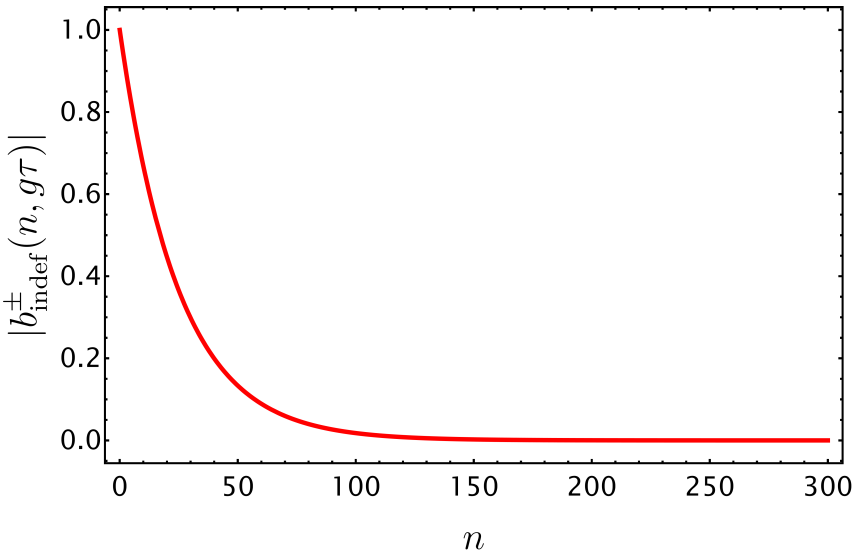

Figure 5.3: **Monotonic decay of $|b^{\pm}_{\text{indef}}(n, g\tau)|$ as a function of n** In line with the order of magnitude of $g\tau$ assumption, here we have $g\tau = 0.2$. As one can see, independently of the inverse temperature $\beta_E = 1/T_E$ and the energy gap ω, $|b^{\pm}_{\text{indef}}(n, g\tau)|$ decreases monotonically with increasing n. Figure obtained from Ref. [30].

where

$$b^{\pm}_{\text{def}}(n, f_E, g\tau) := 1 \pm f_E \left[1 - \cos^{2n}(g\tau)\right] \tag{5.37}$$

and

$$b^{\pm}_{\text{indef}}(n, g\tau) := \pm \cos^{2n}(g\tau). \tag{5.38}$$

The latter quantifies the "amount" of SCO in $\mathcal{B}_{\pm\pm}(n)$. Whenever it is equal to zero, no SCO is left in the post-selected state of the system S. Interestingly, $|b^{\pm}_{\text{indef}}(n, g\tau)|$ decreases *monotonically* for increasing number of collisions n (for of course $0 < g\tau < 1$),

$$|b^{\pm}_{\text{indef}}(n+1, g\tau)| < |b^{\pm}_{\text{indef}}(n, g\tau)|, \quad \forall n \in \mathbb{N} \tag{5.39}$$

asymptotically vanishing ($|b^{\pm}_{\text{indef}}(n \to \infty, g\tau)| = 0$). Moreover, these SCO effects have *no* dependence on the inverse temperature $\beta_E = 1/T_E$ and the energy gap ω. Eq. (5.39) means that *no* non-Markovian effects are involved[8]. These observations are illustrated in Fig. 5.3, where $|b^{\pm}_{\text{indef}}(n, g\tau)|$ is plotted as a function of n for a specific $g\tau$. Interestingly, the inverse temperature $\beta_E = 1/T_E$ and the energy gap ω do influence the post-selected state $\rho^n_{S,\pm}$ through the renormalization imposed by dividing by $p^{\pm}_{\text{post}}(n)$. In fact,

$$\begin{aligned} p^{\pm}_{\text{post}}(n) &= \text{tr}\{\mathcal{B}_{\pm\pm}(n)\} \\ &= \frac{1}{2}\left[b^{\pm}_{\text{def}}(n, f_E, g\tau) + b^{\pm}_{\text{indef}}(n, g\tau)\,\text{tr}\{A_{\text{indef}}\}\right], \end{aligned} \tag{5.40}$$

where the relations $\text{tr}\{A^n_{\text{indef}}\} = \text{tr}\{A_{\text{indef}}\}$ and $\text{tr}\{A^n_{\text{def}}\} = \text{tr}\{A_{\text{def}}\} = 1$ were used.

An important analysis is to check what happens to the aforementioned quantities when the temperature goes to zero $T_E \to 0 \Rightarrow \beta_E \to \infty, f_E \to 1$ and when it goes to

[8] This could be somehow expected, since the environment is composed of non-interacting thermal ancillae and the interaction between control and environment is EC, therefore memory effects do not happen.

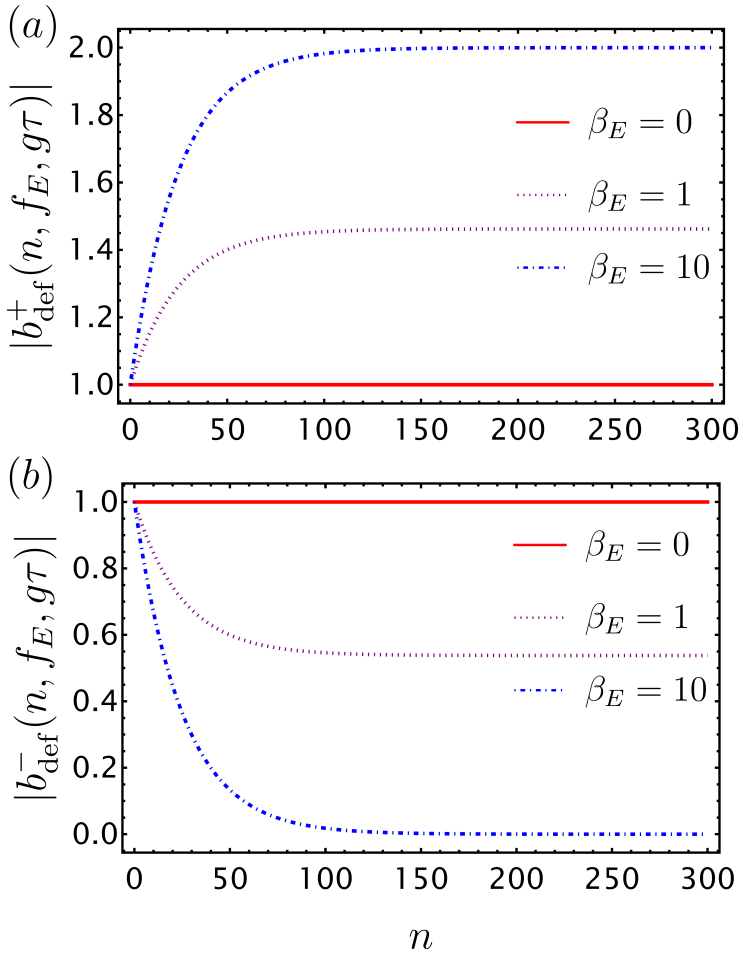

Figure 5.4: **Effect of temperature on $|b^{+}_{\mathbf{def}}(n, f_E, g\tau)|$ (a) and $|b^{-}_{\mathbf{def}}(n, f_E, g\tau)|$ (b) as a function of n.** Three different temperatures are plotted: $\beta_E = 0$ (continuous red line), $\beta_E = 1$ (dotted purple line) and $\beta_E = 10$ (dot-dashed blue line). For low temperatures (high β_E), the definite order term for $|+\rangle_C$ measurement is amplified with increasing n, while for $|-\rangle_C$ measurement it vanishes for the limit of many collisions. On the other hand, for high temperature (low β_E), the definite order term is always the same for both measurement states for all n, as noted in the text. The parameters are $\omega = 1$ and $g\tau = 0.2$. Figure obtained from Ref. [30].

infinity $T_E \to \infty \Rightarrow \beta_E \to 0, f_E \to 0$. In the former, if one then chooses the post-selection state to be $|-\rangle_C$, we have that $b^{-}_{\mathrm{def}}(n, 1, g\tau) = -b^{-}_{\mathrm{indef}}(n, g\tau)$ and then:

$$\begin{aligned} \lim_{\beta_E \to \infty} \rho^{n}_{S,-} &= \frac{b^{-}_{\mathrm{def}}(n, 1, g\tau)(A^{n}_{\mathrm{def}} - A^{n}_{\mathrm{indef}})}{b^{-}_{\mathrm{def}}(n, 1, g\tau)(1 - \mathrm{tr}\{A_{\mathrm{indef}}\})} \\ &= \frac{U^{n}_{S} A_{--} U^{\dagger n}_{S}}{\mathrm{tr}\{A_{--}\}}, \end{aligned} \tag{5.41}$$

which shows that, apart from a local unitary evolution applied to A_{--}, the post-selected state $\rho^{n}_{S,-}$ is *protected* from the decoherence caused by the collisions. However, measuring the control in the $|-\rangle_C$ and finding it there after many collisions is *very* unlikely for

vanishing temperature. Indeed,

$$\begin{aligned}\lim_{\beta_E\to\infty} p^n_{\text{post}}(-) &= \cos^{2n}(g\tau)\frac{(1-\text{tr}\{A_{\text{indef}}\})}{2}\\ &= \cos^{2n}(g\tau)p^0_{\text{post}}(-),\end{aligned} \tag{5.42}$$

thus

$$\lim_{\beta_E,n\to\infty} p^n_{\text{post}}(-) = 0. \tag{5.43}$$

This result is completely reasonable, because when the temperature tends to 0, the environment pushes the control to the thermal state $|+\rangle_C$ (remember that the Hamiltonians of C and E are in the σ_x basis), reducing drastically the probability of finding C in $|-\rangle_C$. On the other hand, if the post-selection state is $|+\rangle_C$, then $b^+_{\text{indef}}(n, g\tau) = 2 - b^+_{\text{def}}(n, 1, g\tau)$ and:

$$\lim_{\beta_E\to\infty} \rho^n_{S,+} = \frac{A^n_{\text{indef}} + b^+_{\text{def}}(n, 1, g\tau)U^n_S A_{--} U^{\dagger n}_S}{p^n_{\text{post}}(+)}, \tag{5.44}$$

where

$$p^n_{\text{post}}(+) = 1 + \text{tr}\{A_{--}\}\left(b^+_{\text{def}}(n, 1, g\tau) - 2\right). \tag{5.45}$$

Therefore, the influence of the environment cannot be suppressed and SCO terms will monotonically fade away.

	Impact of Temperature on QS as $n \to \infty$			
	$\rho^n_{S,-}$	$p^n_{\text{post}}(-)$	$\rho^n_{S,+}$	$p^n_{\text{post}}(+)$
Low-T_E ($\beta_E \to \infty$)	Shielding effect: SCO survives	Goes to 0	SCO is suppressed	Goes to 1
High-T_E ($\beta_E \to 0$)	SCO is suppressed	Goes to $\frac{1}{2}$	SCO is suppressed	Goes to $\frac{1}{2}$

Table 5.1: **Post-measurement state and measurement probability for the states $|\pm\rangle_C$ in the limits of low/high temperature and $n \to \infty$.** When the environment temperature is high ($\beta_E \to 0$), the SCO terms are suppressed irrespective of the post-selection state and the measurement probabilities converge to 1/2. On the other hand, when the temperature is low ($\beta_E \to \infty$), the measurement in the $|+\rangle_C$ state leads to weaker SCO features, while for the $|-\rangle_C$ state these quantities are shielded for high number of collisions. However, this case's probability tends to 0, while for the former situation it tends to 1. Table obtained from Ref. [30].

On the other extreme, when the temperature is very high, asymptotically tending to infinity $T_E \to \infty$, things are different. First, $b^\pm_{\text{def}}(n, 0, g\tau) \equiv 1$, for whatever values of $g\tau$ and number of collisions n, which means that environment effects become invisible to the definite order terms, independently of the post-selection state. Second, the same cannot be said about the SCO terms (linked to $b^\pm_{\text{indef}}(n, g\tau)$), they are *always* affected by the environment, irrespective of whether one measures the control in $|+\rangle_C$ or $|-\rangle_C$. Third,

the behavior of the probabilities $p^n_{\text{post}}(\pm)$ is sensitive on the exact implementation of the QS, as evidenced by the dependence on $\text{tr}\{A_{\text{indef}}\}$:

$$\lim_{\beta_E \to 0} p^n_{\text{post}}(\pm) = \frac{1 + b^{\pm}_{\text{indef}}(n, g\tau)\,\text{tr}\{A_{\text{indef}}\}}{2}. \tag{5.46}$$

In Fig. 5.4 we present plots of $b^{\pm}_{\text{def}}(n, g\tau)$ for specific values of ω, $g\tau$ and for low, intermediate and high temperatures, as functions of the number of collisions n. Also, all the results of this Section are organized in Table 5.1.

5.3 Examples

Having established a general framework from which one can determine temperature induced effects on the operation of the QS, now we pass to concrete examples to benchmark our approach. We start with the situation where the quantum channels are monitoring of *mutually unbiased bases* (MUBs) maps (Section 5.3.1) and then we pass to the QS-based refrigerator, in which the quantum channels are thermalizing maps (Section 5.3.2).

5.3.1 Monitoring of mutually-unbiased bases (MUBs)

Consider the so-called *monitoring maps* [58, 103]:

$$\mathcal{M}^{\epsilon}_{O}(\rho_S) := (1-\epsilon)\rho_S + \epsilon\,\Phi_O(\rho_S), \tag{5.47}$$

where $\epsilon \in [0,1]$ is called the measurement strength and

$$\begin{aligned}\Phi_O(\rho_S) &= \sum_{\alpha=0}^{d_S-1} O_\alpha \rho_S O_\alpha \\ &= \sum_{\alpha=0}^{d_S-1} p_\alpha O_\alpha\end{aligned} \tag{5.48}$$

is a dephasing map in the eigenbasis of $O = \sum_{\alpha=0}^{d_S^2-1} \alpha\, O_\alpha$ ($p_\alpha := \text{tr}\{O_\alpha \rho_S\}$ is the probability of measuring α and O_α are projectors: $O_\alpha O_{\alpha'} = \delta_{\alpha\alpha'} O_\alpha$). The dephasing map is interpreted as a measurement of observable O in which the result is not registered and the final state is a statistical mixture of outcomes. Eq. (5.47) enables one to continuously go from the identity map ($\epsilon = 0$), passing by *weak measurements* ($\epsilon \ll 1$) and to *strong measurements* ($\epsilon \lesssim 1$). In Ref. [58], it is further shown that Kraus decomposition of the monitoring map is achieved by $\{K_j\}_{j\in\{0,1,\ldots,d_S^2-1\}}$, where $K_0 = \sqrt{1-\epsilon}\,\mathbb{1}_S$ and $K_j = \sqrt{\epsilon}\,O_j$ for $j > 0$[9]. Therefore, the monitoring maps are written in the Kraus decomposition as:

$$\mathcal{M}^{\epsilon}_{O}(\rho_S) = \sum_{j=0}^{d_S-1} K_j \rho_S K_j^{\dagger} \tag{5.49}$$

[9] As Kraus operators of a CPTP map, they satisfy the trace preserving condition $\sum_{j=0}^{d_S^2-1} K_j^{\dagger} K_j = \mathbb{1}_S$.

and have the following property [58]:

$$\mathcal{M}_O^{\epsilon} \circ \mathcal{M}_O^{\epsilon'}(\rho_S) = \mathcal{M}_O^{\epsilon''}(\rho_S), \tag{5.50}$$

with $\epsilon'' = \epsilon + \epsilon' - \epsilon\epsilon'$. Still on basic aspects of these maps, in the reference frame of the system, they *always* lower the amount of information contained in the state ρ_S, i.e.

$$\mathcal{I}(\rho_S) - \mathcal{I}(\mathcal{M}_O^{\epsilon}(\rho_S)) \geqslant \epsilon\, \mathfrak{C}_O(\rho_S) \geqslant 0, \tag{5.51}$$

where

$$\mathcal{I}(\rho) := \ln d - \mathcal{S}(\rho) \tag{5.52}$$

is the *available information* of state ρ with dimension d (remember that $\mathcal{S}(\rho) := -\operatorname{tr}\{\rho \ln \rho\}$ is the von Neumann entropy) and

$$\mathfrak{C}_O(\rho_S) := \mathcal{S}(\Phi_O(\rho_S)) - \mathcal{S}(\rho_S) \tag{5.53}$$

is the *relative entropy of coherence* related to observable O. Eq. (5.51) is readily obtained from the concavity of the von Neumann entropy, that it, $\mathcal{S}(\mathcal{M}_O^{\epsilon}(\rho_S)) \geqslant (1-\epsilon)\mathcal{S}(\rho_S) + \epsilon\mathcal{S}(\Phi_O(\rho_S))$. Therefore, we clearly see that the measurement strength and the available information are monotonically linked.

We now restrict these monitoring maps to the case that two operators O and O' have eigenbases $\{|o_j\rangle\}_{j\in\{0,\ldots,d_S-1\}}$ and $\{|o'_j\rangle\}_{j\in\{0,\ldots,d_S-1\}}$, respectively, forming mutually unbiased bases (MUBs), i.e.

$$\langle o_j | o'_{j'} \rangle = \frac{e^{i\phi_{jj'}}}{\sqrt{d_S}}, \tag{5.54}$$

where $\phi_{jj'} \in [0, 2\pi]$ are some phases. Notice that, for systems with very high dimensions ($d_S \gg 1$), the bases are asymptotically orthogonal. By means of the relation between the bases in Eq. (5.54) and $O_j \equiv |o_j\rangle\langle o_j|$, $O'_j \equiv |o'_j\rangle\langle o'_j|$, we get:

$$\Phi_O \circ \Phi_{O'}(\rho_S) = \Phi_{O'} \circ \Phi_O(\rho_S) = \frac{\mathbb{1}_S}{d_S}, \tag{5.55}$$

which in turn gives

$$\mathcal{M}_O^{\epsilon} \circ \mathcal{M}_{O'}^{\epsilon'}(\rho_S) = \mathcal{M}_{O'}^{\epsilon'} \circ \mathcal{M}_O^{\epsilon}(\rho_S), \qquad \forall \epsilon, \epsilon' \in [0,1]. \tag{5.56}$$

Therefore, two monitoring maps of observables O and O' which have as eigenbasis MUBs *commute* for whatever measuring strengths ϵ and ϵ'. Moreover, the explicit expression for the state after two consecutive monitoring maps of MUBs is:

$$\mathcal{M}_O^{\epsilon} \circ \mathcal{M}_{O'}^{\epsilon'}(\rho_S) = (1-\epsilon)(1-\epsilon')\rho_S + \epsilon(1-\epsilon')\Phi_O(\rho_S) + \epsilon'(1-\epsilon)\Phi_{O'}(\rho_S) + \epsilon\epsilon'\frac{\mathbb{1}_S}{d_S}. \tag{5.57}$$

As it is the case for applying only one monitoring map (Eq. (5.51)), when two are applied onto a system S in some state ρ_S, the available information monotonically decays with the measurement strength,

$$\mathcal{I}(\rho_S) \geqslant \mathcal{I}(\mathcal{M}_{O'}^{\epsilon'} \circ \mathcal{M}_O^{\epsilon}(\rho_S)), \qquad \forall \epsilon, \epsilon' \in [0,1] \tag{5.58}$$

This inequality is obtained from

$$\mathcal{I}(\rho_S) - \mathcal{I}(\mathcal{M}^{\epsilon'}_{O'} \circ \mathcal{M}^{\epsilon}_{O}(\rho_S)) \geqslant \epsilon\epsilon' \mathcal{I}(\rho_S) + \epsilon(1-\epsilon')\mathfrak{C}_O(\rho_S) + \epsilon'(1-\epsilon)\mathfrak{C}_{O'}(\rho_S), \tag{5.59}$$

which in turn comes from the concavity of the von Neumann entropy.

For the rest of this section, we consider a simpler situation, where two monitoring maps $\mathcal{M}^{\epsilon}_{O}$ and $\mathcal{M}^{\epsilon}_{O'}$ have the same measuring strength ϵ. Moreover, the monitored operators are $O = \sum_{i=0}^{d_S^2-1} \alpha_i O_i = \sum_{i=0}^{d_S^2-1} \alpha_i |o_i\rangle\langle o_i|_S$ and $O = \sum_{i=0}^{d_S^2-1} \alpha_i O_i = \sum_{i=0}^{d_S^2-1} \alpha'_i |o'_i\rangle\langle o'_i|_S$. Then, the Kraus operators are:

$$M_0 = \sqrt{1-\epsilon}\,\mathbb{1}_S, \quad M_i = \sqrt{\epsilon}\,|o_i\rangle\langle o_i|_S, \quad i \in \{1, \ldots, d_S^2 - 1\}, \tag{5.60}$$

$$N_0 = \sqrt{1-\epsilon}\,\mathbb{1}_S, \quad N_i = \sqrt{\epsilon}\,|o'_i\rangle\langle o'_i|_S, \quad i \in \{1, \ldots, d_S^2 - 1\}. \tag{5.61}$$

Now, imposing the MUB relation between $\{|o_i\rangle_S\}$ and $\{|o'_i\rangle_S\}$, we get:

$$\begin{aligned}\rho^n_{S,\pm} = &\left(\frac{b^{\pm}_{\text{def}}(n, f_E, g\tau) + b^{\pm}_{\text{indef}}(n, g\tau)}{2p^n_{\text{post}}(\pm)}\right) U_S^n \left[\mathcal{M}^{\epsilon}_{O'} \circ \mathcal{M}^{\epsilon}_{O}(\rho_S)\right] U_S^{\dagger n} \\ &+ \epsilon^2 \frac{b^{\pm}_{\text{indef}}(n, g\tau)}{4d_S\, p^n_{\text{post}}(\pm)} \left[\sum_{i,j=0}^{d_S-1} U_S^n \left(e^{2i\phi_{ij}} \langle o'_j|\rho_S\,|o_i\rangle |o_i\rangle\langle o'_j|_S + \text{h.c.}\right) U_S^{\dagger n} - \mathbb{1}_S\right],\end{aligned} \tag{5.62}$$

where h.c. stands for "Hermitian conjugate" and

$$\begin{aligned} p^n_{\text{post}}(\pm) &= \text{tr}\{\mathcal{B}_{\pm\pm}(n)\} \\ &= \frac{b^{\pm}_{\text{def}}(n, f_E, g\tau)}{2} + \frac{b^{\pm}_{\text{indef}}(n, g\tau)}{2}\,\text{Re}\{\chi\} \end{aligned} \tag{5.63}$$

in which

$$\chi = (1-\epsilon)^2 + 2\epsilon(1-\epsilon) + \frac{\epsilon^2}{d_S^{3/2}} \sum_{i,j=0}^{d_S^2-1} e^{i\phi_{ij}} \langle o'_j|\rho_S\,|o_i\rangle. \tag{5.64}$$

The expression in Eq. (5.62) can be applied to any finite-dimensional system S, being therefore very general. To get a grasp of a more restricted situation, consider the case in which the system has $\dim(\mathcal{H}_S) = 2$ with initial state $\rho_S = |+\rangle\langle+|_S$, the Hamiltonian of the system is $H_S = -\omega_S \sigma_x^S/2$, and the monitored operators are $O = \sigma_z$ and $O' = \sigma_x$. Hence, the final post-selected state of the system after the QS and collisions is:

$$\begin{aligned}\rho^n_{S,\pm} = &\frac{1}{2p^n_{\text{post}}(\pm)}\left[\left(1 - \frac{\epsilon}{2}\right)\left(b^{\pm}_{\text{def}}(n, f_E, g\tau) + b^{\pm}_{\text{indef}}(n, g\tau)\right)|+\rangle\langle+|_S\right. \\ &\left. + \frac{\epsilon}{2}\left(b^{\pm}_{\text{def}}(n, f_E, g\tau) + b^{\pm}_{\text{indef}}(n, g\tau)(1-\epsilon)\right)|-\rangle\langle-|_S\right],\end{aligned} \tag{5.65}$$

where

$$p^n_{\text{post}}(\pm) = \frac{1}{2}\left[b^{\pm}_{\text{def}}(n, f_E, g\tau) + b^{\pm}_{\text{indef}}(n, g\tau)\left(1 - \frac{\epsilon^2}{2}\right)\right]. \tag{5.66}$$

Note that the post-selected state is diagonal in the σ_x basis, thus it has no coherences in the same basis (i.e. it has the form of a mixed-state).

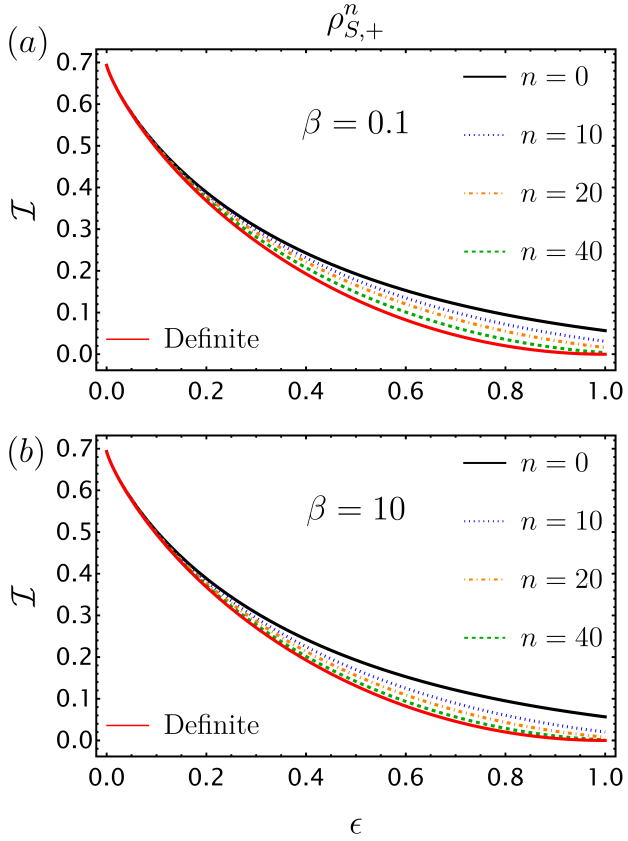

Figure 5.5: **Available information in the system S (a qubit) after applying the QS, collisions and measuring the control in the $|+\rangle_C$ state as a function of the measuring strength ϵ, in the case of monitoring MUBs quantum maps.** The monotonic decay of $\mathcal{I}(\rho^n_+)$ is observed with respect to ϵ, irrespective of the number of collisions n and inverse temperature β, low (a) and high (b). Here $\omega_S = \omega = 1$ and $g\tau = 0.2$. The solid red line represents the available information in the state of the system when the control is traced-out, which corresponds to the definite order scenario. The solid black line depicts the available information for when no collisions happen. All the other curves interpolate between these two. Figure obtained from Ref. [30].

A quantitative analysis of the amount of information contained in the final state can be done by means of the available information defined in Eq. (5.52). The explicit expression is:

$$\begin{aligned}\mathcal{I}(\rho^n_{S,\pm}) = \ & \ln 2 - \frac{1}{2p^n_{\text{post}}(\pm)}\Bigg[\left(\frac{\epsilon}{2}-1\right)\left(b^{\pm}_{\text{def}}(n,f_E,g\tau)+b^{\pm}_{\text{indef}}(n,g\tau)\right) \\ & \times \ln\left(\frac{\left(1-\frac{\epsilon}{2}\right)\left(b^{\pm}_{\text{def}}(n,f_E,g\tau)+b^{\pm}_{\text{indef}}(n,g\tau)\right)}{2p^n_{\text{post}}(\pm)}\right) - \frac{\epsilon}{2}\left(b^{\pm}_{\text{def}}(n,f_E,g\tau)+b^{\pm}_{\text{indef}}(n,g\tau)\,(1-\epsilon)\right) \\ & \times \ln\left(\epsilon\frac{b^{\pm}_{\text{def}}(n,f_E,g\tau)+b^{\pm}_{\text{indef}}(n,g\tau)\,(1-\epsilon)}{4p^n_{\text{post}}(\pm)}\right)\Bigg].\end{aligned} \tag{5.67}$$

In Figs. 5.5 and 5.6 the available information is plotted for the measurement in the $|+\rangle_C$ and $|-\rangle_C$ states, respectively. In the former situation, $\mathcal{I}(\rho^n_{S,+})$ is *always* diminished with

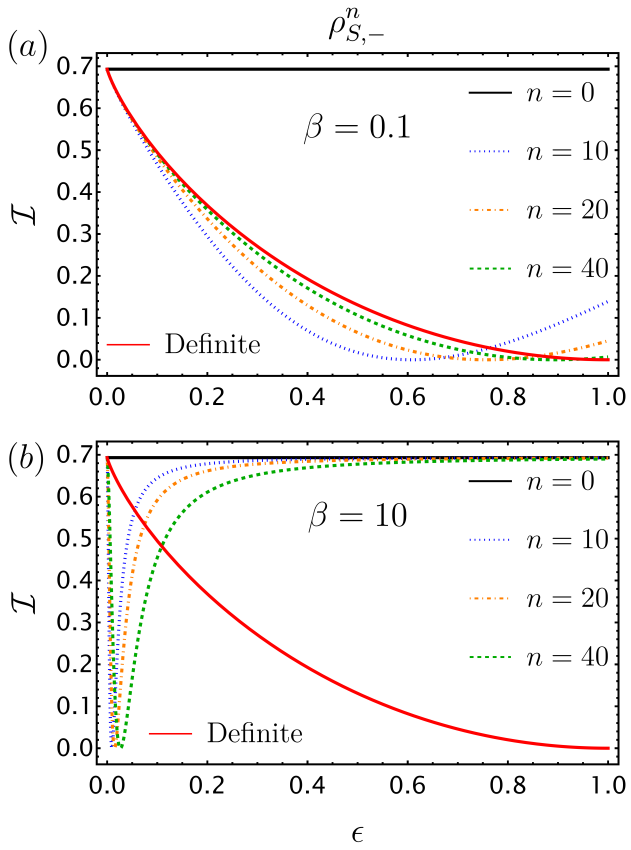

Figure 5.6: **Available information in the system S (a qubit) after applying the QS, collisions and measuring the control in the $|-\rangle_C$ state as a function of the measuring strength ϵ, in the case of monitoring MUBs quantum maps.** The behavior of $\mathcal{I}(\rho^n_-)$ depends strongly on the number of collisions n and the inverse temperature β. (a) For low β, the available information decays monotonically with ϵ for a certain range of collisions, until the moment that for increasing measurement strength $\mathcal{I}(\rho^n_{S,-})$ grows. (b) For high β, the available information – for any number of collisions – decreases fast with small ϵ, but then increases rapidly, reaching the level of maximum available information, achievable for $n = 0$. Here $\omega_S = \omega = 1$ and $g\tau = 0.2$. The solid red line represents the available information in the state of the system when the control is traced-out, which corresponds to the definite order scenario. The solid black line depicts the available information for when no collisions happen. Figure obtained from Ref. [30].

increasing measurement strength ϵ. The more collisions, the faster this decay happens. The qualitative behavior is exactly the same for low and high inverse temperature β of the environment. As one can see, the number of collisions n interpolates the available information between its maximum curve, when no collisions happen, and its minimum curve, obtained from simply tracing out the control DOF, corresponding to the mixture of definite causal orders (Eq. (5.32)). On the other hand, $\mathcal{I}(\rho^n_{S,-})$ has a very different behavior depending on the inverse temperature β. For low β, one has a monotonic decay of the available information for a certain range of collisions. However, as the collisions accumulate, this monotonicity is broken and the available information starts to grow again with ϵ. Moreover, for high β, something even more surprising is observed. Irrespective

of the number of collisions, the available information decreases very fast for small ϵ, but then rises back again to the maximum level, when no collisions happen. This sudden increase is slower as n grows and occasionally ($n \gtrsim 300$) the monotonic decay is recovered, coinciding with the definite order curve.

From studying the situation where the quantum channels composing the QS are monitoring maps of MUBs, we then conclude that the qualitative behavior of the available information with the number of collisions changes drastically according to the chosen measurement state of the control, as shown in Figs. 5.5 and 5.6. In the case of measuring C in $|-\rangle_C$, the behaviour is also dependent on the inverse temperature of the environment β, something that does not happen for measuring the control in $|+\rangle_C$. Hence, by applying our main general equations, we showed that introducing open system dynamics to the control can dramatically change the qualitative behavior of inner features of the state after the QS and subsequent post-selection.

5.3.2 Quantum switch-based refrigerator

In Ref. [18], David Felce and Vlatko Vedral put forward the idea of quantum refrigeration by means of the QS. We apply to it our general framework of open control dynamics, to study how the environment, in a collisional model context, affects the operation of the refrigeration cycle. This feature is considered in between the application of the QS to the composite state system-control and the measurement of the control DOF. The main steps of the modified QS-based refrigeration cycle are shown in Figs. 5.7 and 5.8. The first is a flow chart type of diagram, where arrows point the order of operations. The second is a more artistic representation of the whole protocol, stressing the physical objects involved.

Now we describe the refrigeration cycle step-by-step. Initially, a quantum system S (qubit) with Hamiltonian $H_S = -\omega_S \sigma_z^S/2$ is initialized in the thermal state $\Theta_{\beta_{\text{cold}}} = \exp(-\beta_{\text{cold}} H_S)/Z_S^{\text{cold}}$ ($Z_S^{\text{cold}} = \text{tr}\{\exp(-\beta_{\text{cold}} H_S)\}$ is the partition function) with respect to the inverse temperature β_{cold}. This state reads:

$$\Theta_{\beta_{\text{cold}}} = \left(\frac{1 + f_{\text{cold}}}{2}\right)|+\rangle\langle+|_C + \left(\frac{1 - f_{\text{cold}}}{2}\right)|-\rangle\langle-|_C, \tag{5.68}$$

where $f_{\text{cold}} := \tanh(\beta_{\text{cold}}\omega_S/2)$. This system is put to interact with *at least* two different *cold* baths at the same inverse temperature β_{cold}. The interaction with each bath induces a thermalization map on the state of the system ($\mathcal{M}$ and $\mathcal{N}$, in the case of two baths), described by the Kraus operators:

$$M_i = N_i = \sqrt{\frac{\Theta_{\beta_{cold}}}{2}}\, U_i, \tag{5.69}$$

where $\{M_i\}_{i=0,\ldots,d_S^2-1}$ and $\{N_i\}_{i=0,\ldots,d_S^2-1}$ are the Kraus operators of $\mathcal{M}$ and $\mathcal{N}$, respectively, and $\{U_i\}_{i=0,\ldots,d_S^2-1}$ form a set of orthogonal unitary operators, i.e. $U_i U_j = \delta_{ij} U_j$. These interactions are put in a superposition of orders, according to the QS supermap:

$$\begin{aligned} \mathcal{S}_{\mathcal{M},\mathcal{N}}(\Theta_{\beta_{\text{cold}}} \otimes |+\rangle\langle+|_C) &= \sum_{i,j=0}^{d_S-1} W_{ij} \left(\Theta_{\beta_{\text{cold}}} \otimes |+\rangle\langle+|_C\right) W_{ij}^\dagger \\ &= \frac{1}{2}\left(\Theta_{\beta_{\text{cold}}} \otimes \mathbb{1}_C + \Theta^3_{\beta_{\text{cold}}} \otimes \sigma_x\right) =: \rho^0_{SC} \end{aligned} \tag{5.70}$$

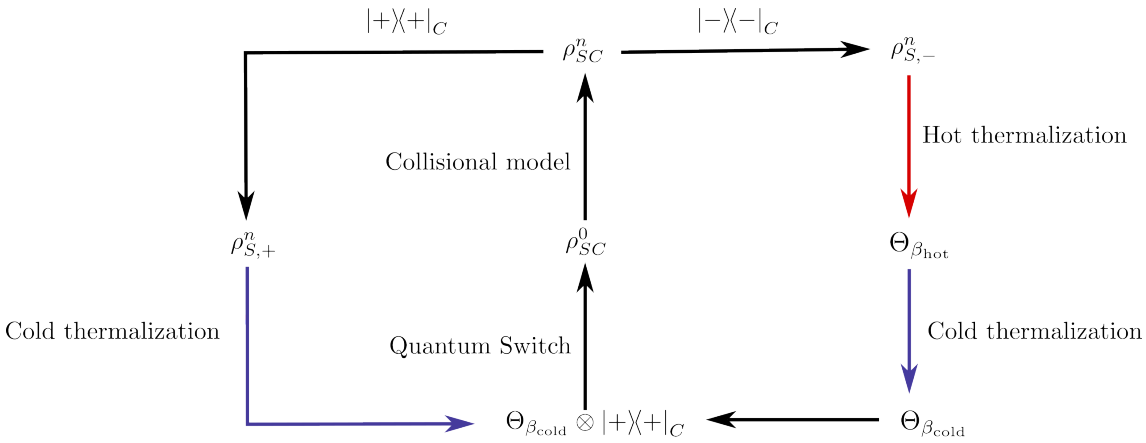

Figure 5.7: **Flow chart depiction of the open control QS-fueled refrigeration cycle.** The composite state system-control (SC) is initialized as the product state $\Theta_{\beta_{\text{cold}}} \otimes |+\rangle\langle+|_C$ and then goes through a quantum switch (QS) transformation controlled by C, in which the order of interaction with two cold baths at the same inverse temperature β_{cold} is controlled coherently. The final state ρ^0_{SC} just on the side of the control DOF goes through open system dynamics, following a collisional model with an environment at inverse temperature β_E. After the interaction with the environment, the system-control composite system is found in state ρ^n_{SC}, which then is measured in the basis of the σ_x operator, just on the side of the control DOF. If C is found to be in $|+\rangle_C$, the final post-selected state $\rho^n_{S,+}$ is classically thermalized with one of the cold baths at inverse temperature β_{cold} and the cycle restarts. On the other hand, if the control is in the $|-\rangle_C$ state, then the post-selected state $\rho^n_{S,-}$ suffers two classical thermalizations in a row: first with a hot bath at inverse temperature β_{hot} and then with one of the cold baths at inverse temperature β_{cold}. The final state is finally reused to in the cycle. Figure taken from Ref. [30].

where $\rho_C = |+\rangle\langle+|_C$ is the state of the control C, a degree-of-freedom (DOF) that controls the order in which the system interacts with the baths and the controlled-Kraus operator is $W_{ij} := M_i N_j \otimes |0\rangle\langle 0|_C + N_j M_i \otimes |1\rangle\langle 1|_C$. In our modified refrigeration cycle, this composite state system-control is put to interact with a thermal environment (bath) E at inverse temperature β_E. This interaction happens just with the subsystem C and is modelled according to the collisional modelled presented in this chapter. The composite state system-control after n collisions is

$$\rho^n_{SC} = \frac{1}{2}\Theta_{\beta_{\text{cold}}} \otimes [\mathbb{1}_C + (1 - b^-_{\text{def}}(n, f_E, g\tau))\ \sigma_x] - \frac{1}{2} b^-_{\text{indef}}(n, g\tau)\, \Theta^3_{\beta_{\text{cold}}} \otimes \sigma_x, \tag{5.71}$$

where $f_E := \tanh(\beta_E \omega/2)$ (ω is the energy gap of C and E). After this, the control is measured in the $\{|+\rangle, |-\rangle\}$ basis and the post-selected states are denoted

$$\rho^n_{S,\pm} = \frac{\Theta_{\beta_{\text{cold}}}}{2 p^n_{\text{post}}(\pm)} \left[b^{\pm}_{\text{def}}(n, f_E, g\tau) + b^{\pm}_{\text{indef}}(n, g\tau) \Theta^2_{\beta_{\text{cold}}} \right], \tag{5.72}$$

in which the measurement probabilities are

$$p^n_{\text{post}}(\pm) = \frac{b^{\pm}_{\text{def}}(n, f_E, g\tau)}{2} + \frac{b^{\pm}_{\text{indef}}(n, g\tau)}{2} \left[1 - \frac{3}{4} \text{sech}^2 \left(\frac{\beta_{\text{cold}} \omega_S}{2} \right) \right]. \tag{5.73}$$

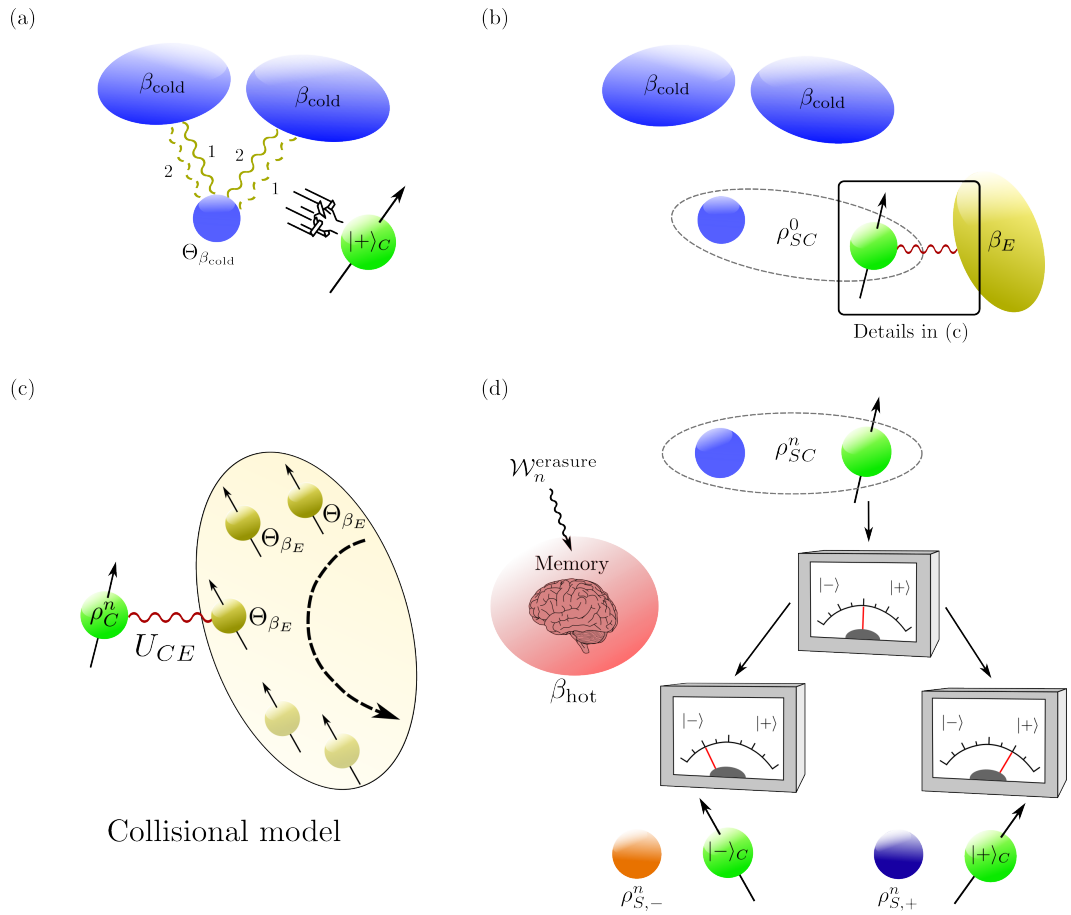

Figure 5.8: **Representation of the open control QS-fueled quantum refrigeration cycle up to the measurement of the control and storage of the result.** Here we represent the steps of the refrigeration cycle up to the classical thermalizations. (a) The system S is initialized in the Gibbs thermal state $\Theta_{\beta_{\text{cold}}}$ and interacts with two thermal baths in the same inverse temperature β_{cold} as S. Whether the order of the interaction is first with one bath then the other or vice-versa (one order is represented by the continuous lines and the other by the dashed ones) is determined by the state of a control qubit C, which starts uncorrelated with the system S. The initial state of C is $|+\rangle_C$, which puts the interaction order in coherent superposition. (b) The system-control state after the controlled-interaction with the cold baths is equal to ρ^0_{SC} and the control C starts to interact with an environment at inverse temperature β_E. (c) Open control model. The control, which has local state ρ^n_C interacts unitarily one-by-one with a stream of qubits (ancillae) in the same Gibbs thermal state Θ_{β_E} through the interaction unitary U_{CE}. All the environment ancillae are uncorrelated in between themselves and with the control C before each interaction. After interacting with C, each environment ancilla is thrown away. This contitutes a collisional model. (d) After n collisions with the environment E, the state of system-control is ρ^n_{SC}. The control is measured in the eigenbasis of σ_x, i.e. $\{|+\rangle, |-\rangle\}$. For the measurement result $|+\rangle_C$ ($|-\rangle_C$), the post-selected state of the system is $\rho^n_{S,+}$ ($\rho^n_{S,-}$). Finally, the outcome of the measurement must be stored in some classical memory, which is considered to be in contact with a thermal bath at inverse temperature β_{hot}. The amount of work to erase the previous result and then store the new one is $\mathcal{W}_n^{\text{erasure}}$.

The protocol then determines that if C is measured in the $|+\rangle_C$ state, the system is classically thermalized to the cold bath temperature $T_{\text{cold}} = 1/\beta_{\text{cold}}$ and the cycle starts all over again. On the other hand, if C is in the other state of the basis, i.e. $|-\rangle_C$, first S is classically thermalized with a hot bath at inverse temperature $\beta_{\text{hot}} < \beta_{\text{cold}}$ and at last with the cold bath at inverse temperature β_{cold}. After this, the cycle is repeated.

When measuring the control, the system's internal energy changes, as well as when it is thermalized with the cold and hot baths. In the "+ branch" (when C is measured in the $|+\rangle$ state), we have the net heat:

$$\mathcal{Q}_{n,+} := \text{tr}_S\left[\left(\rho^n_{S,+} - \Theta_{\beta_{\text{cold}}}\right) H_S\right] + \text{tr}_S\left[\left(\Theta_{\beta_{\text{cold}}} - \rho^n_{S,+}\right) H_S\right] \equiv 0, \tag{5.74}$$

and it *does not* contribute to the energy balance. Meanwhile, in the "- branch" (when C is measured in the $|-\rangle$ state), one has:

$$\mathcal{Q}_{n,-} := \text{tr}_S\left[\left(\rho^n_{S,-} - \Theta_{\beta_{\text{cold}}}\right) H_S\right] + \text{tr}_S\left[\left(\Theta_{\beta_{\text{cold}}} - \Theta_{\beta_{\text{hot}}}\right) H_S\right], \tag{5.75}$$

which explicitly is

$$\begin{aligned}\mathcal{Q}_{n,-} = &-\omega_S \frac{b^-_{\text{indef}}(n, g\tau)}{8 p^n_{\text{post}}(-)} \tanh\left(\frac{\beta_{\text{cold}}\omega_S}{2}\right) \text{sech}^2\left(\frac{\beta_{\text{cold}}\omega_S}{2}\right) \\ &+ \frac{\omega_S}{2}\left[\tanh\left(\frac{\beta_{\text{hot}}\omega_S}{2}\right) - \tanh\left(\frac{\beta_{\text{cold}}\omega_S}{2}\right)\right].\end{aligned} \tag{5.76}$$

The first term in the right-hand side (RHS) of the previous equation comes from the energy variation of the system due to the measurement of C and the second one comes from the classical thermalization with the baths. Thus, the average heat exchanged with the cold baths is:

$$\begin{aligned}\overline{\mathcal{Q}}_n &= p^n_{\text{post}}(+)\mathcal{Q}_{n,+} + p^n_{\text{post}}(-)\mathcal{Q}_{n,-} \\ &= p^n_{\text{post}}(-)\mathcal{Q}_{n,-}.\end{aligned} \tag{5.77}$$

When do we know that we have indeed a refrigeration cycle? It is clearly when (i) $\beta_{\text{hot}} < \beta_{\text{cold}}$, that is, the cold bath is colder than the hot bath and (ii) $\overline{\mathcal{Q}}_n > 0$, because it corresponds to the system gaining energy and the cold bath then losing energy. Take for instance the situation where no collisions happen (closed control), then

$$\overline{\mathcal{Q}}_0 = -\frac{\omega_S\left(\tanh\left(\frac{\beta_{\text{cold}}\omega_S}{2}\right) - 3\tanh\left(\frac{\beta_{\text{hot}}\omega_S}{2}\right)\right)}{8(\cosh(\beta_{\text{cold}}\omega_S) + 1)} > 0. \tag{5.78}$$

The two conditions are combined into one plot and an operation region can be identified in Fig. 5.9.

Given that the mean energetic cost of measuring the control is null for one cycle for every n, i.e.

$$\begin{aligned}\overline{\mathcal{W}}_n &= p^n_{\text{post}}(-)\mathcal{W}_{n,-} + p^n_{\text{post}}(+)\mathcal{W}_{n,+} \\ &= p^n_{\text{post}}(-)\frac{\omega}{2}\left(2p^n_{\text{post}}(+) - 1 + 1\right) + p^n_{\text{post}}(+)\frac{\omega}{2}\left(2p^n_{\text{post}}(+) - 1 - 1\right) \\ &\equiv 0,\end{aligned} \tag{5.79}$$

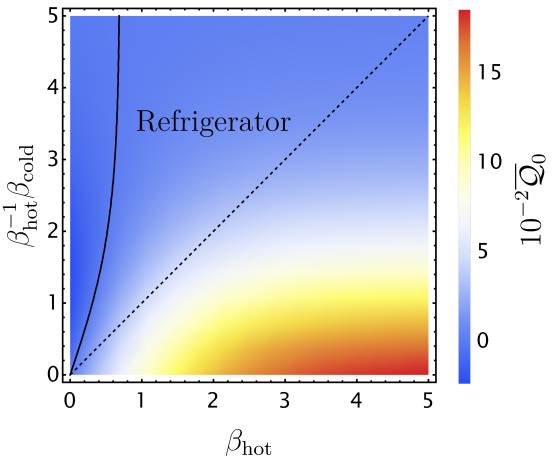

Figure 5.9: **Refrigeration condition for closed control (zero collisions, $n = 0$) as a function of $\beta_{\rm cold}$ and $\beta_{\rm hot}$.** Dashed line determines when $\beta_{\rm hot} = \beta_{\rm cold}$, while continuous line sets where $\overline{Q}_0 = 0$. The energy gap of the system is taken to be $\omega_S = 1.0$. Figure obtained from Ref. [30].

in which we used the fact that $p^n_{\rm post}(+) + p^n_{\rm post}(-) = 1, \forall n \in \mathbb{N}$, the work in the cycle corresponds solely to the work required to erase *one classical bit of information* stored in some classical memory (connected to Landauer's principle [104]):

$$\mathcal{W}_n^{\rm erasure} = -\frac{1}{\beta_{\rm hot}} \sum_{k=\pm} p^n_{\rm post}(k) \ln\left(p^n_{\rm post}(k)\right), \tag{5.80}$$

where we consider that the memory is in contact with the hot bath, in order to preserve the cold bath from undesired heat being dumped into it.

As it is the case for classical refrigeration cycles, the quantifier that is the analogue of the efficiency for heat engines is the *coefficient of performance* (COP), defined as the ratio between the heat being extracted from the cold bath and the amount of work needed to operate the cycle. In our scenario, we define a COP for n collisions, or

$$\mathrm{COP}_n := \frac{\overline{Q}_n}{\mathcal{W}_n^{\rm erasure}}, \tag{5.81}$$

whose explicit expression is obtained from combining Eqs. (5.73), (5.76), (5.77) and (5.80). For a specific set of parameters, we plot the ratio $\mathrm{COP}_n/\mathrm{COP}_0$ as a function of n and $\beta_E/\beta_{\rm hot}$ in Fig. 5.10. It shows that the collisions only worsen the refrigeration capacity of the cycle, even turning it into something else rather than a refrigerator (the gray-scale region, when the sign of COP_n becomes negative). Moreover, we also notice that the larger the ratio $\beta_E/\beta_{\rm hot}$ ($\beta_{\rm hot}$ is fixed, therefore it corresponds to higher β_E, i.e. colder environment), the more resilient the refrigeration cycle is to the collisions, that is, its coefficient of performance decays slower for increasing n.

It is important to consider the possibility that the environment that interacts with the control is in fact one of the cold baths ($\beta_E \equiv \beta_{\rm cold}$). This is a physically reasonable scenario: imagine that we bring the system S close to the cold baths to implement the QS; however, as the control is somehow not completely isolated from the system, it can and

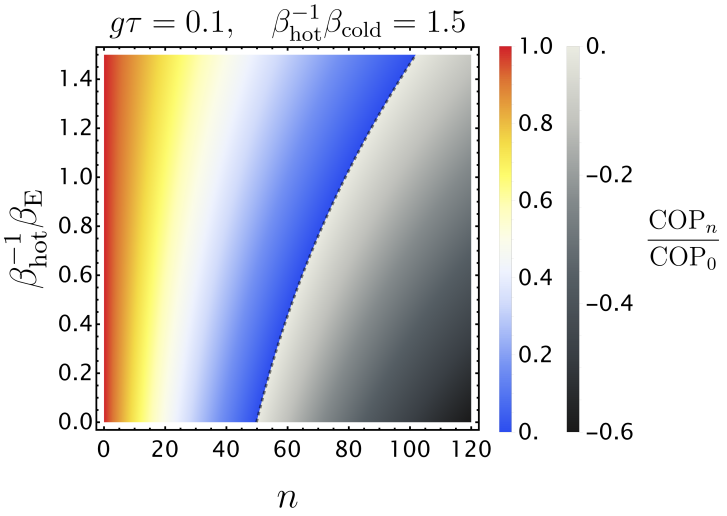

Figure 5.10: **Ratio between the coefficient of performance after n collisions ($\mathbf{COP}_n$) and the coefficient of performance for closed control ($\mathbf{COP}_0$) as a function of n and $\beta_E/\beta_{\mathbf{hot}}$.** We notice that the operation of the refrigeration cycle is only degraded as the number of collisions accumulate up to the point that no refrigeration happens anymore (dashed line in the plot, $\mathrm{COP}_n/\mathrm{COP}_0 = 0$). Here $\omega_S = \omega = 1.0, \beta_{\rm hot} = 1.0, \beta_{\rm cold} = 1.5$ and $g\tau = 0.1$. Figure obtained from Ref. [30].

will interact with the cold baths as well. On one hand the QS happens "instantanously" (in reality, very fast with comparison to the other time scales), and on the other, for some time τ the control will still interact with the cold bath before it is measured. Therefore, as C exchanges energy in the form of heat with the cold bath, it will affect the COP_n. Consider the heat flowing between control and cold bath after each collision:

$$q_n := \mathrm{tr}\{(\rho_C^n - \Theta_{\beta_{\rm cold}})H_C\}, \tag{5.82}$$

or explicitly,

$$\begin{aligned} q_n = &-\frac{3\omega}{8}\mathrm{sech}^2\left(\frac{\beta_{\rm cold}\omega_S}{2}\right) + \frac{\omega}{2}b^-_{\rm def}(n, f_{\rm cold}, g\tau) \\ &+ \frac{\omega}{2}b^-_{\rm indef}(n, g\tau)\left[1 - \frac{3}{4}\mathrm{sech}^2\left(\frac{\beta_{\rm cold}\omega_S}{2}\right)\right]. \end{aligned} \tag{5.83}$$

In Fig. 5.11 this is plotted as a function of $\beta_{\rm cold}/\beta_{\rm hot}$ and ω/ω_S. We can see that depending on the chosen parameters, the control might warm up or cool down, in the former helping with further cooling the cold bath, while in the latter degrading the operation of the refrigeration cycle.

The control heat q_n together with the average heat $\overline{Q}_n$ forms a new entry for the COP,

$$\overline{Q}'_n = \overline{Q}_n + q_n, \tag{5.84}$$

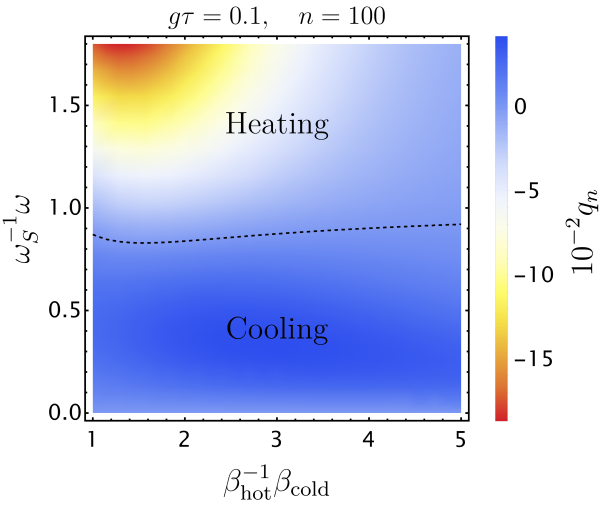

Figure 5.11: **Heat flowing between control C and cold bath, as a function of $\beta_{\rm cold}/\beta_{\rm hot}$ and ω/ω_S, for $n = 100$.** Dashed line ($q_n = 0$) separates the region where the control is heating up ($q_n > 0$) from where it is cooling down ($q_n < 0$). In the former case, extra cooling of the cold bath is attained. Here $\omega_S = 1.0$, $\beta_{\rm hot} = 1.0$ and $g\tau = 0.1$. Figure obtained from Ref. [30].

leading to the modified COP, or COP′:

$$\mathrm{COP}'_n := \frac{\overline{Q}'_n}{\mathcal{W}_n^{\rm erasure}} \tag{5.85}$$

$$= \frac{\overline{Q}_n}{\mathcal{W}_n^{\rm erasure}} + \frac{q_n}{\mathcal{W}_n^{\rm erasure}}. \tag{5.86}$$

The plot of this modified COP for a certain set of parameters, and as a function of ω/ω_S and for $n = 100$ can be seen in Fig. 5.12. We see that for a range of values of ω/ω_S, it is possible to keep the refrigerator operating as a refrigerator for arbitrary number of collisions n, but always with decreased coefficient of performance ($\mathrm{COP}'_n < \mathrm{COP}'_0$).

In this chapter, we have put forward a general expression for the time evolution of the state of a system post-QS with control interacting with an environment in the collisional model framework. Curiously, we found out that the terms that carry the SCO information are independent of the temperature of the environment, which affects primarily the causally ordered terms. However, the temperature dependence appears clearly in the post-selection of the control, in which the chosen measurement basis greatly impacts the behaviour for asymptotic temperatures ($T_E \to 0, \infty$). Starting the control in the $|+\rangle_C$ state and measuring it in $|-\rangle_C$ protects the system's state from decoherence in the low-temperature regime, but the probability of measuring the control in this state also tends to zero. In the high-temperature regime, SCO is always suppressed. However, for control initially in $|+\rangle_C$ and measured in $|+\rangle_C$ after the collisions, the SCO terms are always diminished with increasing n, irrespective of the temperature regime. These results are summarized in Table 5.1. The whole framework was tested in two different examples: first, the QS-based refrigerator proposed in Ref. [18], in which we found out that depending on the environment with which the control interacts, the coefficient of performance

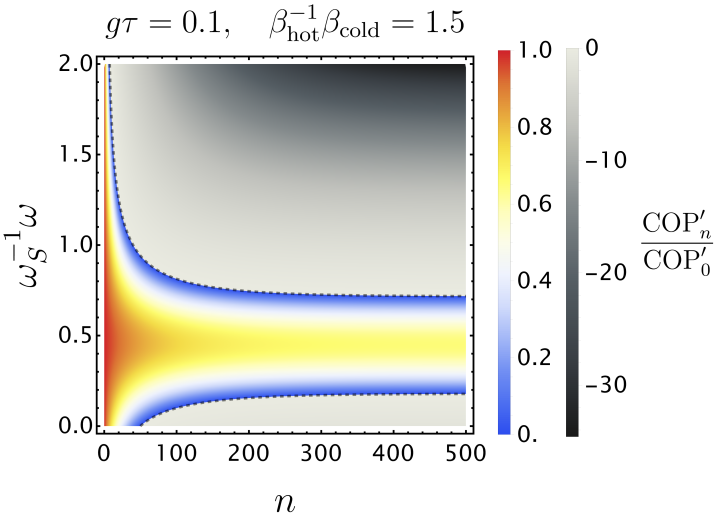

Figure 5.12: **Ratio between the coefficient of performance after n collisions (COP_n) and the coefficient of performance for closed control (COP_0) as a function of n and ω/ω_S, when taking into account the heat from the control q_n.** Dashed lines set where $\text{COP}_n/\text{COP}_0 = 0$. When the environment with which the control interacts is one of the cold baths ($\beta_E = \beta_{\text{cold}}$), one must include the internal energy change of C into the calculation of COP_n. As one can see from the plot, the performance of the refrigeration cycle *always* decays with n for the chosen parameters ($\beta_{\text{hot}} = 1.0, \beta_{\text{cold}} = 1.5$ and $g\tau = 0.1$) and the setup seizes working as a refrigerator for ω/ω_S outside of a determinate range (i.e. in the gray-scale region). Figure obtained from Ref. [30].

of the refrigerator can keep a non-negative value for arbitrarily large number of collisions n. However, in general, the operation of the QS-based refrigerator has its operation degraded by opening the control to interactions with an environment, eventually ceasing to operate as a refrigerator after a certain number of collisions. Second, we also studied the case of monitoring maps of MUBs, where the instabilities of the QS with open control were shown with respect to the asymmetry between control input and output states: if we prepare and measure the control in the $|+\rangle_C$ state, the available information is monotonically decreasing with increasing number of collisions, while for preparation in $|+\rangle_C$ and measurement in $|-\rangle_C$, non-monotonic behaviour with respect to n is found in both low and high temperature regimes.

Chapter 6

Thermodynamics and causal inequalities

"What we observe is not nature itself, but nature exposed to our method of questioning."

— Werner Heisenberg, Physics and Philosophy (1958).

This chapter is devoted to finding out whether thermodynamics through its second law (SLT) constraints indefinite causal order (ICO) processes which violate causal inequalities (CIs). Finding physical limitations on the existence of certain ICO processes is important for fundamental and application reasons. First, knowing which processes are and are not allowed to exist helps steering efforts in understanding the interplay between ICO and some possible quantum gravity (QG) theory. Second, before even starting to apply ICO processes in different scenarios looking for technological advantages, we need to know beforehand if these processes can be in fact engineered. As an example, the *quantum switch* (QS), a special case of controlled-superposition of causal orders (cSCO), which was be treated in Chapter 3, is known to not violate any CI [3, 4] and it is out of our scope, since it is a fact that this kind of ICO process can be manufactured in the laboratory [7–11]. On the other hand, processes like the Oreshkov-Costa-Brukner (OCB) process [25] and the Bäumeler-Wolf (BW) process [26] violate each one a different CI. Their existence/implementation is still a matter of debate, with inconclusive results so far. For instance, it has been *postulated* that processes that cannot be *purified*, i.e. extended to include a global past and a global future, are not physical [24]. The argument goes along a line of reversibility, as process matrices which cannot be purified would map unitary to non-unitary transformations. The postulate sets the OCB (two-party) and BW (three-party) processes to be non-physical and physical, respectively. However, in another work, it was also shown that no two-party process matrices containing ICO can allow extra work extraction with respect to processes not having ICO [27]. The author suggests that this would mean that two-party processes containing ICO do not violate the

SLT, meaning that from the perspective of thermodynamics they are physical. To help solving this impasse, we elaborate a toy model based on the engine of Ref. [29] and the lazy-guess your neighbour's input (LGYNI) game of Ref. [25], where one can violate a certain CI but the extracted work must always be less or equal than zero, as demanded by the SLT. We chose the engine of Ref. [29] for it is a simple model which already links violation of the SLT with the violation of *uncertainty relations* (URs, check Appendix C), so in principle it is already suited for exploring violation of the SLT given some other inequality violation. Our main result is an inequality for quantities related to the two-party process matrix and interestingly, it is *never* violated, even for the maximum violation of the CI, which is given by the OCB process matrix [105]. Also, we get that the violation of CIs is not related to the violation of the SLT. Thus, thermodynamics does not seem to be a constraint for two-party process matrices with two-dimensional systems.

The chapter is organized in the following manner. We begin in Section 6.1 with a straightforward presentation of what are CIs and the two most famous examples from the literature, the OCB and BW processes. Then, in Section 6.2 we give shape to our model. First, in Section 6.2.1 the engine of Hänggi and Wehner [29] is described in its original form, which relates violation of URs with violation of the SLT. Passing to Section 6.2.2, we combine what we learned previously to design what we call a *thermal lazy-guess your neighbour's input* (TLGYNI) game, where two parties, Alice and Bob, play the LGYNI game according to measurement results of their local engines, which are themselves based on the engine of Ref. [29]. After detailed calculations, we show our main result, the inequality on the process matrix terms imposed by the SLT, together with the conclusion that it is never violated when the systems are two-dimensional. In Section 6.2.3 we study the specific case of the OCB process matrix [25] for different states and measurement setups, showing that the violation of CIs and violation of the SLT are uncorrelated. Finally, we finish with Section 6.3, where we discuss the relation of our results with what is available in the literature and what are possible future studies on the overlap between ICO and thermodynamics.

6.1 Causal inequalities

The groundbreaking work of Ref. [25] not only formalized the matter of indefinite causal order (ICO) into the operational framework of process matrices, but it also introduced the concept of causal inequalities (CIs). These are inequalities [25, 26, 50, 53–55] that might be violated only when there is causal non-separability (check Chapter 2 for details). This is a necessary, but not sufficient condition. Indeed, the quantum switch (QS), even though being causally non-separable, does not violate any causal inequality [3, 4, 48, 50] (check Chapter 3 for more information). It is still a topic of active research to understand whether processes that violate CIs can be found in nature and/or can be engineered in the laboratory. We now present some of the known causal inequalities.

In Ref. [25] the authors proposed a game played between two parties, Alice and Bob, each one in a different laboratory and in which locally the laws of quantum mechanics are assumed. Also, we impose uni-directional signalling: only one party can communicate to the other at a time. In Fig. 6.1 one can see a representation of the measurement setup of the local labs. Alice has a hermetically closed laboratory, which opens

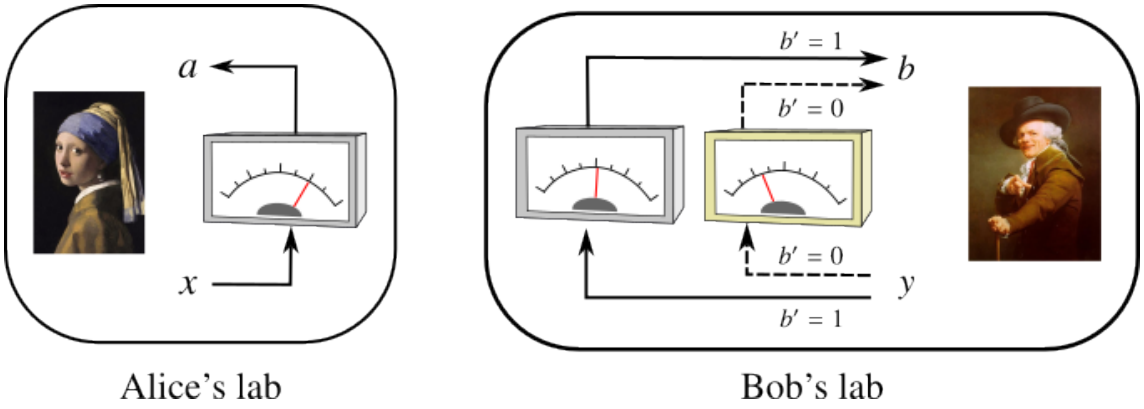

Figure 6.1: **Representation of local laboratories operated by Alice and Bob.** Alice has as input the bit x, which sets what is the measurement that will be performed on a quantum system that enters her laboratory. The output is encoded in the bit a. On the other hand, Bob has an extra bit b' that determines which basis of measurement he will use. The bit y determines the measurement in the basis selected by b' and the output is registered in the bit b. Locally the laws of quantum mechanics hold, but between the laboratories we leave the possibility of indefinite causal order (ICO).

for very brief moments so that a quantum system might enter and be measured and spit out. Given a chosen measurement basis (here we work all the time with two-dimensional systems and measurements), the value of the bit x is what sets the measurement to be performed on the quantum system that entered her laboratory. The outcome is registered in the bit a. Bob, however, has a little more work on his side. He has an extra bit b', which selects if he is going to use one measurement basis or the other. Having the basis set, he then goes on to measure the quantum system according to the bit y and the result is encoded in the bit b. Bob has a similar laboratory than Alice: it opens briefly just for a quantum system to enter and go out after measurements. The probability of success of this game, known as *lazy-guess your neighbour's input* (LGYNI) game [25, 54], which is achieved when Bob correctly guesses the measurement output of Alice or the other way around, is:

$$P_{\text{succ}} := \frac{1}{2}\left[P(x = b|b' = 0) + P(y = a|b' = 1)\right], \tag{6.1}$$

where $P(x = b|b' = 0)$ is the probability that the measurement x of Alice matches the outcome b of Bob when $b' = 0$, while $P(y = a|b' = 1)$ is the other way around, measurement y of Bob equals the output a of Alice when $b' = 1$. In order to obtain these, one must take the marginals of the conditional probability distribution $P(x, y|a, b, b')$:

$$P(x|a, b, b' = 0) = \sum_y P(x, y|a, b, b'), \tag{6.2}$$

$$P(y|a, b, b' = 1) = \sum_x P(x, y|a, b, b'), \tag{6.3}$$

and then we impose $x = b$ in Eq. (6.2) and $y = a$ in Eq. (6.3). For scenarios where the causal order is well-defined between the events of the labs where Alice and Bob are located, the success probability has upper bound [25]:

$$P_{\text{succ}} \leqslant \max P_{\text{succ}}^{\text{causal}} \equiv \frac{3}{4}. \tag{6.4}$$

This upper bound is obtained from the assumption that either Alice is in the causal past of Bob, vice-versa, or they are spatially separated, that is, no communication between them is allowed. Curiously, this bound is the same as in the non-locality scenario famously treated by John Clauser, Michael Horne, Abner Shimony and Richard Holt (the CHSH inequality [106]). If we allow for a resource called *process matrix* W (check Chapter 2 for more information) to contain what is called "causal nonseparability", the above inequality can be violated. In fact, in Ref. [25] the authors found out that a certain process matrix, here called W_{OCB}, allows the success probability to reach a higher value than $3/4$:

$$P_{\mathrm{succ}}^{W_{\mathrm{OCB}}} = \frac{1}{2} + \frac{\sqrt{2}}{4}. \tag{6.5}$$

This happens to be the *maximum* violation of this causal inequality for two-dimensional systems [105]. Once again, this also corresponds to the maximum violation of the CHSH inequality for quantum mechanics, known as the Tsirelson bound [107]. It is quite striking how, in the case of two-dimensional systems, the numerical values of two distinct cases, in one the (lack of) causality in spacetime and in the other non-locality of spatially separated parties, match each other.

Another interesting example of causal inequality that can be violated by ICO is the tripartite one presented in Ref. [26]. Now, instead of two labs commanded by Alice and Bob, we have an additional party, Charlie (see Fig. 6.2). As before, they all have input and output bits, $\{x, a\}$ for Alice, $\{y, b\}$ for Bob and $\{z, c\}$ for Charlie, registering the measurement to be performed and the result to the chosen measurement, respectively. An extra variable with three possible values $m \in \{0, 1, 2\}$ sets which of these parties will have to guess the outcome of measurements done in the other two. Here the success probability for the game is:

$$P_{\mathrm{succ}} = \frac{1}{3}\left[P(x = b \oplus c|m = 0) + P(y = a \oplus c|m = 1) + P(z = a \oplus b|m = 2)\right], \tag{6.6}$$

where $\oplus$ is the sum modulo 2. The probability $P(x = b \oplus c|m = 0)$ is the probability that Alice correctly guesses the output of Bob and Charlie, while $P(y = a \oplus c|m = 1)$ and $P(z = a \oplus b|m = 2)$ are the probabilities that Bob and Charlie manage to guess the output of the other two parties. In the case of predefined causal orders, it was originally found that [108]:

$$P_{\mathrm{succ}} \leqslant \max P_{\mathrm{succ}}^{\mathrm{causal}} \equiv \frac{5}{6}. \tag{6.7}$$

However, by allowing a non-predefined causal order, which is encoded in the process matrix W_{BW} from Bäumeler and Wolf, the violation is maximum, i.e.

$$P_{\mathrm{succ}}^{W_{\mathrm{BW}}} = 1. \tag{6.8}$$

Thus, by using the resource of ICO, one is able to always win the aforementioned game.

In Table 6.1 there is a summary of the bipartite and tripartite CIs. These results point out to the indication that using ICO resources, in this case a certain non-causally separable process matrix, allows for advantages in quantum information tasks, which would then reflect on communication protocols, cryptography, etc. However, a very important

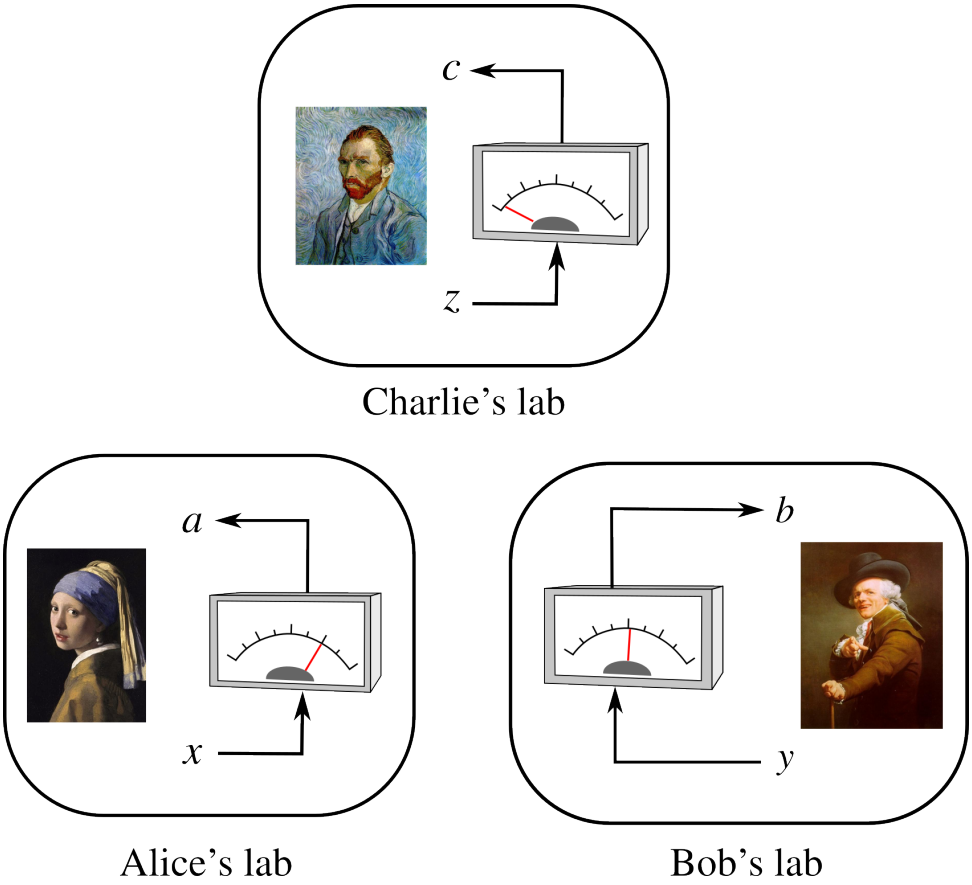

Figure 6.2: **Representation of local labs operated by Alice, Bob and Charlie.** Alice, Bob and Charlie have input bits x, y and z, and output bits a, b and c, respectively. Here we omit an extra variable $m \in \{0, 1, 2\}$ that determines which of the parties must guess the outcome of the other two. Here also locally quantum mechanics is assumed, but global exotic connections in spacetime (e.g. ICO) are allowed.

	$\max P_{\text{succ}}^{\text{causal}}$	ICO violation
Bipartite	$\frac{3}{4}$	$\frac{1}{2} + \frac{\sqrt{2}}{4}$
Tripartite	$\frac{5}{6}$	1

Table 6.1: **Summary of causal upper bounds and ICO violations for bipartite and tripartite systems.** The bipartite CI is due to Ref. [25], where the resource that allows the (maximum) violation of the upper bound is the process matrix W_{OCB}. Meanwhile, the tripartite CI is obtained from Ref. [26], in which the process matrix W_{BW} (maximally) violates the upper bound. In both cases the systems are two-dimensional.

comment here is necessary, which concerns the "physicality" of these process matrices. In Ref. [24] the authors *postulate* that process matrices that are not purifiable, that is, they do not admit a *unitary extension*, are not physical. Unitary extension is the possibility of connecting a given process matrix to another equivalent process matrix with global past and global future. They argue that non-purifiable process matrices break reversibility by

mapping unitary quantum maps onto non-unitary quantum maps, which would then be an unequivocal proof of non-physicality. The authors establish a mathematical criterium based on comparing the rank of the process matrix with the dimension of some special subspace generated by the eigenvectors of the same process matrix. If the rank is superior to the dimension of the special subspace, the process matrix is not purifiable. For further details on how this subspace is constructed, the reader is encouraged to check Ref. [24] in detail. They go on to to apply their criterium to the processes W_{OCB} and W_{BW}, finding out that the former is not purifiable, while the latter is. Even though this result has its mathematical significance, a real proof of the postulate is still missing. A true physical reasoning for why this or that process is physical or not is of utmost importance if we want to understand the underlying physics of ICO.

Noted the striking similarities between causal inequalities and the CHSH inequality (which itself is one specific Bell inequality [5]) in the probability formulation, many questions are raised whether we are talking about the same physical phenomenon in different languages. The question is very tricky, since the main resource that certifies non-locality – quantum entanglement – is not fully understood, even though we very well know how to describe, characterize and manipulate it [109]. Indeed, the scientific community which studies intensively quantum entanglement, most prominently, the scientists devoted to quantum information, has developed an outstanding mathematical toolbox to deal with quantum entanglement and in laboratories all over the world this unique quantum resource is daily manipulated in all sorts of experimental platforms. But, what *is* exactly quantum entanglement? This question might be further rooted in the connection between QM and GR, as it begs for a clear understanding of how the quantum and spacetime are intertwined. Remarkably, the whole field of ICO started with an attempt to describe a future theory of QG in operational terms, without diving into gravity quantization or similarly very hard to solve problems [1, 110]. Thus, scientific inquiry on how ICO works has the potential to help understanding even more what is quantum entanglement.

6.2 Connecting the second law of thermodynamics and causal inequalities

In Ref. [29], Esther Hänggi and Stephanie Wehner showed, by means of a toy model, that the violation of a *fine-grained uncertainty relation* (FGUR) (check Appendix C for definition) implies violation of the SLT. We aim to investigate if such a relationship also holds between the SLT and CIs. From the possible venues to reach this goal, we decide to adapt the engine of Ref. [29] to the scenario of Ref. [25], where the parties play the LGYNI game, such that the non-violation of the SLT will impose some condition on the process matrix connecting the laboratories of Alice and Bob. First, we present how the engine of Ref. [29] works in Section 6.2.1 and then we present our method in Sec. 6.2.2.

6.2.1 The idealized engine of Hänggi and Wehner

The engine cycle is presented in Fig. 6.3. All states and measurement operators are of dimension 2. The engine consists of a container with N particles, which occupy a volume V. The left compartment has a fraction $p_{\mathrm{L}} = 1/2$ of the total number of particles

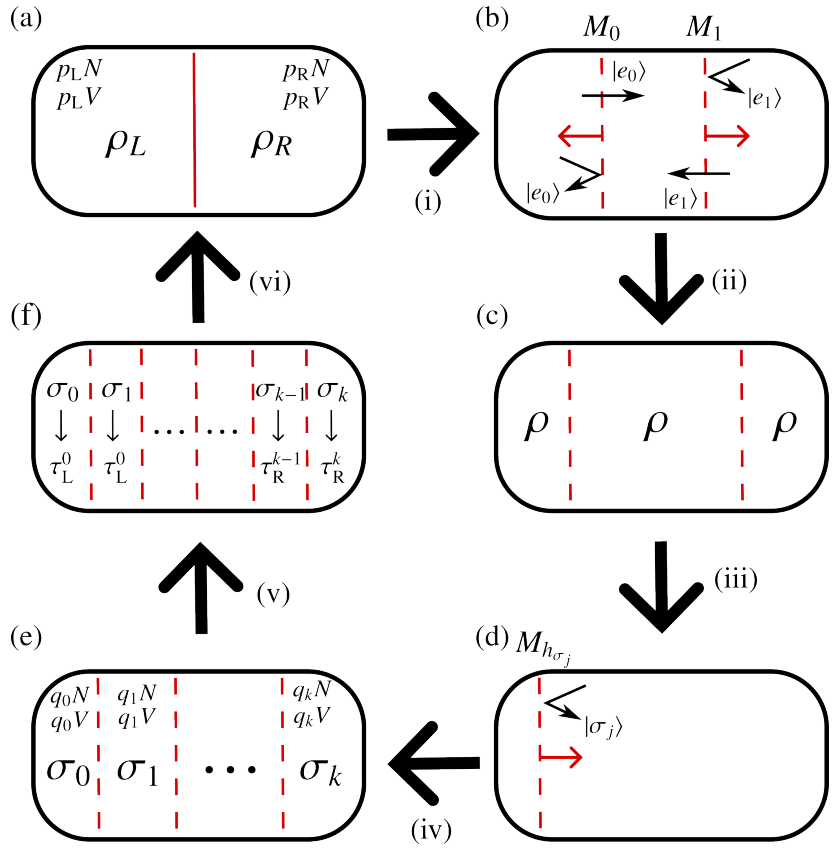

Figure 6.3: **The engine connecting uncertainty relations and the second law of thermodynamics.** (a) We start with a container having N particles occupying a volume V with surrounding temperature T. The container is divided by the red wall in two compartments: left and right. The former has a fraction $p_{\rm L} = 1/2$ of the particles, whose state is $\rho_{\rm L}$, while the latter has a fraction $p_{\rm R} = 1/2$ and state $\rho_{\rm R}$. (i) The red wall is removed and two membranes M_0 and M_1 are inserted. The first is opaque to the state $|e_0\rangle$ and transparent to $|e_1\rangle$, and for the second membrane it is the other way around (opaque to $|e_1\rangle$ and transparent to $|e_0\rangle$). (b) The membranes move apart as particles flow through them and others are blocked. (ii) The process continues until *equilibrium* is reached in (c): the same state $\mathrm{tr}_{\rm Comp.}\{\rho\}$ is found everywhere. (iii) Membranes M_0 and M_1 are removed, while a new set is inserted: $\{M_{h_{\sigma_j}}\}_{j=0,\ldots,k}$ opaque to $|\sigma_j\rangle$ and transparent to the rest. (d) Each membrane moves as the particles bounce back and forth, eventually the whole set reaches equilibrium (iv). (e) The container in the equilibrium situation now has in each partition a fraction q_j of the particles with individual *pure* states $\sigma_j = |\sigma_j\rangle\langle\sigma_j|$. (v) To come back to the initial state of the container, we then transform *unitarily* the states of each compartment. (f) The containers are further subdivided, such that the number of particles is proportional to $p_{\rm L} r^i_{\rm L}$ or $p_{\rm R} r^i_{\rm R}$, where the coefficients $\{r^i_{\rm L(R)}\}_{i=0,\ldots,k'}$ are such that $\rho_{\rm L(R)} = \sum_{i=0}^{k'} r^i_{\rm L(R)} \tau^i_{\rm L(R)}$. The states $\{\sigma_j\}_{j=0,\ldots,k}$ are *unitarily* transformed into $\{\tau^i_{\rm L}\}_{i=0,\ldots,k'}$ or $\{\tau^i_{\rm R}\}_{i=0,\ldots,k'}$. Since all the involved states are pure, the transformations are reversible and have zero work cost. (vi) All the membranes are removed at the same time that a rigid wall is inserted, returning the engine to the original configuration (a).

and their collective state is denoted ρ_{L}, while the right compartment has $p_{\mathrm{R}} = 1/2$ of the particles and state ρ_{R}. These states form what we call the "working fluid" of the engine. Both of them are in the space of density matrices $\mathrm{D}(\mathcal{H}_S)$. The engine state then is:

$$\rho = p_{\mathrm{L}}\,\rho_{\mathrm{L}} \otimes |\mathrm{L}\rangle\langle\mathrm{L}|_{\mathrm{Comp.}} + p_{\mathrm{R}}\,\rho_{\mathrm{R}} \otimes |\mathrm{R}\rangle\langle\mathrm{R}|_{\mathrm{Comp.}}, \tag{6.9}$$

in which $\{|\mathrm{L}\rangle_{\mathrm{Comp.}}, |\mathrm{R}\rangle_{\mathrm{Comp.}}\}$ correspond to the left and right states of the compartment DOF. Note that this "side DOF" is not exactly a quantum system, but solely a physical label and using them as ket states is simply a mathematical notation.

Given the *effects* – a generalization of the concept of measurement operators – representing measurement bases $\mathbf{f} = \{f_0, f_1\}$ and $\mathbf{g} = \{g_0, g_1\}$, the left and right states can be decomposed as:

$$\rho_{\mathrm{L}} = \frac{1}{2}\left(\rho_{f_0} + \rho_{g_0}\right), \tag{6.10}$$

$$\rho_{\mathrm{R}} = \frac{1}{2}\left(\rho_{f_1} + \rho_{g_1}\right), \tag{6.11}$$

where $\{\rho_{f_0}, \rho_{f_1}\}$ and $\{\rho_{g_0}, \rho_{g_1}\}$ are such that for *every* pure state η the corresponding effect e_η fulfills:

$$\mathrm{tr}\{e_\eta\,\rho_{f_{0(1)}}\} = P(e_\eta\,|\,\rho_{f_{0(1)}}) = P(f_{0(1)}\,|\,\eta) = \mathrm{tr}\{f_{0(1)}\,\eta\}, \tag{6.12}$$

$$\mathrm{tr}\{e_\eta\,\rho_{g_{0(1)}}\} = P(e_\eta\,|\,\rho_{g_{0(1)}}) = P(g_{0(1)}\,|\,\eta) = \mathrm{tr}\{g_{0(1)}\,\eta\}. \tag{6.13}$$

These relations represent the duality between *pure* states and *projective* measurements in QM. Consider, for example, $\mathbf{f} = \{0_X, 1_X\}$ and $\mathbf{g} = \{0_Z, 1_Z\}$ being measurements on the basis of the Pauli matrices σ_x and σ_z, respectively, and the state $\eta = |0\rangle\langle 0|$. Therefore, $\rho_{f_0} = |+\rangle\langle +|$, $\rho_{f_1} = |-\rangle\langle -|$, $\rho_{g_0} = |0\rangle\langle 0|$ and $\rho_{g_1} = |1\rangle\langle 1|$, with the effect $e_\eta = 0_Z$.

We then remove the wall separating the containers and insert two mobile membranes M_0 and M_1, the first transparent to $|e_1\rangle$ and the second transparent to $|e_0\rangle$. Effectively, we measure the particles in the measurement basis $\mathbf{e} = \{e_0, e_1\}$. As they are being transmitted and reflected, the particles make these membranes to move until equilibrium is reached. This is identified with the situation that everywhere the local state is equal to $\mathrm{tr}_{\mathrm{Comp.}}\{\rho\} = \rho_{\mathrm{L}}/2 + \rho_{\mathrm{R}}/2$. The work that is extracted in this procedure, in the case that the movement of the membranes is used for some task, is obtained from a calculation of *isothermal expansion* of the membranes: membrane M_0 (M_1) expands from a volume V_0 (V_1) to a volume V_0' (V_1'). Formally:

$$\begin{aligned}\mathcal{W}_{\mathrm{I}} &= NT\int_{V_0}^{V_0'}\frac{\mathrm{d}V}{V} + NT\int_{V_1}^{V_1'}\frac{\mathrm{d}V}{V} &(6.14)\\ &= NT\ln 2\left(-\sum_{i=0}^{1}P(e_i)\log_2 P(e_i) - \frac{1}{2}\sum_{i=0}^{1}H\left(\frac{1}{2}P(e_i\,|\,\rho_{f_i}) + \frac{1}{2}P(e_i\,|\,\rho_{g_i})\right)\right), &(6.15)\end{aligned}$$

where $\ln 2 := \log_e 2$ is the natural logarithm of 2, $H(\alpha) := -\alpha\log_2\alpha - (1-\alpha)\log_2(1-\alpha)$ is the *binary entropy function*, T is the temperature to which the engine is thermalized and $P(e_i) = p_{\mathrm{L}}P(e_i|\rho_{\mathrm{L}}) + p_{\mathrm{R}}P(e_i|\rho_{\mathrm{R}})$. The above quantity is found to be upper bounded:

$$\mathcal{W}_{\mathrm{I}} \leqslant NT\ln 2\left(-\sum_{i=0}^{1}P(e_i)\log_2 P(e_i) - \frac{1}{2}\sum_{i=0}^{1}H(\zeta_{(f_i,g_i)})\right), \tag{6.16}$$

with $\zeta_{(f_i,g_i)}$ being the FGUR upper bound for measurements f_i and g_i. It is possible to saturate this inequality by correctly choosing $\{e_0, e_1\}$ (i.e. *maximally certain effects*).

The second part of the cycle starts with removing membranes M_0 and M_1, while inserting a new set $\{M_{h_{\sigma_j}}\}_{j=0,\dots,k}$, which are transparent to all states, except for $|\sigma_j\rangle$. The membranes then move until accommodating to some equilibrium position, where the space in between membranes has a fraction q_j of the total amount of particles and its state is denoted $\sigma_j \equiv |\sigma_j\rangle\langle\sigma_j|$. The work that is required to transform the engine from the previous configuration to the present one is given by:

$$\begin{aligned}\mathcal{W}_{\text{II}} &= -NT\ln 2\left(\sum_{j=0}^{k} P(h_{\sigma_j} \mid \text{tr}_{\text{Comp.}}\{\rho\})\log_2\left(P(h_{\sigma_j} \mid \text{tr}_{\text{Comp.}}\{\rho\})\right)\right)\\ &= NT\ln 2\,\mathfrak{S}(\text{tr}_{\text{Comp.}}\{\rho\}),\end{aligned} \tag{6.17}$$

where

$$\mathfrak{S}\left(\text{tr}_{\text{Comp.}}\{\rho\}\right) := \min_{\{q_j,\sigma_j\}_{j=0,\dots,k}} H(\{q_0,\dots,q_k\}) \tag{6.18}$$

is the *decomposition entropy* [111] and $H(\{q_0,\dots,q_k\})$ is the Shannon entropy of the set $\{q_0,\dots,q_k\}$.

The final step is then to recover the initial states ρ_{L} and ρ_{R} with a rigid wall between them. This is done by first sub-dividing the partitions such that each one has a fraction of the particles proportional to $p_{\text{L}}r^i_{\text{L}}$ or $p_{\text{R}}r^i_{\text{R}}$, with coefficients $\{r^i_{\text{L(R)}}\}_{i=0,\dots,k'}$, $\{r^i_{\text{R}}\}_{i=0,\dots,k'}$ satisfying:

$$\rho_{\text{L(R)}} = \sum_{i=0}^{k'} r^i_{\text{L(R)}}\tau^i_{\text{L(R)}},$$

where $\{\tau^i_{\text{L(R)}}\}_{i=0,\dots,k'}$ are pure states. In the end, the set of states $\{\sigma_j\}_{j=0,\dots,k}$ is *unitarily* transformed into $\{\tau^i_{\text{L}}\}_{i=0,\dots,k'}$ or $\{\tau^i_{\text{R}}\}_{i=0,\dots,k'}$. These transformations, since the involved states are pure, are *reversible* and have therefore zero work cost. Finally, by removing the membranes and inserting a rigid wall, some work can be extracted, related to the decomposition entropy of each compartment, that is:

$$\mathcal{W}_{\text{III}} = NT\ln 2\left[p_{\text{L}}\,\mathfrak{S}(\rho_{\text{L}}) + p_{\text{R}}\,\mathfrak{S}(\rho_{\text{R}})\right] = NT\frac{\ln 2}{2}\left[\mathfrak{S}(\rho_{\text{L}}) + \mathfrak{S}(\rho_{\text{R}})\right]. \tag{6.19}$$

The total work extracted from the cycle is therefore:

$$\mathcal{W}_{\text{cycle}} = \mathcal{W}_{\text{I}} - \mathcal{W}_{\text{II}} + \mathcal{W}_{\text{III}} \tag{6.20}$$

which is upper bounded by:

$$\begin{aligned}\mathcal{W}_{\text{cycle}} \leqslant NT\frac{\ln 2}{2}\Big(&-2\sum_{i=0}^{1} P(e_i)\log_2 P(e_i) + \mathfrak{S}(\rho_{\text{L}}) + \mathfrak{S}(\rho_{\text{R}})\\ &- 2\mathfrak{S}(\text{tr}_{\text{Comp.}}\{\rho\}) - \sum_{i=0}^{1} H(\zeta_{(f_i,g_i)})\Big),\end{aligned} \tag{6.21}$$

relating directly the violation of FGURs (check Appendix C for definition) with a violation of the SLT, that is, such that $\mathcal{W}_{\text{cycle}} > 0$. Consider, for instance, the case in which

$\mathbf{f} = \{0_X, 1_X\}$ and $\mathbf{g} = \{0_Z, 1_Z\}$, where $0_X = |+\rangle\langle+|$, $1_X = |-\rangle\langle-|$, $0_Z = |0\rangle\langle 0|$ and $1_Z = |1\rangle\langle 1|$. Then:

$$\rho_{\mathrm{L}} = \frac{\mathbb{1}_2}{2} + \frac{\sigma_x + \sigma_z}{4}, \tag{6.22}$$

and

$$\rho_{\mathrm{R}} = \frac{\mathbb{1}_2}{2} - \left(\frac{\sigma_x + \sigma_z}{4}\right). \tag{6.23}$$

In such case, we see that if one traces out the compartment DOF, the result is the maximally mixed state:

$$\mathrm{tr}_{\mathrm{Comp.}}\{\rho\} = \frac{\rho_{\mathrm{L}}}{2} + \frac{\rho_{\mathrm{R}}}{2} \equiv \frac{\mathbb{1}_2}{2}. \tag{6.24}$$

Therefore, the decomposition entropy of $\mathrm{tr}_{\mathrm{Comp.}}\{\rho\}$ is simply:

$$\mathfrak{S}(\mathrm{tr}_{\mathrm{Comp.}}\{\rho\}) = 1, \tag{6.25}$$

the probabilities for the effects are:

$$P(e_0) = P(e_1) = \frac{1}{2} \tag{6.26}$$

and the work per cycle is:

$$\mathcal{W}_{\mathrm{cycle}} = NT \ln 2 \left(H\left(\frac{1}{2} + \frac{\sqrt{2}}{4}\right) - \frac{1}{2} H\left(\zeta_{(0_X,0_Z)}\right) - \frac{1}{2} H\left(\zeta_{(1_X,1_Z)}\right) \right) \tag{6.27}$$

and the maximally certain effects are the eigenvectors of $(\sigma_x + \sigma_z)/\sqrt{2}$. For QM,

$$\zeta_{(0_X,0_Z)} = \zeta_{(1_X,1_Z)} = \frac{1}{2} + \frac{\sqrt{2}}{4}, \tag{6.28}$$

thus

$$\mathcal{W}_{\mathrm{cycle}} \equiv 0, \tag{6.29}$$

meaning that the upper bound of the FGUR is exactly the limit of the SLT, a value that violates this upper bound necessarily violates the SLT.

6.2.2 The thermal lazy-guess your neighbour's input game

Our basic premise is that Alice and Bob in their local laboratories have the same engine as presented in the previous section: a container with two compartments. Each compartment receives a left state ρ_{L} and a right state ρ_{R}, which then correspond to the "working fluid" of these engines: a number N of identical particles. Both of them are in the space of density matrices $\mathrm{D}(\mathcal{H}_S)$. For the sake of simplicity, we assume that the systems entering the compartments are always two-dimensional (qubits). The engine state is described as previously, that is:

$$\rho = p_{\mathrm{L}}\, \rho_{\mathrm{L}} \otimes |\mathrm{L}\rangle\langle \mathrm{L}|_{\mathrm{Comp.}} + p_{\mathrm{R}}\, \rho_{\mathrm{R}} \otimes |\mathrm{R}\rangle\langle \mathrm{R}|_{\mathrm{Comp.}},$$

where from the very beginning we assume that

$$\mathrm{tr}_{\mathrm{Comp.}}\{\rho\} = \frac{\rho_{\mathrm{L}}}{2} + \frac{\rho_{\mathrm{R}}}{2} \equiv \frac{\mathbb{1}_2}{2},$$

and the fractions of the particles in the left and right compartments, p_{L} and p_{R}, are set to $1/2$. This assumption helps simplifying the following expressions, without sacrificing generality, as done in Ref. [29]. What happens then if Alice and Bob dispose of a non-causal resource, for instance a process matrix W violating some CI? In the following, we consider general process matrices which might be causally non-separable, violate CIs, etc. The underlying physical phenomena originating ICO here does not matter much to us, but the operational meaning of disposing of W containing this resource. To implement process matrices in the model, we assume that Alice and Bob play the LGYNI, where the bits of the game – from measurement and state preparation – are relative to measurements and preparations of the *left compartment* of each engine (a mere convention). This double-game of bit guessing plus work extraction is named *thermal lazy-guess your neighbour's input game* (TLGYNI). By playing it, we want to check if additional constraints are imposed to W by the SLT, and in the affirmative, what are these constraints. For instance, we investigate whether there is a one-to-one correspondence between violation of a CI and the violation of the SLT, which would point out to an incompatibility between processes violating CIs with a clear physicality demand, that is, non-violation of the SLT.

Within this framework, we now show how everything can be coherently described together. The following scenario is shown in Fig. 6.4. We start by considering the situation where $b' = 1$. Alice receives a pair of left and right states ρ_{L} and ρ_{R}, respectively, with $\rho_{\mathrm{L}}/2 + \rho_{\mathrm{R}}/2 = \mathbb{1}_2/2$. These are measured by means of the effects $\{e^{\mathrm{A}}_x\}_{x=0,1}$, which is done by using mobile membranes as described in the previous section. She then re-prepares the initial states ρ_{L} and ρ_{R} in the "correct" order, ρ_{L} in the left compartment and ρ_{R} in the right compartment, or in the "opposite" order, ρ_{R} in the left compartment and ρ_{L} in the right compartment. This is encoded in the variable a:

$$\rho_{\mathrm{L(R)}}(a, b' = 1) := \left(\frac{1 + (-1)^a}{2}\right) \rho_{\mathrm{L(R)}} + \left(\frac{1 - (-1)^a}{2}\right) \rho_{\mathrm{R(L)}}. \tag{6.30}$$

Even when the order of the states is opposite to the original one, we consider that the engine operates in a cycle, because we have such a symmetry in this setup: the order of the states does not matter for work extraction. Indeed, for whatever value of a, we have [29]:

$$\begin{aligned}
\mathcal{W}^{\mathrm{A}}_{x|b'=1} &= NT\frac{\ln 2}{2}\left(\mathfrak{S}(\rho_{\mathrm{L}}) + \mathfrak{S}(\rho_{\mathrm{R}}) - \sum_{i=0}^{1} H\left(\frac{1}{2}P(e^{\mathrm{A}}_{i\oplus x}|\rho_{f_i}) + \frac{1}{2}P(e^{\mathrm{A}}_{i\oplus x}|\rho_{g_i})\right)\right) \\
&= NT\frac{\ln 2}{2}\left(\mathfrak{S}(\rho_{\mathrm{L}}) + \mathfrak{S}(\rho_{\mathrm{R}}) - H\left(P(e^{\mathrm{A}}_{x}|\rho_{\mathrm{L}})\right) - H\left(P(e^{\mathrm{A}}_{x\oplus 1}|\rho_{\mathrm{R}})\right)\right) \qquad (6.31) \\
&\leqslant NT\frac{\ln 2}{2}\left(\mathfrak{S}(\rho_{\mathrm{L}}) + \mathfrak{S}(\rho_{\mathrm{R}}) - \sum_{i=0}^{1} H(\zeta_{(f_i,g_i)})\right) \quad \forall x \qquad (6.32)
\end{aligned}$$

with H being the binary entropy function, as defined in Section 6.2.1 and $\mathfrak{S}(\rho_{\mathrm{L(R)}})$ is the decomposition entropy of $\rho_{\mathrm{L(R)}}$, defined similarly to the decomposition entropy found in Eq. (6.18). Also:

$$\rho_{\mathrm{L}} = \frac{1}{2}\left(\rho_{f_0} + \rho_{g_0}\right),$$
$$\rho_{\mathrm{R}} = \frac{1}{2}\left(\rho_{f_1} + \rho_{g_1}\right).$$

Since $\rho_{\mathrm{L}} + \rho_{\mathrm{R}} = \mathbb{1}_2$ and we are in two dimensions, the eigenvalues of ρ_{L} and ρ_{R} are the same. If we parametrize these states in the Bloch sphere as:

$$\rho_{\mathrm{L}} = \frac{\mathbb{1}_2 + \mathbf{r}\cdot\boldsymbol{\sigma}}{2}, \tag{6.33}$$

$$\rho_{\mathrm{R}} = \frac{\mathbb{1}_2 - \mathbf{r}\cdot\boldsymbol{\sigma}}{2}, \tag{6.34}$$

where $\mathbf{r} = (r_1, r_2, r_3)$ is a vector on the Bloch sphere and $\boldsymbol{\sigma} = (\sigma_1, \sigma_2, \sigma_3)$ is the vector containing the Pauli matrices $\{\sigma_i\}_{i=1,2,3}$, the eigenvalues of $\rho_{\mathrm{L(R)}}$ are $(1 \pm |\mathbf{r}|)/2$ and then

$$\mathfrak{S}(\rho_{\mathrm{R}}) \equiv \mathfrak{S}(\rho_{\mathrm{L}}) = H\left(\frac{1}{2} + \frac{|\mathbf{r}|}{2}\right). \tag{6.35}$$

Thus, the work extracted by Alice simplifies to:

$$\mathcal{W}^{\mathrm{A}}_{x|b'=1} = NT \ln 2 \left[H\left(\frac{1}{2} + \frac{|\mathbf{r}|}{2}\right) - H\left(P\left(e^{\mathrm{A}}_x \middle| \frac{\mathbb{1}_2 + \mathbf{r}\cdot\boldsymbol{\sigma}}{2}\right)\right)\right], \tag{6.36}$$

where we further used the fact that the left and right states sum up to the identity, and the same holds for $\sum_x e^{\mathrm{A}}_x = \mathbb{1}_2$.

Due to the process matrix W, the communicated and received states by Alice and Bob are not necessarily the same. In fact, the *effective* states received by Bob are [25]:

$$\tilde{\rho}_{\mathrm{L(R)}}(a, b' = 1) := \frac{1}{2}\,\mathrm{tr}_{A_I A_O B_O}\left\{W\left(\sum_{x=0}^{1} M^{\mathrm{A,L(R)}}_{x|a,b'=1} \otimes \mathbb{1}_{B_I B_O}\right)\right\}, \tag{6.37}$$

where $A_{I(O)}, B_{I(O)}$ are associated to the Hilbert spaces of the input (output) of Alice and Bob, respectively, and $M^{\mathrm{A,L(R)}}_{x|a,b'=1}$ are the CJ matrices of the quantum instrument of Alice for the left and right compartments. The state originally prepared by Alice and sent to Bob is encoded in the inner structure of the quantum instruments $M^{\mathrm{A,L(R)}}_{x|a,b'=1}$. We assume that the CJ matrices of the quantum instruments of Alice are written in the form of measured state tensor product with re-prepared state, i.e. [25]:

$$M^{\mathrm{A,L}}_{x|a,b'=1} = e^{\mathrm{A}}_x \otimes \rho_{\mathrm{L}}(a|b' = 1), \tag{6.38}$$

$$M^{\mathrm{A,R}}_{x|a,b'=1} = e^{\mathrm{A}}_{x\oplus 1} \otimes \rho_{\mathrm{R}}(a|b' = 1). \tag{6.39}$$

From the definition of effective states and the CJ matrices of the quantum instruments of Alice and Bob, we have that:

$$\begin{aligned}\frac{1}{2}\tilde{\rho}_{\mathrm{L}}(a, b' = 1) + \frac{1}{2}\tilde{\rho}_{\mathrm{R}}(a, b' = 1) = \frac{1}{4}\,\mathrm{tr}_{A_I A_O B_O}\{W\,(\mathbb{1}_{A_I} \otimes (\rho_{\mathrm{L}}(a, b' = 1) \\ + \rho_{\mathrm{R}}(a, b' = 1)) \otimes \mathbb{1}_{B_I B_O})\},\end{aligned} \tag{6.40}$$

which simplifies to:

$$\begin{aligned}\frac{1}{2}\tilde{\rho}_{\mathrm{L}}(a, b' = 1) + \frac{1}{2}\tilde{\rho}_{\mathrm{R}}(a, b' = 1) &= \frac{1}{4}\,\mathrm{tr}_{A_I A_O B_O}\left\{W\left(\mathbb{1}_{A_I A_O B_I B_O}\right)\right\} \\ &= \frac{\mathbb{1}_2}{2} + \frac{1}{2}\sum_{i=1}^{3} f_i \sigma_i \\ &= \frac{\mathbb{1}_2 + \mathbf{f}\cdot\boldsymbol{\sigma}}{2}, \qquad \forall a\end{aligned} \tag{6.41}$$

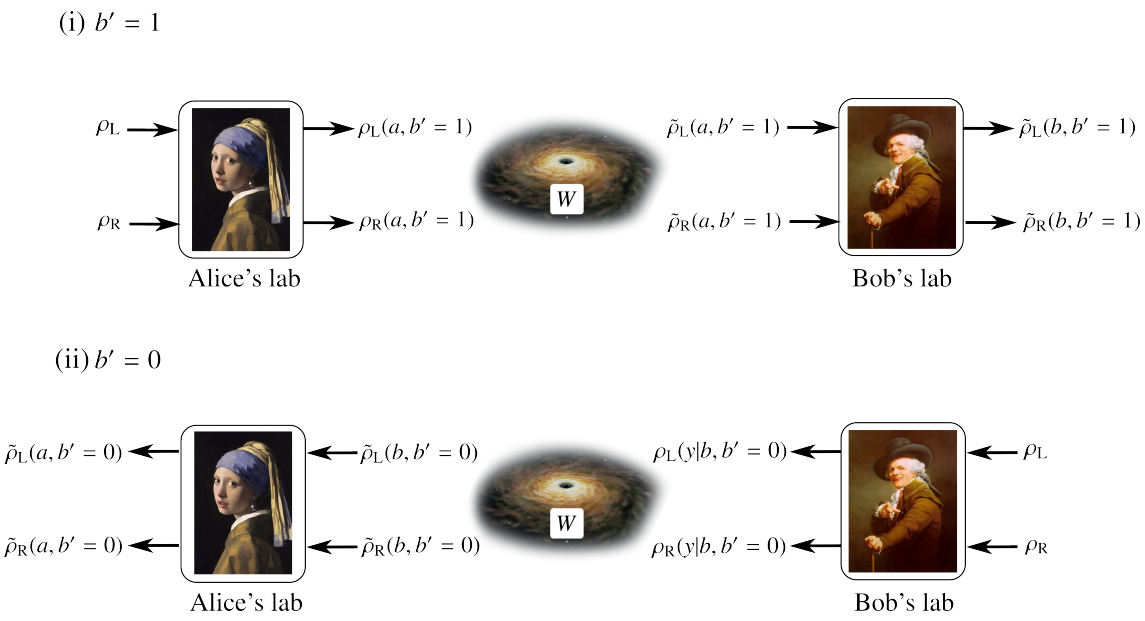

Figure 6.4: **Thermal lazy-guess your neighbour's input (TLGYNI) game played between Alice and Bob from the perspective of communicated and received states.** (i) When $b' = 1$ Alice receives in her lab the left and right states ρ_L and ρ_R, respectively. After measuring them (effects e^A_x), she prepares new states in the compartments: $\rho_L(a, b' = 1)$ and $\rho_R(a, b' = 1)$, such that $\rho_L + \rho_R = \mathbb{1}_2$. Due to the process matrix W, the actual states which are received by Bob are $\tilde{\rho}_L(a, b' = 1)$ and $\tilde{\rho}_R(a, b' = 1)$ (definitions in the text), which in general *do not* fulfill $\tilde{\rho}_L(a, b' = 1) + \tilde{\rho}_R(a, b' = 1) = \mathbb{1}_2$. These states are then processed by Bob through effects $e^B_{y,b'=1}$, whose re-prepared states are $\tilde{\rho}_L(b, b' = 1)$ and $\tilde{\rho}_R(b, b' = 1)$. (ii) On the other hand, when $b' = 0$ Bob is the one to first receive states ρ_L and ρ_R. Following his measurements (projectors $e^B_{y,b'=0}$), he prepares the states $\rho_L(y|b, b' = 0)$ and $\rho_R(y|b, b' = 0)$ (measurement-dependent states), which by means of W will be received by Alice as $\tilde{\rho}_L(b, b' = 0)$ and $\tilde{\rho}_R(b, b' = 0)$ (where $\tilde{\rho}_L(b, b' = 0) = \tilde{\rho}_R(b, b' = 0)$, $\forall b$). After measuring these states through effects e^A_x, we overall have three important quantities: $P^L(y|a, b' = 1)$, $P^L(x|b, b' = 0)$ and $\overline{W}^{AB}_{ab}$, the probabilities for the LGYNI game with respect to measurements of the left compartments and the *average total work* extracted by Alice *and* Bob for outcomes a, b.

where $\{f_i\}_i \in \mathbb{R}$ come from the most general form of the process matrix (check Appendix B). We promptly see that $-1 \leqslant f_i \leqslant 1, \forall i$ and $\sqrt{f_1^2 + f_2^2 + f_3^2} \leqslant 1$, that is, the $\{f_i\}_i$ behave as coordinates of a density matrix on the Bloch sphere.

As a sanity test, we check whether for a direct communication from Alice to Bob we can obtain the expected effective states, that is, simply the re-prepared states by Alice. From the general form of the process matrix (see Chapter 2 or Appendix B), we can write the process matrix of communication from Alice to Bob without memory:

$$W_{A\to B} = \frac{1}{4}\left[\mathbb{1}_{A_I A_O B_I B_O} + \sum_{i,j} c_{ij} \mathbb{1}_{A_I} \otimes \sigma_i^{A_O} \otimes \sigma_j^{B_I} \otimes \mathbb{1}_{B_O}\right], \tag{6.42}$$

from which the effective states received by Bob are:

$$\tilde{\rho}_{\mathrm{L}}(a, b' = 1) = \frac{\mathbb{1}_2 + (-1)^a \left(\sum_i r_i c_{i1}\sigma_1 + \sum_i r_i c_{i2}\sigma_2 + \sum_i r_i c_{i3}\sigma_3\right)}{2}, \tag{6.43}$$

$$\tilde{\rho}_{\mathrm{R}}(a, b' = 1) = \frac{\mathbb{1}_2 + (-1)^{a+1} \left(\sum_i r_i c_{i1}\sigma_1 + \sum_i r_i c_{i2}\sigma_2 + \sum_i r_i c_{i3}\sigma_3\right)}{2}, \tag{6.44}$$

where we again used the Bloch sphere parametrization for the left and right states. For $c_{11} = c_{22} = c_{33} = 1$ and all other c's equal to zero, we get:

$$\tilde{\rho}_{\mathrm{L}}(a, b' = 1) = \frac{\mathbb{1}_2 + (-1)^a \mathbf{r}\cdot\boldsymbol{\sigma}}{2} \equiv \rho_{\mathrm{L}}(a, b' = 1), \tag{6.45}$$

$$\tilde{\rho}_{\mathrm{R}}(a, b' = 1) = \frac{\mathbb{1}_2 + (-1)^{a+1} \mathbf{r}\cdot\boldsymbol{\sigma}}{2} \equiv \rho_{\mathrm{R}}(a, b' = 1), \tag{6.46}$$

like we would expect.

Coming back to the general case, as Bob receives the states modulated by the process matrix, he inserts them into his engine. He disposes of effects $\{e^{\mathrm{B}}_{y,b'=1}\}_{y=0,1}$ for measuring the states in the compartments and he reprepares in similar manner as Alice, but of course resetting now to the states $\tilde{\rho}_{\mathrm{L}}(b, b' = 1)$ and $\tilde{\rho}_{\mathrm{R}}(b, b' = 1)$ (same definition as before, but now $a \to b$). The CJ matrices of his quantum instruments are:

$$M^{\mathrm{B,L}}_{y|b,b'=1} = e^{\mathrm{B}}_{y|b'=1} \otimes \tilde{\rho}_{\mathrm{L}}(b, b' = 1), \tag{6.47}$$

$$M^{\mathrm{B,R}}_{y|b,b'=1} = e^{\mathrm{B}}_{y\oplus 1|b'=1} \otimes \tilde{\rho}_{\mathrm{R}}(b, b' = 1). \tag{6.48}$$

Since his engine is the same as Alice's, the work extracted by Bob is:

$$\begin{aligned}\mathcal{W}^{\mathrm{B}}_{y|a,b,b'=1} = NT\frac{\ln 2}{2}\Bigg(&- 2\sum_{\nu=0}^{1} P(e^{\mathrm{B}}_{\nu|b'=1})(a)\log_2 P(e^{\mathrm{B}}_{\nu|b'=1})(a) + \Im(\tilde{\rho}_{\mathrm{L}}(b, b' = 1)) \\ &+ \Im(\tilde{\rho}_{\mathrm{R}}(b, b' = 1)) - H(P(e^{\mathrm{B}}_{y|b'=1}|\tilde{\rho}_{\mathrm{L}}(a, b' = 1))) \\ &- H\left(P(e^{\mathrm{B}}_{y\oplus 1|b'=1}|\tilde{\rho}_{\mathrm{R}}(a, b' = 1))\right) - 2H\left(\frac{1}{2} + \frac{|\mathbf{f}|}{2}\right)\Bigg),\end{aligned} \tag{6.49}$$

where $P\left(e^{\mathrm{B}}_{\nu|b'=1}\right)(a) = p_{\mathrm{L}} P\left(e^{\mathrm{B}}_{\nu|b'=1}|\tilde{\rho}_{\mathrm{L}}(a, b' = 1)\right) + p_{\mathrm{R}} P\left(e^{\mathrm{B}}_{\nu|b'=1}|\tilde{\rho}_{\mathrm{R}}(a, b' = 1)\right)$ and we used the general expression for the work per cycle, that is, without assuming that the sum of the left and right states is equal to the maximally mixed state. It happens that:

$$P\left(e^{\mathrm{B}}_{\nu|b'=1}\right)(a) = P\left(e^{\mathrm{B}}_{\nu|b'=1}\middle|\frac{\mathbb{1}_2 + \mathbf{f}\cdot\boldsymbol{\sigma}}{2}\right), \quad \forall a \tag{6.50}$$

and then

$$-2\sum_{\nu=0}^{1} P\left(e^{\mathrm{B}}_{\nu|b'=1}\right)(a)\log_2 P\left(e^{\mathrm{B}}_{\nu|b'=1}\right)(a) = 2H\left(P\left(e^{\mathrm{B}}_{y=0|b'=1}\middle|\frac{\mathbb{1}_2 + \mathbf{f}\cdot\boldsymbol{\sigma}}{2}\right)\right). \tag{6.51}$$

Eq. (6.49) is equivalent to:

$$\begin{aligned}\mathcal{W}^{\mathrm{B}}_{x,y|a,b,b'=1} = NT\frac{\ln 2}{2}\Bigg(&\mathfrak{S}(\tilde{\rho}_{\mathrm{L}}(b,b'=1)) + \mathfrak{S}(\tilde{\rho}_{\mathrm{R}}(b,b'=1)) - H\left(P\left(e^{\mathrm{B}}_{y|b'=1}|\tilde{\rho}_{\mathrm{L}}(a,b'=1)\right)\right)\\ &- H\Bigg(1 + P^{\mathrm{L}}(y|a,b'=1) - 2P\Bigg(e^{\mathrm{B}}_{y|b'=1}\Bigg|\frac{\mathbb{1}_2 + \mathbf{f}\cdot\boldsymbol{\sigma}}{2}\Bigg)\Bigg)\\ &- 2H\left(\frac{1}{2} + \frac{|\mathbf{f}|}{2}\right) + 2H\left(P\left(e^{\mathrm{B}}_{y=0|b'=1}\Bigg|\frac{\mathbb{1}_2 + \mathbf{f}\cdot\boldsymbol{\sigma}}{2}\Bigg)\right)\Bigg).\end{aligned} \tag{6.52}$$

We parameterize the above as (it actually is not dependent on x):

$$\begin{aligned}\mathcal{W}^{\mathrm{B}}_{y|a,b,b'=1} = NT\frac{\ln 2}{2}\Bigg(&H\left(\frac{1}{2} + \frac{|\tilde{\mathbf{r}}(b,b'=1)|}{2}\right) + H\left(\frac{1}{2} + \frac{|\tilde{\mathbf{r}}(b\oplus 1,b'=1)|}{2}\right)\\ &- H\left(P\left(e^{\mathrm{B}}_{y|b'=1}|\tilde{\rho}_{\mathrm{L}}(a,b'=1)\right)\right) - H\Bigg(1 + P^{\mathrm{L}}(y|a,b'=1) - 2P\Bigg(e^{\mathrm{B}}_{y|b'=1}\Bigg|\frac{\mathbb{1}_2 + \mathbf{f}\cdot\boldsymbol{\sigma}}{2}\Bigg)\Bigg)\\ &- 2H\left(\frac{1}{2} + \frac{|\mathbf{f}|}{2}\right) + 2H\left(P\left(e^{\mathrm{B}}_{y=0|b'=1}\Bigg|\frac{\mathbb{1}_2 + \mathbf{f}\cdot\boldsymbol{\sigma}}{2}\Bigg)\right)\Bigg),\end{aligned} \tag{6.53}$$

with

$$\tilde{\mathbf{r}}(b,b'=1) = (-1)^b\begin{pmatrix}c_{11} & c_{21} & c_{31}\\ c_{12} & c_{22} & c_{32}\\ c_{13} & c_{23} & c_{33}\end{pmatrix}\begin{pmatrix}r_1\\ r_2\\ r_3\end{pmatrix} + \begin{pmatrix}f_1\\ f_2\\ f_3\end{pmatrix}, \tag{6.54}$$

and the coefficients $\{c_{ij}\}_{i,j} \in \mathbb{R}$ come from the general form of the process matrix.

By identifying

$$P^{\mathrm{L}}(y|a,b'=1) \equiv P\left(e^{\mathrm{B}}_{y|b'=1}|\tilde{\rho}_{\mathrm{L}}(a,b'=1)\right), \tag{6.55}$$

as the probability of Bob's measurement y of the left compartment given Alice's output bit a when $b'=1$, the work extracted by Bob is given by

$$\begin{aligned}\mathcal{W}^{\mathrm{B}}_{y|a,b'=1} = NT\frac{\ln 2}{2}\Bigg(&\sum_{\beta} H\left(\frac{1}{2} + \frac{|\tilde{\mathbf{r}}(\beta,b'=1)|}{2}\right) - H(P^{\mathrm{L}}(y|a,b'=1))\\ &- H\Bigg(1 + P^{\mathrm{L}}(y|a,b'=1) - 2P\Bigg(e^{\mathrm{B}}_{y|b'=1}\Bigg|\frac{\mathbb{1}_2 + \mathbf{f}\cdot\boldsymbol{\sigma}}{2}\Bigg)\Bigg) - 2H\left(\frac{1}{2} + \frac{|\mathbf{f}|}{2}\right)\\ &+ 2H\left(P\left(e^{\mathrm{B}}_{y=0|b'=1}\Bigg|\frac{\mathbb{1}_2 + \mathbf{f}\cdot\boldsymbol{\sigma}}{2}\Bigg)\right)\Bigg),\end{aligned} \tag{6.56}$$

where the dependence on b disappears, because we have two similar terms, one a function of b and the other $b\oplus 1$, thus the actual value of b does not matter and the sum of the terms is taken into account. Therefore, the total work extracted by Alice and Bob when $b'=1$ is:

$$\mathcal{W}^{\mathrm{AB}}_{x,y|a,b'=1} = \mathcal{W}^{\mathrm{A}}_{x|b'=1} + \mathcal{W}^{\mathrm{B}}_{y|a,b'=1}, \tag{6.57}$$

which is explicitly:

$$\begin{aligned}\mathcal{W}^{\mathrm{AB}}_{x,y|a,b'=1} = NT\frac{\ln 2}{2}\Bigg(&\sum_{\beta} H\left(\frac{1}{2}+\frac{|\tilde{\mathbf{r}}(\beta,b'=1)|}{2}\right)+2H\left(\frac{1}{2}+\frac{|\mathbf{r}|}{2}\right)\\ &-2H\left(P\left(e^{\mathrm{A}}_{x}\middle|\frac{\mathbb{1}_2+\mathbf{r}\cdot\boldsymbol{\sigma}}{2}\right)\right)-H(P^{\mathrm{L}}(y|a,b'=1))\\ &-H\left(1+P^{\mathrm{L}}(y|a,b'=1)-2P\left(e^{\mathrm{B}}_{y|b'=1}\middle|\frac{\mathbb{1}_2+\mathbf{f}\cdot\boldsymbol{\sigma}}{2}\right)\right)\\ &-2H\left(\frac{1}{2}+\frac{|\mathbf{f}|}{2}\right)+2H\left(P\left(e^{\mathrm{B}}_{y=0|b'=1}\middle|\frac{\mathbb{1}_2+\mathbf{f}\cdot\boldsymbol{\sigma}}{2}\right)\right)\Bigg).\end{aligned} \tag{6.58}$$

On the other hand, we have the situation where $b'=0$, in which Bob starts manipulating the states and communicates to Alice, who tries to guess Bob's outcome bit b. Bob uses effects $\{e^{\mathrm{B}}_{y|b'=0}\}_{y=0,1}$ by means of membranes, just as previously. His re-preparation follows a similar approach as Alice, but with a dependence on y:

$$\rho_{\mathrm{L(R)}}(y|b,b'=0) := \left(\frac{1+(-1)^{b\oplus y}}{2}\right)\rho_{\mathrm{L(R)}}+\left(\frac{1-(-1)^{b\oplus y}}{2}\right)\rho_{\mathrm{R(L)}}. \tag{6.59}$$

The dependence on y means that the measurement result affects the state re-preparation, a kind of *memory* effect. Likewise Alice when $b'=1$, Bob's extracted work is:

$$\mathcal{W}^{\mathrm{B}}_{y|b'=0} = NT\ln 2\left(H\left(\frac{1}{2}+\frac{|\mathbf{r}|}{2}\right)-H\left(P\left(e^{\mathrm{B}}_{y|b'=0}\middle|\frac{\mathbb{1}_2+\mathbf{r}\cdot\boldsymbol{\sigma}}{2}\right)\right)\right) \tag{6.60}$$

$$\leqslant NT\ln 2\left(H\left(\frac{1}{2}+\frac{|\mathbf{r}|}{2}\right)-\sum_{i=0}^{1}H(\zeta_{(f_i,g_i)})\right). \quad \forall y \tag{6.61}$$

The process matrix W makes the received states $\tilde{\rho}_{\mathrm{L(R)}}(y|b,b'=0)$ by Alice to be different than the actual states prepared by Bob. Analogously to the previous situation, these states are:

$$\tilde{\rho}_{\mathrm{L(R)}}(b,b'=0) := \frac{1}{2}\,\mathrm{tr}_{A_OB_IB_O}\left\{W\left(\mathbb{1}_{A_IA_O}\otimes\sum_{y=0}^{1}M^{\mathrm{B,L(R)}}_{y|b,b'=0}\right)\right\}, \tag{6.62}$$

where the CJ matrices $M^{\mathrm{B,L(R)}}_{y|b,b'=0}$ are:

$$M^{\mathrm{B,L}}_{y|b,b'=0} = e^{\mathrm{B}}_{y|b'=0}\otimes\rho_{\mathrm{L}}(y|b,b'=0), \tag{6.63}$$

$$M^{\mathrm{B,R}}_{y|b,b'=0} = e^{\mathrm{B}}_{y\oplus 1|b'=0}\otimes\rho_{\mathrm{R}}(y|b,b'=0). \tag{6.64}$$

Remarkably, these states are *always* equal to each other:

$$\tilde{\rho}_{\mathrm{R}}(b,b'=0)=\tilde{\rho}_{\mathrm{L}}(b,b'=0)=\frac{\mathbb{1}_2+\tilde{\mathbf{r}}(b,b'=0)\cdot\boldsymbol{\sigma}}{2} \tag{6.65}$$

where

$$\tilde{\mathbf{r}}(b,b'=0)=(-1)^b\begin{pmatrix}\tilde{b}_{11}&\tilde{b}_{12}&\tilde{b}_{13}\\ \tilde{b}_{21}&\tilde{b}_{22}&\tilde{b}_{23}\\ \tilde{b}_{31}&\tilde{b}_{32}&\tilde{b}_{33}\end{pmatrix}\begin{pmatrix}r_1\\r_2\\r_3\end{pmatrix}+\begin{pmatrix}e_1\\e_2\\e_3\end{pmatrix}, \tag{6.66}$$

in which the coefficients $\{\tilde{b}_{ij}\}_{i,j}$ are defined as:

$$\tilde{b}_{ij} := b_{i3j}\cos\left(\theta_{\mathrm{B}}^{b'=0}\right) + b_{i1j}\cos\left(\varphi_{\mathrm{B}}^{b'=0}\right)\sin\left(\theta_{\mathrm{B}}^{b'=0}\right) + b_{i2j}\sin\left(\varphi_{\mathrm{B}}^{b'=0}\right)\sin\left(\theta_{\mathrm{B}}^{b'=0}\right), \tag{6.67}$$

with $\{\theta_{\mathrm{B}}^{b'=0}, \varphi_{\mathrm{B}}^{b'=0}\}$ being the measurement angles of Bob when $b' = 0$:

$$e^{\mathrm{B}}_{y|b'=0} = |\psi_{\mathrm{B}}^{b'=0}\rangle\langle\psi_{\mathrm{B}}^{b'=0}|, \quad |\psi_{\mathrm{B}}^{b'=0}\rangle = \cos\left(\frac{\theta_{\mathrm{B}}^{b'=0}}{2}\right)|0\rangle + e^{i\varphi_{\mathrm{B}}^{b'=0}}\sin\left(\frac{\theta_{\mathrm{B}}^{b'=0}}{2}\right)|1\rangle, \tag{6.68}$$

and the $\{b_{ijk}\}_{i,j,k}$, $\{e_i\}_i \in \mathbb{R}$ come from the process matrix. Thus:

$$\frac{1}{2}\tilde{\rho}_{\mathrm{R}}(b, b' = 0) + \frac{1}{2}\tilde{\rho}_{\mathrm{L}}(b, b' = 0) = \frac{\mathbb{1}_2 + \tilde{\mathbf{r}}(b, b' = 0)\cdot\boldsymbol{\sigma}}{2}. \tag{6.69}$$

After receiving states $\tilde{\rho}_{\mathrm{L}}(b, b' = 0)$ and $\tilde{\rho}_{\mathrm{R}}(b, b' = 0)$, Alice applies her effects $\{e_x^{\mathrm{A}}\}_{x=0,1}$ and re-prepares the same states that she received, but with variables interchanged $b \to a$. In such situation, the CJ matrices describing her quantum instruments are:

$$M^{\mathrm{A,L}}_{x|a,b'=0} = e_x^{\mathrm{A}} \otimes \tilde{\rho}_{\mathrm{L}}(a, b' = 0), \tag{6.70}$$

$$M^{\mathrm{A,R}}_{x|a,b'=0} = e_{x\oplus 1}^{\mathrm{A}} \otimes \tilde{\rho}_{\mathrm{R}}(a, b' = 0). \tag{6.71}$$

Thus the work that she is able to extract from the engine is:

$$\begin{aligned}\mathcal{W}^{\mathrm{A}}_{x|a,b,b'=0} = NT\frac{\ln 2}{2}\Bigg(&\mathfrak{S}(\tilde{\rho}_{\mathrm{L}}(a, b' = 0)) + \mathfrak{S}(\tilde{\rho}_{\mathrm{R}}(a, b' = 0)) \\ &- H\left(P\left(e_x^{\mathrm{A}}|\tilde{\rho}_{\mathrm{L}}(b, b' = 0)\right)\right) - H\left(P\left(e_{x\oplus 1}^{\mathrm{A}}|\tilde{\rho}_{\mathrm{R}}(b, b' = 0)\right)\right) \\ &- 2H\left(\frac{1}{2} + \frac{|\tilde{\mathbf{r}}(a|b' = 0))|}{2}\right) - 2\sum_{\chi=0}^{1} P\left(e_\chi^{\mathrm{A}}\right)(b)\log_2 P\left(e_\chi^{\mathrm{A}}\right)(b)\Bigg),\end{aligned} \tag{6.72}$$

where $P\left(e_\chi^{\mathrm{A}}\right)(b) = p_{\mathrm{L}}P\left(e_\chi^{\mathrm{A}}|\tilde{\rho}_{\mathrm{L}}(b, b' = 0)\right) + p_{\mathrm{R}}P\left(e_\chi^{\mathrm{A}}|\tilde{\rho}_{\mathrm{R}}(b, b' = 0)\right)$. By means of Eq. (6.65), we get:

$$\mathcal{W}^{\mathrm{A}}_{x|b,b'=0} = NT\ln 2\left(-\sum_{\chi=0}^{1} P(e_\chi^{\mathrm{A}})(b)\log_2 P(e_\chi^{\mathrm{A}})(b) - H(P(e_x^{\mathrm{A}}|\tilde{\rho}_{\mathrm{L}}(b, b' = 0)))\right). \tag{6.73}$$

Also, by identifying

$$P^{\mathrm{L}}(x|b, b' = 0) \equiv P(e_x^{\mathrm{A}}|\tilde{\rho}_{\mathrm{L}}(b, b' = 0)) \tag{6.74}$$

as the probability that Alice's measurement of the left compartment is equal to x, given Bob's outcome bit b and that $b' = 0$, we have that:

$$\mathcal{W}^{\mathrm{A}}_{x|b,b'=0} = NT\ln 2\left(-\sum_{\chi=0}^{1} P(e_\chi^{\mathrm{A}})(b)\log_2 P(e_\chi^{\mathrm{A}})(b) - H(P^{\mathrm{L}}(x|b, b' = 0))\right). \tag{6.75}$$

Because $\tilde{\rho}_{\mathrm{L}}(b, b' = 0) = \tilde{\rho}_{\mathrm{R}}(b, b' = 0)$ and $p_{\mathrm{L}} = p_{\mathrm{R}} = 1/2$, we have that:

$$P\left(e_\chi^{\mathrm{A}}\right)(b) = P^{\mathrm{L}}(\chi|b, b' = 0), \tag{6.76}$$

and

$$-\sum_{\chi=0}^{1} P\left(e_{\chi}^{\mathrm{A}}\right)(b)\log_2 P\left(e_{\chi}^{\mathrm{A}}\right)(b) = H\left(P^{\mathrm{L}}(x=0|b,b'=0)\right). \tag{6.77}$$

Considering the symmetry of the binary entropy function,

$$H(P^{\mathrm{L}}(x=0|b,b'=0)) = H(P^{\mathrm{L}}(x=1|b,b'=0)). \tag{6.78}$$

Therefore,

$$\mathcal{W}^{\mathrm{A}}_{x|b,b'=0} \equiv 0, \quad \forall x,b, \tag{6.79}$$

meaning that the work that Alice can extract is *identically* equal to zero and her transformation is always reversible. The total work extracted when $b'=0$ is:

$$\mathcal{W}^{\mathrm{AB}}_{x,y|a,b'=0} \equiv \mathcal{W}^{\mathrm{B}}_{y|b'=0}. \tag{6.80}$$

Finally, since the probabilities that $b'=0$ and $b'=1$ are the same, i.e. $P(b'=0) = P(b'=1) = 1/2$, a fair coin toss, the average work extracted by Alice and Bob *together* in the winning condition for the LGYNI game ($x=a$ when $b'=0$ and $y=b$ when $b'=1$) is:

$$\overline{\mathcal{W}}^{\mathrm{AB}}_{a,b} = \frac{\mathcal{W}^{\mathrm{AB}}_{x=b,y=a|a,b'=1}}{2} + \frac{\mathcal{W}^{\mathrm{AB}}_{x=b,y=a|b,b'=0}}{2}, \tag{6.81}$$

which equals:

$$\begin{aligned}\overline{\mathcal{W}}^{\mathrm{AB}}_{a,b} = NT\frac{\ln 2}{4}\Bigg(&4H\left(\frac{1}{2}+\frac{|\mathbf{r}|}{2}\right) + \sum_{\beta=0}^{1} H\left(\frac{1}{2}+\frac{|\tilde{\mathbf{r}}(\beta|b'=1)|}{2}\right) - 2H\left(P\left(e^{\mathrm{A}}_{x=b}\middle|\frac{\mathbb{1}_2+\mathbf{r}\cdot\boldsymbol{\sigma}}{2}\right)\right)\\ &- 2H\left(P\left(e^{\mathrm{B}}_{y=a|b'=0}\middle|\frac{\mathbb{1}_2+\mathbf{r}\cdot\boldsymbol{\sigma}}{2}\right)\right) + 2H\left(P\left(e^{\mathrm{B}}_{y=0|b'=1}\middle|\frac{\mathbb{1}_2+\mathbf{f}\cdot\boldsymbol{\sigma}}{2}\right)\right) - 2H\left(\frac{1}{2}+\frac{|\mathbf{f}|}{2}\right)\\ &- H(P^{\mathrm{L}}(y=a|b'=1)) - H\left(1+P^{\mathrm{L}}(y=a|b'=1) - 2P\left(e^{\mathrm{B}}_{y=a|b'=1}\middle|\frac{\mathbb{1}_2+\mathbf{f}\cdot\boldsymbol{\sigma}}{2}\right)\right)\Bigg).\end{aligned} \tag{6.82}$$

Thus, assuming that the SLT cannot be violated for any a, b, i.e. $\overline{\mathcal{W}}^{\mathrm{AB}}_{a,b} \leqslant 0\ \forall a,b$, we have the following inequality holding for *every* bipartite process matrix W in the two-level LGYNI scenario:

$$\begin{aligned}&4H\left(\frac{1}{2}+\frac{|\mathbf{r}|}{2}\right) + \sum_{\beta=0}^{1} H\left(\frac{1}{2}+\frac{|\tilde{\mathbf{r}}(\beta|b'=1)|}{2}\right) - 2H\left(P\left(e^{\mathrm{A}}_{x=b}\middle|\frac{\mathbb{1}_2+\mathbf{r}\cdot\boldsymbol{\sigma}}{2}\right)\right)\\ &- 2H\left(P\left(e^{\mathrm{B}}_{y=a|b'=0}\middle|\frac{\mathbb{1}_2+\mathbf{r}\cdot\boldsymbol{\sigma}}{2}\right)\right) + 2H\left(P\left(e^{\mathrm{B}}_{y=0|b'=1}\middle|\frac{\mathbb{1}_2+\mathbf{f}\cdot\boldsymbol{\sigma}}{2}\right)\right) - 2H\left(\frac{1}{2}+\frac{|\mathbf{f}|}{2}\right)\\ &- H(P(y=a|b'=1)) - H\left(1+P(y=a|b'=1) - 2P\left(e^{\mathrm{B}}_{y=a|b'=1}\middle|\frac{\mathbb{1}_2+\mathbf{f}\cdot\boldsymbol{\sigma}}{2}\right)\right) \leqslant 0, \quad \forall a,b.\end{aligned} \tag{6.83}$$

where we dropped the "L", as it is now redundant. Therefore, the SLT sets a bound which in principle constraints some of the parameters $(\{f_i\}_i, \{b_{ijk}\}_{i,j,k}\{c_{ij}\}_{i,j})$ of the two-party process matrix. We say in principle, because we ought to investigate whether the

upper bound can indeed be violated. If not, there is no actual limitation imposed by the SLT onto the parameters of the bipartite process matrix.

In the Wolfram Mathematica notebook available in GitHub[1], we show the surprising result that, for whatever values of a, b, the measurement angles of Alice and Bob (θ_{A}, φ_{A}, $\theta_{\mathrm{B}}^{b'=0(1)}$, $\varphi_{\mathrm{B}}^{b'=0(1)}$), the initial states ($\rho_{\mathrm{L}}$, ρ_{R}) and the parameters of the process matrix ($\{a_{ij}\}_{i,j}$, $\{b_{ijk}\}_{i,j,k}$, $\{c_{ij}\}_{i,j}$, $\{d_{ijk}\}_{i,j,k}$, $\{e_i\}_i$, $\{f_i\}_i$, $\{g_{ij}\}_{i,j}$), it is *not* possible to violate the inequality of Eq. (6.83). In the notebook we numerically arrive at this result, that is, no combination of the parameters, properly defined in their domain of validity, can surpass the upper bound of our main inequality when we apply a maximization function of Mathematica. The Mathematica notebook is properly commented and it should be straightforward for the reader to understand the calculations done in it. To have a taste of how it works in specific cases, we present some combinations of initial states and measurements in the next sections for the situation in which the process matrix is the OCB process matrix [25]. These cases are also treated in the same Mathematica notebook referenced before.

6.2.3 Example

As a didactic case, consider the OCB process matrix:

$$W_{\mathrm{OCB}} = \frac{1}{4}\left[\mathbb{1}_{A_I A_O B_I B_O} + \frac{1}{\sqrt{2}}\left(\mathbb{1}_{A_I} \otimes \sigma_3^{A_O} \otimes \sigma_3^{B_I} \otimes \mathbb{1}_{B_O} + \sigma_3^{A_I} \otimes \mathbb{1}^{A_O} \otimes \sigma_1^{B_I} \otimes \sigma_3^{B_O}\right)\right]. \quad (6.84)$$

For this process matrix, we will study two different situations: (i) initial state pre-defined and free measurement choices; and (ii) free initial state choices and measurements pre-defined. The inequality in Eq. (6.83) reduces to:

$$\begin{aligned} &4H\left(\frac{1}{2}+\frac{|\mathbf{r}|}{2}\right) + 2H\left(\frac{1}{2}+\frac{\sqrt{2}}{2}r_3\right) - 2H\left(\frac{1}{2}+\frac{r_1}{2}\sin(\theta_{\mathrm{A}})\cos(\varphi_{\mathrm{A}}) + \frac{r_2}{2}\sin(\theta_{\mathrm{A}})\sin(\varphi_{\mathrm{A}})\right. \\ &\left. + \frac{r_3}{2}\cos(\theta_{\mathrm{A}})\right) - 2H\left(\frac{1}{2}+\frac{r_1}{2}\sin\left(\theta_{\mathrm{B}}^{b'=0}\right)\cos\left(\varphi_{\mathrm{B}}^{b'=0}\right) + \frac{r_2}{2}\sin\left(\theta_{\mathrm{B}}^{b'=0}\right)\sin\left(\varphi_{\mathrm{B}}^{b'=0}\right)\right. \\ &\left. + \frac{r_3}{2}\cos\left(\theta_{\mathrm{B}}^{b'=0}\right)\right) - 2H\left(\frac{1}{2}+\frac{\sqrt{2}}{4}\cos\left(\theta_{\mathrm{B}}^{b'=1}\right)\right) \leqslant 0, \end{aligned} \quad (6.85)$$

which we see already that is *independent* of the variables a and b.

6.2.3.1 Initial states well-defined

Consider the case in which:

$$r_1 = r_2 = 0, \quad r_3 = 1, \quad (6.86)$$

that is, the initial states

$$\rho_{\mathrm{L}} = |0\rangle\langle 0|, \quad \rho_{\mathrm{R}} = |1\rangle\langle 1| \quad (6.87)$$

[1] https://github.com/dmolitoroa/phdthesis.

are the the eigenstates of the σ_3 operator (i.e. they are the up and down spin states, respectively). In this case, the inequality of Eq. (6.85) is saturated for:

$$\theta_{\rm A} = \pi, \quad \varphi_{\rm A} = \theta_{\rm B}^{b'=1} = \varphi_{\rm B}^{b'=1} = \theta_{\rm B}^{b'=0} = \varphi_{\rm B}^{b'=0} = 0, \tag{6.88}$$

for which the success probability is:

$$P_{\rm succ}^{\rm OCB} \approx \frac{2}{3} < \frac{3}{4} \equiv \max P_{\rm succ}^{\rm causal}, \tag{6.89}$$

that is, by saturating the upper bound of the inequality, we do not violate the upper bound of the causal inequality. On the other hand, the maximization of the success probability,

$$\max P_{\rm succ}^{\rm OCB} = \frac{1}{2} + \frac{\sqrt{2}}{4} > \frac{3}{4}, \tag{6.90}$$

which is achieved for

$$\theta_{\rm A} = \varphi_{\rm A} = \theta_{\rm B}^{b'=1} = \varphi_{\rm B}^{b'=1} = \varphi_{\rm B}^{b'=0} = 0, \quad \varphi_{\rm B}^{b'=0} = \pi/2, \tag{6.91}$$

gives a LHS of Eq. (6.85) equal to -2, that is, not saturated.

Another situation is when

$$r_1 = r_3 = \frac{1}{\sqrt{2}}, \quad r_2 = 0, \tag{6.92}$$

which means that:

$$\rho_{\rm L} = |+\rangle\langle+|, \quad \rho_{\rm R} = |-\rangle\langle-|, \tag{6.93}$$

i.e., the eigenstates of the operator σ_1 ($|\pm\rangle = (|0\rangle + |1\rangle)/\sqrt{2}$). The saturation of our main inequality is achieved for:

$$\theta_{\rm A} = \theta_{\rm B}^{b'=0} = \frac{3\pi}{4}, \quad \varphi_{\rm A} = \varphi_{\rm B}^{b'=0} = \pi, \quad \theta_{\rm B}^{b'=1} = \varphi_{\rm B}^{b'=1} = 0. \tag{6.94}$$

For this combination of measurement angles, we get:

$$\max P_{\rm succ}^{\rm OCB} \approx \frac{11}{16} < \frac{3}{4} \equiv \max P_{\rm succ}^{\rm causal}, \tag{6.95}$$

and again the saturation of the inequality does not coincide with violating the CI. For the maximum violation of the latter, we need:

$$\theta_{\rm A} = \varphi_{\rm A} = \theta_{\rm B}^{b'=1} = \varphi_{\rm B}^{b'=1} = \varphi_{\rm B}^{b'=0} = 0, \quad \theta_{\rm B}^{b'=0} = \frac{\pi}{2}, \tag{6.96}$$

which gives

$$\max P_{\rm succ}^{\rm OCB} = \max P_{\rm succ}^{\rm causal} = \frac{3}{4}, \tag{6.97}$$

such that one loses the capacity of violating the CI. Moreover, the LHS of Eq. (6.85) is then equal to -2.4035, even lower than in the previous case, when the initial states were the eigenstates of the σ_3 operator.

Finally, we pass to the case where:

$$r_1 = r_2 = \frac{1}{\sqrt{2}}, \quad r_3 = 0, \tag{6.98}$$

meaning that the initial states

$$\rho_{\mathrm{L}} = \frac{1}{2}\left(|+\rangle + |+i\rangle\right)\left(\langle +| + \langle +i|\right), \quad \rho_{\mathrm{R}} = \frac{1}{2}\left(|-\rangle + |-i\rangle\right)\left(\langle -| + \langle -i|\right), \tag{6.99}$$

with $|\pm i\rangle = (|0\rangle \pm i|1\rangle)/\sqrt{2}$ being the eigenstates of the operator σ_2, are on the *equator* of the Bloch sphere, that is, *perpendicular* to the computational basis (z-axis). In this situation, for the combination of measurement angles:

$$\theta_{\mathrm{A}} = \theta_{\mathrm{B}}^{b'=0} = \pi/2, \quad \varphi_{\mathrm{A}} = \varphi_{\mathrm{B}}^{b'=0} = 5\pi/4, \quad \theta_{\mathrm{B}}^{b'=1} = \varphi_{\mathrm{B}}^{b'=1} = 0, \tag{6.100}$$

the inequality of Eq. (6.85) is saturated. Here, however, for *any* set of measurement angles, the success probability is *always*:

$$P_{\mathrm{succ}}^{\mathrm{OCB}} \equiv \frac{1}{2} < \frac{3}{4}, \tag{6.101}$$

that is, the same as randomly playing the guessing game. This result can be understood from the structure of the OCB process matrix, where the z-axis is picked as a favored direction and sets an important symmetry for all states and measurements.

6.2.3.2 Measurements well-defined

On the other hand, one might have measurements already pre-defined in the laboratories instead of the states entering the engines. Consider the case in which Alice measures along the z-axis and Bob along the z-axis (x-axis) when $b' = 1$ ($b' = 0$). It is equivalent to:

$$\theta_{\mathrm{A}} = \varphi_{\mathrm{A}} = \theta_{\mathrm{B}}^{b'=1} = \varphi_{\mathrm{B}}^{b'=1} = \varphi_{\mathrm{B}}^{b'=0} = 0, \quad \theta_{\mathrm{B}}^{b'=0} = \frac{\pi}{2}. \tag{6.102}$$

In this case, the state that saturates the inequality in Eq. (6.85) is the maximally-mixed state in two dimensions:

$$\rho_{\mathrm{L}} = \rho_{\mathrm{R}} = \frac{\mathbb{1}_2}{2}, \tag{6.103}$$

that is,

$$r_1 = r_2 = r_3 = 0, \tag{6.104}$$

which gives

$$P_{\mathrm{succ}}^{\mathrm{OCB}} = \frac{1}{2} < \frac{3}{4}. \tag{6.105}$$

This result is straightforward: by making use of the maximally-mixed state, we have a situation analogous to tossing a fair coin. The success probability is maximized for

$$r_1 = r_2 = 0, \quad r_3 = 1, \tag{6.106}$$

such that

$$\max P_{\mathrm{succ}}^{\mathrm{OCB}} = \frac{1}{2} + \frac{\sqrt{2}}{4} > \frac{3}{4}, \tag{6.107}$$

and the LHS of Eq. (6.85) is equal to −2.

Another combination is for Alice to still measure along the z-axis and Bob along the same axis when $b' = 1$, but when $b' = 0$ he measures along the y-axis. In this case,

$$\theta_{\mathrm{A}} = \varphi_{\mathrm{A}} = \theta_{\mathrm{B}}^{b'=1} = \varphi_{\mathrm{B}}^{b'=1} = 0, \quad \theta_{\mathrm{B}}^{b'=0} = \varphi_{\mathrm{B}}^{b'=0} = \frac{\pi}{2}. \tag{6.108}$$

In this scenario, the LHS of Eq. (6.85) is again saturated by the maximally-mixed state, just as in the previous situation. Similarly, the success probability is still equal to 1/2, as one would expect from the maximally-mixed state. The maximization of the success probability gives:

$$\max P_{\mathrm{succ}}^{\mathrm{OCB}} = \frac{2}{3} < \frac{3}{4}, \tag{6.109}$$

being achieved, as before, by the computational basis:

$$r_1 = r_2 = 0, \quad r_3 = 1. \tag{6.110}$$

Again, the LHS of our inequality equals −2.

The last case to be considered is when Alice measures along the x-axis and Bob along the x-axis (y-axis) when $b' = 1$ ($b' = 0$). Thus,

$$\varphi_{\mathrm{A}} = \varphi_{\mathrm{B}}^{b'=1} = 0, \quad \theta_{\mathrm{A}} = \theta_{\mathrm{B}}^{b'=1} = \theta_{\mathrm{B}}^{b'=0} = \varphi_{\mathrm{B}}^{b'=0} = \frac{\pi}{2}. \tag{6.111}$$

Once more, the state that saturates the upper bound of Eq. (6.85) is the maximally-mixed state and the success probability is 1/2. In analogy to the situation where we started with states on the equator of the Bloch sphere, here the success probability is *always* equal to 1/2 and the LHS of our inequality can reach its minimum of −4.79825 when the initial states are pure and on the z-axis ($r_1 = r_2 = 0$, $r_3 = 1$).

6.3 Relation to already existing results and future directions

In Ref. [27] it was found that in a setup of two non-correlated and non-interacting singlets, a pair of subsystems with Alice and the other pair with Bob, in which a LGYNI game is played with the help of the Oreshkov-Costa-Brukner (OCB) process matrix, *no* extra work can be extracted when compared to the definite order scenario. It was pointed out as being a signature of non-violation of the SLT. We moved forward and showed by means of a toy model, the thermal LGYNI or TLGYNI, which combines the idealized engine of Ref. [29] with the LGYNI game of Ref. [25], that the SLT imposes an inequality over binary entropy functions that depend on the components of the process matrix (in our case we have bipartite processes with two-dimensional systems). However, by analyzing the parameters of general process matrices numerically and studying the specific case of the OCB process matrix [25] with different states and measurement setups, we conclude that *no* process matrix is limited by the SLT. We also found out that the violation of CIs and of the SLT are not related, that is, violating one does not mean violating the other. Thus, the SLT is not a physical constraint for the implementation of any two-party process

matrix with two-dimensional systems, as no parameters are bounded by it. The only bound to the parameters comes from QM, something already shown for a long time [25]. Our result reinforces what was obtained in Ref. [27].

As previously mentioned in the text, Araújo *et al.* [24] postulated that only purifiable process matrices are physical. This was argued on the basis that non-purifiable process matrices map unitary channels to non-unitary CPTP maps, which then would ruin reversibility. The OCB process matrix, for instance, would be nonphysical following their criterion, because it is not purifiable. Nonetheless, as commented by the authors of Ref. [24], they consider the collapse of the wave function, the "standard" mechanism for explaining measurements in QM to be a non-physical process, for it is irreversible. So here is the linking point between their, our and the results of Ref. [27], *measurement in QM*. Indeed, for our and Ref. [27] results, being able to projectively measure quantum states is taken for granted, since we are not interested in the philosophical debate whether collapse is real or not. We treat measurement as a *statistical tool* to obtain probabilities and this fact gives us distributions that do not violate the SLT for bipartite and two-dimensional process matrices. The SLT as a universal law for physicality points in a optimistic direction to the real existence of (at least) bipartite ICO processes violating CIs. Of course, if we move to the discussion of unitarity in QM, something that originates the *black hole information paradox* debate, for instance, then we might doubt the physicality of non-purifiable process matrices in a cohesive unitary theory. This, on the other hand, is in conflict with thermodynamics itself, which dictates that the entropy of a closed system is always non-decreasing. As a matter of fact, our life experience is highly irreversible, we see it everywhere. It could be argued that it is the result of growing complexity as we go from simple and very small to complex and very large (macroscopic) systems. Stochastic thermodynamics [97, 112], for instance, is a theory that helps solving the problem, as it allows entropy to rarely decrease for very small systems, but *always* increase on average. A definitive adjustment of measurements in QM to the SLT was, at the moment that this thesis is being written, not yet established. Finally, we consider the following solution to the problem: as far as ideal projective measurements can be implemented[2], bipartite and two-dimensional ICO processes seem to be physical under the SLT.

For the continuation of this work, we can think of at least two questions concerning the relationship between SLT and ICO processes violating CIs that can be investigated. First, our proof concerns bipartite processes with two-dimensional systems. It would be interesting to increase the number of parties to three and more, as well as considering systems with higher dimensions, such as *qudits* and continuous-variable systems, to check if for some number of parties and/or dimension of the system, the SLT is violated. Second, we do not know what is the real energetic cost of having a process matrix violating a CI at first place. In the literature the process matrix is always considered as a given mathematical object. This is natural when we think about quantum states, we assume that some process, natural or not, produces infinite many copies of some state. When it comes to process matrices violating CIs, it is not anymore the case, since we do not know in detail what are the physical mechanisms that can generate them. It can be the case

[2]This point is indeed sensitive, since ideal projective measurements demand infinite resources (i.e. energy) to be implemented [113]. However, this can be seen as a technicality issue that solely limits the efficiency with which a certain quantum information task is performed (being able to projectively measure is key to the majority, if not all, quantum information protocols).

that the amount of resources needed to produce the phenomena are so prohibitive that in practice they are impossible to be implemented and are rarely found naturally. Or even worse, it could be the case that any possible protocol to generate these special process matrices is in disagreement with the SLT, which then would cross them out of existence definitely. While the first question is very technical and can be readily answered, the second is way more fundamental and needs a further development of the physical theory behind ICO, which sets it to not be soon answered.

Chapter 7

Conclusion

"It's the job that's never started as takes longest to finish."

— Sam Gamgee, The Fellowship of the Ring.

The main goal of this thesis was to study the relationship between indefinite causal order (ICO), a hypothesized feature of a successful theory of quantum gravity (QG), and thermodynamics. More specifically, we aimed at finding out whether the second law of thermodynamics (SLT) imposes some *physical* constraint on ICO processes which can violate the so-called causal inequalities (CIs). These are theoretical processes that have not yet been detected and/or engineered in the laboratory. Therefore, this project was very challenging and ambitious, having as goal a breakthrough result on the physicality of special process matrices violating CIs. The certification that there are no physical limitations for their existence is of importance if they are to be really considered as physical phenomena or just mathematical constructs. The SLT, one of the pillars of physical theory, and known to be a universal law, was chosen as a decisive test for studying the physicality of processes violating CIs. By combining the idealized engine of Esther Hänggi and Stephanie Wehner [29] (see Section 6.2.1) with the lazy-guess your neighbour's input game (LGYNI) of Ognyan Oreshkov, Fabio Costa and Časlav Brukner [25] (see Section 6.1), we showed that given the symmetries of the problem, the SLT does not seem to constrain any parameter of bipartite and two-dimensional process matrices (check Section 6.2.2). Even for the maximum violation of the two-party CI, given by the Oreshkov-Costa-Brukner (OCB) process matrix [25] for any initial states and measurement setups (see Section 6.2.3) we could not violate the SLT in our setup. This means that the SLT *seems not* to be a physical constraint for the existence of two-party process matrices with two-dimensional systems. Nevertheless, this is a "negative" result, in the sense that we were not able to certify with certainty whether thermodynamics limits or not the existence of process matrices violating CIs. It might happen that our setup, based on the engine of Ref. [29], has just the right symmetries to decouple completely the SLT from CIs, which would make our model biased. This is something that must be checked in the future. Even though "negative", our results are very important in the effort of understanding non-causal process matrices from a physical perspective and motivates more

tests for their validation.

Moreover, a previous work by Gianluca Francica [27] showed also in a toy model of work extraction that bipartite and two-dimensional ICO processes do not lead to advantages when compared to the definite causal order scenario. The author suggested that this would be a signature of compliance with the SLT. Indeed, our result goes in line with this idea, at least for this class of ICO processes (bipartite, two-dimensional). Finally, Araújo *et al.* [24] postulated the physicality of processes violating CIs on the basis of purification: only purifiable processes would be physical, as they do not violate reversibility. The reversibility condition is imposed as a condition for a correct physical theory. This, nonetheless, comes from the opinion of the authors that the collapse of the wave-function is not real and (projective) measurements are taken apart from quantum theory, a unitary (reversible) theory. Following their postulate, the OCB process would then be not physical, which contradicts our result and the suggestion of Ref. [27]. However, we find a solution to the impasse: if ideal projective measurements do exist and can be implemented, then bipartite and two-dimensional ICO processes violating CIs seems to be physical according to the SLT. We affirm that we are not interested in the philosophical debate of unitarity in quantum theory (or any other theory), but we make use of the projective measurements as statistical tools to calculate the probabilities that enter the CIs. Thus, as much as the operationality of Born's rule is concerned, our result holds. Nevertheless, apart from the aforementioned matter of model bias, other physical constraints might exist for the existence of ICO-violating process matrices. Indeed, Venkatesh Vilasini and Renato Renner [28] presented physicality constraints on ICO processes based on the relativity of a *classical spacetime*.

Very important are also our technical results concerning the controlled-superposition of causal orders (cSCO) implementation known as the quantum switch (QS). These processes, as discussed in Chapter 3 do not violate any CI and were already implemented in the laboratory [7–11]. In Chapter 4, we describe the works of Ref. [23]. We investigated the instabilities of the QS when the control DOF is subject to interaction with an environment. Our main result is a general expression for the state of the composite state system-control, as well as for the post-selected state of the system when measuring the control in the $|\pm\rangle_C$ state, after some arbitrary number of collisions of ancillae modelling a thermal environment. It was found that in the asymptotic limits of low and high temperature of the environment, the "indefinite order terms" in the post-selected state are very sensitive to the measurement state: measuring in the $|+\rangle$ state always leads to decreasing ICO effects for increasing number of collisions, while measuring in the $|-\rangle_C$ state can provide some "shielding" for the ICO effects in the limit of low-temperatures, even though the probability of measuring the control in such a state asymptotically tends to zero. This QS with open control framework is applied to two examples: monitoring maps of mutually-unbiased bases (MUBs) and the QS-based quantum refrigerator of Ref. [18]. These examples show that, in general, the interaction between control and environment diminishes the ICO effects for increasing number of collisions, exception made for peculiar situations treated in the Chapter. For instance, in the right conditions the QS-based quantum refrigerator can have a non-vanishing coefficient of performance (COP) for arbitrarily large number of collisions with the environment, and the monitoring maps of mutually-unbiased bases can have memory effects, evidenced by "revivals" of available

information. Moreover, in Chapter 4, the thermodynamic problem of activation of passive states is treated in the context of the QS. We show that the QS alone is *not* a thermodynamical resource, that is, extra resources on the side of the control must be present to ensure state activation (i.e. coherence in the state of the control and non-diagonal Hamiltonian of the control in the computational basis). We then arrive at necessary but not sufficient conditions for state activation of both the composite state system-control and the state of the system alone. To benchmark our results, we apply our framework to test in the cases that the system is composed of (i) a two-level system (qubit) with unitaries as rotations around the Bloch sphere and (ii) a quantum harmonic oscillator with unitaries as displacement and squeeze operators. The results clearly show that state activation is *very* case-sensitive and depends a lot on the initial and measurement states of the control.

The thesis as a whole explores in a coherent and comprehensive manner aspects of the relationship between ICO and thermodynamics, in both fundamental and technical terms. Our result of Chapter 6 points to an interesting and exciting perspective: bipartite and two-dimensional ICO process matrices violating CIs are not in conflict with thermodynamics, presenting an argument for their physicality. This, nonetheless, is not a sufficient condition, since other constraints for their physicality can be considered (as presented in Ref. [28], for instance). Indeed, it is possible, for example, that the phenomena originating these process matrices need an infinite amount of resources, limiting their existence or at least making them very improbable. This is in fact a possible route of investigation for the future, demanding however a more concrete formulation of the physics behind ICO. Also, our results hold for bipartite and two-dimensional process matrices violating CIs, an immediate follow up is to move to higher number of parties and dimensions. The technical results of Chapters 4 and 5 are also important, as they deal with applications of the QS, which in turn was already implemented in the laboratory and has been shown to offer advantages in different fields, such as quantum computation, quantum communications, quantum metrology and quantum thermodynamics.

Appendix A

Choi-Jamiołkowski matrices

Based on the famous mathematical isomorphism between linear operators and maps by Man-Duen Choi [63] and Andrzej Jamiołkowski [62], Choi-Jamiołkowski (CJ) matrices [25, 48] are very important in the process matrix treatment of indefinite causal order (ICO).

Consider the Hilbert space $\mathcal{H}_A$, in which the computational basis is written as $|i\rangle_A$, with $i \in \mathbb{N}$, as well as an *isomorphic* Hilbert space $\mathcal{H}_{A'}$ with computational basis $|i'\rangle_{A'}$ in one-to-one correspondence to $|i\rangle_A$. In this scenario, the non-normalized maximally entangled state is given by:

$$|\mathbb{1}\rangle\!\rangle_{AA'} := \sum_{i=0}^{d_A-1} |i\rangle_A \otimes |i'\rangle_{A'}, \tag{A.1}$$

where $d_A := \dim(\mathcal{H}_A)$ is the dimension of the Hilbert space $\mathcal{H}_A$ (since $\mathcal{H}_A$ and $\mathcal{H}_{A'}$ are isomorphic, they have the same dimensions).

In the above we use the so-called "double-ket notation". It is also used to determine the *CJ vector* of a certain linear operator $O : \mathcal{H}_A \to \mathcal{H}_B$,

$$\begin{aligned} |O\rangle\!\rangle &:= (\mathbb{1}_A \otimes O)\,|\mathbb{1}\rangle\!\rangle_{AA} \\ &= \sum_{i=0}^{d_A-1} |i\rangle_A \otimes O\,|i\rangle_A\,. \end{aligned} \tag{A.2}$$

Moreover, analogously we define the CJ matrix for a linear map $\mathcal{M} : \mathcal{L}(\mathcal{H}_A) \to \mathcal{L}(\mathcal{H}_B)$,

$$\begin{aligned} J(\mathcal{M}) \equiv M &:= [(\Im_{A\to A} \otimes \mathcal{M})\,(|\mathbb{1}\rangle\!\rangle\langle\!\langle \mathbb{1}|_{AA})]^{\intercal} \\ &= \left[\sum_{j,j'=0}^{d_A-1,d_A-1} |j\rangle\langle j|_A \otimes \mathcal{M}(|j\rangle\langle j|_A)\right]^{\intercal}, \end{aligned} \tag{A.3}$$

where the double summation is implicit, $^{\intercal}$ denotes the transposition operation and $\Im_{A\to A}$ is the identity map from the Hilbert space $\mathcal{H}_A$ to itself:

$$\begin{aligned} \Im_{A\to A}(\rho_A) &= \sum_{j,j'=0}^{d_A-1,d_A-1} |j\rangle\langle j|_A\,\rho_A\,|j'\rangle\langle j'|_A \\ &= \mathbb{1}_A\,\rho_A\,\mathbb{1}_A \\ &= \rho_A. \end{aligned} \tag{A.4}$$

An important example is of the identity map between two different Hilbert space $\Im_{A\to B}$, that is, a one-to-one mapping from $\mathcal{H}_A$ to $\mathcal{H}_B$,

$$\Im_{A\to B}(\rho_A) = \rho_B, \tag{A.5}$$

where $|i\rangle_A \mapsto |i\rangle_B \ \forall i \in \mathbb{N}$. Thus:

$$\begin{aligned} J(\Im_{A\to B}) &= [(\Im_{A\to A}\otimes\Im_{A\to B})(|\mathbb{1}\rangle\!\rangle\langle\!\langle\mathbb{1}|_{AA})]^{\mathsf{T}} \\ &= \left[\sum_{j,j'=0}^{d_A-1,d_B-1} |j\rangle\langle j'|_A \otimes \Im_{A\to B}(|j\rangle\langle j'|_A)\right]^{\mathsf{T}} \\ &= \left[\sum_{j,j'=0}^{d_A-1,d_B-1} |j\rangle\langle j'|_A \otimes |j\rangle\langle j'|_B\right]^{\mathsf{T}}. \end{aligned} \tag{A.6}$$

In the quantum circuit language, this is the CJ matrix of a line connecting one Hilbert space to another, for instance, the output of a quantum channel (A_O) to the input of another (B_I) (see Fig. A.1). For this case, we have to be careful with the proper Hilbert spaces, such that:

$$J(\Im_{A_O\to B_I}) = = \left[\sum_{j,j'=0}^{d_{A_O}-1,d_{B_I}-1} |j\rangle\langle j'|_{A_O} \otimes |j\rangle\langle j'|_{B_I}\right]^{\mathsf{T}}. \tag{A.7}$$

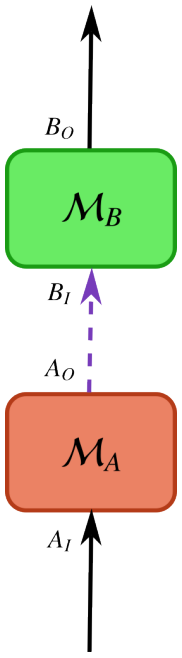

Figure A.1: **Circuit connection between quantum channels.** The quantum channels $\mathcal{M}_A$ and $\mathcal{M}_B$ have input (output) Hilbert spaces A_I (A_O) and B_I (B_O), respectively. The purple dashed arrow is the line that connects one Hilbert space to the other and its Choi-Jamiołkowski (CJ) matrix is given by Eq. (A.6).

Appendix B

Process matrix characterization

Define sets of matrices $\{\xi_i^{A_{I(O)}}\}_{i=0}^{d_{A_{I(O)}}^2-1}$ and $\{\xi_i^{B_{I(O)}}\}_{i=0}^{d_{B_{I(O)}}^2-1}$, where $d_{A_{I(O)}}$ and $d_{B_{I(O)}}$ are the dimensions of $\mathcal{H}_{A_{I(O)}}$ and $\mathcal{H}_{B_{I(O)}}$, such that:

$$\xi_0^{A_{I(O)}} = \mathbb{1}_{A_{I(O)}}, \qquad \xi_0^{B_{I(O)}} = \mathbb{1}_{B_{I(O)}}, \tag{B.1}$$

$$\mathrm{tr}\left\{\xi_i^{A_{I(O)}}\xi_j^{A_{I(O)}}\right\} = d_{A_{I(O)}}\delta_{ij}, \qquad \mathrm{tr}\left\{\xi_i^{B_{I(O)}}\xi_j^{B_{I(O)}}\right\} = d_{B_{I(O)}}\delta_{ij} \tag{B.2}$$

and

$$\mathrm{tr}\{\xi_i^{A_{I(O)}}\} = \mathrm{tr}\{\xi_i^{B_{I(O)}}\} = 0, \quad \forall i. \tag{B.3}$$

These form Hilbert-Schmidt bases in $\mathcal{H}_{A_{I(O)}}$ and $\mathcal{H}_{B_{I(O)}}$. For example, when $d_{A_{I(O)}} = d_{B_{I(O)}} = 2$, these are simply the Pauli matrices. Thus, any element of $\mathcal{L}(\mathcal{H}^{A_I} \otimes \mathcal{H}^{A_O} \otimes \mathcal{H}^{B_I} \otimes \mathcal{H}^{B_O})$ can be decomposed as:

$$W = \sum_{i,j,k,l} w_{ijkl}\left(\xi_i^{A_I} \otimes \xi_j^{A_O} \otimes \xi_k^{B_I} \otimes \xi_l^{B_O}\right), \tag{B.4}$$

in which $w_{ijkl} \in \mathbb{R}$ for the sake of Hermiticity. Similarly, one has that the CJ matrices of CPTP maps can be written in the same bases:

$$M^{\mathrm{Alice}} = \sum_{i,j} m_{ij}^{\mathrm{Alice}}\left(\xi_i^{A_I} \otimes \xi_j^{A_O}\right), \qquad M^{\mathrm{Bob}} = \sum_{i,j} m_{ij}^{\mathrm{Bob}}\left(\xi_i^{B_I} \otimes \xi_j^{B_O}\right). \tag{B.5}$$

The first constraint is imposed by Eq. (2.18), which leads to:

$$m_{00}^{\mathrm{Alice(Bob)}} = \frac{1}{d_{A_O(B_O)}}, \qquad m_{i0}^{\mathrm{Alice(Bob)}} = 0, \quad \forall i > 0. \tag{B.6}$$

Hence,

$$M^{\mathrm{Alice}} = \frac{1}{d_{A_O}}\left(\mathbb{1}_{A_IA_O} + \sum_{i>0}\lambda_i^{\mathrm{Alice}}\left(\mathbb{1}_{A_I} \otimes \xi_i^{A_O}\right) + \sum_{i,j>0}\kappa_{ij}^{\mathrm{Alice}}\left(\xi_i^{A_I} \otimes \xi_j^{A_O}\right)\right), \tag{B.7}$$

$$M^{\mathrm{Bob}} = \frac{1}{d_{B_O}}\left(\mathbb{1}_{B_IB_O} + \sum_{i>0}\lambda_i^{\mathrm{Bob}}\left(\mathbb{1}_{B_I} \otimes \xi_i^{B_O}\right) + \sum_{i,j>0}\kappa_{ij}^{\mathrm{Bob}}\left(\xi_i^{B_I} \otimes \xi_j^{B_O}\right)\right), \tag{B.8}$$

where $\mathbb{1}_{XY} \equiv \mathbb{1}_X \otimes \mathbb{1}_Y$ and $\lambda_i^{\text{Alice/Bob}}, \kappa_{ij}^{\text{Alice/Bob}} \in \mathbb{R}$, $\forall i, j$.

A parenthesis here is convenient. Imagine for a moment that there is just one party: Alice. In such a case, we have a process matrix W_A restricted to $\mathcal{L}(\mathcal{H}_{A_I} \otimes \mathcal{H}_{A_O})$. The normalization condition gives:

$$\begin{aligned}\text{tr}\left\{W_A M^{\text{Alice}}\right\} = \frac{1}{d_{A_O}}\Big[W_A\Big(\mathbb{1}_{A_I A_O} + \sum_{i>0} \lambda_i^{\text{Alice}}\left(\mathbb{1}^{A_I} \otimes \xi_i^{A_O}\right) \\ + \sum_{i,j>0} \kappa_{ij}^{\text{Alice}}\left(\xi_i^{A_I} \otimes \xi_j^{A_O}\right)\Big)\Big] = 1,\end{aligned} \tag{B.9}$$

which by expansion into the Hilbert-Schmidt basis for $W_A = \sum_{i,j} w_{ij}\left(\xi_i^{A_I} \otimes \xi_j^{A_O}\right)$ is:

$$d_{A_I}\left(w_{00} + \sum_{i>0} w_{0i}\,\lambda_i^{\text{Alice}} + \sum_{i,j>0} w_{ij}\,\kappa_{ij}^{\text{Alice}}\right) = 1, \tag{B.10}$$

hence:

$$w_{00} = \frac{1}{d_{A_I}}, \qquad w_{0i} = w_{i,j} = 0, \quad \forall i, j > 0. \tag{B.11}$$

A process matrix limited to one party is then written in the Hilbert-Schmidt basis as:

$$\begin{aligned} W_A &= \frac{1}{d_{A_I}}\left(\mathbb{1}_{A_I A_O} + \sum_{i>0} v_i\left(\xi_i^{A_I} \otimes \mathbb{1}_{A_O}\right)\right) \\ &= \frac{1}{d_{A_I}}\left(\mathbb{1}_{A_I} + \sum_{i>0} v_i\,\xi_i^{A_I}\right) \otimes \mathbb{1}_{A_O} \\ &= \rho_{A_I} \otimes \mathbb{1}_{A_O}, \end{aligned} \tag{B.12}$$

where $v_i := w_{i0}$. Eq. (B.12) has the same form as a density matrix in a larger Hilbert space, i.e. a state in $\mathrm{D}(\mathcal{H}_{A_I}) \otimes \mathbb{1}_{A_O}$. This simplified case of one party shows to us that the process matrix can be seen as a generalization of the density matrix for multi-partite systems.

Now we come back to the bi-partite case. Here we do it in three steps. First, fix $M^{\text{Bob}} = \mathbb{1}_{B_I B_O}/d_{B_O}$, then the normalization condition gives:

$$d_{A_I} d_{B_I}\left(w_{0000} + \sum_{i>0} w_{0i00}\,\lambda_i^{\text{Alice}} + \sum_{i,j>0} w_{ij00}\,\kappa_{ij}^{\text{Alice}}\right) = 1, \quad \forall \lambda_i^{\text{Alice}}, \kappa_{ij}^{\text{Alice}} \in \mathbb{R}, \tag{B.13}$$

which leads to:

$$w_{0000} = \frac{1}{d_{A_I} d_{B_I}}, \qquad w_{0i00} = w_{ij00} = 0, \quad \forall i, j > 0. \tag{B.14}$$

Second, we now fix $M^{\text{Alice}} = \mathbb{1}_{A_I A_O}/d_{A_O}$, for which the normalization condition imposes the values:

$$w_{000i} = w_{00ij} = 0, \quad \forall i, j > 0. \tag{B.15}$$

Third and last step, for general M^{Alice} and M^{Bob}, we get:

$$\begin{aligned}&\sum_{i,k>0} w_{0i0k}\, \lambda_i^{\text{Alice}}\, \lambda_k^{\text{Bob}} + \sum_{i,k,l>0} w_{0ikl}\, \lambda_i^{\text{Alice}}\, \kappa_{kl}^{\text{Bob}} + \sum_{i,j,k>0} w_{ij0k}\, \kappa_{ij}^{\text{Alice}} \lambda_k^{\text{Bob}} \\ &+ \sum_{i,j,k,l>0} w_{ijkl}\, \kappa_{ij}^{\text{Alice}}\, \kappa_{kl}^{\text{Bob}} = 0, \qquad \forall \lambda_i^{\text{Alice}}, \lambda_k^{\text{Bob}}, \kappa_{ij}^{\text{Alice}}, \kappa_{kl}^{\text{Bob}} \in \mathbb{R}.\end{aligned} \tag{B.16}$$

Finally, the most general form of a bipartite process matrix is:

$$W = \frac{1}{d_{A_I} d_{B_I}} \left(\mathbb{1}_{A_I A_O B_I B_O} + \xi_{B\to A} + \xi_{A\to B} + \xi_{A\leftrightarrow B}\right), \tag{B.17}$$

where

$$\xi_{B\to A} := \sum_{i,j>0} a_{ij} \left(\xi_i^{A_I} \otimes \mathbb{1}_{A_O} \otimes \mathbb{1}_{B_I} \otimes \xi_j^{B_O}\right) + \sum_{i,j,k>0} b_{ijk} \left(\xi_i^{A_I} \otimes \mathbb{1}_{A_O} \otimes \xi_j^{B_I} \otimes \xi_k^{B_O}\right), \tag{B.18}$$

$$\xi_{A\to B} := \sum_{i,j>0} c_{ij} \left(\mathbb{1}_{A_I} \otimes \xi_i^{A_O} \otimes \xi_j^{B_I} \otimes \mathbb{1}_{B_O}\right) + \sum_{i,j,k>0} d_{ijk} \left(\xi_i^{A_I} \otimes \xi_j^{A_O} \otimes \xi_k^{B_I} \otimes \mathbb{1}_{B_O}\right), \tag{B.19}$$

$$\begin{aligned}\xi_{A\leftrightarrow B} = &\sum_{i>0} e_i \left(\xi_i^{A_I} \otimes \mathbb{1}_{A_O} \otimes \mathbb{1}_{B_I} \otimes \mathbb{1}_{B_O}\right) + \sum_{i>0} f_i \left(\mathbb{1}_{A_I} \otimes \mathbb{1}_{A_O} \otimes \xi_i^{B_I} \otimes \mathbb{1}_{B_O}\right) \\ &+ \sum_{i,j>0} g_{ij} \left(\xi_i^{A_I} \otimes \mathbb{1}_{A_O} \otimes \xi_j^{B_I} \otimes \mathbb{1}_{B_O}\right),\end{aligned} \tag{B.20}$$

with $a_{ij}, b_{ijk}, c_{ij}, d_{ijk}, e_i, f_i, g_{ij} \in \mathbb{R}$. It is important to note that, these parameters should be such that

Appendix C

Uncertainties

One of the most striking features of quantum mechanics is the existence of *uncertainty relations* (URs). First introduced by Werner Heisenberg as *uncertainty principle* [114], this is a fundamental limitation on *simultaneous* determinism in physical reality of certain quantities. The most prominent example, and the classic textbook case, is that of position and momentum[1] [115, 116]:

$$\Delta x \, \Delta p \geqslant \frac{\hbar}{2}, \tag{C.1}$$

which means that product between standard deviation of the measurement of position,

$$\Delta x := \sqrt{\langle x^2 \rangle - \langle x \rangle^2}, \tag{C.2}$$

with $\langle x \rangle$ and $\langle x^2 \rangle$ being the expectation value of x and x^2, respectively, and the standard deviation of the measurement of momentum,

$$\Delta p := \sqrt{\langle p^2 \rangle - \langle p \rangle^2}, \tag{C.3}$$

of a quantum particle is lower bounded by a universal quantity. Strikingly, if we acquire very precise knowledge about the position of a particle (e.g. an electron), that is $\Delta x \sim 0$, necessarily what we know about the momentum at that *same time* must be very imprecise ($\Delta p \to \infty$). Note that we stress the expression "same time", because the uncertainty principle states the impossibility of simultaneous knowledge of pairs of *observables* (i.e. operators that are measurable in the lab). Of course that, if a fresh new particle, identical to the previous one, comes to the measurement apparatus and we obtain precise knowledge of the momentum, than the knowledge of the position will suffer from extreme uncertainty. The same reasoning applies to state preparation: if we cannot measure with infinite precision certain pairs of observables, we cannot as well imprint them with striking precision at the same time to the preparation of a quantum system. Interestingly, the physical constant $\hbar$, first introduced by Max Planck in an effort to solve a very specific problem, the ultraviolet catastrophe in the radiation of a blackbody [117, 118][2], turned out to be a *universal* lower bound permeating the whole micro-world, and by consequence the totality of physical reality.

[1] In the following we take $\hbar \neq 1$.

[2] Actually, the constant's father introduced the h, from which $\hbar = h/2\pi$ is obtained.

The uncertainty principle might be extended to two general observables A and B, as fist proved by Howard Robertson [119]:

$$\Delta A \Delta B \geqslant \frac{1}{2} |\langle\psi|[A, B]_-|\psi\rangle| , \tag{C.4}$$

for some quantum state $|\psi\rangle \in \mathcal{H}$, and $\Delta A := \sqrt{\langle A^2\rangle - \langle A\rangle^2}$, $\Delta B := \sqrt{\langle B^2\rangle - \langle B\rangle^2}$ are the standard deviations of the observables A and B, respectively. Here we already see that commutativity, a mathematical feature of the linear spaces formed from Hilbert spaces ($\mathcal{L}(\mathcal{H})$) where A and B live, is what defines the lower bound of the uncertainty relation between the observables. In the case that A and B commute, thus, they have the same eigenvectors, or equivalently, they can be simultaneously diagonalized, the lower bound of the uncertainty relation is 0, and both A and B can be known very infinite precision at the same time. Moreover, when one considers the commutation relation between the position and momentum operators, $[x, p] = i\hbar\,\mathbb{1}$, automatically Eq. (C.1) is recovered.

Expressing URs in the standard deviation formulation of Eqs. (C.1) and (C.4), although historically and conceptually important, has its flaws when taken into consideration real physical scenarios. First, as pointed out in the Review [120], in the case of finite spectrum observables, that is, observables that have a finite number of eigenvectors ($\dim(\mathcal{H}) \neq \infty$), it can become tricky. As an example, consider the *algebra* of the Pauli operators:

$$[\sigma_j, \sigma_k]_- = 2i \sum_{l=1}^{3} \epsilon_{jkl}\, \sigma_l, \tag{C.5}$$

where ϵ_{jkl} is the *Levi-Civita symbol*, defined by:

$$\epsilon_{\alpha\beta\gamma} = \begin{cases} +1, & \text{if } (j,k,l) = (1,2,3), (3,1,2), (2,3,1) \\ -1, & \text{if } (j,k,l) = (2,1,3), (1,3,2), (3,2,1) \\ 0, & \text{if } j = k, k = l, j = l \end{cases}$$

thus, if we pick so to say $j = 1$ and $k = 2$, from Eq. (C.4) we get:

$$\Delta\sigma_1 \Delta\sigma_2 \geqslant |\langle\psi|\sigma_3|\psi\rangle| = |\langle\sigma_3\rangle|, \tag{C.6}$$

which is problematic. If a state lies on the xy-plane of the Bloch sphere, then $\langle\sigma_3\rangle = 0$ and $\Delta\sigma_1\Delta\sigma_2 \geqslant 0$, i.e. it's a trivial inequality. On top of that, if we have the state being the eigenstate of σ_1 ($\{|+\rangle, |-\rangle\}$) or of σ_2 ($\{|+i\rangle, |-i\rangle\}$), then $\Delta\sigma_1 = 0$ or $\Delta\sigma_2 = 0$ and the inequality is tight, that is, the lower bound is reached even for non-zero standard deviation of the other observable of the pair. For any other state apart from these eigenvectors the inequality is not tight and then not an optimized quantifier of uncertainty. Here it's clear that having a *multiplication* of standard deviations on the LHS of the inequality is what creates this technical complication. Second, using the standard deviation to investigate statistical quantities might lead to very counter-intuitive scenarios. One of these in pointed out in Ref. [120]: take for instance a spin-1 particle with equally distributed probabilities for each spin value along the z-axis $P(s_3) = 1/3$ for $s_3 \in \{-1, 0, 1\}$. Thus, the standard deviation of the angular momentum operator S_3 is $\Delta S_3 = \sqrt{2/3}$. Moreover, by some inquiry method, we find out that $s_3 \neq 0$, which leaves just two non-zero probability values

$s_3 \in \{-1, 1\}$ with equal probabilities $P(s_3) = 1/2$. Calculating again the standard deviation one finds that now $\Delta S_3 = 1$. Surprisingly, the standard deviation *increases*, even though the amount of possible values for the spin decreased. Another situation, as described in Ref. [121], is of the spatial position of a particle. Imagine a two-dimensional box (the width is considered to be very small compared to the length and the height) of length L with its center at the $x = 0$ position. An idealized particle, or classical, in the sense that it's a rigid zero-dimensional entity, is known to be very close to one of the endings of this box, due to some barriers keeping it at one of these positions. Therefore, two positions are available with equal probability $P(-L/2) = P(L/2) = 1/2$ and the variance of the position is:

$$\begin{aligned} \Delta x^2 &= \int_{-L/2}^{L/2} a^2\, P(a)\, \mathrm{d}a - \left(\int_{-L/2}^{L/2} a\, P(a)\, \mathrm{d}a \right)^2 \\ &\sim P(-L/2)\left(-\frac{L}{2} + \frac{L^2}{4} \right) + P(L/2)\left(+\frac{L}{2} + \frac{L^2}{4} \right) \\ &= \frac{L^2}{4}, \end{aligned} \tag{C.7}$$

hence the standard deviation:

$$\Delta x \sim \frac{L}{2}. \tag{C.8}$$

Then, the barriers are removed and the particle can be equally found anywhere $P(x) = 1/L \forall x \in \{-L, L\}$. The variance in this case is:

$$\begin{aligned} \Delta x^2 &= \int_{-L/2}^{L/2} a^2\, P(a)\, \mathrm{d}a - \left(\int_{-L/2}^{L/2} a\, P(a)\, \mathrm{d}a \right)^2 \\ &= \frac{1}{L}\left[\frac{a^3}{3} \right]_{-L/2}^{L/2} + \frac{1}{L^2}\left[\frac{a^2}{2} \right]_{-L/2}^{L/2} \\ &= \frac{L^2}{12}, \end{aligned} \tag{C.9}$$

thus the standard deviation becomes:

$$\Delta x = \frac{L}{\sqrt{12}}. \tag{C.10}$$

This result is completely counter-intuitive, the particle becomes less-constrained and it can be found anywhere in a larger region, but the standard deviation becomes *more* concentrated around the central position $x = 0$. Finally, an interesting case discussed in Ref. [120] is when the system under study has non-numerical labels and then the standard deviation has no meaning at all. For instance, the fundamental particle known as *neutrino* is known to exist in three different "flavours": "electron", "muon" and "tau" types. Evidently, here the standard deviation has zero room to be used, *no* quantitative measures are presented. Nonetheless, identifying the uncertainty in scenarios like this is of great relevance and can be captured by other quantifiers, such as the *(information) entropy* (also known as *Shannon measure of information*, SMI).

C.1 Alternative formulations of URs

As pointed out above, the standard deviation approach to URs, although the most known one, is in many scenarios not convenient. Thus, we shall provide viable alternatives for treating uncertainty of the measurement of some observable. Below we present two other possible ways to express URs: *entropic uncertainty relations* (EURs) and *fine-grained uncertainty relations* (CGURs).

C.1.1 Entropic uncertainty relations (EURs)

A more "modern" and application-suited way of expressing URs is through the use of the information entropy (i.e. Shannon and von Neumann entropies for classical and quantum systems, respectively). The relationship of this kind of entropy with the thermodynamic entropy is given by Boltzmann constant k_B.

The first EUR was brought to light in 1957 [122, 123], but it was not until 1975 that an improved version was developed [124, 125]:

$$h(x) + h(p) \geqslant \log_2\left(\frac{e\pi\hbar}{l_x l_p}\right), \tag{C.11}$$

where

$$h(x) = -\int_{-\infty}^{\infty} \mathfrak{p}(a) \log \mathfrak{p}(a) \mathrm{d}a \tag{C.12}$$

and

$$h(p) = -\int_{-\infty}^{\infty} \mathfrak{p}(q) \log \mathfrak{p}(q) \mathrm{d}q \tag{C.13}$$

are the *differential entropies* of the probability density distributions $\mathfrak{p}(x)$ and $\mathfrak{p}(p)$ of the position and momentum operators, respectively[3]. The parameters l_x and l_p are called the position and momentum scales, respectively, and serve to make the argument of the logarithm dimensionless. Remarkably, in Ref. [125] it was even shown that the EUR of Eq. (C.11) is stronger than Eq. (C.1) and thus implies it.

However, in a scenario where quantum information is concerned, we would like to employ some quantifier that is more suited for the situation, such as the Shannon entropy for finite spectrum observables. The works of Refs. [126] and [127] laid the ground for the most-well known EUR developed in Ref. [128]:

$$H(A) + H(B) \geqslant \log_2\left(\frac{1}{c}\right), \tag{C.14}$$

with $H(X) = -\sum_x P_X(X = x) \log_2 P_X(X = x)$ being the Shannon entropy associated with the probability distribution $P_X(x)$ over the stochastic variable X, which has possible outcomes x. Here we see the observable as a stochastic variable to the extent that measuring it spits out a result with a probability associated to it. Moreover, in the RHS of Eq. (C.14), c is the *maximum* overlap between pairs of eigenvectors of the operators A and B. That is,

$$c = \max_{a,b} c_{a,b} \tag{C.15}$$

[3]The logarithm base 2 is merely a convention, we can also use base e, for instance.

where

$$c_{a,b} = |\langle a|b\rangle|^2 \tag{C.16}$$

and $|a\rangle$, $|b\rangle$ are eigenvectors of observables A, B respectively ($A|a\rangle = a|a\rangle$ and $B|b\rangle = b|b\rangle$). A striking characteristic of the EUR in Eq. (C.14) is that it's *state-independent*, differently from the standard deviation-based UR of Eq. (C.4). The maximum overlap c is found to be in the value range:

$$\frac{1}{d} \leqslant c \leqslant 1, \tag{C.17}$$

where $d = \dim(\mathcal{H})$ is the dimension of the Hilbert space where the eigenvectors of A and B live in. The previous bounds on c lead to

$$0 \leqslant \log_2\left(\frac{1}{c}\right) \leqslant \frac{1}{d}. \tag{C.18}$$

The lower bound is trivial (i.e. equal to zero) when A and B have at least one pair of eigenvectors in common. On the other hand, when the eigenvectors of the observables form *mutually unbiased bases* (MUBs), one has that $\log_2(1/c) = 1/d$. What is interesting about the latter case is that what sets the limit on the common knowledge of the observables A and B is a geometric feature of the Hilbert space of the system, that is, its dimensionality. Finding tighter bounds for different entropic measures and various physical scenarios is a research topic on its own, thus for more information we direct the reader to the excellent review found in Ref. [120].

Arguments for the use of EURs instead of standard URs based on the standard deviation are varied. First, there are the counter-intuitive features of the latter presented in the first part of this Chapter. Second, there are positive arguments for EURs; David Deutsch in Ref. [126] noted that changing the labels of outcomes *doesn't* change the information entropy, since it encodes the "amount of information" in the given set and this cannot change by mere relabelling. In contrast, the standard deviation is prone to variation when outcomes are relabelled. Moreover, as noted in Refs. [129, 130], information entropy is non-decreasing under *random relabelling*, that is, relabelling the outcomes in a way that randomness is injected (e.g. by erasure of information). Thus, the EUR cannot be violated by merely manipulating what one already knows (or even by forgetting part of it). As also noted in Ref. [120], EURs are fit to encompass correlated quantum systems, constituting a powerful tool for studying for instance entanglement. From an applications point of view, EURs are also interesting, because entropies are operationally meaningful for quantifying randomness extraction and data compression, two essential features for development of security of quantum key distribution and quantum cryptography [120].

C.1.2 Fine-grained uncertainty relations (FGURs)

A similar approach to the EUR is called by the name of *fine-grained uncertainty relations* (FGUR). First proposed in Ref. [131], this kind of UR accounts for differences in probability distributions to which EURs are blind to, i.e. there are different probabilities distributions that have the same entropy. In regard to this fact that they carry the name "fine-grained". A FGUR look like the following [131, 132]:

$$\left\{ \sum_{r=1}^{n} P(r)P(x^{(r)}|\rho) \leqslant \zeta_{\boldsymbol{x}} \,\middle|\, \boldsymbol{x} \in \mathbf{B}^{\times n} \right\}, \tag{C.19}$$

which consists of a set of inequalities Each inequality corresponds to a set of outcomes $\boldsymbol{x} = \{x^{(1)}, \ldots, x^{(n)}\}$ of n measurements performed on some system initialized in the state ρ. The quantity $P(r)$ is the probability that measurement with label r is chosen, $P(x^{(r)}|\rho)$ is the probability of getting the outcome $x^{(r)}$ when measurement labelled r is applied on the state ρ and $\mathbf{B}^{\times n}$ is the set containing all possible combinations of measurements outcomes. The upper bound $\zeta_{\boldsymbol{x}}$ is obtained through maximization of the LHS, i.e.

$$\zeta_{\boldsymbol{x}} = \max_{\rho} \sum_{r=1}^{n} P(r) P(x^{(r)}|\rho) \tag{C.20}$$

and the state $\rho_{\boldsymbol{x}}$ that saturates this maximum is called the *maximally certain state* [131].

Previous works have pondered how a violation of a FGUR leads to the violation of some other physical property. For instance, in Ref. [131] the authors consider measurements performed on two or more systems and find out that a violation of the Tsirelson bound [107] implies a violation of a FGUR. Also, in Refs. [29, 132] the authors devise thermodynamic cycles in which it is argued that violating a specific FGUR leads to violation of the second law of thermodynamics (SLT), and vice-versa.

Bibliography

[1] L. Hardy, *Probability theories with dynamic causal structure: a new framework for quantum gravity*, 2005.

[2] G. Chiribella, Phys. Rev. A **86**, 040301 (2012).

[3] M. Araújo, C. Branciard, F. Costa, A. Feix, C. Giarmatzi, and Č. Brukner, New Journal of Physics **17**, 102001 (2015).

[4] T. Purves and A. J. Short, Phys. Rev. Lett. **127**, 110402 (2021).

[5] J. S. Bell, Physics Physique Fizika **1**, 195 (1964).

[6] R. F. Werner, Phys. Rev. A **40**, 4277 (1989).

[7] L. M. Procopio, A. Moqanaki, M. Araújo, F. Costa, I. Alonso Calafell, E. G. Dowd, D. R. Hamel, L. A. Rozema, Č. Brukner, and P. Walther, Nature Communications **6**, 7913 (2015).

[8] G. Rubino, L. A. Rozema, A. Feix, M. Araújo, J. M. Zeuner, L. M. Procopio, Č. Brukner, and P. Walther, Science Advances **3**, e1602589 (2017).

[9] M. M. Taddei, J. Cariñe, D. Martínez, T. García, N. Guerrero, A. A. Abbott, M. Araújo, C. Branciard, E. S. Gómez, S. P. Walborn, L. Aolita, and G. Lima, PRX Quantum **2**, 010320 (2021).

[10] G. Rubino, L. A. Rozema, D. Ebler, H. Kristjánsson, S. Salek, P. Allard Guérin, A. A. Abbott, C. Branciard, C. Č. Brukner, G. Chiribella, and P. Walther, Phys. Rev. Res. **3**, 013093 (2021).

[11] M. Antesberger, M. T. Quintino, P. Walther, and L. A. Rozema, PRX Quantum **5**, 010325 (2024).

[12] G. Chiribella, G. M. D'Ariano, P. Perinotti, and B. Valiron, Phys. Rev. A **88**, 022318 (2013).

[13] M. Araújo, F. Costa, and C. Č. Brukner, Phys. Rev. Lett. **113**, 250402 (2014).

[14] D. Ebler, S. Salek, and G. Chiribella, Phys. Rev. Lett. **120**, 120502 (2018).

[15] K. Wei, N. Tischler, S.-R. Zhao, Y.-H. Li, J. M. Arrazola, Y. Liu, W. Zhang, H. Li, L. You, Z. Wang, Y.-A. Chen, B. C. Sanders, Q. Zhang, G. J. Pryde, F. Xu, and J.-W. Pan, Phys. Rev. Lett. **122**, 120504 (2019).

[16] Y. Guo, X.-M. Hu, Z.-B. Hou, H. Cao, J.-M. Cui, B.-H. Liu, Y.-F. Huang, C.-F. Li, G.-C. Guo, and G. Chiribella, Phys. Rev. Lett. **124**, 030502 (2020).

[17] X. Zhao, Y. Yang, and G. Chiribella, Phys. Rev. Lett. **124**, 190503 (2020).

[18] D. Felce and V. Vedral, Phys. Rev. Lett. **125**, 070603 (2020).

[19] X. Nie, X. Zhu, K. Huang, K. Tang, X. Long, Z. Lin, Y. Tian, C. Qiu, C. Xi, X. Yang, J. Li, Y. Dong, T. Xin, and D. Lu, Phys. Rev. Lett. **129**, 100603 (2022).

[20] K. Simonov, G. Francica, G. Guarnieri, and M. Paternostro, Phys. Rev. A **105**, 032217 (2022).

[21] P. R. Dieguez, V. F. Lisboa, and R. M. Serra, Phys. Rev. A **107**, 012423 (2023).
[22] K. Simonov, S. Roy, T. Guha, Z. Zimborás, and G. Chiribella, *Activation of thermal states by coherently controlled thermalization processes*, 2023.
[23] O. A. D. Molitor and Ł. Rudnicki, Entropy **26**, 153 (2024).
[24] M. Araújo, A. Feix, M. Navascués, and Č. Brukner, Quantum **1**, 10 (2017).
[25] O. Oreshkov, F. Costa, and Č. Brukner, Nature Communications **3**, 1092 (2012).
[26] Ä. Baumeler and S. Wolf, New Journal of Physics **18**, 013036 (2016).
[27] G. Francica, Phys. Rev. A **106**, 042214 (2022).
[28] V. Vilasini and R. Renner, Phys. Rev. Lett. **133**, 080201 (2024).
[29] E. Hänggi and S. Wehner, Nature Communications **4**, 1670 (2013).
[30] O. A. D. Molitor, A. H. A. Malavazi, R. D. Baldijão, A. C. Orthey, I. L. Paiva, and P. R. Dieguez, Communications Physics **7**, 373 (2024).
[31] V. Scarani, M. Ziman, P. Štelmachovi č, N. Gisin, and V. Bu žek, Phys. Rev. Lett. **88**, 097905 (2002).
[32] M. Ziman, P. Štelmachovi č, V. Bu žek, M. Hillery, V. Scarani, and N. Gisin, Phys. Rev. A **65**, 042105 (2002).
[33] D. Karevski and T. Platini, Phys. Rev. Lett. **102**, 207207 (2009).
[34] G. T. Landi, E. Novais, M. J. de Oliveira, and D. Karevski, Phys. Rev. E **90**, 042142 (2014).
[35] F. Barra, Sci. Rep. **5**, 14873 (2015).
[36] P. Strasberg, G. Schaller, T. Brandes, and M. Esposito, Phys. Rev. X **7**, 021003 (2017).
[37] G. D. Chiara, G. Landi, A. Hewgill, B. Reid, A. Ferraro, A. J. Roncaglia, and M. Antezza, New J. Phys. **20**, 113024 (2018).
[38] F. L. S. Rodrigues, G. De Chiara, M. Paternostro, and G. T. Landi, Phys. Rev. Lett. **123**, 140601 (2019).
[39] O. A. D. Molitor and G. T. Landi, Phys. Rev. A **102**, 042217 (2020).
[40] F. Ciccarello, S. Lorenzo, V. Giovannetti, and G. M. Palma, Phys. Rep. **954**, 1 (2022).
[41] M. Schlosshauer, Rev. Mod. Phys. **76**, 1267 (2005).
[42] Stanford Encyclopedia of Philosophy, *Philosophical issues in quantum theory*, `https://plato.stanford.edu/entries/qt-issues/#EntaNonlNons` (visited on 07/26/2024).
[43] T. Clifton, P. G. Ferreira, A. Padilla, and C. Skordis, Physics Reports **513**, Modified Gravity and Cosmology, 1 (2012).
[44] A. Zee, *Quantum field theory in a nutshell*, 2nd Edition (Princeton University Press, 2010).
[45] C. Kiefer, *Quantum gravity – an unfinished revolution*, 2023.
[46] A. R. Brown, H. Gharibyan, S. Leichenauer, H. W. Lin, S. Nezami, G. Salton, L. Susskind, B. Swingle, and M. Walter, PRX Quantum **4**, 010320 (2023).
[47] S. Fedida, A.-C. de la Hamette, V. Kabel, and Č. Brukner, *Knot invariants and indefinite causal order*, 2024.
[48] J. Wechs, H. Dourdent, A. A. Abbott, and C. Branciard, PRX Quantum **2**, 030335 (2021).
[49] H. Barnum, C. A. Fuchs, J. M. Renes, and A. Wilce, *Influence-free states on compound quantum systems*, 2005.

[50] O. Oreshkov and C. Giarmatzi, New Journal of Physics **18**, 093020 (2016).
[51] A. Feix, M. Araújo, and Č. Brukner, New Journal of Physics **18**, 083040 (2016).
[52] Y. Aharonov, J. Anandan, S. Popescu, and L. Vaidman, Phys. Rev. Lett. **64**, 2965 (1990).
[53] Ä. Baumeler, A. Feix, and S. Wolf, Phys. Rev. A **90**, 042106 (2014).
[54] C. Branciard, M. Araújo, A. Feix, F. Costa, and Č. Brukner, New Journal of Physics **18**, 013008 (2015).
[55] A. A. Abbott, C. Giarmatzi, F. Costa, and C. Branciard, Phys. Rev. A **94**, 032131 (2016).
[56] T. Baumgratz, M. Cramer, and M. B. Plenio, Phys. Rev. Lett. **113**, 140401 (2014).
[57] A. Streltsov, G. Adesso, and M. B. Plenio, Rev. Mod. Phys. **89**, 041003 (2017).
[58] P. R. Dieguez and R. M. Angelo, Phys. Rev. A **97**, 022107 (2018).
[59] K.-D. Wu, T. Theurer, G.-Y. Xiang, C.-F. Li, G.-C. Guo, M. B. Plenio, and A. Streltsov, npj Quantum Inf. **6**, 22 (2020).
[60] S. Designolle, R. Uola, K. Luoma, and N. Brunner, Phys. Rev. Lett. **126**, 220404 (2021).
[61] T. Giordani, R. Wagner, C. Esposito, A. Camillini, F. Hoch, G. Carvacho, C. Pentangelo, F. Ceccarelli, S. Piacentini, A. Crespi, et al., Sci. Adv. **9**, eadj4249 (2023).
[62] A. Jamiołkowski, Reports on Mathematical Physics **3**, 275 (1972).
[63] M.-D. Choi, Linear Algebra and its Applications **10**, 285 (1975).
[64] F. Costa, Quantum **6**, 663 (2022).
[65] M. Steiner, Phys. Rev. A **67**, 054305 (2003).
[66] F. Giacomini, E. Castro-Ruiz, and Č. Brukner, New Journal of Physics **18**, 113026 (2016).
[67] S. Koudia and A. Gharbi, *Quantum non-gaussianity from an indefinite causal order of gaussian operations*, 2021.
[68] R. Haag, D. Kastler, and E. B. Trych-Pohlmeyer, Communications in Mathematical Physics **38**, 173 (1974).
[69] A. Lenard, Journal of Statistical Physics **19**, 575 (1978).
[70] W. Pusz and S. L. Woronowicz, Communications in Mathematical Physics **58**, 273 (1978).
[71] A. E. Allahverdyan, R. Balian, and T. M. Nieuwenhuizen, Europhysics Letters **67**, 565 (2004).
[72] D. Šafránek, D. Rosa, and F. C. Binder, Phys. Rev. Lett. **130**, 210401 (2023).
[73] R. Alicki and M. Fannes, Phys. Rev. E **87**, 042123 (2013).
[74] X. Liu, D. Ebler, and O. Dahlsten, Phys. Rev. Lett. **129**, 230604 (2022).
[75] M. A. Nielsen and I. L. Chuang, *Quantum computation and quantum information: 10th anniversary edition* (Cambridge University Press, 2010).
[76] G. S. Agarwal, *Quantum optics* (Cambridge University Press, 2012).
[77] M. M. Nieto and D. R. Truax, Fortschritte der Physik/Progress of Physics **45**, 145 (1997).
[78] P. A. Guérin, A. Feix, M. Araújo, and C. Č. Brukner, Phys. Rev. Lett. **117**, 100502 (2016).
[79] P. A. Guérin, G. Rubino, and C. Č. Brukner, Phys. Rev. A **99**, 062317 (2019).
[80] M. T. Quintino, Q. Dong, A. Shimbo, A. Soeda, and M. Murao, Phys. Rev. Lett. **123**, 210502 (2019).

[81] D. Jia and F. Costa, Phys. Rev. A **100**, 052319 (2019).
[82] A. A. Abbott, J. Wechs, D. Horsman, M. Mhalla, and C. Branciard, Quantum **4**, 333 (2020).
[83] F. Chapeau-Blondeau, Phys. Rev. A **103**, 032615 (2021).
[84] D. Xie, C. Xu, and A. Wang, Chinese Physics B **30**, 090304 (2021).
[85] G. Chiribella, M. Banik, S. S. Bhattacharya, T. Guha, M. Alimuddin, A. Roy, S. Saha, S. Agrawal, and G. Kar, New Journal of Physics **23**, 033039 (2021).
[86] F. Chapeau-Blondeau, Phys. Rev. A **104**, 032214 (2021).
[87] M. J. Renner and C. Č. Brukner, Phys. Rev. Lett. **128**, 230503 (2022).
[88] F. Chapeau-Blondeau, Physics Letters A **447**, 128300 (2022).
[89] Q. Liu, Z. Hu, H. Yuan, and Y. Yang, Phys. Rev. Lett. **130**, 070803 (2023).
[90] P. Yin, X. Zhao, Y. Yang, Y. Guo, W.-H. Zhang, G.-C. Li, Y.-J. Han, B.-H. Liu, J.-S. Xu, G. Chiribella, G. Chen, C.-F. Li, and G.-C. Guo, *Experimental super-heisenberg quantum metrology with indefinite gate order*, 2023.
[91] K. Goswami, C. Giarmatzi, M. Kewming, F. Costa, C. Branciard, J. Romero, and A. G. White, Phys. Rev. Lett. **121**, 090503 (2018).
[92] K. Goswami and J. Romero, AVS Quantum Science **2**, 037101 (2020).
[93] M. Caleffi and A. S. Cacciapuoti, IEEE Journal on Selected Areas in Communications **38**, 575 (2020).
[94] Stanford Encyclopedia of Philosophy, *Copenhagen interpretation of quantum mechanics*, `https://plato.stanford.edu/entries/qm-copenhagen/` (visited on 08/01/2024).
[95] H. P. Breuer and F. Petruccione, *The theory of open quantum systems* (Oxford Univ. Press, 2002).
[96] M. Esposito, K. Lindenberg, and C. V. den Broeck, New Journal of Physics **12**, 013013 (2010).
[97] G. T. Landi and M. Paternostro, Rev. Mod. Phys. **93**, 035008 (2021).
[98] R. Clausius, Annalen der Physik **169**, 481 (1854).
[99] R. Clausius, Annalen der Physik **201**, 353 (1865).
[100] H. B. Callen, *Thermodynamics and an introduction to thermostatistics*, 2nd ed. (Wiley, 1985).
[101] R. Dann and R. Kosloff, Phys. Rev. Res. **3**, 023006 (2021).
[102] F. Ciccarello and V. Giovannetti, Physica Scripta **2013**, 014010 (2013).
[103] O. Oreshkov and T. A. Brun, Phys. Rev. Lett. **95**, 110409 (2005).
[104] R. Landauer, IBM J. Res. Dev. **17**, 525 (1961).
[105] Z. Liu and G. Chiribella, *Tsirelson bounds for quantum correlations with indefinite causal order*, 2024.
[106] J. F. Clauser, M. A. Horne, A. Shimony, and R. A. Holt, Phys. Rev. Lett. **23**, 880 (1969).
[107] B. S. Tsirelson, Letters in Mathematical Physics **4**, 93 (1980).
[108] Ä. Baumeler and S. Wolf, in *Proceedings of international symposium on information theory* (IEEE, Piscataway, 2014), pp. 526–530.
[109] R. Horodecki, P. Horodecki, M. Horodecki, and K. Horodecki, Rev. Mod. Phys. **81**, 865 (2009).
[110] L. Hardy, Journal of Physics A: Mathematical and Theoretical **40**, 3081 (2007).
[111] A. J. Short and S. Wehner, New Journal of Physics **12**, 033023 (2010).

[112] G. Manzano, J. M. Horowitz, and J. M. R. Parrondo, Phys. Rev. X **8**, 031037 (2018).
[113] Y. Guryanova, N. Friis, and M. Huber, Quantum **4**, 222 (2020).
[114] W. Heisenberg, Zeitschrift für Physik **43**, 172 (1927).
[115] E. H. Kennard, Zeitschrift für Physik **44**, 326 (1927).
[116] H. Weyl, *Gruppentheorie und quantenmechanik* (Hirzel, Leipzig, 1928).
[117] M. Planck, Verhandl. Dtsch. phys. Ges. **2** (1900).
[118] M. Planck, Annalen der Physik **4** (1901).
[119] H. P. Robertson, Phys. Rev. **34**, 163 (1929).
[120] P. J. Coles, M. Berta, M. Tomamichel, and S. Wehner, Rev. Mod. Phys. **89**, 015002 (2017).
[121] I. Białynicki-Birula and Ł. Rudnicki, in *Statistical complexity*, edited by K. D. Sen (Springer Netherlands, Dordrecht, 2011), pp. 1–34.
[122] H. Everett, Rev. Mod. Phys. **29**, 454 (1957).
[123] I. I. Hirschman, American Journal of Mathematics **79**, 152 (1957).
[124] W. Beckner, Annals of Mathematics **102**, 159 (1975).
[125] I. Białynicki-Birula and J. Mycielski, Communications in Mathematical Physics **44**, 129 (1975).
[126] D. Deutsch, Phys. Rev. Lett. **50**, 631 (1983).
[127] K. Kraus, Phys. Rev. D **35**, 3070 (1987).
[128] H. Maassen and J. B. M. Uffink, Phys. Rev. Lett. **60**, 1103 (1988).
[129] S. Friedland, V. Gheorghiu, and G. Gour, Phys. Rev. Lett. **111**, 230401 (2013).
[130] Z. Puchała, Ł. Rudnicki, and K. Życzkowski, Journal of Physics A: Mathematical and Theoretical **46**, 272002 (2013).
[131] J. Oppenheim and S. Wehner, Science **330**, 1072 (2010).
[132] L.-H. Ren and H. Fan, Phys. Rev. A **90**, 052110 (2014).